

Hillslope evolution of heterolithic landscapes – Investigating processes and controls on
geomorphic development of staircase landscapes

by

Nicholas Reilly McCarroll

B.S., Pennsylvania State University, 2017

M.S., Utah State University, 2019

AN ABSTRACT OF A DISSERTATION

submitted in partial fulfillment of the requirements for the degree

DOCTOR OF PHILOSOPHY

Department of Geography and Geospatial Sciences
College of Arts and Sciences

KANSAS STATE UNIVERSITY
Manhattan, Kansas

2024

Abstract

This dissertation explores different components commonly associated with layered landscapes, using the Flint Hills in northeast Kansas as a natural laboratory and inspiration. The geology of the Flint Hills results in a distinctive stair-step hillslope profile covered in large rock fragments and boulders that armor the slopes. The research presented in the dissertation focuses on three components of layered landscapes: boulder armor transport, boulder armor production, and the influence of stratigraphy on landscape evolution. The investigation employs a combination of thorough fieldwork, geochronologic techniques, and computer modeling to gain deeper insights into these areas.

In Chapter 2, I find that boulder armor in soil-mantled landscapes like the Flint Hills is primarily transported downslope through creep processes. The complex relationship between boulder size and distance downslope suggests that boulders undergo in-situ weathering via fragmentation. Chapter 3 extends the timeline, finding that boulder armor and bedrock bench surfaces date back to the Late Pleistocene during the Last Glacial Maximum. This study suggests that block production and transport were most active during this glacial period, with subsequent warming leading to a slowdown in the system. The boulder armor on the hillslopes is considered relict features representing a time of increased activity. Chapter 4 involves modeling layered landscapes, providing insights into their long-term dynamics. The results suggest that the efficiency of boulder armor is related to the spacing between layers and the transport efficiency of the boulders. While layered landscapes attempt to establish a dynamic steady state, boulder armor and stratigraphic architecture may prevent them from achieving such a state for extended periods of geologic time.

When the findings of these chapters are considered together, it is suggested that boulder armor production may be an intrinsic part of layered landscapes influenced by glacial climates. In locations where moisture conditions are suitable, creep processes spread the boulders out and down the slopes to form discrete boulder armor, rather than a blanket of colluvium like a boulder field. Future research can further explore the timing of bench and boulder production across all the bedrock benches on the hillslope to test whether boulder production is a bottom-up base-level process or a top-down climate-driven process. The Flint Hills, along with layered landscapes in general, offer valuable opportunities for advancing our understanding of geomorphology.

Hillslope evolution of heterolithic landscapes – Investigating processes and controls on
geomorphic development of staircase landscapes

by

Nicholas Reilly McCarroll

B.S., Pennsylvania State University, 2017

M.S., Utah State University, 2019

A DISSERTATION

submitted in partial fulfillment of the requirements for the degree

DOCTOR OF PHILOSOPHY

Department of Geography and Geospatial Sciences
College of Arts and Sciences

KANSAS STATE UNIVERSITY
Manhattan, Kansas

2024

Approved by:

Major Professor
Arnaud J. A. Temme

Copyright

© Nicholas McCarroll 2024.

Abstract

This dissertation explores different components commonly associated with layered landscapes, using the Flint Hills in northeast Kansas as a natural laboratory and inspiration. The geology of the Flint Hills results in a distinctive stair-step hillslope profile covered in large rock fragments and boulders that armor the slopes. The research presented in the dissertation focuses on three components of layered landscapes: boulder armor transport, boulder armor production, and the influence of stratigraphy on landscape evolution. The investigation employs a combination of thorough fieldwork, geochronologic techniques, and computer modeling to gain deeper insights into these areas.

In Chapter 2, I find that boulder armor in soil-mantled landscapes like the Flint Hills is primarily transported downslope through creep processes. Complex relationships between boulder size and distance downslope suggests that boulders undergo in-situ weathering via fragmentation. Chapter 3 extends the timeline, finding that boulder armor and bedrock bench surfaces date back to the Late Pleistocene during the Last Glacial Maximum. The study suggests that block production and transport were most active during this glacial period, with subsequent warming leading to a slowdown in the system. The boulder armor on the hillslopes is considered relict features representing a time of increased activity. Chapter 4 involves modeling layered landscapes, providing insights into their long-term dynamics. The results suggest that the efficiency of boulder armor is related to the spacing between layers and the transport efficiency of the boulders. While layered landscapes attempt to establish a dynamic steady state, boulder armor and stratigraphic architecture may prevent them from achieving such a state for extended periods of geologic time.

When the findings of these chapters are considered together, it is suggested that boulder armor production may be an intrinsic part of layered landscapes influenced by glacial climates. In locations where moisture conditions are suitable, creep processes spread the boulders out and down the slopes to form discrete boulder armor, rather than a blanket of colluvium like a boulder field. Future research can further explore the timing of bench and boulder production across all the bedrock benches on the hillslope to test whether boulder production is a bottom-up base-level process or a top-down climate-driven process. The Flint Hills, along with layered landscapes in general, offer valuable opportunities for advancing our understanding of geomorphology.

Table of Contents

List of figures	xiii
List of tables.....	xiv
Acknowledgements.....	xv
Dedication.....	xvii
Chapter 1 – Introduction	1
1.1 Motivations for dissertation research.....	1
1.2 Hillslope types and evolution	3
1.2.1 Soil-mantled hillslopes.....	4
1.2.2 Soil-poor hillslopes	6
1.2.3 Patchy-cover hillslopes	7
1.3 Bedrock controls on landscape form	7
1.3.4 Simple cliffs	8
1.3.5 Staircase and cuesta landscapes	9
1.4 Hillslope boulder armor	10
1.4.6 What is a boulder?	11
1.4.7 Influence of boulder armor	11
1.4.8 Production of boulder armor	13
1.4.9 Hillslope transport of boulders.....	13
1.5 The dissertation.....	17
1.5.10 Dissertation structure	18
1.5.11 Methods used to address research questions.....	20
1.6 Geochronology for Holocene and Pleistocene geomorphology	21
1.6.12 Radiocarbon	22
1.6.13 Optically stimulated luminescence	23
1.6.14 Cosmogenic surface exposure dating.....	23
1.6.15 ³⁶ Cl exposure dating	24
1.7 Landscape evolution modeling.....	25
1.7.16 Mathematical modeling in geomorphology	26
1.7.17 Hillslope transport laws	28

1.7.18 Modeling investigations into heterolithic landscapes	32
1.8 Holocene and Pleistocene geomorphology of the Flint Hills region	33
Chapter 2 – Transport and weathering of large limestone blocks on hillslopes in heterolithic sedimentary landscapes	38
2.1 Abstract.....	38
2.2 Plain language summary	39
2.3 Introduction and conceptual framework.....	40
2.4 Geology and geography of study area	46
2.5 Methods	50
2.5.19 Cliff measurements	50
2.5.20 Block measurements	51
2.6 Results.....	53
2.6.21 Size, shape, weathering.....	54
2.6.22 Changes downslope.....	57
2.6.23 Interaction with soil	61
2.7 Discussion.....	62
2.7.24 Block size and surface weathering.....	62
2.7.25 Transport and block shape	68
2.7.26 Effects of vegetation cover	70
2.7.27 Block transport mechanisms	73
2.8 Conclusions.....	76
Chapter 3 - The lasting legacy of glacial landscape dynamics: Capturing the transport of boulder armor and hillslope retreat with geochronology in the Flint Hills of Kansas.....	78
3.1 Abstract.....	78
3.2 Introduction.....	79
3.2.28 Plain language summary	79
3.2.29 Introduction and conceptual framework	79
3.2.30 Production of hillslope boulder armor	82
3.2.31 Boulder armor impacts.....	83
3.2.32 Boulder armor transport and removal	85
3.2.33 Geology and geography	87

3.2.34 Regional Pleistocene hillslope activity	88
3.3 Methods	90
3.3.35 ³⁶ Cl exposure dating	90
3.3.36 Sample location determination and surface sampling	91
3.3.37 Shielding evaluation.....	95
3.3.38 Sample preparation and age calculation.....	96
3.3.39 Modeling Cosmogenic Inheritance and Lateral Exhumation	96
3.3.40 Calculating boulder movement rates	99
3.4 Results.....	100
3.4.41 Rock chemistry	100
3.4.42 Raw ages	100
3.4.43 Accounting for weathering and inheritance	103
3.5 Discussion.....	109
3.5.44 LGM timing of landscape activity	109
3.5.45 Relation to holocene activity.....	114
3.5.46 Boulder transport and lateral retreat of benches	115
3.6 Conclusions.....	117
Chapter 4 - Fossil hillslopes and the stratigraphic control on rates of adjustment in multi-layered landscapes.....	119
4.1 Abstract.....	119
4.2 Introduction.....	119
4.2.47 Plain language summary	119
4.2.48 Introduction and conceptual framework	120
4.3 The model	121
4.4 Results.....	126
4.4.49 Basic processes of layered landscapes	126
4.4.50 Stratigraphy, armoring, and uplift rates	129
4.4.51 Landscape response, adjustment times, and behavior.....	129
4.5 Discussion.....	131
4.5.52 Modeled outcomes and real hillslopes	131
4.5.53 Stratigraphic controls and dynamic steady state	133

4.5.54 Time to steady state.....	134
4.5.55 Optimum armoring and fossil hillslopes.....	136
4.6 Conclusion	137
Chapter 5 - Layered landscapes future laboratories of hillslope dynamics	139
5.1 Abstract.....	139
5.2 Introduction.....	139
5.2.56 The Flint Hills	140
5.3 Results of the previous three research chapters	141
5.3.57 Chapter 2 – Limestone boulders (blocks) and hillslope transport	142
5.3.58 Chapter 3 – Timing and rate of boulder movement and production.....	143
5.3.59 Chapter 4 – Modeling of heterolithic hillslopes.....	144
5.4 Chapter 5 – Synthesis	146
5.4.60 Boulder armor and glacial climates	146
5.4.61 Boulder weathering in the Flint Hills.....	153
5.4.62 Stratigraphic architecture, geometry, and boulder armor interactions.....	155
5.4.63 Climate and boulder armor effects.....	158
5.5 Synthesis – New Flint Hills insights.....	161
5.5.64 Long timescale behavior of the Flint Hills.....	161
5.5.65 Boulder and armor dynamics	165
5.5.66 Hillslope erosional signals	167
5.6 The future of layered landscape research	170
5.6.67 Signal shredding in heterolithic hillslope	170
5.6.68 Cliff preservation and fracture soil routing.....	171
5.6.69 Improved modeling of hillslope armor	177
5.7 Future research in the Flint Hills	178
5.7.70 Understanding bedrock bench and cliff morphology.....	178
5.7.71 Creeping boulders and grass sliding	180
5.7.72 Expanded cliff retreat chronology.....	184
5.7.73 Hilltop gravels and dating the age of the current landscape	186
5.8 Conclusions.....	187
References.....	190

Appendix A Chapter 2	221
Appendix B Chapter 3	222

List of figures

Figure 2. 1 Models of blocks movement	43
Figure 2. 2 Study location map and landscape stratigraphy	48
Figure 2. 3 Hillslope survey schematic.....	51
Figure 2. 4 Hillslope block (boulder) surface weathering and size data.....	56
Figure 2. 5 Block (boulder) property with distance from bedrock bench.....	60
Figure 2. 6 Block (boulder) geometry association analysis	62
Figure 2. 7 Conceptual model of block fragmentation	66
Figure 3. 1 ³⁶ Cl sampling location field map and site photography	88
Figure 3. 2 Renderings of sample sites	94
Figure 3. 3 Age-distance regression of boulder and bench surface ages	103
Figure 3. 4 Inheritance modeling curves.....	106
Figure 3. 5 Comparison of paleoclimatic and geomorphic activity to ³⁶ Cl chronology	110
Figure 4. 1 Examples of simulated landscapes and examples of real layered landscapes.....	124
Figure 4. 2 Simulated layered landscape dynamics examples	127
Figure 4. 3 Effect of the presence or absence of armor and response to uplift change	128
Figure 4. 4 Relationship between hardness ratio landscape properties	131
Figure 5. 1 Conceptual model of climate driven boulder armor production and transport	149
Figure 5. 2 End-member types of hillslope armor	158
Figure 5. 3 Conceptual model of fracture piping and field examples.....	172
Figure 5. 4 Mass balance model of bench morphology	177
Figure 5. 5 Optically stimulated luminescence record of block movement.....	184
Figure 5. 6 Models of erosional signal propagation in layered landscape	186

List of tables

Table 2. 1 Properties of large blocks separated by block shape as well as vegetation cover.	55
Table 3. 1 Cosmogenic exposure result for hillslope boulder armor and bedrock bench surfaces	101
Table 3. 2 Boulder and bench surface exposure ages corrected for inheritance based on lateral hillslope retreat.....	107

Acknowledgements

I would like to acknowledge the people and organizations who helped to make this PhD dissertation possible. First, I would like to thank the Purdue University PRIME lab for helping support and fund my work through their seed grant program. I would like to thank the Geological Society of America for their funding of this research through their graduate student research grant program. I would also like to thank the Kansas State Department of Geography and Geospatial Sciences for their support and funding of my work through the various grants, scholarships, and fellowships made available to me. I would like to thank the NSF Long Term Ecological Research program at the Konza Prairie Biological Station for allowing me to conduct my research within the tall grass Prairie.

Thank you to my fellow graduate students for being there for me and helping with the weird odds and ends that come to PhD research. I would like to especially thank Nathan Brownstein and Clay Robertson who have been great friends during my time here at Kansas State. I would like to thank my committee members Abigail Langston, Chuck Martin, Joel Spencer, and David Pompeani for providing me feedback and helping plan a path to completing my PhD.

I want to thank my mother, Judy McCarroll, for her constant love and support during not only my time completing my PhD, but throughout my entire life. I would also like to thank my Father Todd McCarroll, one of the smartest men I know, for his constant love and support throughout my life. I must also thank my dad for helping me formulate the seeds of dissertation while we were hiking in Konza Prairie right after I moved to Manhattan. My parents are two of the staunchest and supportive advocates that any son could ask for and I am eternally grateful for them. Without their guidance, love, and support, a little boy from Lehman, PA, obsessed about

how the water flowed over the ground after it rained, wouldn't have reached his goal of becoming a scientist and gaining his PhD. Thanks to my brothers Andrew and Will who are always there to help me and are two of the best friends a brother could ask for. Massive thanks to my fiancée Dr. Mary Evans, who has been at my side through this entire process, while also gaining her own PhD! Thank you, Mary, for helping me proofread and provide expert grammar and organizational feedback. Mary I will forever be thankful for all your help over this 5-year journey, you have seen this dissertation and the corrections as well, even when I grumbled.

Finally, I would like to give a big thanks to my Advisor Arnaud Temme. I will be forever grateful that Arnaud decided to take me on and mentor me. Arnaud has provided me with so many opportunities to move out of my comfort zone both as a scientist and as a person. His optimism and energy are infectious. His door was always open to me whenever I need to ask him questions or run something by him. I am happy that I can now count him as one of my friends now in life and thankful I could learn so much from him.

As I move into the next part of my life, capping it off with this achievement that I have always dreamed of reaching, I am optimistic that my time here at the KSU Geography and Geospatial Sciences Department has prepared me for wherever my path may take me.

-Nicholas Reilly McCarroll

Dedication

For the little boy from Lehman Pennsylvania who always wanted to be “a doctor, but not that kind of doctor”. I hope that he would be proud of the “doctor” he became all those years later.

Chapter 1 – Introduction

1.1 Motivations for dissertation research

The ultimate driver of landscape evolution across the globe is downward erosion, which occurs primarily through the river and stream channels. The rate at which a river erodes the landscape determines the rate of change in the surrounding area. However, much of the landscape consists of hillslopes, where weathering processes break down and alter rocks into soil, which is then transported down-gradient. This production and transport of soil is controlled by a multitude of factors including lithology, climate, biology, tectonics, vegetation, and hydrology, all of which can vary on both regional and local scales. The natural heterogeneity of landscapes on both local and regional scales of soil production and transport results in a myriad of forms that occur across the Earth's surface. Understanding how factors like lithology and climate influence hillslope evolution is important due to their direct control over the development of the hillslope portions of landscapes.

Through investigation and experimentation, the geomorphic community has developed a robust understanding of hillslope behavior and processes. From this understanding of how this natural system works, the geomorphic community has developed mathematical relationships that are numerical distillations of those geomorphic processes and mechanisms that we can observe shaping the landscapes found across the globe. These mathematical relationships describe the transport of mass across the Earth's surface and so are called transport laws. For hillslope evolution, we use the hillslope diffusion transport law. Hillslope diffusion is the process by which individual particles that make up the surface of the hillslope move imperceptibly slowly in the downslope direction (Dietrich et al., 1987; Roering et al., 1999). Hillslope diffusion is a random process for each particle, which can be moved downslope by various processes like

bioturbation, cyclic wetting and drying, freeze-thaw cycles, rainsplash, and tree throw (Carson and Kirkby, 1972; Black and Montgomery, 1991; Heimsath et al., 1997). In bulk, the movement of these particles results in significant amounts of mass being moved down and off the hillslopes over geomorphic times.

However, due to the complicated interplay of these factors (i.e., climate, vegetation, lithology, etc...) in natural settings, it can be difficult to disentangle and understand their individual effects on hillslope diffusion and evolution in the context. To simplify this complexity within hillslope diffusion, we combine these factors into a single term used in mathematical equations that describes the rate at diffusion occurs, diffusivity (D). Fortunately, landscape evolution modeling using the geomorphic transport laws allows the geomorphic community to examine how each factor independently contributes to the hillslope system is a hypothetical landscape. A virtual landscape that mimics the form and behavior that is observed based on these transport laws, has been a crucial tool in disentangling how different factors and geomorphic processes influence the development of individual hillslopes as well as entire landscapes.

The geomorphic community has been dedicated to gaining a better understanding of how individual factors such as biology, lithology, climate, and hydrology affect the morphology, developmental history, and geomorphometric properties of hillslopes. The underlying lithology is particularly important to landscape evolution because the physical and chemical properties of rock are fundamental to the long-term behavior of landscape change and development. In this dissertation, I will examine how factors related to lithology exert control over hillslope evolution.

1.2 Hillslope types and evolution

Hillslopes can be defined as any land not submerged in water or occupied by a stream (Grieve et al., 2016). Although hillslopes may vary in terms of their underlying geological, climatic, and biological factors, hillslopes can be grouped into two broad-end member types: soil-mantled and rocky soil-poor hillslopes (Neely et al., 2019; Shobe et al., 2021). These two end members reflect the competition between soil production, transport, and slope stability thresholds (Dietrich et al., 2003; Neely et al., 2019).

On both types of hillslopes, transport of soil and regolith from the top to the bottom still occurs, but the processes by which that is achieved are different. Transported material can accumulate at the hillslope's base, eventually burying the flanks of the hillslope (Ward et al., 2011). Hillslopes are nearly always bounded by a stream near the foot of the hillslopes (Gilbert 1909; Schumm, 1977). Material from the hillslope is transported via hillslope processes to a nearby stream channel where the regolith is carried away by the fluvial system from that portion of the landscape (Gilbert and Murphy, 1914; Schumm, 1977; Harvey, 2002; Shobe et al., 2021). Therefore, hillslopes function as conveyor belts that move material from different portions of the hillslope into local streams. Hillslopes do not naturally exist in isolation; they connect to their corresponding channels at their bases. Different sets of processes govern these end-member types of hillslopes and produce the hillslopes we observe today. For the purposes of this study, I will focus on fully developed soil-mantled hillslopes. A review of the distinct end member types of hillslopes is provided below to provide the larger context for the hillslopes that are the focus of this dissertation. Due to my focus on soil-mantled hillslope more detail has been provided for this type of hillslope in the below review.

1.2.1 Soil-mantled hillslopes

Soil-mantled hillslopes are smooth, rounded features typically found in regions where the hillslope has had significant amounts of time to become adjust to the tectonic, hydrologic, and climatic factors that ultimately control rock weathering and soil erosion (Gilbert, 1909; Carson and Kirkby, 1972; Johnstone and Hilley, 2014). Hillslopes that achieve this balance between bedrock weathering, soil production, and erosion rates are described as being in “steady state” or “equilibrium” (Heimsath et al., 1997; Roering, 2008). Soil-mantled hillslopes are a well-known feature in geomorphology, first studied by the father of American geomorphology, G.K. Gilbert (1909). These hillslopes are smooth, rounded, convex features that occur across a range of landscapes (Gilbert, 1909; Heimsath et al., 1997; Roering, 2008). The ubiquitous nature of these types of hillslopes would suggest that many portions of the Earth’s surface have achieved equilibrium currently or at some time in the past.

A layer of physically and chemically weathered bedrock that varies in thickness based on local conditions such as climate and lithology, blankets these hillslopes (Mudd and Furbish, 2004; Johnstone and Hilley, 2014; Langston et al., 2015). This layer of material is the portion of the hillslope that undergoes transport through small-scale, local, processes. Due to the dominance of small-scale processes such as rain splash, bioturbation, shrinking and swelling of soil, the geomorphic community classifies these hillslopes as “diffusive” (Heimsath et al., 1997; Roering et al., 1999; Roering, 2008). Despite the small scale of these processes, they result in the continuous creep of material in the downhill direction, creating mass movement that can be measured by researchers over human timescales (Brooks et al., 2002; Heimsath et al., 2005).

The rate at which mass movement occurs via processes like creep is a function of the gradient of the hillslope (Gilbert 1909) The gradient of soil-mantled hillslopes increases

monotonically with distance from the apex, resulting in a mature convex upward form (Gilbert, 1909; Heimsath et al., 1997; Roering, 2008). Gilbert (1909) proposed that the average velocity of creep for soil-mantled hillslopes must increase downslope because soil-mantled hillslopes have a uniform thickness of regolith. To maximize the effect of gravity on the rate of creep, the hillslope must increase its gradient to accommodate the compounding amount of material coming in from above at any given point. This relationship between the local slope and the rate of transport results in the convex upward form that is strongly associated to the concept of the soil-mantled hillslope. The form of these hillslopes remains stable through time once established and indicates that the hillslope has reached equilibrium between the weathering of bedrock, production of soil, and the downslope transport of material (Montgomery, 2001; Roering et al., 2001). A convex upward hillslope can function as a visual indicator to geomorphologists that a hillslope as well as the overall landscape has experienced similar conditions for significant amounts of geomorphic time (Montgomery, 2001).

The convex upward soil-mantled hillslope is a ubiquitous feature across many landscapes across the world, as such the geomorphic community has studied them since the earliest days of modern geomorphology (i.e Gilbert 1909). Over a century of study, the geomorphic community has distilled the concepts and observations into mathematical relationships that allow for simulations of these features through time (Culling, 1960; Dietrich et al., 2003; Tucker and Hancock, 2010; Temme et al., 2013). The development of the hillslope diffusion transport laws has allowed for the exploration of individual factors that may control the geomorphology of individual hillslopes but the larger overall landscape as well.

1.2.2 Soil-poor hillslopes

On the other hand, rocky, soil-poor hillslopes are steeper, more jagged, and linear in the downslope direction. These soil-poor hillslopes are commonly found in areas with high relief, such as mountains or canyons, which have experienced recent base level or tectonic changes (Cason and Kirkby, 1972; Schmidt and Montgomery, 1995; Dietrich et al., 2003; Neely et al., 2019). In these cases, hillslope erosion rates locally have exceeded rates of soil production, resulting in removal of the soil mantle and exposure of bare bedrock (Neely et al., 2019). Momentum and gravity are the primary drivers of the transport of material across and down these hillslopes (Caviezel et al., 2021). Materials that are liberated from their origin can move quite far downslope, sometimes all the way to the bottom of the hillslope due to the considerable amounts of potential energy available in these settings (DiBiase et al., 2017; Caviezel et al., 2021). This type of transport is known as non-local, as particles move far from their “local” starting point. Examples of non-local transport on these steep hillslopes include rock falls, avalanches, and landslides. These movement events are temporally discontinuous but can achieve significant amounts of movement for each individual particle. Factors, such as the surface roughness of the hillslope, the angle of the hillslope, and the size and shape of the particles govern the downslope transport distance (DiBiase et al., 2017). For instance, if the steep hillslope is a talus cone, the surface would be composed of pockets or crevasses that could catch and instantaneously stop particles that are smaller than the roughness feature (DiBiase et al., 2017). Due to the more dynamic and temporally discontinuous nature of transport on soil-poor hillslopes, mathematical laws have not yet been specifically developed for these types of hillslopes. However, modifications of the soil-mantled hillslope law have been developed by Roering et al. (1999) to cover cases where non-local transport occurs.

1.2.3 Patchy-cover hillslopes

Recently, intermediate conditions in steep landscapes with partial rock and partial soil cover have garnered greater attention in geomorphic observations and investigations. In these steep environments, significant portions of the hillslopes are covered in soil, whereas others are bare rock. These locations bridge the gap between the two endmembers of hillslopes. Neely et al. (2019) suggests that patchy soil cover is due to local differences in bedrock properties (i.e., fracture densities) that allow for the heterogeneous production and accumulation of regolith and soil that is magnified by vegetation that stabilizes each soil patch. These settings show that soil-mantled hillslopes can develop in locations that the geomorphic community would otherwise predict would be bare rock slopes.

1.3 Bedrock controls on landscape form

The end-member types of hillslopes presented above can occur across different climatic and lithological settings. Indeed, different landforms of interest, like hogbacks, cliffs, and escarpments could fall under one or both endmembers present above depending on the underlying conditions of a given landscape. This dissertation will focus on the latter, the effects of the underlying lithology on soil-mantled hillslope development and evolution. The characteristics of the underlying lithology are one of the fundamental controls on landscape evolution (Stock and Montgomery, 1999; Sklar and Dietrich, 2001; Forte et al., 2016). Typically, the relative hardness or erodibility of the rock in a particular landscape determines its nature. For instance, very resistant rocks, such as quartzites, can produce landscapes with large reliefs, while very erodible rocks, like shale, produce low-relief landscapes (Stock and Montgomery, 1999; Sklar and Dietrich, 2001). A review of the types of landforms that develop due to differences in lithologic properties can be found below. This phenomenon of lithological controlled landforms

is key for understanding the study location as well as the staircase hillslopes that this dissertation focuses on.

1.3.4 Simple cliffs

The simplest example of how differences in rock erodibility result in a landform is the formation of a vertical cliff face. Less erodible rock acts as a cap that preserves the topography and protects the softer lithology underneath from further erosion. A significant amount of work understanding the formation and evolution of large cliffs - also known as escarpments - in arid settings, such as those on the Colorado Plateau has already been performed (Koons, 1955; Schmidt, 1996; Shumm and Chorely, 1996; Ward et al., 2011). Generally composed of one hard rock unit that overlies a much softer lithology, these large escarpments can reach hundreds of meters in height and produce significant amounts of rock debris that mantle the slopes directly below the cliff. The lithology of the rock itself can also exert a direct control over the form of a landscape. For example, carbonates dissolve quickly in climates where water is plentiful and are unable to hold up relief, whereas in arid climates, carbonates often form the rock units that produce ridges and high points in a landscape (Wahrhaftig, 1965; Bernard et al., 2019). On a regional scale, differences in erodibility and layer spacing for tilted rocks can result in cuesta landscapes, whereas for horizontal strata, the lateral extent of a resistant rock layer can control the size and distribution of features such as plateaus and mesas (Migón and Duszyński, 2022; Duszyński et al., 2019; Ward, 2019; Glade et al., 2019; Forte et al., 2016; Ward et al., 2011). The term “heterolithic” is used here in this dissertation to describe the property of a sequence of lithologic units that have regular alternation between relative hard and soft lithologies. In most landscapes, simple large cliffs are not common. Instead, globally, heterolithic rock units typically

form multiple smaller cliffs or breaks in slope stacked on top of each other (Duszyński et al., 2019; Duszyński and Migón, 2022).

1.3.5 Staircase and cuesta landscapes

Staircase landscapes, have a distinctive stair-step pattern resulting from quasi-horizontal rocks made up of repeating layers of varying erodibility (Frye, 1955; Yanites et al., 2017; Vero et al., 2018; Duszyński and Migón, 2022). The thickness, configuration, and relative hardness of these layers can differ from location-to-location due to past sea level, accommodation space, and paleogeography (Cecil, 1990; Schalger, 1993; Cecil and Edgar, 2003). The softer lithologies form the slopes, while the harder layers create the benches or slope breaks and when conditions are right are expressed as small vertical cliff faces (Frye, 1955; Vero et al., 2018). When viewed in cross-section, the larger overall hillslope may display a complex morphology of sub-slopes delineated by the position of harder lithologies vertically in the hillslope (Frye, 1955; Vero et al., 2018). When the resistant layers begin to dip more steeply, resistant layers form a series of inclined scarps known as cuestas (Ahnert 1960). The sequence of cuesta scarps will be distributed laterally across the landscape, outcropping wherever the dipping resistant unit intersects the surface. These cuesta scarps are also known as “hogbacks” due to their distinctive shape (Glade et al., 2017).

Despite these observations, questions regarding the formation, evolution, and processes governing staircase landscapes remain unanswered. We lack a well-defined understanding of how the arrangement of hard and soft layers and their relative thickness have on the long-term development of the hillslope. Recent focusing on the large escarpments of the American Southwest has established that the resistant layers that form benches, hogbacks, and cliffs can play an active rather than a passive role in landscape evolution (Glade et al., 2017; Glade et al.,

2019; McCarroll et al., 2021; Shobe et al., 2021). In places where likelihood for resistant layers to disaggregate as boulders or debris is high, these pieces of hard rock can blanket and protect the hillslope. In effect an “armor” layer is formed that protects the softer underlying rock from weathering or transport. It is unclear how this armor interacts with heterolithic landscapes, however what is clear that the presence of hillslope armor is an important factor when considering the evolution of hillslopes.

1.4 Hillslope boulder armor

Early research on the evolution of landscape features such as cliffs, valley walls, hogbacks, and cuerdas assumed that these features were passive actors in landscape evolution (Koons, 1955; Yeend, 1973; Abrahams et al., 1984). While these features can respond to climatic and tectonic signals, they were believed to have little influence on changes in the surrounding landscape. However, recent work suggests that these features are active participants in landscape development (Glade et al., 2017; Duszyński et al., 2019; Glade et al., 2019). Cliffs and valley walls, for example, can deposit large rock boulders onto hillslopes, modulating the timing and rate of erosional signals propagating through a landscape. This process results in the production of hillslope boulder armor, which can modulate and complicate the ongoing landscape change in areas below where these cliffs, benches, and hogbacks occur (Glade et al., 2017; Glade et al., 2019; Shobe et al., 2021). Boulder armor, or more generally hillslope armor, is a layer of large fragments of resistant rock that cover the portions of the hillslope composed of weaker rock. The armor protects the hillslope from weathering and erosion slowing down the rate of hillslope change.

Thus, the production of hillslope armor from an active cliff face makes it an active participant in landscape evolution, in contrast to the assumptions of earlier researchers. This

dissertation will focus on various aspects of boulder armor within a soil-mantled hillslope setting across the three research chapters. Due to the importance of hillslope boulder armor in hillslope evolution, the following sections examines what boulder armor is, how it influences the hillslope, how it is produced, and how it can be transported across and off hillslopes. In the context of the dissertation boulder armor is a central topic in all three research chapters, with each examining a different aspect of boulder armor in the context of field location, which is covered in a following section.

1.4.6 What is a boulder?

Recent studies have investigated the impact of boulder armor on hillslope processes and landscape evolution (Glade et al., 2017; Shobe et al., 2018; Glade et al., 2019; Chilton and Spotila, 2020; McCarroll and Temme, 2021; Shobe et al., 2021). Boulder armor refers to multiple large rock fragments and grains on the hillslope surface that collectively have an overall large-scale impact on the wider hillslope. Although technically a boulder is any sediment grain larger than 256mm (Wentworth, 1922), this definition is not useful in hillslope geomorphology, which requires a more specific definition. Shobe et al. (2021) defines boulders as grains large enough to restrict the motion of smaller, more mobile grains and trigger significant geomorphic change. Throughout this dissertation we adopt this definition when we determine what clasts on hillslopes should be classified as hillslope armor and “boulders”.

1.4.7 Influence of boulder armor

The role of boulders and coarse material in protecting slopes from erosion has been a long-standing concept in hillslope geomorphology. According to Bryan (1940) and Mills (1984), depressions in hillslopes such as gullies fill up with coarse colluvial material from a more resistant rock unit above, resulting in armoring of that location. The armor shields that part of the

hillslope from future erosion caused by runoff and diverts the focus of erosion to another nearby location. Over time, the armored part of the hillslope becomes a strained high point or hilltop (Bryan, 1940; Mills, 1984; Chilton and Spotila, 2020). This process of “Gully Gravure” demonstrates the ability of hillslope armor to drive topographic inversion over both geomorphic and geologic time scales. In later studies, this type of armoring by a colluvial package has become a fundamental theory in examining the evolution of large arid escarpments and associated landforms, including talus flatirons (Koons, 1955; Elorza and Martinez, 2001; Oh et al., 2020; McCarroll et al., 2021). However, more recent research has shifted its focus to individual large boulders and rock fragments scattered across a hillslope and their impact on slope protection against erosion.

Boulders can affect regolith flux in various ways, such as trapping regolith on the upslope side and decreasing the rate at which underlying bedrock is converted into regolith, which reduces the removal of material from soil-mantled hillslopes and forces them to steepen (Granger et al., 2001; Chilton and Spotila, 2020; Glade et al., 2017; Glade and Anderson, 2018). In steep landscapes, boulders produce depressions and pockets that capture smaller grains, inhibiting dry ravel and increasing surface roughness, which decreases the effectiveness of erosion caused by overland flow (DiBiase et al., 2017; Bunte and Poesen, 1993). The influence of these boulders on hillslope evolution is an emergent effect of each individual boulder shielding slopes from erosion as well as catching material on their upside depending on their three-dimensional geometry. However, researchers must consider boulder movement and removal when understanding their temporal and spatial impacts on the landscape. Rates of boulder removal, residence times, and rates of downslope boulder movement remain unknown in landscape evolution models. Another

open question is what the efficiency of boulder armor is based on boulder properties and spatial distribution.

1.4.8 Production of boulder armor

Recent studies have shown that the production of hillslope armor is a result of lateral erosion of various land features such as cliffs, bluffs, hogbacks, and bedrock benches (Duszyński et al., 2019; Shobe et al., 2021). While significant amounts of research have been conducted on the large escarpments in arid regions such as the Colorado Plateau (Koons, 1955; Schmidt, 1996; Shumm and Chorely, 1996; Ward et al., 2011; McCarroll et al., 2021), these towering cliffs are not typical of most cliffs and hillslopes around the world. Cliffs and escarpments ranging in size up to several meters are more prevalent (Duszyński et al., 2019). In scenarios where thin caprock is present, block-by-block weathering, release, retreat, and subsequent block (boulder) transport are crucial factors governing hillslope evolution with intra-slope cliffs (Koons, 1955; Yeend, 1973; Abrahams et al., 1984). The removal of material beneath the caprock results in slumping and detachment of a portion of the escarpment face as a discrete block that may begin to move downslope (Yeend, 1973). This process is usually gradual and slow, resulting from a combination of dissolution and frost wedging, as opposed to the catastrophic rock avalanches of larger escarpments (Yeend, 1973; Koons, 1955; Ward, 2011). Cliffs and escarpments of varying sizes, including modest bedrock benches, produce boulder armor that can significantly impact hillslope evolution.

1.4.9 Hillslope transport of boulders

Large rocks or boulders deposited on hillslopes can influence the movement of regolith and shield the underlying rock from weathering. Recent research has shown that boulders on hillslopes beneath a tough rock unit, typically in the form of a cliff, can significantly affect and

govern the evolution of landforms over time (Duszyński and Migoń, 2015; Glade et al., 2017; Glade and Anderson, 2018; Shobe et al., 2021). However, this review pertains to boulders in soil-mantled hillslopes due to the focus of this dissertation on such hillslopes and field location chosen for this research, the Flint Hills of Kansas, United States. In a soil-mantled landscape boulders and coarse rock fragments cannot be removed through higher-energy transport processes such as landsliding or tumbling (Caviezel et al., 2021). Even in a soil-covered setting, boulders must still be removed from the hillslope and the wider landscape through processes like, rock fall, landslide rafting, or sheet wash lubricated sliding (Schumm, 1967; Duszyński and Migón, 2015; Glade et al., 2017).

The processes that drive the downslope transport of hillslope armor are influenced by several factors including the properties of the boulder itself. Recent research shows that block size is a key control on momentum-based downhill transport and erosional processes. DiBiase et al. (2017) found that when clast size is smaller than the microtopography of the hillslope, the probability of clast interception and storage on the hillslope is high. In contrast, Caviezel et al. (2021) showed that in steep landscapes dominated by momentum-based transport, block shape controls the movement trajectory. However, there is no detailed examination of the relationships between size, shape, and movement of boulders in lower-gradient, soil-mantled hillslopes where there is no momentum-based transport. Insights from previous studies on the geomorphic processes and mechanisms that drive the movement of rock fragments or boulders can be useful when interpreting the findings of this dissertation. In the following paragraphs I present a review of previous research establishing mechanisms by which transport of boulders and rock fragments can be achieved.

Early studies of rock fragment movement focused on bare rock slopes in arid and alpine environments. Schumm (1976) found that thin, tile-shaped rock fragments are highly mobile on arid shale slopes of the Colorado Plateau. He proposed that rock fragments move by sliding, caused by sheet, wash and rafting on creeping regolith. Perez (1985) observed that talus of varying size and shape on alpine slopes in the Andes move through a combination of creep driven by temperature fluctuations and needle-ice action. In another arid landscape, Turkey, Govers and Poesen (1996) demonstrated that downhill clast movement on debris-covered slopes can be caused by dislodging by animals and subsequent rolling. In a different context, Grab et al. (2008) identified frost jacking and gelifluction as the primary drivers of boulder movement on slopes in the mountains of New Zealand. Although these studies are limited to specific environments, they provide valuable insights into the various mechanisms driving rock fragment movement in different conditions.

Recent research by Duszyński and Migón (2015), Glade et al. (2017), and DiBiase et al. (2017) has highlighted the significance of clast size in understanding the transport of discrete cobble and larger clasts on hillslopes. These studies build upon earlier research, dating back to the 1970s, that examined the transport of rock fragments on hillslopes. For example, Schumm (1976), Perez (1985), Govers and Poesen (1996), Grab et al. (2008), and Shobe et al. (2020) all explored this topic. Glade et al. (2017) observed that cubic boulders on hillslopes collect soil behind their upslope face and move in response to significant amounts of hillslope undermining. They also found that the size of blocks produced by hard sedimentary layers decreases systematically in the downslope direction due to weathering. Based on these observations, Glade et al. suggested that sub-meter and meter-sized rock cubic boulders resist the downslope

movement of the soil mantle, resulting in an intermittent process of block movement triggered by hillslope undermining.

Duszyński and Migón (2015) found that large boulders ($\sim 10^3 \text{ m}^3$) in eastern Germany and western Poland do not move once deposited on a slope below or next to a cliff face, suggesting that they resist the downslope movement of soil and regolith. Later, Duszyński et al. (2017) proposed that these large blocks can only be carried downslope passively on mass movements such as shallow rotational landslides. This process may explain the unexpected position of massive blocks dozens of meters in length more than 100 m from the cliff face, as observed by Duszyński and Migón (2015). An alternative process would be the retreat of the scarp itself laterally away from the exceptionally large boulder through physical weathering of the caprock into sand grains that are washed away (Migón et al., 2020).

When transport is not achievable passive removal would be to weather the boulders away in place. By weathering the armor chemically (Darmody et al., 2005) or physically (Epps et al., 2010; McGrath et al., 2013; Epps et al., 2020) the rock fragments become small enough to become part of the mobile regolith and can then be transported away. The transport of newly created fragments is also dependent on lithology, physical properties, and climate conditions (Wells et al., 2008; Roman-Sanchez et al., 2019)

The investigations presented above demonstrate that the most common mechanisms for moving sub-meter to meter-sized boulders and rock fragments downslope are creep, sheet wash-induced sliding, and discrete tumbling. However, for boulders $\sim 10^3 \text{ m}^3$ in size, they may only be transported through landslide rafting. While size is a crucial factor in understanding the transport of boulders, it may not be the only control on the processes regulating boulder armor movement in a soil-mantled setting. Apart from Schumm (1967), who explicitly described the shape of rock

fragments studied, other studies assume that boulders are cubic in shape. However, based on geometric principles, the shape of the boulders should also influence the mechanisms and rates of downslope block movement. Therefore, there is an opportunity to examine the role of boulder shape in these processes.

1.5 The dissertation

There is still much that the geomorphic community does not understand about heterolithic landscapes. While there has been groundbreaking work on the fluvial side of these landscapes, little research has been focused on the hillslopes, and connections between the distinct aspects of these landscapes have not been fully explored (see previous discussion). I will use the local heterolithic landscape of the Flint Hills, Kansas, as the model landscape in my investigations here in the dissertation. There are three areas that require further investigation. Firstly, the influence of the geometric properties of large grains and boulders on their downslope transport on less steep, soil-mantled hillslopes are not well understood. Secondly, there is a lack of chronology for the production and transport of coarse hillslope armor on hillslopes. I will perform this portion of my research focused on the limestone boulders and bench surfaces found in the Konza Prairie portion of the Flint Hills outside of Manhattan, KS. While chronology exists for the fine portion of hillslope material in the Flint Hills region, it is unknown if the coarse hillslope armor is currently being transported actively. Thirdly, while it is understood that the underlying rock properties have a direct effect on landscape morphology and evolution, little is known about how the arrangement of these layers affects the larger landscape. The behavior of hillslopes has been ignored until recently. Therefore, in this dissertation, I aim to answer the following research questions:

R1: How do the size and shape of large rock boulders on temperate soil-mantled hillslopes affect their downslope transport?

R2: What is the timing and long-term rate of boulder armor production and transport on soil-mantled hillslopes in the Flint Hills?

R3: What are the stratigraphic controls on hillslope development and evolution for heterolith landscapes?

Each research question will be addressed individually in one of the chapters of my dissertation. Answering these research questions will expand our understanding of hillslope development overall and will especially contribute to the discussion on heterolith landscapes. Furthermore, this research will produce rarely quantified rates of boulder movement that can be used as an important input to future landscape evolution modeling studies. Finally, this research will increase our knowledge of a type of landscape that does not receive much attention from the geomorphic community.

1.5.10 Dissertation structure

This dissertation will focus solely on the different aspects of hillslopes found in heterolithic landscapes. Each research chapter in this dissertation will focus on a different aspect of the heterolithic hillslope system and the armor that is on that hillslope. The model landscape for this research is Flint Hills, Kansas. The hillslopes due to the alternating relatively hard and soft rocks and the plentiful hillslope armor of various size and shapes make it perfect natural laboratory for my research. The dissertation is composed of three chapters, each one a separate research project, and a fourth, final chapter where the findings of this dissertation are put in context on one another and what they mean more broadly.

Chapter 2 is a field-based study in the Flint Hills. Chapter 2 specifically focuses on the measurement of many individual boulder and rock fragment properties to gain a significant amount of data to perform robust statistical analysis. Using this statistical analysis, I aim to answer the first primary research question of this dissertation (**R1**). This first chapter examines if there is a connection between the size and shape of the hillslope armor and how it is transported downslope. More specifically in Chapter 2 I establish a new model of boulder weathering and transport for soil mantled hillslopes.

Chapter 3 is a field-based study in the same study location. Chapter 3 specifically focuses on the establishment of the geochronology of boulder armor production and transport. A total of 20 limestone surfaces, 10 boulder armor and 10 bedrock benches, were sampled in order for their surfaces to be dated. The data set created from these samples is used to answer the second primary research question of this dissertation (**R2**). From this geochronologic data set I calculated rates of block movement as well as rates that the bedrock bench is uncovered by a laterally retreating hillslope. This boulder-bench geochronology is also used in Chapter 3 to compare the activity of transport and production of hillslope armor in the field location to other records of hillslope activity across the Flint Hills region. I also examine the timing of activity to paleoclimate records to propose a model of climate driven armor production based within Ice Age time periods.

Chapter 4 considers the larger heterolithic hillslopes more abstractly in mathematical simulations. This chapter focuses on how the underlying stratigraphic arrangement of hard and soft layers may control the development, evolution, and rate of change of heterolithic hillslopes using landscape evolution modeling. The metrics harvested from the simulated landscapes are used to answer the third primary research question of this dissertation (**R3**). I

examined the relationship between hillslope boulder armor and the underlying organization of the stratigraphy. Simulations were performed to examine how heterolithic hillslopes of different stratigraphic arrangement react to changes in the rate of uplift. Modeling also presented the opportunity to develop new insights into denudating hillslopes like those in the field area of the Flint Hills.

Chapter 5 considers the findings of the three research chapters and integrates them into a new more comprehensive understanding. This new understanding focuses on two areas, the first what do these new insights mean in the context of heterolithic hillslopes across all landscapes. The second area is what do these insights mean more specifically for the Flint Hills. I also propose where future research into the topic of heterolithic hillslopes and the Flint Hills should focus.

Each chapter builds on the previous. Chapter 2 will provide insights into the processes responsible for armor transport. Chapter 3 will provide rates at which armor transport occurs. Chapter 4 will provide insights into how the overall heterolithic hillslope behaves over long geomorphic time scales. From those three research chapters, Chapter 5, will synthesize the findings of these three investigations into new insights for the Flint Hills landscape as well as heterolithic landscapes more generally. The data needed to produce these new insights needs specific methodologies unique to each chapter. In the following section I detail how different methodological approaches are used to produce the needed data as well as address one of the main research questions covered in each of the three research chapters.

1.5.11 Methods used to address research questions

To address the research questions a three-pronged methodological approach was used for this dissertation research. The first prong is used in Chapter 2 where I collect many

point measurements of different physical and landscape properties of each boulder and rock fragment on hillslope in Konza Prairie portion of the Flint Hills. Statistical analysis is performed on the robust data set of boulder and rock fragment armor to assess hypotheses regarding the processes that may be responsible for the transport and deposition of the armor across the hillslope. The second prong is used in Chapter 3 where I utilize the geochronological technique of cosmogenic surface exposure dating to constrain the age of boulder and bench surfaces. This technique is discussed in more detail below. The ages are used in combination with the samples relative positions on the hillslope to establish rates of movement and change. I also combine surface ages with some mathematical modeling to establish the timing of boulder production and transport for the study portion of the Flint Hills. The third and final prong used in Chapter 4 is using landscape evolution modeling to examine the relationships between the underlying stratigraphy organization and the behavior of the hillslopes over geomorphic time scales (10^6 years). In this third chapter, I will alter the thickness and spacing of resistant layers in the underlying virtual stratigraphy to examine how it affects hillslope evolution. Together these methods have been used to create new insights into the heterolithic hillslope system, Chapter 5. In the following sections I discuss the techniques that are used in this dissertation in more detail.

1.6 Geochronology for Holocene and Pleistocene geomorphology

A key component of geomorphology and quaternary studies has been the use of absolute dating techniques. These techniques provide a specific age, within a margin of error, based on the detection of some kind of signal that accumulates in the dated material (Libby et al., 1949; Aitken, 1985; Balco et al., 2008). For geomorphic investigations that require geochronology, dateable material will be targeted within a feature or deposit of interest. In certain cases, more than one technique may be used to compare to the others and check the

validity of the results that are being produced (Banerjee et al., 2003; Lee et al., 2011). Three techniques are commonly considered when performing geomorphic investigations within the Holocene or Pleistocene. These techniques are radiocarbon, optically stimulated luminescence, and cosmogenic nuclide dating. Each one of these techniques has pros and cons which may make one more appealing depending on the specific properties of a study site as well as the type of geomorphic question one is trying to answer. In this dissertation I use cosmogenic ^{36}Cl geochronology to address the primary research question addressed in Chapter 2. Due to the use of other geochronologic techniques in geomorphic investigations of the Flint Hills I provide them as well to give context to the choice of method for this research and field site.

1.6.12 Radiocarbon

Radiocarbon dating is based on the comparison of a radioactive isotope of carbon (^{14}C) to stable isotopes of carbon in organic materials (^{12}C) (Libby et al., 1949; Atkinson 1975; Ramsey, 2008). Radiogenic carbon is produced in the atmosphere to the interaction with high-energy cosmic rays (Libby et al., 1949; Atkinson 1975). This radiogenic carbon is incorporated into the biomass of all living organisms (Libby et al., 1949; Atkinson 1975). This results in some amount of radiocarbon being present in all organic materials. As such, it is extremely useful when dating organic materials, like bones, plant fibers, or charcoal when present (Ramsey, 2008). Once the creature dies the radiocarbon clock begins to tick, as this technique is based on the amount of ^{14}C remain in a sample which radioactively decays over time (Libby et al., 1949; Atkinson 1975; Ramsey, 2008). Radiocarbon dating has an upper limit of about 60,000 years due to the ever-smaller amount of ^{12}C in the sample (Atkinson 1975; Ramsey, 2008). Due to this upper limit, this technique is commonly used for investigating geomorphic topics that occurred over the

Holocene (0-12,000 years ago) or into the Pleistocene (12,000 – 2.58 x10⁶ years ago), specifically the late Pleistocene.

1.6.13 Optically stimulated luminescence

Optically stimulated luminescence based on the accumulation of electrons inside of individual quartz or feldspar crystals (Aitken 1985; Madsen and Murray, 2009). This technique is especially useful due to the rate ubiquitous nature of quartz in most sedimentary deposits due to its toughness and stability (Madsen and Murray, 2009). Luminescence geochronology can determine the “burial” age of a deposit, which is the last time a grain of quartz or feldspar saw the sun (Aitken 1985; Madsen and Murray, 2009). Once buried, ambient radioactive activity causes a signal to build up inside the crystal lattice of quartz or feldspar grains (Aitken 1985; Madsen and Murray, 2009). This signal can build up until the lattice becomes saturated and is a function of how radioactive the surrounding material is. If the grain is exposed to light again, the signal inside the quartz or feldspar grain is reset (Aitken 1985; Madsen and Murray, 2009; Nelson et al., 2015). When collecting these samples, care must be taken so the sampled material is not exposed to light (Nelson et al., 2015). Optically stimulated luminescence typically has an upper limit of about 350,000 years (Murray and Olley, 2002; Wallinga and Cunningham, 2014). However, in places where the rate of accumulation of a signal is extremely slow, this limit can theoretically be extended to longer timescales (Banerjee et al., 2003; Chapot et al., 2016). Due to the temporal range of this technique, it is commonly used for investigations into the Holocene as well as all the late Pleistocene (12,000 – 129,000 years ago) and into the Middle Pleistocene.

1.6.14 Cosmogenic surface exposure dating

Cosmogenic nuclide dating techniques rely on the accumulation of isotopes, such as ¹⁰Be, ²⁶Al, ¹⁴C, and ³⁶Cl, that are produced when cosmic rays interact with minerals in rock (Lal, 1991;

Balco et al., 2008; Alfimov and Ochs, 2009). The isotopes build up in the mineral proportionally to the duration of exposure to cosmic radiation (Nishiizumi et al., 2007). Most of the nuclear reactions that produce cosmogenic nuclides occur in the first two meters of exposed bedrock (Balco et al., 2008; Alfimov and Ochs, 2009). The rate of production quickly drops off with increasing depth into the rock (Balco et al., 2008; Alfimov and Ochs, 2009). The rate at which cosmogenic nuclides are produced varies through time due to the shifting strength in the Earth's magnetic field, however chronologies of this variation has been established by geochronologists (Nishiizumi et al., 1989; Lifton et al., 2014;). Using a calibrated cosmogenic production rate has become standard across the discipline of cosmogenic geochronology (Balco et al., 2008; Marrero et al., 2016; <https://hess.ess.washington.edu/>). Cosmogenic surface exposure dating has an upper limit determined by the half-life of radionuclide use are using for your geochronology (Balco et al., 2008). The half-life is the time it takes for half the radionuclides present to decay into a more stable element. However, the age range that the cosmogenic nuclide is used for geochronology in his dissertation (^{36}Cl) can range from one thousand years to ten million years (Balco et al., 2008). Due to the range of cosmogenic dating, it is extremely useful for Pleistocene geomorphology as well as a sizable portion of the Miocene (5 to 23 million years ago).

1.6.15 ^{36}Cl exposure dating

For this dissertation, I am limited to using ^{36}Cl as the target nuclide due to the target landforms, limestone boulder armor and cliffs, are composed primarily of calcite (CaCO_3). Due to my target landforms being composed of calcite other geochronologic techniques like optically stimulated luminescence are not viable. I am also limited to what type of radionuclide we will be using to date these surfaces. I must use radiogenic ^{36}Cl as my geochronometer. When cosmic rays interact with the calcite, they convert ^{40}Ca to ^{36}Cl (Alfimov and Ochs, 2009). This is the

primary way ^{36}Cl concentrations increase near the surface, although low energy muon interactions can produce ^{36}Cl at lower rates in deeper rock (Alfimov and Ochs, 2009). By measuring the concentration of these isotopes in rock, one can determine the time since the rock surface was last exposed (Granger and Muzikar, 2001; Balco et al., 2008). Cosmogenic nuclide dating has successfully dated a range of geologic features and processes, including hillslope evolution (Dunne et al., 1999; Granger et al., 2001; Heimsath et al., 2002).

1.7 Landscape evolution modeling

Landscape evolution modeling to simulate landscapes at multiple scales has become an important tool in the geomorphic community's search to understand the development of landforms and landscapes. Before a series of advances in computing, topographic data, and geochronology, landscape evolution models in geomorphology were closer to conceptual models. These landscape evolution models describe how landscapes develop over time or how a process occurs qualitatively. These early models were based on observations of reality and explained those real landscapes in terms of form and process. An example of one of an early landscape evolution model is that of the development of the Henry Mountains due to differences in lithology (Gilbert, 1877). In the case of this dissertation, a foundational early landscape evolution model is that on the convexity of soil-mantled hillslopes (i.e., Gilbert, 1909). These theoretical models then gave way to a series of physical analogue models to better understand the role of specific processes in landscape evolution (Horton, 1945; Leopold et al., 2020). Flume experiments are a ubiquitous type of physical model that uses a scale representation of a river to better understand form and process in a controlled way (Schumm et al., 1987). Presently, landscape evolution models have taken to mean using mathematical theories created to describe the various geomorphic processes driving the evolution of a landscape or landform through time

(Pazzaglia, 2003). A single landscape evolution model can have many multiple different processes occurring with each one governed by an equation (Tucker and Hancock, 2010; Temme et al., 2017). Each process equation can interact with any other. These models are much too complex to be “solved,” and so landscape modelers must approximate the solutions of these various equations by simulating and landscape virtually thought time (Tucker and Hancock, 2010; Temme et al., 2017). As such, the term landscape evolution modeling refers not only to the mathematical equations that may a particular landscape processes, but also to the computer programs and code used to calculate the numerical solutions to these equations (Pazzaglia, 2003; Tucker and Hancock, 2010).

1.7.16 Mathematical modeling in geomorphology

The simulation of landscapes using computers is dependent on the creation of geomorphic transport laws that describe a process that results in the transport of material across the landscape as a mathematical statement. Geomorphic transport laws have been formulated to describe fluvial erosion in both transport- and detachment-limited settings and to simulate the processes related to hillslope diffusion (Braun et al., 2001; Roering et al., 2001; Dietrich et al., 2003) among others. These transport laws begin by examining a process, like hillslope diffusion, and break it down into a mass balance (Tucker and Handcock, 2010; Temme et al., 2017). A mass balance examines the inputs and outputs of an idealized version of a portion of the landscape. This mass balance has been used to create transport laws for fluvial and hillslope systems (Dietrich et al., 2003; Tucker and Handcock, 2010; Temme et al., 2017). The inputs and outputs can be the result of various processes depending on the portion of the landscape of interest. The exact inputs and outputs can vary depending on local conditions; however, once accounted for, the inputs and outputs can simply be subtracted from each other to calculate a

change in mass. All landscape evolution models describe a change in mass that can be applied by the transport law across an entire simulated landscape. When the transport law is applied to the virtual landscapes, it results in a change in the surface elevation that is dependent on the relative amounts of mass coming in or out of a location.

Landscape evolution models have been used to address a wide range of different questions in the field of geomorphology. Much of this modeling is to gain better conceptual understanding of the processes that we believe are shaping a given landscape. This type of modeling is exploratory in nature and allows for us to establish connections between patterns we observe and geomorphic processes (Dietrich et al., 2003; Strudley et al., 2006; Tucker and Hancock, 2010). Landscape evolution models have become the choice for geomorphologists when the scale –either spatial, temporal, or both– is difficult to replicate in physical laboratories or observe out in the field (Kirkby, 1984; Jerolmack and Paola, 2010; Tucker and Hancock, 2010; Ward, 2019). These models simulate landscapes and the resulting geomorphic landscape metrics (i.e., elevation distributions, slope gradients, curvatures) can then be compared to field collected metrics. These comparisons allow for testing of conceptual models on how morphology might be affected by difference in boundary conditions (i.e., climate or rates of landscape uplift), process, or even the parameters that are used to represent properties of a landscape (Perron and Fagherazzi, 2012; Whittaker, 2012). These transport laws have been utilized to understand the developmental history of landscapes, project their evolution into the future, and constrain sediment fluxes (Rhoads, 2006; Temme et al., 2013; Langston et al., 2015; Temme et al., 2017). The use of landscape evolution modeling has become a corner stone of modern geomorphology due to their flexibility in helping answer questions across a wide range of temporal and spatial scales that are of interest to the geomorphic community. In this dissertation, I am interested in

the evolution of hillslopes. In the following section I provide the derivation of the primary geomorphic transport law related to hillslopes, the hillslope diffusion equation, which will be used in Chapter 3 of this dissertation. Other transport laws exist for processes like river erosion and fluvial transport of sediment but due to those portions of the landscape not being the focus of this research will not be covered in the following review.

1.7.17 Hillslope transport laws

As discussed in the sections above, hillslopes are responsible for transporting material from higher to lower points in the landscape, and their importance has led to the development of mathematical relationships that conceptualize and replicate hillslopes. Not all geomorphic transport laws are equally applicable in every situation. In the case of the modeling work presented here we will only focus on the hillslopes. In a study concerned with the evolution of the larger landscape, transport laws for fluvial erosion would also have to be included, however since I am not focusing on those processes those set of equations do not have to be used. As such in this section, we will focus on the development of hillslope diffusion transport laws.

The first diffusion transport law developed was the linear diffusion model, which was derived from equations that describe chemical diffusion (Culling, 1960; Roering et al., 1999). This transport law was the impetus for modeling hillslope evolution (Culling, 1960; Roering et al., 1999). According to the linear diffusion model, the flux of material transported across a hillslope is directly proportional to the topographic gradient (Culling, 1960; Hirano, 1968). This earliest hillslope diffusion transport law reflects the findings of Davis (1892) and Glibert (1909) that the convex shape of a soil-mantled hillslope in steady-state state with climate and uplift results from slope-dependent processes. Davis and Gilbert observed that from the crest of the hillslope to the toe of the hillslope, the amount of material that must be transport increases, each

position having to transport not only what new material being created from rock weathering but also what is coming in from locations above. To keep up with all this material, the hill's slope increases in gradient to transport the evermore amounts of material present as you move down the hillslope. Based on these observations, the flux of hillslope material ($q_{s,l}$) is proportional to the local hillslope gradient multiplied by the local hillslope diffusivity:

$$q_{s,l} = DS \quad \text{Equation 1.1}$$

Where S is the local slope at a particular position on the hillslope and D is a diffusivity term. The term D establishes how diffusive a landscape or in other words how quickly can any hillslope transport material and respond to erosional signals. We discuss the D term in more detail below.

The main criticism of the linear diffusion transport law is this model failed to replicate observations of hillslope curvature in steep landscape positions (Roering et al., 1999). Specifically, steep enough hillslopes assumed to be under equilibrium were found to have linear curvature as opposed to convex curvature. To address this issue, a non-linear diffusion model was developed, which more accurately replicates observed hillslope profiles. This version of the hillslope diffusion model integrates the theory and observation that as hillslope gradients begin to approach the angle of repose or critical slope the regolith transport begins to increase non-linearly (Roering et al., 1999). Effectively near the critical slope, the transport becomes effectively infinite, instantaneously decreasing the gradient of the slope. In the context of a real landscape this would be the equivalent of processes of landsliding which transport a significant amount of material downslope in a small amount of time. This model can simulate cases where rates of flux become nearly infinite, such as landsliding, which is not typically captured in the linear diffusion model. However, the non-linear diffusion model combines these two processes in

a single transport law (Roering et al., 1999; Martin, 2000; Dietrich et al., 2003). The non-linear model quantifies hillslope regolith flux ($q_{s,nl}$) as:

$$q_{s,nl} = \frac{DS}{1-(S/S_c)^2} \quad \text{Equation 1.2}$$

where S is the hillslope gradient, and S_c is a limiting slope steepness beyond which sediment fluxes become infinite (through landsliding). Practically, S_c is often defined as the steepest slope present in an uplifting landscape that has reached equilibrium with erosion. However, not all steady state landscapes may necessarily attain slope steepness near S_c and so S_c may remain a purely assumed value for low-gradient landscapes (Neely et al., 2019). While this diffusion law reflects an improved understanding of hillslope dynamics there are issues when slope gradients approach the critical slope (S_c). In simulations where portions of the hillslope achieve steepness approaching S_c , the soil fluxes become extremely large and can remove a volume of regolith greater than what is available to move, leading to model instability (Perron, 2011). To address this issue, dynamic time-stepping must be implemented to decrease the size of the timestep used by the model, allowing it to maintain stability until the over-steepened location is flattened enough for normal time-stepping to resume (Perron, 2011). A drawback to this solution is the increase in model run times when these dynamic time stepping conditions are met within a model. In context of the modeling work done in Chapter 4 the non-linear diffusion law is not used in the modeling due to stability issues and run times greatly increasing due to dynamic timestepping.

Following the creation of the non-linear diffusion law studies conducted by Roering (2004), Heimsath et al. (2005), and Johnstone and Hilley (2014) have shown that the rate of soil creep through a soil profile is dependent on the depth. Specifically, the rate of soil creep is highest at the surface and decreases exponentially as depth increases (Roering, 2004).

This pattern has been observed across various spatial and temporal scales and in different climatic settings and soil textures (Roering, 2004). Thus, it is essential to consider the depth dependence of soil flux in the mobile regolith when formulating hillslope geomorphic transport laws. Johnstone and Hilley (2014) present a revision of both the linear and non-linear diffusion soil flux laws that consider integrates over the thickness of soil. Depth dependent soil flux ($q_{s,depth}$) is thus represented as:

$$q_{s,depth} = q_0 h_t \left(1 - e^{-\frac{H}{h_t}}\right) \quad \text{Equation 1.3}$$

Where q_0 is flux of regolith due to linear or non-linear diffusion (Equations 1 and 2), H is the thickness of the soil, and h_t is a characteristic soil thickness representing the depth scale of soil transport. Johnstone and Hilley (2014) and later Glade et al. (2017) employed the linear hillslope diffusion law to model hillslopes with varying lithologies, by varying D . This version of the hillslope transport law will be utilized in the modeling of hillslopes composed of alternating layers of hard and soft rock in Chapter 3 of this dissertation.

As demonstrated above, the geomorphic community has been improving their understanding of hillslope transport theory. However, the diffusivity term, D , which is a constant that combines factors such as vegetation, lithology, regolith properties, and climate, is still poorly understood. Although the use of D keeps landscape evolution model as simple as possible, it reveals knowledge gaps regarding how these factors interact to influence hillslope and sediment transport, requiring tuning of D for each studied landscape. Examples of understudied settings that affect hillslope transport include hillslope boulder armor and the stratigraphic arrangement of underlying lithology, which have only recently been explored (Glade et al., 2017, 2019; Johnstone and Hilley, 2014). These settings present opportunities for

further geomorphic investigation, and this dissertation aims to increase our understanding of their effects on hillslope evolution (Chapters 2 and 4).

1.7.18 Modeling investigations into heterolithic landscapes

Recent modeling explorations have emphasized the significance of regional scale stratigraphic organization in landscape development (Glade et al., 2019; Ward, 2019; Yanites et al., 2017; Forte et al., 2016; Ward et al., 2011). Forte et al. (2016) demonstrated how waves of accentuated erosion can progress up a fluvial system as a river erodes through rocks with different erodibilities. In addition, Yanites et al. (2017) demonstrated that the timing of erosion can significantly vary due to the underlying lithologies' geometric relationships, causing baselevel signals to become delayed while traveling up the river network. In landscapes with complex underlying geometries, various parts of the landscape experience distinct timing of erosional signals. Ward (2019) revealed that landscapes developed in tilted heterogeneous stratigraphy have incision rate thresholds that may regulate the formation of strike valleys. The incision rate threshold is proportional to the spacing and dip of resistant layers. Moreover, Ward (2019) observed that the response times of these structurally controlled heterolith landscapes may be longer than late Quaternary variations in incision rates. Interestingly, Ward (2019) suggested that the escarpment's formed in heterolithic landscapes may preserve information about regional incision rates on timescales different from those documented in the fluvial network. Despite the significant insight provided by these studies on signal propagation through landscapes with variable lithology and increasingly complicated structural geology, they primarily focused on the fluvial portion of landscapes, with little attention paid to the hillslopes.

Only recent modeling work has explored the impact of lithology on hillslope evolution, but this research has primarily focused on the formation of cliffs and hogbacks, while

relatively little attention has been paid to the role of stratigraphic organization in hillslope evolution, particularly in landscapes where rocks are horizontal (Shobe et al., 2021; Tucker, 2019; Glade et al., 2019; Glade et al., 2017; Johnstone and Hilley, 2015; Ward et al., 2011). The rate of lateral cliff retreat in landscapes with two adjacent lithologic units has been shown to depend on the rate of erosion of the soft underlying rock and the large rocky debris armor (Ward et al., 2011). More recently, Glade et al. (2017, 2019) investigated the influence of debris armor from an upper resistant lithology on hillslope evolution and found that large rock blocks can modulate hillslope change over geomorphic timescales and affect the flux of material downslope, storing hillslope material on their upslope sides. However, there is still a significant gap in understanding the impact of stratigraphic organization on hillslope evolution, especially for landscapes with horizontal rock layers, even though large areas of the continental interior are composed of flat-lying rocks (Duszyński and Migón, 2022).

1.8 Holocene and Pleistocene geomorphology of the Flint Hills region

The Flint Hills exhibit distinctive hillslope profiles that resemble stair steps, with alternating layers of nearly horizontal shale and limestone controlling their morphology (Frye, 1955). The soft shale layers form the soil-covered portions of the hillslopes, while the limestone layers can form small bedrock cliffs and ledges that curve along the landscape. These benches and cliffs are aligned with the stream valleys incised by first-order ephemeral streams. At the points where these streams intersect with the limestone benches, there is a noticeable increase in tree cover and an amphitheater hillslope morphology that is centered around the stream. The limestone layers that form the cliffs are well-fractured into regular units at approximately one-meter intervals, and the resulting boulders and blocks are deposited on the shale slopes beneath the cliffs (Frye, 1955). The blocks come in varying shapes, ranging from cubic to tile-shaped,

and are thought to move through tumbling and soil rafting processes, as previously hypothesized above.

The Flint Hills physiographic province covers an area of approximately 26,000 km² and is the result of the erosion of Permian age limestones and shales (Dort, 1987; Aber, 1991; Oviatt, 1999). This landscape configuration is believed to be between 2 and 3 million years old (Frye, 1955; Oviatt, 1999). Evidence of the previous landscape configuration can be found in the form of hilltop gravels rich in chert, which have pebble lithologies that suggest they originated from areas farther west than the modern-day drainages of the Flint Hills reach. The drainage network that deposited these gravels originated from eastern Colorado and western Kansas and flowed primarily in an east-west direction before the establishment of the modern drainage network (Aber, 1997; Aber, 2018). However, the exact process or event that reorganized the drainages in the region is not well understood. One explanation is glaciation of the region during pre-Illinoian times (Frye, 1955; Oviatt, 1999). However, further investigations are necessary to determine the underlying causes.

The region has also undergone significant environmental changes during the Pleistocene epoch. In this period, glaciers advanced and retreated across the area. The glaciers reached their maximum extent during the pre-Illinoian glaciation, which occurred around 650,000 years ago. At that time, the glaciers moved into the northeastern corner of Kansas, leading to the damming of the Kansas River near Wamego, KS and the formation of Glacial Lake Kaw (Todd, 1903). Later, during the Late Pleistocene and Holocene, the valleys and hillslopes in north-eastern Kansas remained topologically stable but underwent changes in response to shifts in climate, according to studies by Smith (1991), Beeton and Mandel (2011), and Lyzell and Mandel (2020).

In the Holocene, the proportion of C3 and C4 carbon isotopes in soil organic matter (SOM) can indicate the prevailing climatic conditions. The type of photosynthesis pathway used by a plant determines the relative proportions of C3 or C4 in its biomass (Monson et al., 1984; Kohn, 2010). C3 plants are adapted to cooler climates and can tolerate wet or dry conditions, while C4 plants are adapted to warmer climates and can tolerate moist or dry conditions. In the study area of Great Plains and Flint Hills paleosols, the relative proportions of C3/C4 in SOM are linked to the proportions of short(C3) to tall(C4) grasses present in the landscape during soil formation, including big bluestem, Indian grass, little bluestem, and switchgrass (Briggs et al., 2002; Lyzell and Mandel, 2020). Changes in the C3/C4 isotopic ratios in soil profiles suggest that six periods of upland hillslope destabilization occurred between 10,000 C¹⁴ yr B.P. and 900 yr. B.P., resulting in the shedding of fine-grained material that lasted approximately 500 years, followed by major periods of stream aggradation that lasted equally long or longer (Gorynski and Mandell, 2009; Lyzell and Mandel, 2020). These destabilization periods are characterized by the deposition of low-gradient fine-grained alluvial fans at the base of hillslopes. Once a new vegetation regime is established, sediment flux effectively ceases, and the times of destabilization are followed by periods of stream aggradation and valley filling. The Konza Prairie portion of the Flint Hills experienced stream aggradations approximately 8,000 yr B.P., 3,000 yr B.P., and 1,700 yr B.P. (Smith, 1991). These periods of stream aggradation are followed by evacuation and erosion. King's Creek, the primary stream in Konza, began evacuating material again around 180 yr B.P. and is currently deeply incised into its own alluvium and partially into bedrock. This Holocene history is like that of other streams in the Flint Hills, such as Fox Creek, located approximately 100 km south of my study location (Beeton and Mandel, 2011).

According to Lyzell and Mandel (2020), the records indicate that shifts over the past 10,000 years affected only the fine-grained portion of the mobile hillslope, and there is no evidence that boulder armor was ever transported from their upland positions during this time, suggesting that their positions have been relatively stable for at least 10,000 years or longer. However, this finding is intriguing as observations from the modern-day hillslope suggest that boulders are transported along with the creeping regolith, and we would expect that during times of increased fine sediment flux, proportional amounts of armor would be carried downslope as well (Schumm, 1967). Therefore, a chronology needs to be established in the region to examine when these boulders and limestone benches were actively producing and transporting armor downslope.

The dissertation presented in the following chapters is concerned with developing a better understanding of heterolithic landscapes and hillslope armor. The Flint Hills provides an opportunity to address the major research questions of this dissertation. Its location is prime due to Kansas State University managing a local portion, the Konza Prairie, within a short driving distance from the university. An increased amount of research has been performed on this portion of the Flint Hills and so provides a rich research background that can be utilized to put the findings of this research in context of the larger landscape it takes place in. The presence of abundant hillslope boulder armor makes it an optimal location to address the first of the primary dissertation research questions (**R1**) in Chapter 2. The regularly fractured limestone that outcrop as small cliffs and benches along with the boulder armor below make the Flint Hills opportune for the second of the main research dissertation questions (**R2**) in Chapter 3. While Chapter 4 uses landscape evolution modeling to answer the third primary dissertation research question (**R3**) The Flint Hills acts as the model landscape that is used when interpreting the model. For all

three chapters, the Flint Hills is an important part of the research performed here in this dissertation.

Chapter 2 – Transport and weathering of large limestone blocks on hillslopes in heterolithic sedimentary landscapes

2.1 Abstract

Geomorphic transport laws that describe the movement of material across landscapes generally hide the role of lithological and climatic boundary conditions behind proportionality terms. The geomorphic community aims to characterize the role of these boundary conditions and include them in mechanistic transport laws. A more detailed mechanistic understanding is needed for hillslopes formed in heterolithic rock that weathers into weak regolith and hard blocks (boulders), such as in hogbacks. The properties of such blocks may determine both the process and rate of their transport downslope. I focused on soil mantled hillslopes in the Flint Hills of Kansas in the United States, where I studied the role of block (boulder) shape and size under a limestone cliff that breaks up approximately into equal amounts of cubic and tile-shaped clasts. Based on previous studies on the transport of rock clasts, I hypothesized that cubic and tile-shaped blocks should be transported differently, leading to different distributions of size and orientation with increasing distance from the cliff. Block shape does have significant influence over how soil collects and is stored on the hillslope near blocks. Yet, few cubic blocks appear to be transported through tumbling in contrast with assumptions in recent modeling work. I found complex relationships between block size and distance from the cliff face, and I propose that this is due to weathering via fragmentation. This process produces discrete smaller fragments from a larger parent block. The data suggests that at least in Kansas both cubic and tile-shaped blocks are transported primarily by creep processes.

A version of this chapter was submitted to the *Journal of Geophysical Research: Earth Surface* on January 21st, 2022 and accepted after going through peer review on August 26th, 2022. The citation of the journal article is: McCarroll, N. R., & Temme, A. J. A.M. (2022). Transport and weathering of large limestone blocks on hillslopes in heterolithic sedimentary landscapes. *Journal of Geophysical Research: Earth Surface*, 127, e2022JF006609. <https://doi.org/10.1029/2022JF006609>.

2.2 Plain language summary

In steep landscapes like those of the Rocky Mountains or the Canyons of the Colorado Plateau, large boulders and blocks move downslope quickly and violently under the force of gravity. Recent research has shown that the general shape of these blocks (boulders) is important for how they tumble and how far they can travel downhill. However, in much flatter landscapes, like those of the Great Plains, we generally don't have a well-defined understanding of how these large rock blocks move downhill. I hypothesize that blocks that are broadly cubic or tile-shaped will move differently downslope and so should lead to them occupying different positions in these flatter landscapes. My investigation is focused on the Flint Hills of Kansas. I show that in this landscape of soil-covered hills and shallow slopes that all blocks, despite shape, must be transported downslope via a process known as creep. I also present evidence that the blocks on these hills quickly break apart into halves and quarters and this may be helped along by factors such as fire. My results lead me to believe that block shape is not as an important consideration in downslope movement for landscapes like the Flint Hills.

2.3 Introduction and conceptual framework

Geomorphic transport laws are mathematical relationships that describe the mass flux of material over a landscape. The formulation of such laws is central to the modern field of landscape evolution modeling (Dietrich et al., 2003; Temme et al., 2017; Tucker & Hancock, 2010). Landscape evolution models have been used in constraining sediment fluxes, understanding the developmental history of landscapes, and projecting the evolution of landscapes into the future (Dietrich et al., 2003; Temme et al., 2017; Tucker & Hancock, 2010). Laws have been formulated to describe fluvial erosion in both transport and detachment limited settings, and to simulate the processes related to hillslope diffusion (Braun et al., 2001; Dietrich et al., 2003; Roering et al., 2001), among others. The earliest diffusion transport law was the linear diffusion model, derived from equations describing chemical diffusion (Culling, 1960; Roering et al., 1999). This transport-law initiated landscape modeling of hillslope evolution (Culling, 1960; Roering et al., 1999). The linear diffusion model states that the flux of hillslope material is directly proportional to topographic gradient (Culling, 1960; Hirano, 1968). However, this model failed to replicate observations of hillslope curvature in steep landscape positions (Roering et al., 1999). In response to this shortcoming, the non-linear diffusion model was formulated, which better replicates observed hillslope profiles, yet still lumps processes ranging from creep to landsliding (e.g., Dietrich et al., 2003; Martin, 2000; Roering et al., 1999.). The non-linear model quantifies hillslope regolith flux (q_s) as:

$$q_{s,nl} = \frac{DS}{1-(S/S_c)^2} \quad \text{Equation 2.1}$$

where S is the hillslope gradient, and S_c is a limiting slope steepness beyond which sediment fluxes become infinite (through landsliding). Practically, S_c is often defined as the steepest slope present in a landscape that has reached equilibrium. However, not all steady state

landscapes may necessarily attain slope steepness near S_c and so may remain as a theoretical value for low-gradient landscapes. The proportionality parameter D is a constant combining the role of vegetation, lithology, regolith properties, and climate, among others. This collection of many factors into one term can be done to simplify our landscape evolution models. However, this simplification also reveals our knowledge gaps concerning how these factors come together and interact to influence hillslope and sediment transport, thus requires tuning of D to each new studied landscape (e.g., DiBiase et al., 2017; Marston, 2010; Roering et al., 2001).

Climate, lithology, and vegetation cover are known significant controls on the flux of material (e.g., Govers & Poesen, 1998; Marston, 2010; Roering et al., 2001). The geomorphic community has recognized this and is attempting to understand how climate, lithology, and vegetation are reflected in proportionality terms such as D (e.g., Carriere et al., 2020; Johnstone & Hilley, 2015; Pelletier & Rasmussen, 2009). One of the factors that has recently received attention is the lithological composition of the hillslope, particularly in heterolithic settings. The different lithologies in these settings can each produce distinct weathering products with different properties. These properties—grain or clast size, shape, erodibility, and density—can act as controls on material transport (as illustrated for fluvial regimes by Menting et al. (2015)). Of specific interest, the transport of large rock blocks (boulders) from hard lithologies down a hillslope and into a fluvial channel can significantly modulate erosional signals propagating through a landscape (Duszynski et al., 2017; Glade & Anderson, 2018; Glade et al., 2019; Roth et al., 2020; Shobe et al., 2018, 2021). Therefore, knowing how and when large rock blocks are transported downslope by hillslope processes is important for understanding broader aspects of landscape evolution. Recent work focusing on hillslope transport of discrete cobble and larger clasts by Duszynski and Migon (2015), Glade et al. (2017), and DiBiase et al. (2017) has shown

that clast size is important in understanding how and at what rates clasts are transported downslope. These studies build upon earlier work beginning in the 1970s examining the transport of large, cobble to boulder-sized, rock fragments downslope (e.g., Govers & Poesen, 1998; Grab et al., 2008; Pérez, 1985; Schumm, 1967; Shobe et al., 2020). Early work on the movement of rock fragments was done on arid and alpine bare rock slopes (Pérez, 1985; Schumm, 1967). These studies focused on measuring rates of surficial movement of talus material or rock fragments over a finer-grained regolith. Schumm (1967) found that thin, tile-shaped rock fragments are highly mobile on the arid shale slopes of the Colorado Plateau. He proposed that rock fragments on bare regolith slopes move through a combination of sliding, caused by sheet, wash and rafting on creeping regolith. Pérez (1985) observed that talus of varying size and shape on alpine slopes in the Andes moves through a combination of creep driven by temperature fluctuations and needle-ice action. In a similarly arid landscape like the Colorado Plateau, Turkey, Govers and Poesen (1998) showed that dislodging by animals and subsequent rolling can drive downhill clast movement on debris covered slopes. Grab et al. (2008) invokes frost jacking and gelifluction as the primary mover of boulders on slopes in the mountains of New Zealand. Recent work has established that block size has also emerged as a key control on momentum-based downhill transport and erosional processes. DiBiase et al. (2017) examined the relationship between hillslope topographic roughness and the size of bouncing clasts in steep, soil-poor topographies. They found that when clast size is smaller than the microtopography of the hillslope, the probability of clast interception and storage on the hillslope is high. Caviezel et al. (2021) showed that in steep landscapes dominated by momentum-based transport, block shape has a strong control over movement trajectory: tile-shaped blocks have a greater lateral spread in depositional location at the bottom of steep

hillslopes than cubic blocks. However, no examination of these size and shape relationships has been conducted for lower gradient soil-mantled hillslopes. Glade et al. (2017) observed that ~1 m rock blocks on hillslopes collect soil behind their upslope face, and that blocks had presumably moved in response to significant amounts of hillslope undermining below the block.

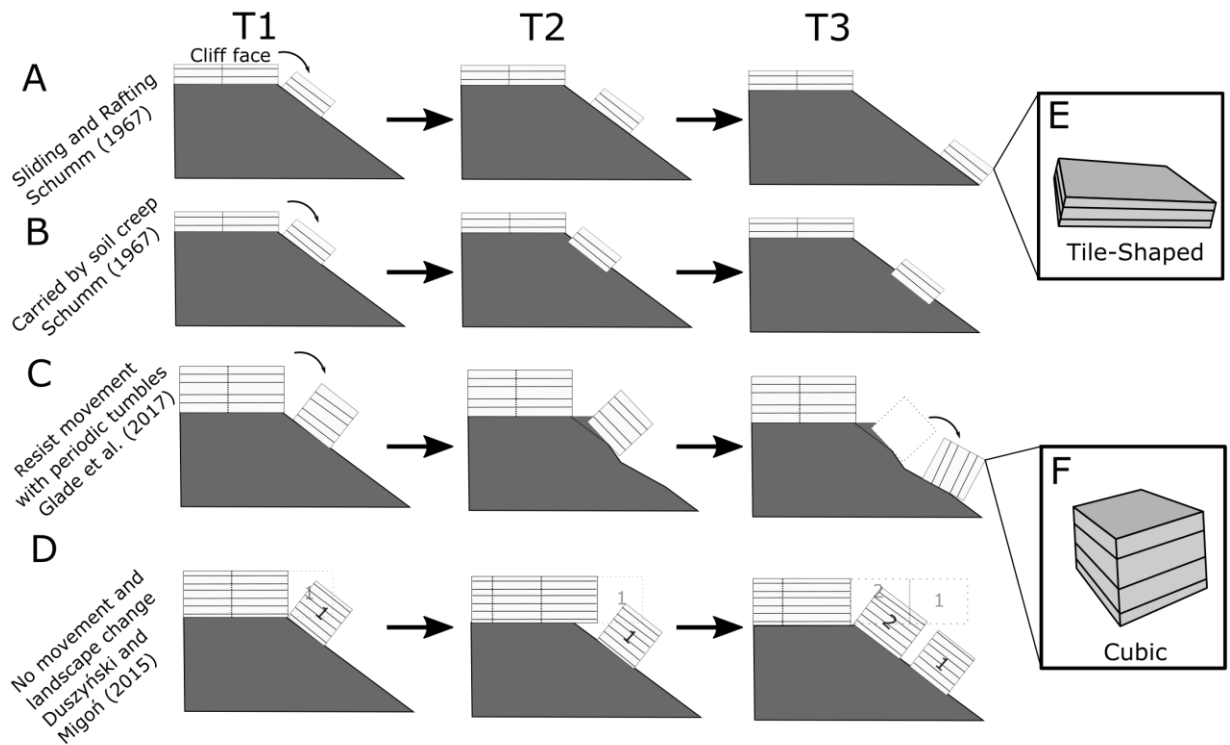


Figure 2. 1 Models of blocks movement

Proposed modes of block movement on hillslopes in literature. Each model is simplified into a three-step progression through time. (a) Block movement rate is faster than soil diffusion due to sliding (Schumm, 1967). (b) Block movement is at the rate of hillslope diffusion and is the result of the block being embedded and transported with the mobile regolith (Schumm, 1967). (c) Blocks resist downslope movement with regolith but are moved through a combination of slope undermining and upslope soil damming resulting in instability and tumbling (Glade et al., 2017). The rate of block movement will be slower than hillslope soil diffusion. (d) Blocks are too large to move and stay where they are deposited (Duszyński & Migon, 2015). The rate of block movement will be zero. The hillslope around the block lowers and the cliff laterally retreats away resulting in the appearance of downslope block transport. (e) Conceptual example of a tile-shaped block where the long and intermediate axes of the block are much larger than the shortest axis. (f) Conceptual example of a cubic block where the longest, intermediate, and shortest axes are approximately similar in length.

Glade et al. (2017) also observed that the size of blocks produced by hard sedimentary layers systematically decreases in the downslope direction—supposedly through weathering. Based on these field observations, they postulated a resistance of sub-meter and meter-sized rock

blocks to the downslope movement of the soil mantle. The implication of that assumption is that the movement of boulder-sized blocks on soil-mantled hillslope is an intermittent process where movement is triggered by undermining of the hillslope beneath the block resulting in blocks that move slower than the mobile regolith. Duszynski and Migon (2015) suggested that $\sim 10^3 \text{ m}^3$ rock blocks, observed in eastern Germany, do not move once they are deposited on a slope below or next to a cliff face, successfully resisting the downslope movement of soil and regolith. In later work, Duszynski et al. (2017) suggested that such blocks, too large to move otherwise,

can only be carried downslope passively on mass movements, such as shallow rotational landsliding. This process of landslides carrying massive blocks is a possible explanation for the unexpected position of blocks dozens of meters in length more than 100 m from the cliff face, as observed by Duszynski and Migon (2015). The research presented above demonstrates the most common mechanisms for moving sub-meter to meter sized blocks downslope are creep, sheet wash-induced sliding, and discrete tumbling, whereas blocks $\sim 10^3 \text{ m}^3$ in size may be transported only through landslide rafting (Figure 2.1). Size may not be the only control on the processes regulating a block's movement. Apart from Schumm (1967), who explicitly described the shape of blocks studied, other studies largely observe or assume blocks that are generally cubic in shape. However, based on geometric principles, one should expect the shape to influence mechanisms and rates of downslope block movement. To explore this influence, in this project we can simplify block shape into two conceptual categories: cubic and tile-shaped (Figures 2.1e and 2.1f). Glade et al. (2017) proposed that cubic blocks may be rather immobile on slopes except for short intermittent moments of movement. Such cubic blocks, when compared to tile-shaped blocks, have less downward-facing surface area in contact with the hillslope. Subsequently, the force of swelling hillslope material may be unable to overcome the cubic

block's greater pressure, which precludes movement by creep. Instead, movement may primarily result from downslope undermining and slope steepening, causing block instability, tumbling, or sliding (Glade et al., 2017). On the other hand, tile-shaped blocks as observed by Schumm (1967) are transported in a continuous fashion. Schumm described two primary transport pathways. Tile-shaped blocks can move rapidly via sliding induced by reductions in slope shear strength due to the moisture or surface runoff. Alternatively, tile-shaped blocks can be moved gradually by creep as part of the mobile hillslope regolith. Repeated lifting and lowering related to the periodic shrinking and swelling of material, or frost heave, results in downslope block transport in a similar manner to creep. In either case, tile-shaped blocks appear to be passive actors in downslope transport and depend on the activity of the soil. The lack of a systematic study on the effect of particle shape or size on downslope block transport in a low gradient soil mantled hillslope setting leads me to ask, "How does block size and shape affect downslope transport as well as soil-block interactions on creep dominated hillslopes?"

To begin answering this research question, I test four hypotheses. These are:

H1: Total block surface area decreases with increasing distance from the cliff face.

H2: Visible signs of surface weathering increase with increasing distance from the cliff face.

H3: Cubic blocks collect soil behind their upslope side, whereas tile-shaped blocks will be surrounded by soil.

H4: The average difference between the slope of a block and the slope of the surrounding hillslope (quantified as Block Relative Slope [BRS]) is large for cube-shaped blocks compared to tile-shaped blocks.

I test these hypotheses in the Flint Hills in north-eastern Kansas. Hard, sub-horizontal limestone layers of the Flint Hills weather into blocks that range in shape from cubes to tiles and are transported over hillslopes mainly weathered from shale. This property of my study location allows me to examine how the initial properties of large rock fragments, particularly shape and size, affect downslope block transport while controlling for lithology, vegetation, and climate history.

2.4 Geology and geography of study area

Our research is conducted in the Konza Prairie Biological Station portion of the Flint Hills (39°05' N, 96°35'W) outside of Manhattan, KS (Figures 2.2a and 2.2b). Konza Prairie spans approximately 35 km² of unplowed tallgrass prairie and has been little modified by humans. The Flint Hills physiographic province (Figure 2.2a) is approximately 26,000 km² in area and was formed by the erosion of a sequence of quasi-horizontal Permian age limestones and shales (Aber, 1991; Dort, 1987; Oviatt, 1999). The current landscape configuration is estimated to be approximately 2–3 million years old (Frye, 1955; Oviatt, 1999). Evidence of the previous landscape configuration is present as chert-rich hilltop gravels found across the Flint Hills and eastern Kansas. The drainage network that deposited the gravels sourced its material from eastern Colorado and western Kansas and ran primarily in an east-west direction before the establishment of the modern drainage network (Aber, 1997, 2018).

In more recent times, the region has experienced the Pleistocene advance and retreat of glaciers. Glaciers extended into the north-eastern corner of Kansas, at their maximum extent during the pre-Illinoian (~650 ka) glaciation, culminating in the damming of the Kansas River near Wamego, KS and giving rise to Glacial Lake Kaw (Aber, 1991; Balco et al., 2009; Bierman

et al., 1999). My study site is approximately 10 km from the terminal limit of the pre-Illinoian Glaciation (Figure 2.2a). During the Late Pleistocene and Holocene, valleys, and hillslopes in north-eastern Kansas were topologically stable, but responding to climatic changes (Beeton & Mandel, 2011; Layzell & Mandel, 2020; Smith, 1991). For example, the Konza Prairie portion of the Flint Hills experienced stream aggradations and incisions at approximately 8,000, 3,000, and 1,700 yr B.P. (Smith, 1991). The primary stream in Konza, King's Creek, began evacuating material again around 180 yr B.P. and is currently deeply incised into its own alluvium and partially into bedrock. This Holocene history mimics that of other streams in the Flint Hills, such as Fox Creek, which is nearly 100 km south of my study location (Beeton & Mandel, 2011). The Flint Hills are known for their stairstep hillslope profiles, whose morphology is controlled by alternating layers of quasi-horizontal shale and limestone (Frye, 1955) (Figure 2.2c). The soft shales form soil-mantled parts of hillslopes, whereas the limestones can form small (up to 2 m high) bedrock ledges and cliffs which contour

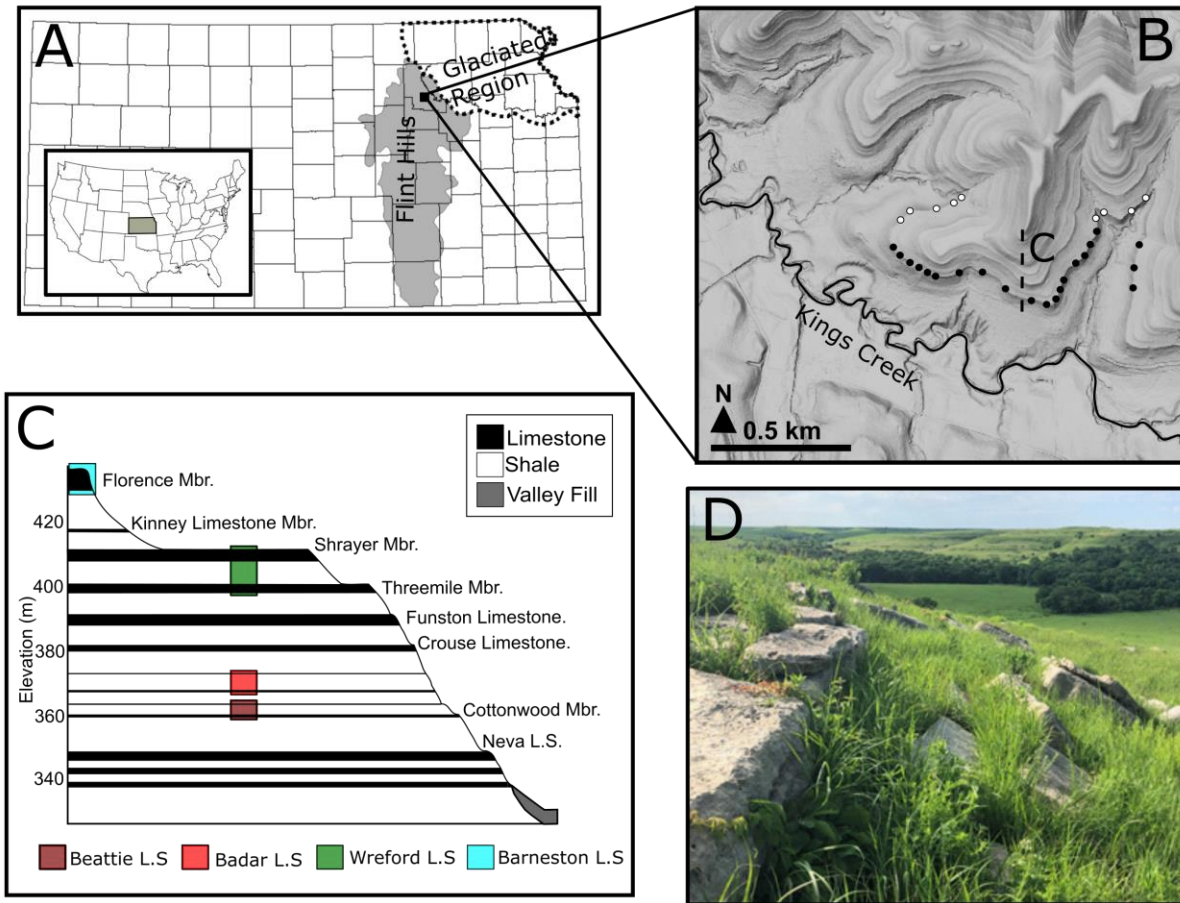


Figure 2. 2 Study location map and landscape stratigraphy

(a) Physiographic provinces of Kansas, the Flint Hills and the Glaciated Region. The location of Konza Prairie is denoted with rectangle. (b) Hillshade map of a small study portion of Konza Prairie demonstrating the characteristic staircase hillslope morphology of the Flint Hills region. Slope block survey locations are denoted with circles. White points represent transects in forest setting; black points represent transects in grassland setting. The major stream in Konza Prairie, Kings Creek, is traced with a solid black line. The dashed line represents typical stair-step hillslope represented in panel (c) which depicts lithologic controls on landscape morphology. (c) Stratigraphic cross-section of the region demonstrating the lithologic control particular limestone units have on landscape morphology. Major bench or cliff forming limestone units are named. Colored regions represent major limestone lithologic units that have been split up into limestone member sub-units. The abbreviation “L.S.” represent “limestone,” and “Mbr” represents “member.” Adapted from Smith (1991) and not to scale. (d) Example of small limestone cliffs formed from Badar Limestone and large rock blocks on slopes common in Konza Prairie, KS. Limestone cliff in left-hand portion of photo is approximately 0.25 m in height and rock is pre-fractured into $\sim 1 \times 1 \times 0.25$ m blocks. Large rock blocks are in center and right-hand portion of photo. Large rock blocks are found up to approximately 10 m downslope.

along the landscape. The benches and cliffs thus primarily run parallel with stream valleys cut by first-order ephemeral streams. Locations where streams cross limestone benches are marked by increases in tree cover and the development of amphitheater hillslope morphology centered on

the stream. The cliff-forming limestones are well-fractured into regular units at approximately one-m intervals that eventually form the boulders and blocks that are deposited on the shale slopes below the cliffs (Frye, 1955) (Figure 2.2d). The blocks vary between cubic and tile-shaped and are assumed to move via tumbling and soil rafting respectively, as hypothesized above.

I studied a prominent limestone bench formed from the Cottonwood Limestone Member of the Beatie Limestone (Aber & Grisafe, 1982; Imbrie et al., 1964) (Figures 2.2b and 2.2c). The studied section of cliff mainly faces south and east, with some sections facing north. This limestone unit was primarily chosen due to its prominence in the landscape, with clear vertical separation from the next-higher bench-forming Morrell Limestone. The vertical separation caused the formation of an approximately 50 m long slope, with few to no observable blocks in its lowest 10 m in most locations, which should prevent contamination from Morrell-limestone blocks (boulders) in the studied part of the hillslope under the Cottonwood Limestone member.

The study cliff formed by the Cottonwood Limestone and the hillslope under it are covered by mostly grassland and some forest. Forested sections are occupied by a combination of trees and dense woody underbrush that grow on top of and in the fractures of the cliff face and around the blocks on the hillslope under it. These forests take the form of gallery forests that parallel streams of the region (Knight et al., 1994). Four species of tree, the American Elm (*Ulmus americana*); the Honey Locust (*Gleditsia triacanthos*); the Hackberry (*Celtis occidentalis*); and the Eastern red cedar (*Juniperus virginiana*); account for approximately 90% of the trees in the area (Briggs et al., 2002). Grassland portions are dominated by tall grasses with infrequent large woody plants occupying some cliff face positions. Dominant grass species

are big bluestem (*Andropogon gerardii*); Indian grass (*Sorghastrum nutans*); little bluestem (*Schizachyrium scoparius*); and switch grass (*Panicum virgatum*) (Briggs et al., 2002).

2.5 Methods

Properties of the Cottonwood Limestone cliff and blocks (boulders) on the hillslopes under it were recorded every approximately 25 m for a 2 km distance along the cliff, excluding locations near trails. This spacing between measurements was implemented to capture spatial variations in cliff properties and in blocks on the underlying slope. Examples of properties of interest include cliff height, bedrock fracture spacing, surface weathering, and block size and shape. This survey scheme resulted in observations from 30 transect locations along the cliff (Figure 2.2b).

2.5.19 Cliff measurements

A set of four cliff measurements were collected for each location separated by 2 m to capture local variability (Figure 2.3, red circles). Surface weathering of the cliff surface was again visually estimated as the percentage of surface area affected by spalling, flaking, and pitting. Fracture spacing and orientation were recorded in two pairs to reflect the presence of two primary fracture directions and to calculate the size of future blocks before their release. Fracture orientation was measured as an azimuth and fracture spacing was measured as a distance separating one fracture to another (Figure 2.3). These measurements allowed me to quantify the expected initial dimensions of blocks deposited on hillslopes in this landscape.

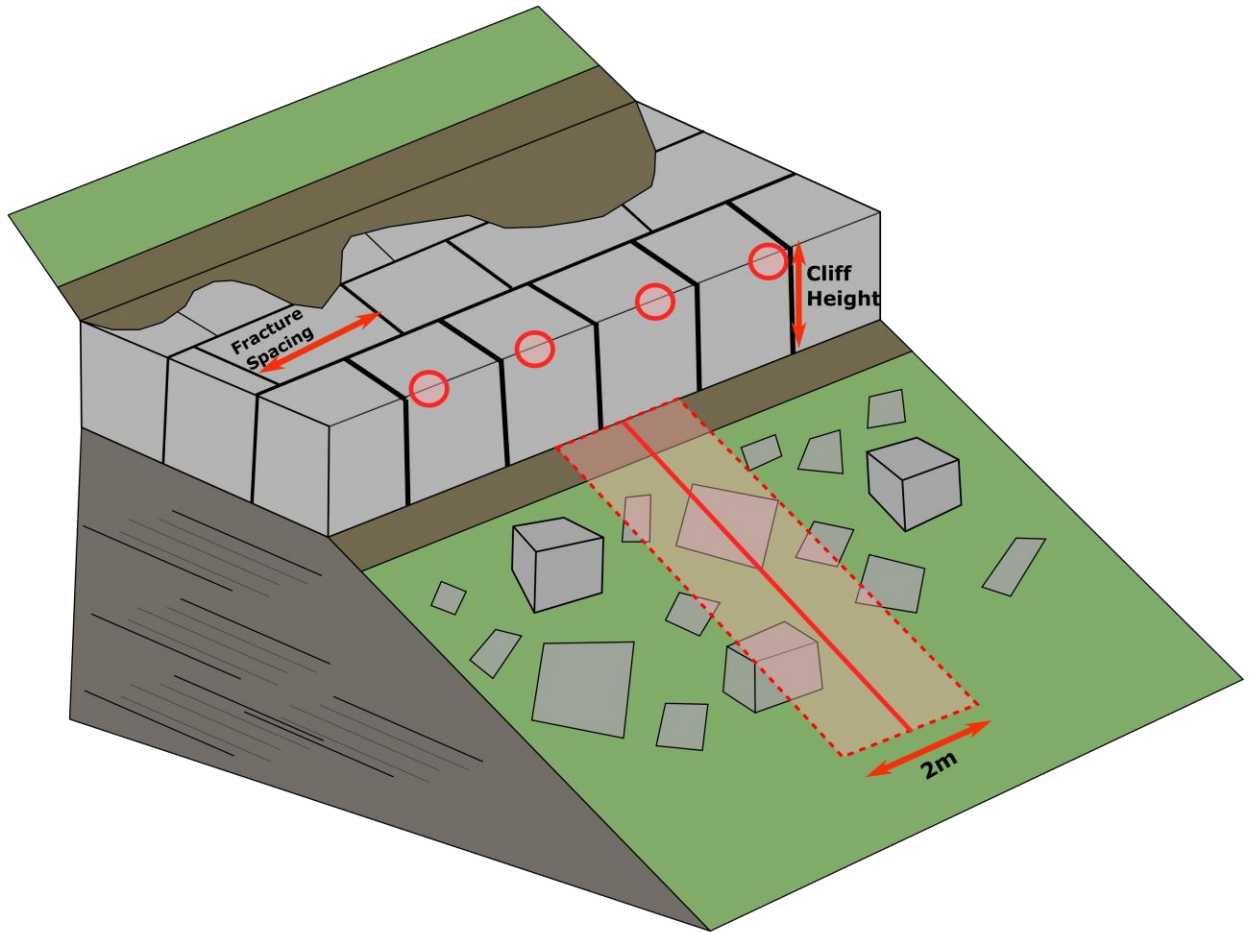


Figure 2. 3 Hillslope survey schematic

Schematic of slope block transect and cliff measurements. A slope transect is shown as a red line surrounded by the 2 m-wide transect area. Red circles on the cliff face represent where cliff property measurements were taken. Cliff property measurement locations are separated by approximately 2 m. All blocks touching or partially overlapping the transparent red transect survey block were measured.

2.5.20 Block measurements

Block (boulder) properties were measured for all blocks in a 30 m long, 2 m wide transect straight down the slope from the cliff face formed by the Cottonwood Limestone (Figure 2.3). Block properties such as size, weathering, and downslope dip were then aggregated over 3 m distance intervals during data analysis. Minimum block size observed was set at 64 mm (corresponding to a 0.004 m² surface area). This minimum represents the cutoff between pebble and cobble-sized rock fragments and represents the smallest grain size that can be easily

observed in the grassy study location. Distances between all blocks and the overlying cliff were measured along the transect line from the center of the slope block. Block size was recorded as two measurements: the length of the longest and intermediate axes of the block. Each axis was perpendicular to the other. Size was reported as an area calculated by multiplying these two measurements. While I did not measure the short axis of blocks, I categorized them by shape. Blocks that had a short axis $<0.5 * \text{intermediate axis}$ were recorded as “tile-shaped” and blocks that have a short axis $>0.5 * \text{intermediate}$ and long axis were recorded as “cubic” (Figures 2.1e and 2.1f). This distinction

was implemented as it best reflected my initial first order field observations and categorization of rock blocks into categories of “cubic” and “tile-shaped.” For ease of communication, I continue to use the terms “tile-shaped” and “cubic” when referring to the two shape classes of hillslope blocks in the results and discussion sections. Blocks were designated “undetermined” if this distinction could not be confidently made. This designation was made for 65 of 842 blocks measured.

Weathering state was assessed visually as the percentage of the visible block surface that was occupied by surface pitting or spalling. I recognize that this method may underestimate the surface affected by weathering if spalling has removed large thin flakes that make the new surface look un-weathered. This process of spalling may be a mechanism by which the surface of these blocks weather through time. Spalling may lead to a decreasing relationship between distance and weathering. However, I do not believe that the process of surface spalling is fast enough to significantly affect the surface of a block that is occupied by pitting. I was not able to observe many instances where large portions of a block surface were reset by spalling. Yet, I

acknowledge that my values for surface weathering percentage may be a minima controlled by the process of surface spalling.

Block dip in the downhill direction was measured in degrees using a digital inclinometer placed at the center of the block. Hillslope steepness was calculated at a 2 m resolution (derived from a 2 m lidar-derived DEM, Blackmore (2019)). The calculated hillslope steepness was then subtracted from the block dip to obtain a BRS. The azimuth of the surface of each block was calculated from the DEM using aspect of the hillslope at the block position. These observations were collected to quantify spatial relationships that reflect transport processes that could move large blocks downslope.

Additionally, qualitative observations of stability, burial, and embedding were recorded to deduce transport processes. Block stability was recorded as stable or unstable depending on if movement or rotation resulted from the force of a human foot pushing the block. Burial condition was based on how embedded a block was in soil. The perimeter of embedded blocks was probed with either a soil knife or rock hammer to estimate the depth at which the bottom of the block occurred and in extension how much of the block was buried below the soil surface. If at least 50% of the block's short axis was embedded, then a block was described as buried in soil. Blocks that were less than 50% embedded were recorded as unburied. For blocks that were buried, a secondary designation was given based on how the block was embedded. If a block was surrounded by soil, it was recorded as buried on all sides, whereas blocks only buried on the upslope or downslope faces were recorded as such.

2.6 Results

A total of 30 slope block survey transects were performed, resulting in a total of 842 block observations. Three hundred sixty blocks were cubic and 417 blocks were tile-shaped. A

large majority of blocks were in grassland transects (717), while 108 blocks were observed in forest transects. Seventeen blocks were observed in a transitional region between forest and grassland.

2.6.21 Size, shape, weathering

Before release from the cliff, the average block (boulder) size is $2.12 \pm 1.82 \text{ m}^2$. In grassland, pre-release blocks have an average size of $2.07 \pm 1.38 \text{ m}^2$, whereas in forest, pre-release blocks have an average area of $2.31 \pm 2.66 \text{ m}^2$. These differences between forest and grassland are small and not significant at the 0.05 level. On hillslopes under the cliff, the average size of blocks of both shape classes is $0.39 \pm 0.67 \text{ m}^2$. Tile-shaped blocks have an average size of $0.50 \pm 0.80 \text{ m}^2$, and cubic blocks have an average size of $0.32 \pm 0.56 \text{ m}^2$. This size difference between tile-shaped and cubic blocks is large and significant (t-test, $p < 0.001$). Blocks in forest ($0.38 \pm 1.11 \text{ m}^2$) are also overall larger than blocks in grassland ($0.32 \pm 0.50 \text{ m}^2$, t-test, $p < 0.001$), although this difference is less substantial. I report other statistics for block properties in Table 2.1.

Table 2. 1 Properties of large blocks separated by block shape as well as vegetation cover.

	All Blocks n = 842	Cubic Blocks n = 360	Tile-shaped Blocks n = 417	Grassland Blocks n = 717	Forest Blocks n = 108
Size (m²)					
Average ± SD	0.39 ± 0.67	0.32 ± 0.56	0.50 ± 0.80	0.32 ± 0.55	0.38 ± 1.11
Median	0.17	0.14	0.20	0.14	0.39
Minimum	0.01	0.01	0.01	0.01	0.02
Max	7.20	6.44	7.20	7.20	6.44
Block Relative Slope (Degrees)					
Average ± SD	9.00 ± 10.64	10.16 ± 12.60	8.36 ± 9.30	8.65 ± 10.53	9.69 ± 10.78
Median	6.00	6.52	5.89	5.48	6.86
Minimum	0.00	0.01	0.00	0.00	0.01
Max	82.36	82.36	71.87	82.36	65.01
Azimuth (Degrees)					
Average ± SD	203.36 ± 70.05	207.10 ± 67.30	203.30 ± 72.58	198.70 ± 59.69	250.60 ± 101.89
Median	215	209.50	215.00	215.00	306.00
Minimum	75	75.00	75.00	104.00	75.00
Max	355	355.00	355.00	352.00	355.00
Surface Weathering (% of surface occupied by pitting)					
Average ± SD	19.45 ± 15.54	23.00 ± 16.69	17.08 ± 14.60	17.82 ± 14.58	28.17 ± 17.84
Median	15.00	20.00	15.00	15.00	25.00
Minimum	0.00	0.00	0.00	0.00	1.00
Max	80.00	80	73.00	80.00	80.00

The average BRS for all blocks is $9.00 \pm 10.64^\circ$. This means that there is an average difference between the dip of a block and the steepness of the local hillslope of 9° . The average BRS of tile-shaped and cubic blocks are $8.36 \pm 9.3^\circ$ and $10.16 \pm 12.6^\circ$, respectively. This small difference between them is not significant (t-test $p = 0.08$). In grassland, blocks have an average BRS of $8.65 \pm 10.53^\circ$, whereas in forest, blocks have an average BRS of $9.69 \pm 10.78^\circ$. This difference between forest and grassland is also small and not statistically significant ($p = 0.351$). The average azimuth for hillslope blocks is $203.36 \pm 70.05^\circ$. Grassland blocks have an average azimuth of $198.70 \pm 59.69^\circ$, whereas forest blocks have an average azimuth of $250.60 \pm 101.89^\circ$ (t-test $p < 0.001$). The average azimuth of tile-shaped and cubic blocks is $207.10 \pm 67.30^\circ$ and

$203.30 \pm 72.58^\circ$, respectively. Differences on account of block shape are not significant at the 0.05 level.

Cliff face surfaces have an average estimated surface weathering of $30\% \pm 12\%$. The mean value for surface weathering of blocks on slopes under the cliff is substantially lower, at $19.5\% \pm 15\%$. This difference is statistically significant (t-test, $p < 0.001$). Tile-shaped blocks appeared less weathered ($17\% \pm 14\%$) than cubic blocks ($23\% \pm 16\%$, t-test $p < 0.001$). Large blocks ($>1 \text{ m}^2$) appear to be overall more weathered than smaller blocks ($<1 \text{ m}^2$) (Figure 1.4a).

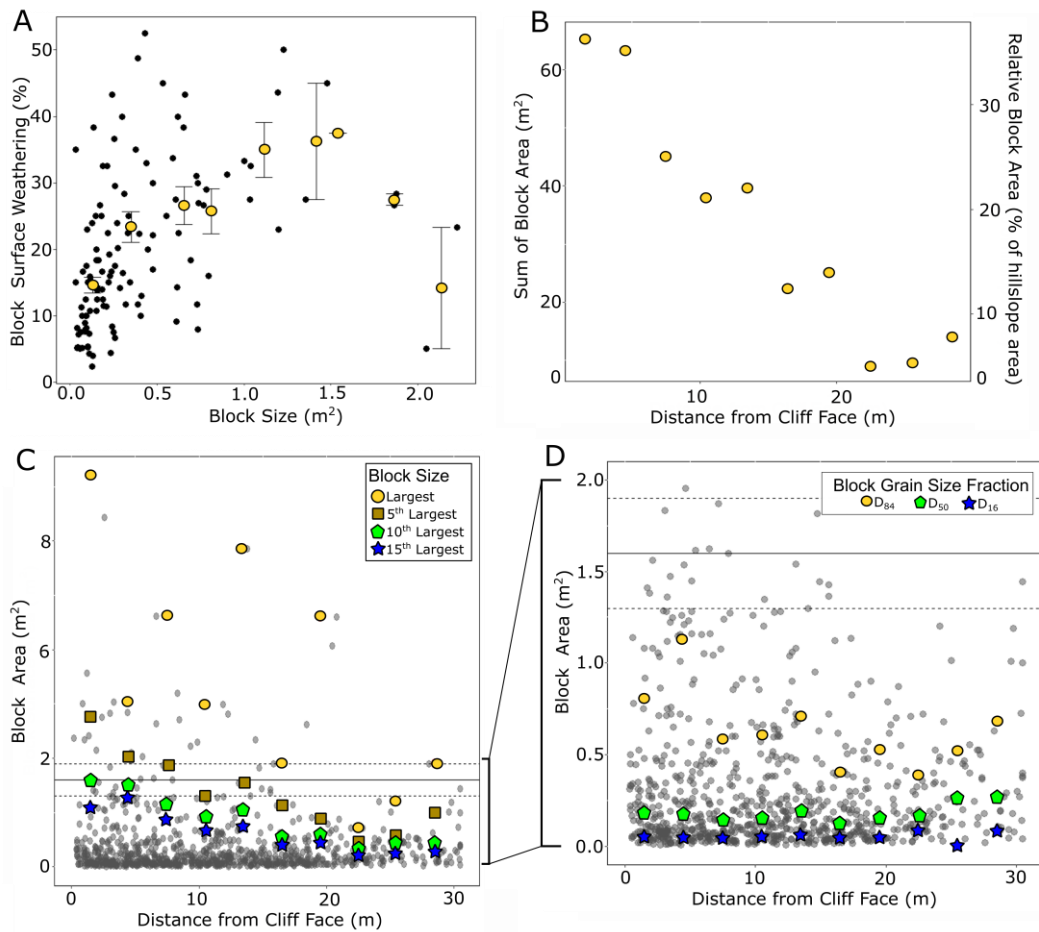


Figure 2. 4 Hillslope block (boulder) surface weathering and size data

(a) Surface weathering plotted as a function of block size. Yellow points are mean values of distance and weathering calculated at 0.25 m^2 interval. The standard error of surface weathering for each interval is shown with error bars. (b) Sum of block area of hillslope blocks for 3 m intervals. Secondary axis shows the block area as a portion of the hillslope area. (c). Block size as a function of distance for the cliff face. Grey points are individual measured

hillslope blocks. Colored points are the largest blocks in intervals of 3 m to capture trends in surface area on account of block size. The black horizontal line is the median surface area of fractured limestone unit calculated from fracture spacing. Black dashed lines are confidence intervals of the median. (d) Subset of data presented from panel (c), showing block sizes from 0 to 2.0 m². Colored points are specific grain size fractions in intervals of 3 m to capture trends in surface area on account of block size. The black horizontal line is the median surface area of fractured limestone unit calculated from fracture spacing. Black dashed lines are confidence intervals of the median.

2.6.22 Changes downslope

There is a strong and significant decrease in block size with distance from cliff ($b = -0.0002 \text{ m}^2/\text{m}$, $p = 0.019$, Figure 2.4c). There is also a strong and significant linear decrease in total block area when aggregating over 3 m downslope intervals ($b = -0.41 \text{ m}^2/\text{m}$, $p < 0.001$) (Figure 2.4b). Most blocks, 60%, are found within the first 12 m below the cliff face. There appears to be a visual decrease in the maximum block size with increasing distance from the cliff (Figure 2.4c). When the largest sized blocks for 3-m distance intervals are examined, there is a substantial and significant decrease (Figure 2.4c) in maximum size and distance ($b = -1.60 \text{ m}^2/\text{m}$, $p = 0.02$). This seemingly linear decrease is also present for the 5th ($p < 0.001$), 10th ($p < 0.001$), and 15th ($p < 0.001$) largest rock blocks ($b = -0.71, -0.47, -0.37 \text{ m}^2/\text{m}$, respectively). When specific grain size fractions are calculated over 3 m distance intervals (Figure 1.4d) there is no significant linear trend for the D16, D50, or D84 ($b = 3 \times 10^{-4}, 0.003, -0.014 \text{ m}^2/\text{m}$ respectively) with distance from the cliff ($p = 0.78, 0.10, \text{ and } 0.08$ respectively). The average values of these grain size fractions are $0.05 \pm 0.02 \text{ m}^2$, $0.18 \pm 0.05 \text{ m}^2$, $0.63 \pm 0.22 \text{ m}^2$, respectively. Only the largest grain size fraction, D95 ($1.3 \pm 0.5 \text{ m}^2$), has a substantial and significant decreasing size with increasing distance from cliff ($b = -0.46 \text{ m}^2/\text{m}$, $p = 0.007$). There is no significant difference between cubic and tile-shaped blocks in terms of decrease in size with distance, and therefore, tile-shaped blocks remain larger than cubic blocks. There is no significant difference between forest and grassland blocks in terms of decrease in size with distance, either.

When lumped into 3 m intervals, no overall trend can be observed between surface weathering and distance from the cliff face for either tile-shaped or cubic blocks (Figure 2.5a). However, there appears to be a moderate increasing trend for a subset of blocks at distances 9–27 m from the cliff face. In this interval, it can be observed both cubic and tile-shaped blocks overall increase surface weathering with increasing downslope position. For all distance intervals, the mean surface weathering percentage of both tile-shaped and cubic blocks are substantially below the mean surface weathering of the modern cliff face. In fact, the mean surface weathering percentage for tile-shaped blocks for distance intervals 0–12 m is significantly below the standard deviation of cliff face surface weathering values. Mean weathering below the standard deviation of cliff face weathering also occurs for distance intervals 15–18 m, and 21–24 m for tile shaped blocks.

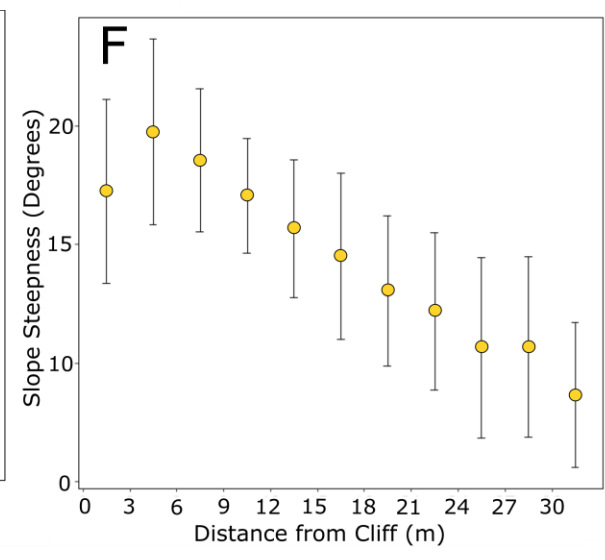
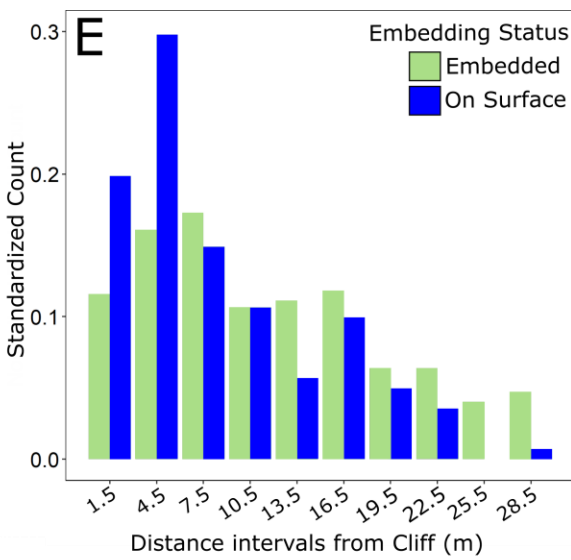
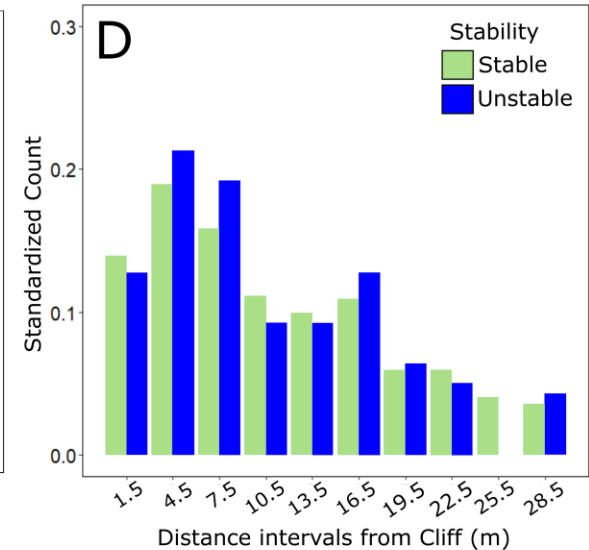
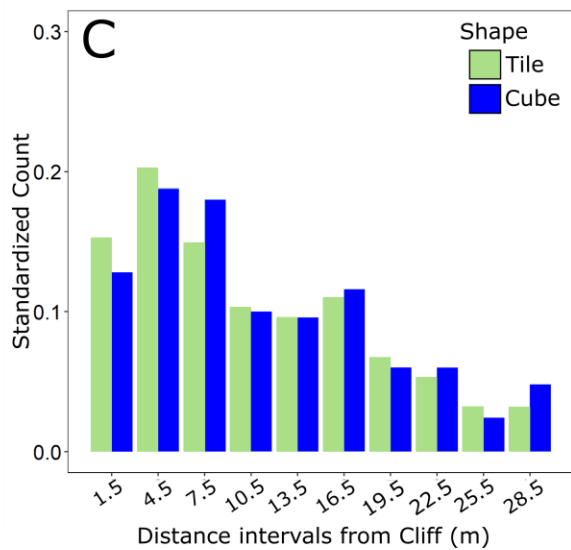
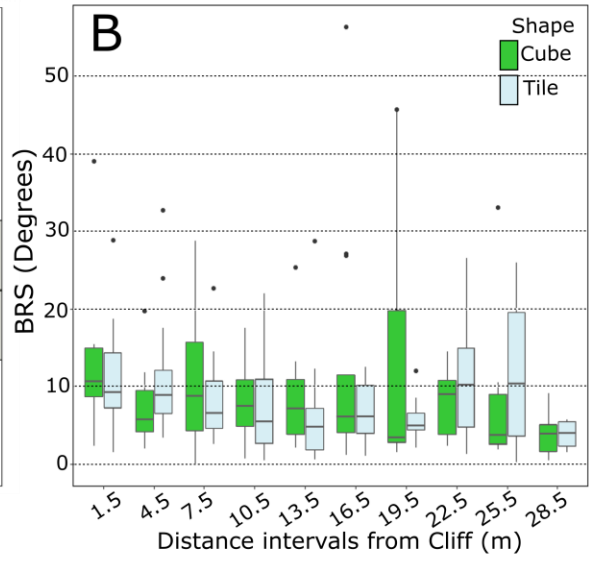
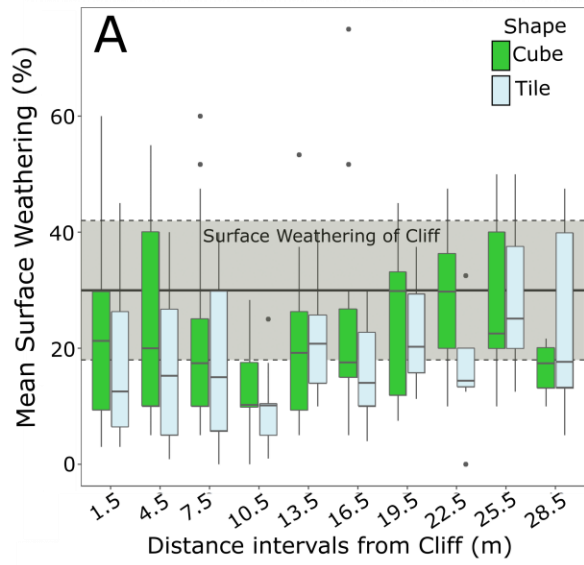


Figure 2. 5 Block (boulder) property with distance from bedrock bench

(a) Box plot of average surface weathering of hillslope blocks for 30 slope transects in 3 m intervals. Solid black horizontal line is the average surface weathering of cliff face surfaces via pitting. The dashed black line is the standard deviation of average surface pitting of cliff faces. Each bin of the histograms represents a 3 m interval downslope from the cliff face. To better compare cubic and tile-shape block spatial patterns on hillslopes, the number of individual blocks in each bin has been standardized. Standardization was done by dividing number of points in the bin by the total number of tile-shaped or cubic blocks respectively. (b) Box plot of difference between hillslope blocks and hillslope slope for 30 slope transects for 3 m intervals. Horizontal dashed lines mark 10° increments of Block Relative Slope. (c) Histogram showing distribution of cubic and tile-shaped blocks on slopes. (d) Histogram showing the distribution of stability of blocks on slope. (e) Histogram showing burial status of blocks on slopes. Significant peak of unburied, surface blocks in distance interval 3–6 m. (f) Average hillslope slope profile was calculated from slope values extracted every 3 m along transect survey lines. Average slope value for each distance interval along transects lines is plotted with its standard deviation. The pattern of the data reflects the concave-up hillslope morphology common to hillslopes below this limestone layer.

All BRS values are greater than zero for both cubic and tile-shaped blocks, reflecting that all blocks are inclined more than the local hillslope. BRS appears to decrease moderately for both cubic and tile-shaped blocks with downslope distance from the cliff face (Figure 2.5b). Blocks in the first 3 m downslope from the cliff face have an average BRS of 11° , whereas those furthest from the cliff have an average BRS of 3° . This difference is significant (t-test, $p < 0.001$). This signal is present for both tile-shaped and cubic blocks: tile-shaped blocks in the first 3 m of the cliff face have a BRS of 11.1° compared to those furthest from the cliff with a value of 3.8° (t-test, $p < 0.001$) and cubic blocks in the first 3 m of the cliff face have a BRS of 12.5° compared to those furthest from the cliff with a value of 3.9° (t-test, $p = 0.001$). There is no substantial or significant relationship between azimuth and BRS or between azimuth and surface weathering for the entire data set or for tiles and cubes separately. Shape is not related to block position on hillslopes: there is no significant difference between cubic and tile-shaped blocks in relation to position (two-sample Kolmogorov-Smirnov test, $p = 0.91$, Figure 2.5c). Unstable and stable blocks also appear to be in about the same position on slopes, with slightly more unstable than stable blocks in the 3–9 m range ($p = 0.65$, Figure 2.5d). There is no overall significant difference in distribution of blocks that are embedded in the soil or sitting on the

surface (Kolmogorov-Smirnov test, $p = 0.41$), there are substantial differences between embedded and on surface blocks in cliff proximal positions (0–6 m from the cliff face (Figure 2.5e).

2.6.23 Interaction with soil

Most blocks (543, or 64%) were embedded in the hillslope soil to some degree. Three hundred eleven blocks were surrounded by soil, 202 had soil only behind the upslope face, and 30 had soil covering only the downslope face. I used a χ^2 test to determine whether block shape and the type of embedding are related for all blocks, for grassland blocks, and for forest blocks (Figure 2.6). The null hypothesis for this test is that shape and embedding status are independent. This hypothesis was rejected ($p < 0.001$): there is a relationship between block shape and how the block is embedded in hillslope soil. Cubic blocks have more individuals embedded in soil only on the upslope side. Tile-shaped blocks are more often embedded in the soil on all sides. The strength of the association between embedding type and block shape, expressed as Cramer's V , is 0.33, indicating moderate associations for the entire data set (Figure 6). For blocks in forest locations, Cramer's V is 0.25 (low association strength), while in grassland locations, Cramer's V is 0.34 (moderate association strength).

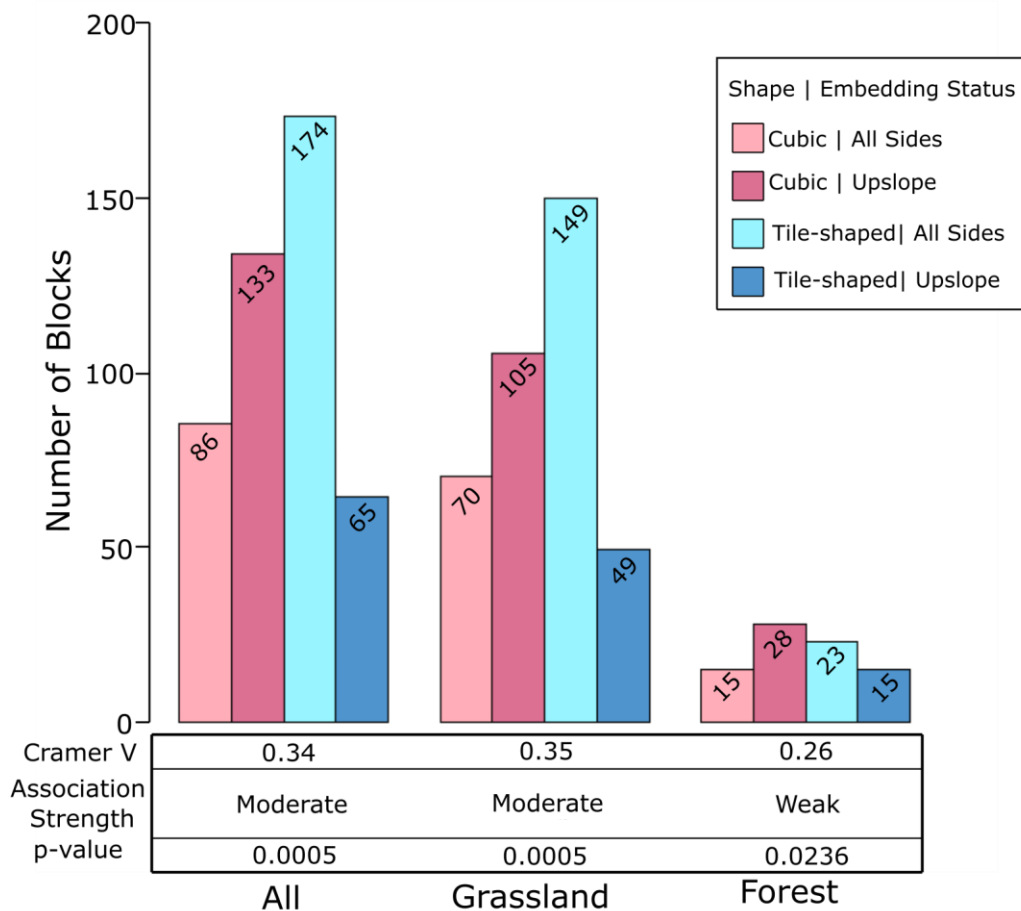


Figure 2. 6 Block (boulder) geometry association analysis

Association analysis results between embedding status and block shape. Results are reported for all blocks measured and then separated out by vegetation cover type. The Cramer V test produces an output between 0 and 1, where 0 is no association, and any value that is above 0.5 is considered a strong association. Associations between 0.3 and 0.5 are moderate strength. Associations below 0.3 are weak associations. This histogram visualizes data used in each combination of block shape and embedding status classes.

2.7 Discussion

2.7.24 Block size and surface weathering

Results clearly show that blocks are decreasing in size through time via weathering processes as they move downslope. There is also a significant decrease in total block size with distance from the cliff face, leading me to accept my first main hypothesis. We can further

observe that the size of the largest individual blocks (D_{95} , and the largest, 5th, 10th, and 15th largest blocks) decreases with distance from the cliff. For semi-arid and arid landscapes, Glade et al. (2017) and McGrath et al. (2013) observed a logarithmic decrease in size with distance for the largest particles on the hillslopes. For this landscape, I do not find this to be true. Instead, the largest size fractions decrease in size linearly (Appendix A – Table A.1). I propose these trends reflect the fundamental nature of chemical and physical weathering of limestone blocks in this landscape. As a limestone fragment breaks apart and dissolves, the surface area continues to increase relative to the total block volume. This increase in the ratio between surface area and volume through time corresponds with an increase in weathering which would manifest as a continual decrease in block size. If this is the case, we would expect to see a continual decrease in size along the hillslope toposequence, which we observe here in the data.

This location also shares Glade et al. (2017) observation that the smallest particle fraction (D_{16}) remains constant across slope positions. This relationship holds true for a significant portion of my observed clast sizes. However, where Glade et al. (2017) interpreted the constancy of the smallest grain size fraction (D_{16}) as evidence of the constant provision of weathered fragments of larger blocks, I suggest that in this case the stable D_{16} of blocks more strongly reflects the minimum observable rock size more than a physical process. In my study, I did not observe rock fragments smaller than a cobble due to visibility problems in the dense grassy vegetation. This measurement scheme results in an artificial minimum block size that is related to methodology rather than a physical minimum. As a result, I proceed cautiously when making interpretations concerning the smallest grain sizes in my data set. However, the overall implication of block size changes along the topo-sequence remains, weathering reduces block size.

At the same time, I do not observe a significant increase in signs of surface weathering with increasing distance from the cliff, leading me to reject my second main hypothesis. My initial assumption that limestone blocks weather primarily via flaking and dissolution of small fragments from the surface would have led to increasing signs of surface weathering on the blocks as they move downslope and become smaller. In keeping with that hypothesis, it also seemed reasonable to expect that blocks would inherit the surface weathering that accumulated when they were part of the cliff face. If that would have been the case, we would expect average block surface weathering near the average cliff surface weathering in cliff proximal positions (Figure 2.5a). One would also expect that in cliff distal positions the block surface weathering would be greater than the average cliff surface weathering. In contrast to both of those expectations, we see that in cliff proximal positions block surfaces are less weathered than cliff faces. Only at more distal hillslope positions does block weathering begin to increase again and becomes closer to the average cliff weathering. To explain why we do find smaller blocks but not more signs of weathering, I propose that fragmentation into discrete fragments drives a reduction in total block size, produces complex size-distance patterns, and creates new unweathered block surfaces along fracture planes.

Fragmentation is the process by which large clast break up into discrete smaller fractional portions of the original (Wells et al., 2008). This process has most recently been described by Román-Sánchez et al. (2019) who present two broad conceptual fragmentation pathways. In the first broad pathway, particles break into discrete halves, thirds, quarters, and so on. In the second broad pathway, larger particles break off significantly smaller particles and decrease slightly in size themselves. I initially expected the latter in Konza (through spalling), but my observations point to some combination of the two, favoring the former model. As the largest blocks weather

via fragmentation and are transported downslope, they decrease in size (Figures 2.4c and 2.7), losing portions of themselves as small fragments or larger discrete daughter blocks. The presence of both types of fragmentation also results in the complex size-distance patterns observed on these hillslopes (Figures 2.4c and 2.4d). Yet, when sum together the size of individual rock fragments and large blocks in the downslope direction (Figure 2.4b) we see a strong linearly decreasing relationship in total block size. This trend would reflect that while the largest block present may decrease with distance from the cliff face, a decreasing proportion of the original large block is preserved on the hillslope. Some of the original material of these large blocks is permanently lost through dissolution or fragmentation to a grain size that cannot be differentiated from the mobile regolith (Figure 2.4b). This clear relationship is a significant result, as it reflects fundamental landscape relationship between the rate at which large blocks break apart and the rate at which these discrete fragments are transported downslope.

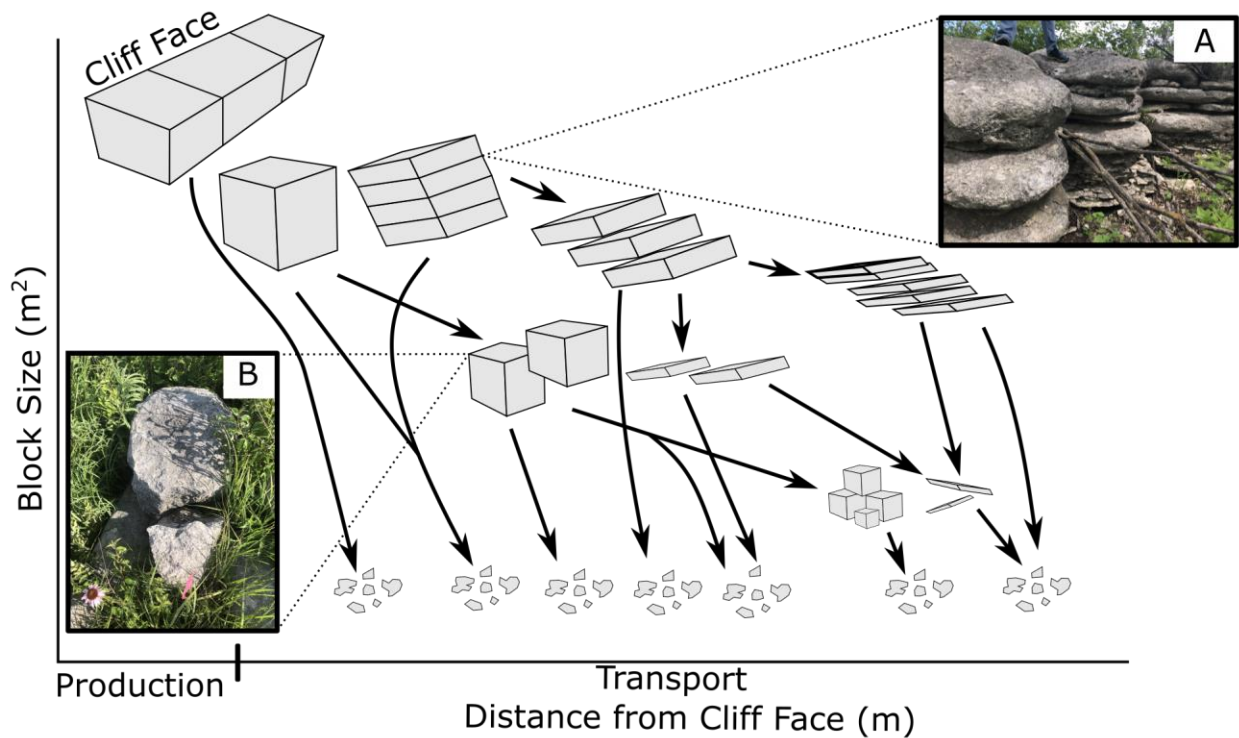


Figure 2. 7 Conceptual model of block fragmentation

Generalized conceptual pathways of block (boulder) fragmentation. Tile-shaped blocks will maintain or slowly decrease in area whereas cubic blocks will decrease in area as they break apart along a vertical face. Irregular rock fragments along the bottom represent the smallest rock fragment sizes observed. These smallest fragments can have tile or cubic shapes. Fragmentation is always occurring, resulting in small fragments at all distance intervals from the hillslope. (a) Photograph of limestone block breaking along pre-existing horizontal planes. These are blocks that are still part of, or just disconnected from the cliff face. (b) Photograph of limestone block breaking along vertical irregular weakness of crack. Block in photograph is approximately 3–6 m from the modern cliff face.

One can also observe that most blocks, even in positions very close to the cliff face, are substantially smaller and less weathered than the average and median of limestone fracture spacing. This suggests that substantial fragmentation occurs immediately upon release of limestone blocks onto the hillslope, creating fresh non-weathered surfaces on daughter blocks. This is supported by visual field observations of blocks that have broken apart and are resting directly on the hillslope surface (Figures 2.2d and 2.5e) in response to slumping, falling, or tumbling from their cliff face positions. If blocks do indeed have a high likelihood of instant break-up, it would help explain why there is not a significant decrease in block size with distance

from the cliff for most size fractions of blocks—the largest decrease has already occurred before the block has moved away from the cliff face. Fragmentation into few large fragments can explain both the absent increase in surface weathering with increasing distance from the cliff (Figure 2.7) and the fact that blocks are overall less weathered than the average cliff face by providing a process that creates new, unweathered block surfaces. This process can also explain the roughly positive relationship between surface weathering and block size (Figure 2.4a)—larger blocks have had more time to accumulate signs of surface weathering, whereas smaller blocks are mostly fragmentation products with newly exposed surfaces.

Finally, fragmentation into few, relatively large new blocks can explain the observation that tile-shaped blocks have larger average areas than cubic blocks. I propose that the limestone that forms the slope blocks can break apart in two styles. On one hand, large blocks can break apart into a series of large regular tile-shaped blocks along horizontal weaknesses, resulting from original sedimentary layering (Figure 2.7a). This mode of break-up would preserve the large surface formed by the largest and intermediate axes of the parent block and create equally large un-weathered surfaces, thus depressing the observed surface weathering of tile-shaped blocks. On the other hand, blocks can break apart into more cubic halves, quarters, thirds, and so on, breaking along cracks that may have formed after the block separated from the cliff face (Figure 2.7b). This style of fragmentation would create new cubic blocks with a smaller surface area than the parent block, but fewer new un-weathered surfaces.

As a result of the findings discussed above, I propose fragmentation of large blocks into a small number of smaller blocks provides a simple explanation for the complex observed relationships between block size and distance (Figures 2.4c and 2.4d). It also provides a simple explanation for the absent relationship between block weathering and distance (Figure 2.4a).

Finally, the difference in style of block break-up discussed above explains why we observe tile-shaped blocks that are less weathered yet larger than cubic blocks (Figure 2.7).

2.7.25 Transport and block shape

I hypothesized based on previous work by Schumm (1967), Glade et al. (2017), Glade and Anderson (2018), and Caviezel et al. (2021) that different block shapes result in different transport mechanisms. This difference would be caused by block geometry controlling the block center of gravity as well as the volume of soil that can collect behind it. We do indeed observe a similar process of upslope soil collection and downslope soil depletion with cubic blocks (Figure 2.6), as proposed by Glade et al. (2017). On the other hand, soil builds up equally along all sides of tile-shaped blocks. This shows that block shape plays an important role in how soil is stored on and routed down hillslopes. Thus, we accept my third hypothesis—there is indeed a significant correlation between the shape of a block and the distribution of hillslope material around a block. However, my observations subsequently do not support a different transport process for different shapes.

If cubic blocks would have transported via slow tumbling or rotation, we should have observed overall greater values of BRS. For a cubic block undergoing rotational movement, we would expect surfaces to occupy inclinations ranging from parallel to the slope to nearly standing on edge. Cubic blocks would occupy these high inclinations before tumbling or rotating would happen when a block's center of gravity moves beyond its lower edge. This would result in BRS values that would range from 0° to 25° , assuming a hillslope of 20° . However, this was not observed; both tile-shaped and cubic blocks have similar, low BRS values between 5° and 15° , while hillslope steepness ranges from 20° to 10° (Figures 2.5b and 2.5f). Thus, I reject my fourth hypothesis. Instead, I propose that both cubic and tile-shaped blocks are mainly transported by

soil creep, as first proposed by Schumm (1967) for substantially smaller tile-shaped clasts in arid settings.

Nonetheless, blocks on occasion do tumble downslope. This tumbling occurs in locations near cliffs where slope steepness is highest (around 20° , Figure 2.5f). In the field near cliffs, I observe meter and sub-meter scale blocks that are unstable and not embedded in the hillslope in these locations (Figures 2.5d and 2.5e). The number of not-embedded blocks reaches its peak in the first 12 m of slopes and so may indicate more recent or frequent movement in this zone (Figure 2.5e). We also observe that BRS in this region (Figure 2.5b), specifically in the first 9 m, is at its highest, which suggests an increased likelihood of unstable spatial configurations for a small number of blocks on steeper hillslopes. Recent movement is consistent with the low percentage of surfaces presenting evidence of weathering so close to the cliff (Figure 2.5a). My interpretation is that in this cliff-proximal zone, slopes are steeper, and the likelihood of especially newly- or recently released blocks rotating or tumbling is higher, leading to more fragmentation via breakage, exposure of fresh surfaces, and blocks sitting directly on the hillslope surface rather than being embedded in the soil. Furthermore, I propose that the small amount of rotation seen for all blocks (Figure 2.5b) is most likely related to downslope soil mining and upslope soil storage as proposed by Glade et al. (2017). While in the field I see evidence of rotation related to this process, we do not see evidence of the ultimate effect of downslope movement. This may be due to this landscape not being steep enough to allow for sporadic movement, but rather slight surface rotation while creep processes move the blocks downslope like a conveyor belt.

Further work focusing on whether and how large blocks break apart because of tumbling should be done to confirm or refute these suggestions as well as the mechanism that produces the

small amounts of rotation for all blocks. This future work would also need to consider lithologic characteristics that allow for easier break up of some blocks over others. Carbonate rocks in this region as covered above have relatively regular fractures and joints that generally control the dimensions of the block that is first deposited on the hillslope. I also observe in the field that there is lateral variation in thickness of bedding in the Cottonwood limestone (Aber & Grisafe, 1982). These bedding planes act as a primary weakness that the rock may break along once the block detaches from the cliff face (Dredge, 1992; Ruedrich et al., 2011). We may expect a higher proportion of tile-shaped blocks below cliff locations with thinner beds and thus more bedding planes along which failures can occur. Another lithologic characteristic of interest may be the level of dolomitization of the rock. Carbonate rocks in the region have undergone levels of conversion from limestone to dolostone that can vary laterally (Imbrie et al., 1964). Dolomite has a higher tensile strength (5–25 mPa) than calcite (1–15 mPa) and is less reactive to chemical weathering (Baykasoglu et al., 2008; Drever, 1982; Paronuzzi & Serafini, 2009; Szramek et al., 2011). In places where the cliff face is composed of more dolomite, we would expect slope blocks to be larger compared to blocks sourced from purely limestone cliffs. This difference would arise due to dolomite's comparatively greater “toughness” to both physical and chemical weathering.

2.7.26 Effects of vegetation cover

While not one of the initial goals of this research, I found that there is a significant size difference between blocks under forest cover and blocks under grassland (Appendix A – Table A.1 and Figure A.1). Blocks in forest cover are slightly larger (0.38 ± 1.11) than grassland blocks (0.32 ± 0.55), and the difference is statistically significant (t-test, $p < 0.001$). The difference cannot be attributed to a difference in pre-release fractured bedrock between grassland

($2.07 \pm 1.38 \text{ m}^2$) and forest sections ($2.31 \pm 2.66 \text{ m}^2$) of the limestone cliff—there is no significant difference between the two (t-test, $p = 0.63$). Furthermore, while there is a significant difference in hillslope gradients between forest and grassland (t-test, $p = 0.005$), it is not substantial with average hillslope gradients being $17.6 \pm 7.1^\circ$ and $16.5 \pm 9.7^\circ$, respectively. Therefore, I tentatively reject differences in hillslope gradient as a possible reason for differences in block size between the two vegetation cover types. Interestingly, we can also observe a difference in block surface weathering between the two vegetation cover types (Table 2.1). The surface weathering of blocks is higher in the forest ($28.17\% \pm 17.84\%$) than in the grassland areas ($17.84\% \pm 14.58\%$, t-test, $p < 0.001$). This difference in surface weathering suggests the observed differences in size may be the result of differential rates of weathering between the land cover types. I explore below three other possible reasons for the block size difference.

First, block size difference could result from differences in long term fire-related processes between forest and grassland. Grasslands have about three times more intense and energetic fires than forests (Gomes et al., 2020). These differences in fire intensities can lead to stronger physical weathering (through fragmentation and spalling) and thus to smaller blocks in grasslands. This explanation requires that the forest-grassland transition has been spatially largely constant over block-weathering timescales, which I assume to be at least centuries. Indeed, prairie grasses have dominated this portion of the Great Plains region since at least 30,000 yr B.P. (Axelrod, 1985; Johnson et al., 2007; McLauchlan et al., 2013). Over this period, the spatial extent of forests has been primarily contained to areas near stream and river channels (Axelrod, 1985; Knight et al., 1994). Over shorter timescales, the gallery forests expand and contract based on factors such as water availability or grazing patterns, but never reach into higher hillslopes (Knight et al., 1994). Along with the relative spatial stability of the grassland-

forest boundary, wildfires have had a significant presence in these grassland landscapes over both human and geomorphic time scales (Gorynski & Mandel, 2009). Fire has been shown to weaken rocks and increase post-fire susceptibility to weathering (Goudie et al., 1992). Micro-cracks can form through individual grains within a rock in response to fire heating, creating new internal weaknesses (Dorn, 2003), which can then lead to macro-scale fractures, breaks, and exfoliation (Dorn, 2003; Goudie et al., 1992; Shtober-Zisu & Wittenberg, 2021). In the context of this landscape, increased fire related weathering in grassland vegetation cover could therefore result in faster rates of fragmentation and increased amounts of fresh surfaces being exposed compared to forest settings. This difference in fire intensity between grasslands and forest could be one explanation for differences in surface weathering as well as block size between the vegetation cover types.

Second, the block-size difference may be the result of landcover-associated microclimatic variations (Eppes & Keanini, 2017; McFadden et al., 2005). Globally, except for the boreal regions, forests dampen the diurnal temperature range that is experienced in a location (Duveiller et al., 2018; Lee et al., 2011). Trees in forested locations shade blocks from direct sunlight, reducing thermal expansion and contraction cycles and thus limiting physical weathering. Due to differential amounts of thermal expansion due to microclimatic controls, the rate of spalling and fragmentation would be lower in forest settings (Eppes & Keanini, 2017). This lower rate of forest fragmentation would result in slower block breakup, larger blocks, and less fresh surface being exposed compared to the grassland locations.

Third, the observed difference may be the result of leaf litter cover in forested areas covering and obscuring smaller blocks that would be exposed and therefore observed in the

grassland setting. However, it is difficult to validate this hypothesis without removing the leaf litter and vegetation.

Further research focusing on the role of microclimate, vegetation shielding, and fire frequency in relation to block weathering in grasslands will be needed to test these propositions. Of the three proposed explanations, I believe that wildfire differences may be the best supported by previous research and be the easiest to investigate. Monitoring the post fire evolution of cracks and fractures that may develop in a block (i.e., Goudie et al., 1992) may be the simplest way to measure resulting differences between forest and grassland fires. However, that still does not give us an insight into crack formation during the fire event itself. Therefore, it may be advantageous to monitor crack propagation during a fire event. For example, the installation of geophones on select large hillslope blocks (boulders) may allow us to “hear” the cracking as it takes place. Doing this in both forest and grassland settings may allow us to establish differences in fracture propagation intensity for the two different wildfire types. The Konza Prairie research station would be an optimal location to perform this future work due to regular prescribed burns of both forested and grassland locations as well as the bed rock geology that allow the targeting of large blocks of the same lithology for this monitoring.

2.7.27 Block transport mechanisms

Topography, specifically slope steepness, must be a first order control over block transport. Transport of blocks and clasts over hillslopes in very steep mountain settings is primarily driven by the pull of gravity (Caviezel et al., 2021; DiBiase et al., 2017). Yet, in landscapes where hillslope gradients are lower, such momentum-based transport will be rare. However, even on less steep slopes, it stands to reason that block transport via soil interaction

and block rotation increases with slope steepness, and that transport through rotation becomes harder on flatter slopes. In my study location, the slopes below limestone cliff are on average 15°, and I find little evidence of rotational-based transport. We could expect that undercutting and rotation-based transport may be observable or even dominant in steeper settings. Steeper slopes increase the potential for rotation-based movement and transport. Furthermore, based on my findings, shape does not have a particularly strong control over the type of mechanism moving blocks downslope in the Flint Hills as opposed to steep landscapes (i.e., Caviezel et al., 2021). Regardless of block geometry, transport occurs mainly along with the mobile regolith via creep.

In addition, I postulate that seasonal temperature and moisture fluctuations are important in determining whether creep processes can move blocks downslope. Grab et al. (2008) showed that in alpine regions, frost jacking and gelifluction can be a primary movement driver of large meter-scale blocks on soil-mantled hillslopes. This type of strongly frost-driven transport occurs irrespective of clay content of the soil (Grab et al., 2008). In less extreme climatic conditions, we could expect that frequent formation and melting of frost in the near surface may be able to repeatedly lift and lower blocks, resulting in movement in the downslope direction in a similar manner as creep. Locations where winters are wet and frequent temperature fluctuations from above to below freezing occur would maximize this type of process's contribution to transport. The climate of my study location may not be ideal for maximizing the cycles of lifting and lowering blocks due to its temperate mid-continental climate characterized by cold, dry winters and warm, wet summers. Most of the precipitation (75%) falls during the agricultural growing season, May through September (Hayden, 1998). However, autumn and spring diurnal temperature swings from above to below freezing coupled with precipitation or

substantial soil moisture may result in some amount of lifting and lowering over the course of a year due to near surface frost formation. A fair test of the role of climate in frost-jacking transport of large blocks would be possible by finding a climatic gradient along which other conditions remain approximately equal. An example would be examining hillslope blocks below a cliff forming unit that runs along climatic gradient where frost formation frequency decreases. Reduction in frost formation would result in decreased creep efficiency, resulting in more transport being accomplished by slope steepening and tumbling rather than creep. We could perhaps also expect that the frequency of blocks would be lower near cliff proximal positions in climatic conditions where creep is efficient enough to carry away the blocks from the cliff face in northern locations.

A final factor that I believe contributes to creep transport of blocks is the proportion of expansive clays that compose hillslope soils. When clays (especially expansive 2:1 clays such as smectite and vermiculite) wet, they expand and can cause soil heave. In extreme settings where soils are nearly entirely composed of these 2:1 clays, this swelling can result in damage to building foundations (Kalantari, 2012). This process can lead to lateral movement of slope blocks sitting on top of the soil, rather than rotating or tumbling. Repeated expansions and contractions over time would result in slow downslope movement, just as with frost heave. In experimental settings, a bentonite expansive clay exerted a maximum swelling pressure between 1,000 and 2,500 kPa when wetted (Bhanwariwal & Ravi, 2021). A cubic 1 m^3 limestone block of $\rho = 2,000 \text{ kg/m}^3$ with 1 m^2 surface area would exert merely 20 kPa of downward force on the soil surface, much less than that of the experiment's pure bentonite. Clearly, in natural settings, the force exerted by swelling clays would be less because clay percentages are lower; many clays are less expansive than bentonite, and expansion can to some extent happen in directions other

than upward. Yet, a role for clay-expansion in block transport via creep seems warranted. In my study location, hillslope soils form primarily from upland loess and the shale that form the hillslopes which result in high proportions of silt and clay. Furthermore, as the limestones of this landscape weather, they too release clays as the calcite around them eventually dissolves away.

2.8 Conclusions

Rock blocks on hillslopes under cliffs in Konza Prairie appear to display complex relationships between size and distance from the modern cliff face. I find that the larger size fraction of blocks exhibits a clear decrease in size with distance from the cliff; however, the relationship is less clear for smaller block sizes. Furthermore, I observe a clear decrease in total block size with increasing downslope distance from the cliff when the size of individual blocks is summed together in 3 m intervals. The sum of hillslope block size for these 3 m intervals does appear to decrease with distance strongly linearly (Figure 4b). I propose that fragmentation of large blocks is a simple explanation for the weak relationship between block size and distance from cliff for moderate and small blocks. Fragmentation allows for the largest blocks to decrease in size, while acting as a mechanism for the production of the small and moderate sized blocks and rock fragments found across the entire hillslope. Field observations lead me to conclude that the process of fragmentation differs between cubic and tile-shaped blocks leading to tile-shaped blocks being larger in size and less weathered compared to cubic blocks.

When these observations are considered together, I conclude that in this temperate mid-continental landscape limestone blocks weather primarily through fragmentation. Furthermore, this process occurs while the block moves downslope through time. I also find that block shape may play an important role in how soil is spatially distributed around large hillslope blocks. Cubic blocks are more likely to collect soil on their upslope side and act as repositories of soil,

whereas tile-shaped blocks are surrounded on all sides by soil, suggesting that soil may move around them more easily. Yet, block shape does not appear to play as important a role in block transport as expected at the beginning of my investigation. I show that most blocks, regardless of three-dimensional geometry, are transported in a fashion first described by Schumm (1967)—on top of moving regolith with creep. This conclusion is based on the following observations: we find on similar values of relative slopes for both tile-shaped and cubic blocks as well as both shape classes having nearly the same distribution of hillslope positions.

Finally, I observe that differences in slope block size and surface weathering is related to differences in vegetation cover types. I propose that this difference may be caused by microclimatic as well as wildfire intensity differences between grassland and forest vegetation cover. Wildfires can weaken rock and speed up the process of fragmentation, whereas microclimate differences can affect weathering rates. However, further research will be needed to decide between the relative importance of these two possible reasons.

**Chapter 3 - The lasting legacy of glacial landscape dynamics:
Capturing the transport of boulder armor and hillslope retreat
with geochronology in the Flint Hills of Kansas**

3.1 Abstract

I present new geochronological data derived from hillslope boulder armor in the Flint Hills in northeastern KS, United States, that provides insights into the rates and timing of lateral retreat in this landscape. My results show that the surfaces of these limestone boulders date back to the Pleistocene era, well within the last glacial period. I also found that there is a significant increase in the ages of hillslope armor with increasing distance downslope from the modern limestone bench, the source of the boulders. Based on the age-distance relationship of the boulders, I estimate the rate of lateral retreat in this landscape to be 0.02 mm/yr, which falls between the geometrically estimated retreat rates based on calculated denudation rates of the Flint Hills region. I propose that the cooler temperatures and higher effective moisture due to less efficient evapotranspiration during the late Pleistocene period resulted in more effective freeze-thaw and transport processes, such as creep due to soil expansion and contraction. The production and transport of new boulder armor would then have effectively ceased once the climate transitioned to warmer conditions during the Holocene. My findings suggest that the boulder armor observed on the soil mantled hillslopes today are relict features from before the LGM-Holocene transition. These results provide important insights into the long-term evolution of these ubiquitous layered sedimentary landscapes.

A version of this chapter was submitted to the Journal *Geomorphology* on June 23rd, 2023, and accepted after going through peer review on November 13th, 2023. The citation of the journal article is: McCarroll, Nicholas Reilly, and Arnaud Temme. "The lasting legacy of glacial landscape dynamics: Capturing the transport of boulder armor and hillslope retreat with geochronology in the Flint Hills of Kansas." *Geomorphology* 445 (2024): 108980.

3.2 Introduction

3.2.28 Plain language summary

Limestone boulders found on hillslopes in Konza Prairie, Kansas date to the Pleistocene period, specifically to glacial times. The age of the boulders indicates that the cooler temperatures and higher moisture levels during the Pleistocene period provided more favorable conditions for processes like ice wedging, resulting in more boulders being produced and transported away from the limestone benches on the landscape. I estimated the rate of lateral change in the landscape at 0.02 mm/yr, and the apparent rate of boulder transport at 0.12 mm/yr. The boulder armor found on the hillslopes today is therefore relict features from the most recent Ice Age, produced and transported during the Pleistocene period. The research suggests that the climate fluctuations over geologic timescales may result in conditions that speed up or slow down landscape activity, and my estimated long-term averaged rates of lateral retreat are consistent with the vertical denudation rate of 0.1 mm/yr published for this location. Understanding the history and processes that shaped the landscape can provide valuable insights into how it may continue to change in the future.

3.2.29 Introduction and conceptual framework

The rate of landscape development and response to exogenic changes determined by the rate at which material can be removed from the landscape. This rate of material flux out of a

landscape is directly controlled by the rate at which material can be weathered, transported down a hillslope, and eventually carried away by the fluvial system (Glade et al., 2019; Shobe et al., 2021). The rate of material transport is controlled by the efficiency at which various geomorphic processes proceed (Sweeney et al., 2015; Richardson et al., 2019; Neely et al., 2019). On one hand, internal geomorphic drivers like the underlying lithology, precipitation patterns, changes in vegetation cover, and biologic activity exert considerable influence on the processes that drive material flux on both hillslopes and the fluvial system (Govers and Poesen, 1998; Roering et al., 2001; Marston, 2010; Schanz and Montgomery, 2016). On the other hand, external boundary conditions, such as climate, tectonics, and base level changes, can significantly control the effectiveness and relative dominance of the different internal geomorphic drivers that drive the processes that transport material out of a landscape (Gran et al., 2013; Zondervan et al., 2020; Marshall et al., 2021). These process drivers and boundary conditions can, individually or together, exaggerate or mute these different processes and thus speed up or slow down the rate of material transport and in turn the rate of overall landscape change (Glade et al., 2017; Glade and Anderson, 2018; Glade et al., 2019; Shobe et al., 2021; Chapter 2). The geomorphic community has made significant progress in understanding the effects of geomorphic drivers and processes on landscape change. In the case of hillslopes, the key processes are: bedrock weathering, debris flows, and soil creep (Roering et al., 1999; Mudd and Furbish, 2004). Recently, the geomorphic community's attention has shifted to examine less obvious or harder measured landscape properties that can also influence geomorphic drivers and processes. Hillslope armor, formed by rock fragments and boulders, is one such landscape property that has received increased attention by the geomorphic community (Glade et al., 2019; Chilton and Spotila, 2020; Shobe et al., 2021;

Chapter 2). This surface armor may function as a dynamic boundary condition at the hillslope and regional landscape scale.

Rock fragments of varying sizes from a harder lithology can cover and protect underlying, more erodible rock or soil, which can modulate erosion in both hillslope and fluvial settings (Glade et al., 2019). On hillslopes this armor works by trapping regolith on the upslope side and reducing the rate at which the bedrock beneath the armor is converted into regolith and eroded away (Granger et al., 2001a). The ability of boulder armor to reduce the rate of material removal off a hillslope is an important control in landscapes composed of alternating lithologies with differing erodibility. In such landscapes, portions of slopes underlain by weaker lithologies can be armored by boulders sourced from outcrops of resistant lithologies. Model simulations indicate boulder armor can significantly increase the geomorphic lifespan of landforms as well as modulate ongoing river incision and hillslope adjustment (Thaler and Covington, 2016; Glade et al., 2017; Glade et al., 2019). However, we have yet to constrain the rate at which such material is provided to and transported over the hillslopes. Understanding how and when large rock boulders are transported downslope by hillslope processes is important for comprehending the longevity of this control on landscape evolution.

I seek to establish a chronology of the production and movement of hillslope boulder armor for hillslopes in the Konza Prairie portion of the Flint Hills of Kansas, where a record of fine sediment fluxes off the hillslopes has already been established (Gorynski and Mandel, 2009; Layzell and Mandel, 2020). The Flint Hills are formed from many repeating layers of shale and limestone that create a distinct stair-step hillslope profile (Frye, 1955). Many of the slopes are armored by boulders and rock fragments sourced from the limestone layers (Frye, 1955; Chapter 2). Using cosmogenic ^{36}Cl collected from benches and boulders on two hillslopes, this chapter

will provide insights into rates of boulder transport as well as an estimate of how quickly these hillslopes are retreating laterally.

3.2.30 Production of hillslope boulder armor

The lateral migration and erosion of various land features such as cliffs, bluffs, hogbacks, as well as bedrock benches, are a critical source of hillslope armor in the form of deposited boulders, as noted in recent studies (Duszyński et al., 2019; Shobe et al., 2021; Fame et al., 2023). The production of hillslope armor from an active cliff face makes it an active participant in landscape evolution, as it regulates rates of erosion and weathering below the cliff face (Glade et al., 2017; Glade and Anderson, 2018; Glade et al., 2019). A significant portion of research has focused on the large escarpments in arid settings, such as the Colorado Plateau (Koons, 1955; Schmidt, 1996; Schumm and Chorely, 1966; Ward et al., 2011; McCarroll et al., 2021). These towering escarpments, several hundred meters high, are primarily composed of a hard rock unit that overlays a much softer lithology, creating a significant amount of rock debris that mantles the slopes directly below the cliff (Koons, 1955; Schmidt, 1996; Schumm and Chorely, 1966; Ward et al., 2011). While impressive, these colossal cliffs are not typical of most cliffs and hillslopes around the world. Cliffs and escarpments ranging in size from several meters to tens of meters are more prevalent (Duszyński et al., 2019). In these scenarios, thin caprock, block-by-block weathering, boulder release, cliff retreat, and subsequent boulder transport are crucial factors governing hillslope evolution. In locations with prefractured or jointed caprock, this mode of cliff-retreat is dominant (Koons, 1955; Yeend, 1973; Abrahams et al., 1984). The removal of material beneath the caprock ultimately results in slumping and detachment of a portion of the escarpment face as a discrete boulder that may begin to move downslope (Yeend,

1973) This process is usually gradual and slow as opposed to the catastrophic rock avalanches of much larger escarpments (Yeend, 1973; Koons, 1955; Ward et al., 2011; Chapter 2).

3.2.31 Boulder armor impacts

The concept of colluvial armor protecting hillslopes from erosion is not new in hillslope geomorphology. Bryan (1940) and later Mills (1981) described a process where depressions in hillslopes, such as gullies or heads of streams, fill up with coarse colluvial material sourced from a more resistant rock unit from above and armor that location. The armor shields that part of the hillslope from future erosion via runoff and diverts the focus of erosion to another nearby location. Eventually, the armoring effect can result in a location where the protected part of the hillslope becomes a stranded high point or hilltop (Bryan, 1940; Mills, 1981; Chilton and Spotila, 2020). This type of armoring of a portion of a hillslope by a colluvial package has become a fundamental theory in later work examining the evolution of large arid escarpments and the development of associated landforms, such as talus flatirons (Koons, 1955; Gutiérrez Elorza and Sesé Martín, 2001; Oh et al., 2019; McCarroll et al., 2021). However, the focus has shifted from examining the effect of armoring via a continuous colluvial package to the impact of individual large boulders scattered across a hillslope.

A combination of recent field and landscape modeling studies have started to investigate the impact of discrete boulder armor on hillslope processes and landscape evolution (Glade et al., 2017; Glade et al., 2019; Chilton and Spotila, 2020; Shobe et al., 2021; Chapter 2). Boulder armor can be defined as multiple individual large rock fragments on a hillslope that influence hillslope activity at their individual location and collectively have a large-scale impact on the hillslope. Although a boulder is technically any sediment grain larger than 256 mm (Wentworth, 1922), this definition is not useful in hillslope geomorphology as it includes a wide range of

grains with scales from submeter to decameter. Shobe et al. (2021) pragmatically defined boulders as grains large enough to restrict the motion of smaller, more mobile grains and trigger significant geomorphic change. I adopted this definition of boulders for this discussion.

Conceptually, boulders can affect regolith flux in several ways. They can trap regolith on the upslope side and decrease the rate at which underlying bedrock is converted into regolith and eroded even if it's already weathered, thereby reducing the removal of material from soil-mantled hillslopes and forcing them to steepen (Granger et al., 2001b; Chilton and Spotila, 2020; Glade et al., 2017; Glade and Anderson, 2018). In steep landscapes, boulders produce depressions and pockets that capture smaller grains, inhibiting dry ravel, and increase surface roughness, which decreases the effectiveness of erosion caused by overland flow due to the microtopography capturing grains in local topographic lows thus making them energetically unfavorable to transport (DiBiase et al., 2017; Bunte and Poesen, 1993). However, the movement and removal of boulders must be considered when understanding the durability of their impact on the landscape. Such rates of boulder production, boulder removal, residence times, and rates of downslope boulder movement have only started to be constrained recently (Denn et al., 2017; Del Vecchio et al., 2018; Fame et al., 2023). Due to the scarcity of known rates of boulder armor residence times there is still an immense need for more data across a variety climatic and geologic settings so that a natural range of residence times can be established by the geomorphic community.

Numerous studies have attempted to estimate or derive the rates of landscape denudation and regolith diffusion; however, with such little data concerning boulder armor it is difficult to assess their residence times on hillslopes. Shobe et al. (2021) estimated the residence time of boulders based on the landscape's average boulder size and known denudation rates. However,

this approach assumes that boulder armor is relatively immobile, that boulders weather in place, and that the landscape is in equilibrium. Several studies suggest that hillslope boulder armor residence times are short enough that armor can be transported into fluvial channels before weathering processes can disintegrate the boulders while still on the hillslopes (Ouimet et al., 2007; Glade et al., 2019; Shobe et al., 2021). So, while we know that boulders are produced, deposited on hillslopes, and transported by geomorphic processes, the geomorphic community has yet to establish the rates of those processes with modern geochronology.

Ideally landscape evolution models would model boulder movement using physical laws that reproduce those rates of boulder production and movement that are measured in landscapes. However, up until now our landscape evolution models have solely used rules that govern under what conditions a boulder may move in the downslope direction (Glade et al., 2017; Glade et al., 2019).

3.2.32 Boulder armor transport and removal

Once a boulder is emplaced on a hillslope, it can theoretically affect the transport of regolith and protect the underlying rock from weathering. Recent studies have highlighted how large cubic boulders on hillslopes beneath a resilient boulder-producing rock unit, typically in the form of a cliff, can significantly alter and control the evolution of landforms over time (Duszyński and Migoń, 2015; Glade et al., 2017; Glade and Anderson, 2018; Shobe et al., 2021). In this study, I am concerned with boulders in a soil-mantled hillslope setting that cannot be removed through higher-energy transport processes like landsliding or tumbling (Caviezel et al., 2021). However, even in a soil-mantled setting, these boulders must either weather in place or be removed from the hillslope and transported out of the landscape. The most apparent way to accomplish this is by chemically (Darmody et al., 2005) and physically weathering (Eppes et al.,

2010; McGrath et al., 2013; Eppes et al., 2020) the boulders into smaller, more easily transportable components (Wells et al., 2008; Román-Sánchez et al., 2019; Chapter 2). However, if the rate of boulder weathering is slow enough, then boulder armor can be transported off the hillslope by geomorphic processes like creep. This would result in a removal rate faster than what may be expected if weathering was the only process at work.

Several conceptual models have been proposed to explain the movement or stability of rock boulders and fragments on hillslopes, including those by Schumm (1967), Abrahams et al. (1984), Duszyński and Migón (2015), Glade et al. (2017, 2019), and Chapter 2. Some research found that boulders are highly mobile downslope (Schumm, 1967; Glade et al., 2017; Glade et al., 2019). Various mechanisms, such as soil creep, frost jacking, animal trampling, and sheet wash, have been proposed as the primary causes of this movement (Schumm, 1967; Abrahams et al., 1984; Govers and Poesen, 1998; Duszyński and Migón, 2015; Duszyński et al., 2019). In other cases, studies found that boulders are resistant to movement, even as the hillslope and landscape around them erode (Duszyński and Migón, 2015; Duszyński et al., 2019). Computer modeling suggests that such large boulders primarily move due to periodic tumbles downslope but are otherwise immobile for extended periods of time (Glade et al., 2017, 2019). Field measurements presented in Chapter 2 suggest that in soil mantled landscapes, boulder armor (up to meter scale) is generally transported by creep independent of boulder geometry.

Due to the transport mechanism being practically the same between cubic and tile shaped boulders in the Flint Hills we expect both shape classes to experience similar residence times and transport rates (Chapter 2). The data presented in Chapter 2 suggests that outside of creep driven transport, fragmentation of boulders is the only other mechanism by which boulder armor can be effectively removed from hillslopes in the landscape.

3.2.33 Geology and geography

The Flint Hills, covering an area of approximately 26,000 km², is a physiographic province formed by the erosion of quasi-horizontal Permian age limestones and shales (Frye, 1955; Dort Jr., 1987; Oviatt, 1999). The contrasting erodibility between the shales and limestones has resulted in the development of stairstep hillslope profiles (Figure 3.1B and C). The resistant limestone forms small bedrock benches and cliffs that contour the landscape, while the shales create convex soil-mantled hillslopes that sit between the limestone layers stratigraphically. The limestones in the region are approximately orthogonally joined and fractured into regular units that eventually form the cubic and tile-shaped boulders found on the hillslopes below the modern limestone bench. My focus will be on the Konza Prairie Biological Station portion of the Flint Hills (39.05' N, 96.35' W) located outside of Manhattan, KS (Figures 3.1A). Konza Prairie spans approximately 35 km² of unplowed tallgrass prairie and has undergone little modification by humans.

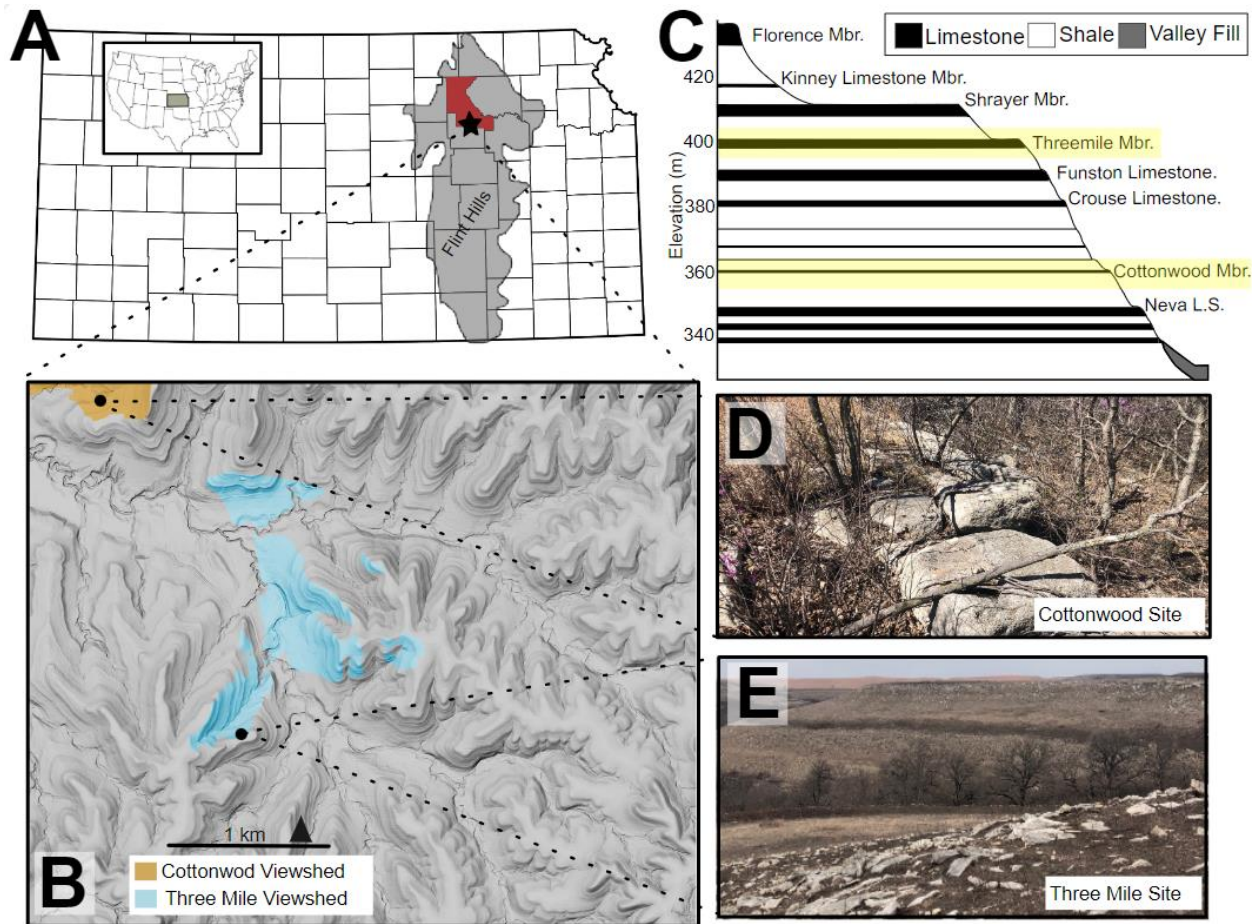


Figure 3. 1 ^{36}Cl sampling location field map and site photography

(a) The physiographic province of the Flint Hills of Kansas (grey). Riley county Kansas is highlighted in red while the location of the study location, Konza Prairie is denoted with a star. (b) A Hillshade map of the study portion of Konza Prairie demonstrating the stairstep morphology of the landscape. Points on the hillshade denote the locations of the two study sites where cosmogenic sampling took place. The shaded portions of the map represent the viewsheds of my two sampling locations that were used to evaluate topographic shielding for my cosmogenic surface exposure ages. The relief of the hillslopes in the study area is approximately 60 meters on average. (c) Is a stratigraphic cross-section of the region demonstrating the lithologic control specific limestone units have on landscape morphology. Limestone units that were targeted in this study are highlighted in yellow. The abbreviation “L.S.” represents “limestone”, and “Mbr” represents “member” Adapted from Smith (1991) and not to scale. (d) Photograph of the large boulders right next to the modern Cottonwood Limestone bench face that were sampled. (e) Photograph of the Three Mile limestone bench and sampling location from afar. Note the abundance of hillslope boulder armor in the foreground.

3.2.34 Regional Pleistocene hillslope activity

During the late Pleistocene and Holocene periods, the Great Plains region, including the Flint Hills region of Kansas remained topologically and topographically stable, without major fluvial reorganization, but has responded to climatic changes (Smith, 1991; Beeton and Mandel,

2011; Layzell and Mandel, 2020). Several studies, including those within the Flint Hills, used the stable carbon isotope ($\delta^{13}\text{C}$) of soil organic matter (SOM) to track changes in the relative contributions of ^{12}C and ^{13}C to biomass found in sequences of buried colluvial deposits and hence through time. The proportions of ^{12}C and ^{13}C carbon isotopes in biomass are determined by the type of pathway a plant uses to sequester carbon dioxide during photosynthesis (Monson et al., 1984; Kohn, 2010). These different carbon fixation pathways produce either a three carbon (C3) or a four carbon (C4) sugar and have different affinities for lighter or heavier isotopes of carbon. C3 plants tolerate moist or dry conditions and are adapted to cooler climates, while C4 plants tolerate moist or dry conditions and are adapted to warmer climates. The relative proportions of $^{12}\text{C}/^{13}\text{C}$ in Great Plains Holocene and Pleistocene deposits are linked to the proportions of short(C3) to tall (C4) grasses present in the landscape at the time of soil formation, and thus to climatic conditions (Layzell and Mandel, 2020). In the study area, the dominant grasses currently are big bluestem (*Andropogon gerardii*), Indian grass (*Sorghastrum nutans*), little bluestem (*Schizachyrium scoparius*), and switchgrass (*Panicum virgatum*) all of which are C4 tall grasses (Tieszen et al., 1997; Briggs et al., 2002).

Based on findings from several sites near the study area, shifts in relative proportions of short and tall grasses repeatedly caused upland hillslopes to become unstable, resulting in shedding of fine-grained material that lasted approximately 500 years, followed by major periods of stream aggradation that lasted equally long or longer. Six such destabilization events occurred between 10,000 C₁₄ yr. B.P. and 900 yr. B.P. (Gorynski and Mandel, 2009; Layzell and Mandel, 2020). The deposition of low-gradient fine-grained alluvial fans at the base of hillslopes characterizes these destabilization periods (Layzell and Mandel, 2020). Once the shifts in the relative amounts of short and tall grasses have stabilized, sediment flux effectively ceases.

However, these records only suggest that the fine-grained portion of the mobile hillslope was affected by these shifts over the past 10,000 years (Layzell and Mandel, 2020). There is no evidence that boulder armor was transported from hillslope positions during this time, suggesting that their positions may have been stable over the last 10,000 years or longer. This is curious, as observations from the modern-day hillslope would suggest that boulders are transported along with the creeping regolith (i.e Chapter 2) and during times of increased fine-sediment flux off hillslopes we might also expect proportional amounts of armor being carried downslope as well.

3.3 Methods

3.3.35 ^{36}Cl exposure dating

Cosmogenic nuclide dating techniques rely on the accumulation of isotopes such as ^{10}Be , ^{26}Al , ^{14}C , and ^{36}Cl that are produced when cosmic rays interact with minerals in rock (Lal, 1991; Balco et al., 2008; Alfimov and Ivy-Ochs, 2009). The isotopes build up in the mineral proportionally to the duration of exposure to cosmic radiation (Nishiizumi et al., 2007). In my study area, we are limited to using ^{36}Cl as the target nuclide because the limestone boulder armor and cliffs are composed primarily of calcite (CaCO_3), which, when interacting with cosmic rays, converts ^{40}Ca to ^{36}Cl (Alfimov and Ivy-Ochs, 2009). This is the primary way ^{36}Cl concentration increases near the surface, although low energy muon interactions can produce ^{36}Cl at lower rates in deeper rock (Alfimov and Ivy-Ochs, 2009). By measuring the concentration of these isotopes in rock, we can determine the time since the rock surface was last exposed (Granger and Muzikar, 2001; Balco et al., 2008). Cosmogenic nuclide dating has successfully dated a range of geologic features and processes, including hillslope evolution (Dunne et al., 1999; Granger et al., 2001a; Heimsath et al., 2002). The use of ^{36}Cl nuclide dating has the advantage of being less

sensitive to shielding effects from overlying rock or sediment compared to other cosmogenic nuclides (Nishiizumi et al., 2007).

3.3.36 Sample location determination and surface sampling

We studied two significant limestone benches formed from the Three Mile and the Cottonwood Limestone Member of the Beatie Formation (Imbrie et al., 1964; Aber and Grisafe, 1982). Before collecting any samples for ^{36}Cl surface dating, I examined limestone boulders in the field. The sampling criteria for each site were tailored to the type of boulders present and the purpose of sampling. However, in all cases I gave preference to boulders whose surfaces showed minimal signs of weathering, such as flaking, to avoid the possibility of obtaining an erroneously youthful age due to the loss of a portion of the surface. Additionally, I collected samples from the in-situ limestone bedrock bench to attempt to account for the effect of cosmogenic inheritance from when the boulder was still part of the bedrock bench and buried but near the surface and was able to accumulate signal from slow muon capture.

The Three Mile Limestone is stratigraphically and topographically located above the Cottonwood Limestone. The specific limestone bench I studied is situated on a prominent hilltop that is isolated laterally from the next bench-forming unit above it by nearly 170 m. The edge of the bench reaches a maximum height of one meter, with most parts measuring about half a meter in height. Our study focused on a northwest-facing position and is exclusively covered by grasses. At this location I focused on boulder armor along a 30 m long topo-sequence perpendicular to the bedrock bench formed by the Three-Mile Limestone (Figure 3.1E). I elected to sample from “tile-shaped” boulders, which I previously used as a geometric classification to distinguish between broadly 3-dimensional “cube-shaped” boulders and 2-dimensional, tile-shaped boulders (Chapter 2). I selected tile-shaped boulders based on field observations and an

original conceptual model that they would be more resistant to flipping over than cubic-shaped boulders due to hillslope processes. Studies by Caviezel et al. (2021) found that even in high-energy environments, flipping of tile-shaped boulders is difficult, and they move downslope via sliding. In Chapter 2, I also showed that tile-shaped boulders in this location appear more stable than cube-shaped boulders and show little evidence of the possibility of rotational movement. This stability is important as it would imply that the same face of the boulder has been exposed to the sky over its whole lifetime on the hillslope. However, I also show in Chapter 2, that tile-shaped and cubic-shaped boulders appear to both transported via creep with little evidence that either shape class experiences frequent rotational movement. This refutes the original conceptual model that I used to inform my sampling procedures and as such the chronology presented here should be representative of both shape classes of boulder armor on these hillslopes.

I targeted boulders for sampling that were at least 0.5×0.5 m in size, and samples were collected near the center of the boulder to reduce edge effects that might be caused by preferential weathering of corners or edges. I collected a total of 10 samples, including 8 samples from boulder armor and 2 samples from the modern cliff face. I collected at least a kilogram of material for each sample. Each rock sample was limited to 4 cm in thickness due to tool constraints.

The Cottonwood Limestone (Figure. 3.1D) is situated lower in the landscape and forms a prominent 1.5-m-high “cliff” that outcrops in most parts of the region. Grassland mostly covers the Cottonwood Limestone and the hillslope underneath it, with some forested sections that consist of a combination of trees and dense woody underbrush growing on top of and within fractures of the cliff face and around the boulders on the hillslope below. The study area forests are mainly gallery forests that grow along streams (Knight et al., 1994). The studied section of

this layer faces northwest, and both the cliff and the hillslope below are covered by forest vegetation because of their close position to the stream network. At this location, I followed a similar sampling scheme: I sampled large boulders that are found immediately under the modern limestone bench (Figures. 3.1D and 3.2B). These boulders are large cubic boulders of limestone, approximately $2 \times 2 \times 1.5$ m, which have slumped and detached from the limestone bench. I collected samples along a perpendicular transect relative to the modern bedrock bench edge, focusing on the only two large cubic boulders present in this location. Samples were collected from both the horizontal tops of the boulders as well as the sides of the boulders. I used the top surfaces of the boulders to estimate the rate of lateral exhumation of the limestone bench, while the vertical surfaces were sampled to estimate the rates of actual boulder detachment from the limestone bench. I collected samples as far away from the edge of the boulder as reasonably possible with the available equipment.

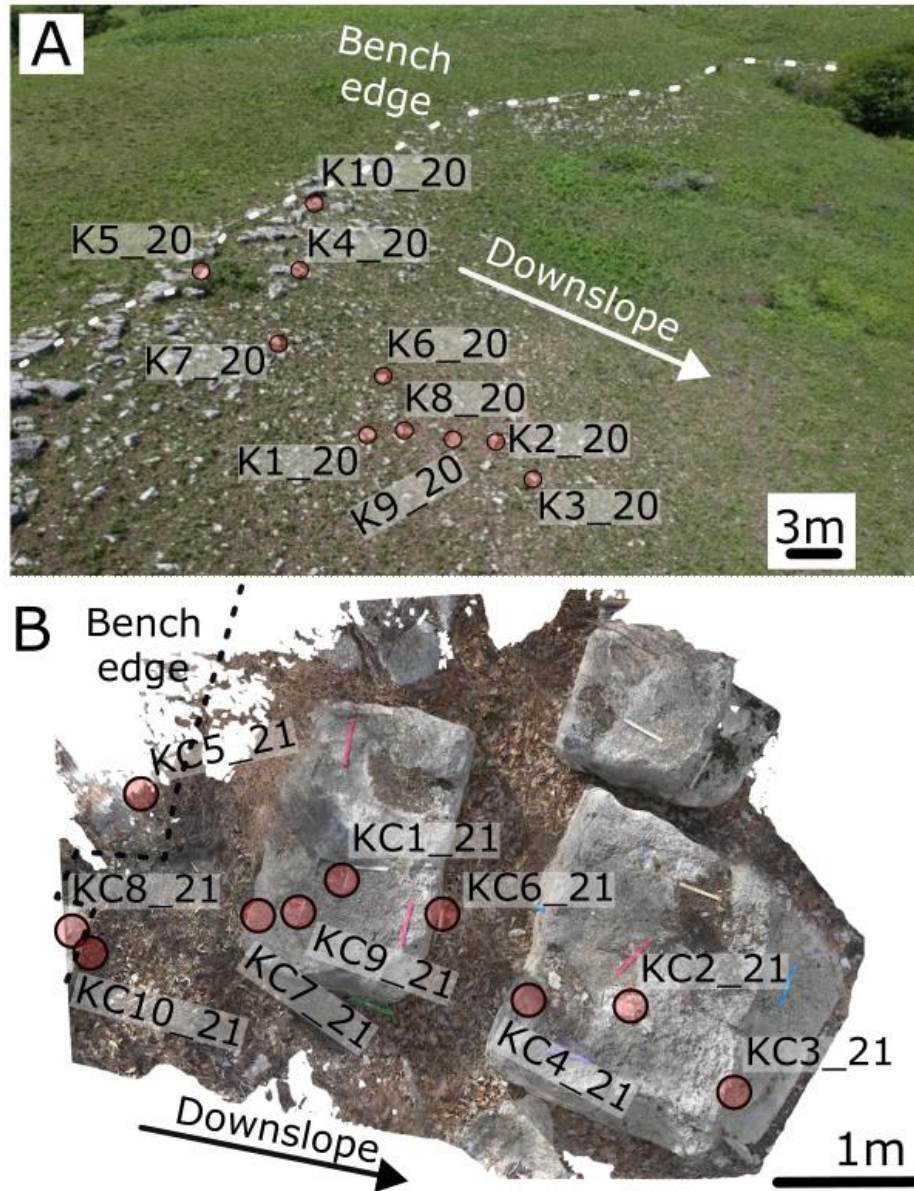


Figure 3. 2 Renderings of sample sites

Overview of Threemile Limestone bench and hillslope sampling location. The location of each sample is denoted by a transparent circular points and denoted with the sample ID. The white dashed line outlines the edge of the limestone bench at the sample location. The arrow labeled “Downslope” points in the downslope direction. (b) Orthophotograph of Cottonwood Limestone slump boulders (blocks) generated in Agisoft Metashape. Sample locations are denoted as transparent circular points and labeled with the sample ID. The black dashed lines follow the edges of the modern cliff edge. The black arrow points in the downslope direction.

3.3.37 Shielding evaluation

To calculate the correct shielding factor for my sites, I determined the large-scale topographic shielding factor for both sites, and additionally the local shielding due to complex boulder geometries at the Cottonwood Limestone site. To calculate topographic shielding, I used the concept of a viewshed to determine the horizon line (Figure. 3.1). The horizon line is a physical boundary formed by the topography of the surrounding landscape that delimits the sky and thus blocks some portion of the incoming cosmic radiation. I used the “skyline” code (2018 revised version) developed by Balco et al. (2008) to calculate topographic shielding values.

For the sample locations below the Three-Mile Limestone (Figure 3.2a), I only considered topographic shielding because boulder surfaces were nearly parallel with the hillslope surface, boulders were well separated laterally, and their shapes relatively flat and tabular. The (topographic and overall) shielding factor for this location is approximately 0.96, which is fitting for the open nature of this portion of the landscape.

The sampling site beneath the Cottonwood Limestone (Fig. 3.2b) is locally more complex than the previous one. The large cubic boulders are situated close to the modern bench face and close to each other and are in locations similar to their original positions before detachment through slumping. The nearly horizontal surfaces of the boulders that face the sky are simple cases when it comes to shielding, as the only obstruction to the sky on these surfaces is the landscape. However, for the nearly vertical surfaces I sampled, substantial portions of the sky may be obstructed by the nearest boulder. To accurately capture shielding in this situation, I used the 3D shielding calculator of Balco (2014). The shielding calculator provides a Monte-Carlo-based estimate of the shielding factor based on a 3D model of the feature of interest. Balco’s

code requires photogrammetry to build a 3D model of the feature of interest. I performed photogrammetry on this large bench proximal boulders and used Agisoft Metashape (v.1.7.5) to produce my 3D model (Fig. 3.2B) that I exported for use in Balco's (2014) MATLAB code. With this code, I found that the horizontal surface shielding ranged from 0.95 to 1.00, while the vertical surface shielding ranged from 0.75 to 0.87 (Table 2.2).

3.3.38 Sample preparation and age calculation

Samples were chemically prepared using methods outlined by Stone et al. (1996), and subsequent AMS measurement of ^{36}Cl was conducted at the Purdue Rare Isotope Measurement (PRIME) Lab at Purdue University. Bureau Veritas Mineral Laboratories in Vancouver, BC conducted geochemical analyses of the samples. The measured concentrations of ^{36}Cl , simulated shielding values, and rock geochemistry were used to calculate exposure ages using the community standard CRONUS Earth Web Calculator (Balco et al., 2008; Marrero et al., 2016; <https://hess.ess.washington.edu/>). This calculator employs several different cosmogenic nuclide production rate scaling schemes that use the same nuclide concentration inputs (St, Lal, 1991; Stone, 2000, Lm, Lal, 1991; Nishiizumi et al., 1989, LSDn, Lifton et al., 2014). The resultant age estimations from the different scaling schemes varied by no more than 10 %, which is less than the 10–15 % analytical uncertainty of the AMS measurements. More importantly, the relative ages of my samples did not change between scaling schemes. I present all my ages as scaled by the time-dependent model (LSDn) of Lifton et al. (2014), which incorporates magnetic field fluctuations, solar modulation, and atmospheric pressure.

3.3.39 Modeling Cosmogenic Inheritance and Lateral Exhumation

We conducted a modeling experiment to gain insight into the potential levels of inheritance resulting from subsurface accumulation of ^{36}Cl in the bedrock bench before the

limestone bench was exhumed and started to produce discrete boulders. In this experiment, I made the simplifying assumption that the landscape topography and hillslope profile is in equilibrium and remains similar in form as the landscape retreats laterally and exposes new limestone surfaces. In the case of my stair-step landscape of the Flint Hills I use the geometric relationships of an idealized system in topographic equilibrium for making prediction of the relationship between denudation and lateral retreat (Glade and Anderson, 2018; McCarroll, 2019). With equilibrium topography, for every amount of vertical incision there is a corresponding amount of lateral retreat. I believe that this assumption is correct as this landscape is composed of nearly horizontal strata, the landscape is lowering, and the stream channels are not significantly migrating towards or away from hillslope over time (Glade and Anderson, 2018). Glade and Anderson (2018), suggest that in this type of scenario the landscape profile will be stable through time as the hillslope retreats laterally backwards. In this case of lateral retreat the vertical rates of erosion across the non-caprock portions of the hillslope are constant through time, unlike hogbacks formed out of tilted rocks (Glade and Anderson, 2018).

To begin to understand how inheritance levels relate to the rate of cliff retreat, I focused solely on the production of ^{36}Cl via spallation in the near surface and negative muon capture (Balco et al., 2008; Alfimov and Ivy-Ochs, 2009). Neutron spallation is the primary mechanism by which ^{36}Cl accumulates at the surface with quickly decreasing in the first meter of soil and rock. At depth below a meter, lower energy muon capture of ^{40}Ca should also be considered (Braucher et al., 2013). Braucher et al. demonstrated that ^{36}Cl can accumulate at depths of up to 25 m, at a rate of approximately 1 atom/g/yr, for typical rock densities of 2.63 g/cm^3 . At this slow yet significant rate, bedrock could accumulate concentrations like those measured in my

samples in a few hundred thousand years, given significantly slow rates of lateral erosion and exhumation, before the overlying material is removed.

I modeled the in-situ production and radioactive decay of ^{36}Cl as a function of depth below the retreating hillslope (Gosse and Phillips, 2001; Alfimov and Ivy-Ochs, 2009).

$$N_{36\text{Cl}}(z, t) = N_{36\text{Cl}}^{\text{inh}} * e^{(-\lambda_{36\text{Cl}}*t)} + P(z) \quad \text{Equation 3.1}$$

where $N_{36\text{Cl}}$ is the concentration of ^{36}Cl , $N_{36\text{Cl}}^{\text{inh}}$ is the inherited concentration of ^{36}Cl , $\lambda_{36\text{Cl}}$ is the decay constant for ^{36}Cl , and $P(z)$ is the depth dependent production of ^{36}Cl . I characterize the production of ^{36}Cl as the following:

$$P(z) = P_{\text{sp}}(z) + P_{\text{muon}}(z) \quad \text{Equation 3.2}$$

$$P_{\text{sp}}(z) = P_{\text{sp}}^{36}(0) * [\text{Ca}] * e^{-\frac{z}{z^*}} \quad \text{Equation 3.3}$$

$$P_{\text{muon}}(z) = Y_{\text{muon}}^{\text{Cl}36} * R_{\text{muon}}(z) \quad \text{Equation 3.4}$$

$$R_{\text{muon}}(z) = R_{\text{muon}}(0) * \sum_k p_{k,\text{muon}} * e^{-\frac{z}{z^*_{k,\text{muon}}}} \quad \text{Equation 3.5}$$

where P_{sp} is the production of ^{36}Cl via neutron spallation at the surface and in the near-surface and P_{muon} is production of ^{36}Cl due to capture of slow muons at greater depths (Stone et al., 1996; Stone, 2000; Heisinger et al., 2002, b; Alfimov and Ochs, 2009). The production rate at the surface, $P_{\text{sp}}^{36}(0)$, is 48.8 ± 1.7 (atoms $^{36}\text{Cl}/\text{g_Ca}/\text{yr}$) (Stone et al., 1996). The fraction of rock that is Ca, $[\text{Ca}] = 0.59$ (g_Ca/g_rock), and z^* is the attenuation length for neutron spallation (160 g/cm 2). R_{muon} is the stopping rate of muons (stopped muons/g/yr) and the yield of ^{36}Cl per stopped negative muon is $Y_{\text{muon}}^{\text{Cl}36} = 0.012$ (^{36}Cl atoms/ stopped muon) (Stone et al., 1996). $R_{\text{muon}}(z)$ is depth dependent, I use the approximation of Schaller et al., (2004) which is discussed in detail by Alfimov and Ochs (2009). I use the approximation of $R_{\text{muon}}(0) = 160$ stopped muons/g/yr of Heisinger et al., (2002b).

To establish an approximation of the corresponding lateral rates of erosion, I can use geometric relationships between vertical and lateral changes in the landscape. Assuming topographic steady state, I can estimate the amount of lateral retreat to vertical denudation using the geometric prediction from McCarroll's M.S. thesis (2019).

$$x = \frac{z}{\tan \alpha + \tan \beta} \quad \text{Equation 3.6}$$

where x is the amount of lateral cliff or landscape retreat and z is the amount of vertical incision in the landscape, and α is the dip of the bed rock. I use a local hillslope gradient β of 10 and a rock dip α of ~ 0.9 . (Smith, 1991). I input known estimates and calculations of denudation of Wooster (1903) and Macpherson and Sullivan (2019) to calculate the rate of lateral bench exhumation at 0.1 mm/yr and 0.4 mm/yr respectively. These estimated rates of lateral bench exhumation are used to constrain the range of retreat rates that one may reasonably expect in this landscape. I also use a rate of 0.2 mm/yr that is inferred from the Cottonwood Limestone bench chronology presented below. I model the lateral exhumation of a bedrock bench based on the Cottonwood Limestone bench sample location. The hillslope covering the bench retreats laterally away thought time while its profile remains the same. I vary the retreat rate for each scenario for a period of 40,000 years.

3.3.40 Calculating boulder movement rates

When measuring the distance downslope of the samples collected from boulders at the Three Mile site (Figure 3.2a) I used the edge of the modern bench face as my base line. I use the distances from bench and geochronology to estimate an apparent rate of downslope boulder movement via linear regression. However, this is not the true rate of downslope boulder movement because the edge of the bench has been retreating backwards through time and so this base line has not been constant through time. This backwards movement of the cliff face

exaggerates the rates of boulder movement based on their position relative to the modern bench edge following (Appendix B – Figure B.1):

$$x_{BM} = x_{ABM} - \left(\frac{y_{LR}}{\cos(\beta)}\right) \quad \text{Equation 3.7}$$

Here, X_{BM} is the actual rate of downslope boulder movement, X_{ABM} is the apparent rate of boulder movement, and Y_{LR} is the rate of lateral retreat of the bedrock bench. The steepness of the hillslope below the bench that the boulders are on is β – here equal to 10 degrees.

3.4 Results

3.4.41 Rock chemistry

The geochemistry of the Three-Mile and Cottonwood limestones are approximately similar (Appendix B – Tables B.1 to B.8). However, one can observe a difference in the rock geochemistry within the Three-Mile limestone samples. I found that the relative proportions of Ca decrease with distance from the modern bedrock bench face, while Si increases. This may represent the increasing amounts of calcite that have been removed from the boulders due to chemical weathering as they sit on the hillslopes.

3.4.42 Raw ages

The ages of boulder armor below the Three-Mile limestone range from 25 ± 1.4 ka to 48 ± 3.5 ka, increasing in age with distance from the modern bedrock bench face in linear fashion (Table 3.1 and Figure 3.3). Linear regression on these data indicates a rate of age increase of 821 years per meter downslope ($R^2 = 0.76$). The in-situ bedrock of the modern limestone bench has a spread of ~5 thousand years, ranging from 25 ± 1.4 ka to 30 ± 2.2 ka. Assuming that the rate of cliff retreat is much slower than the actual rate of hillslope boulder transport (Equation 3.7), I estimate the movement of boulder armor on this hillslope to be 0.0012 m/yr (1.2 mm/yr) by taking the reciprocal of the slope of the linear regression.

Table 3. 1 Cosmogenic exposure result for hillslope boulder armor and bedrock bench surfaces

Sample ID	PRIME ID	Distance from bench (m)	Sample Mass (g)	Dilution Spike (mg)	36 Ratio ($\times 10^{-15}$)		[^{36}Cl] ^a (atoms g ⁻¹)		Exposure ^b Age (ka)		
					M	$\pm\sigma$	μ (10^6)	$\pm\sigma$ (10^4)	μ (Int)	$\pm\sigma$ (Ext)	$\pm\sigma$
Three-Mile Limestone											
K1-20	202101162	12.4	30.290	1.1376	1021	30.0	1.36	5.04	36.5	1.5	2.5
K2-20	202101163	18.2	30.312	1.1848	930.1	28.5	1.40	7.83	36.7	2.3	3.1
K3-20	202101164	21.2	30.127	1.1671	1098	32.0	1.89	8.74	48.3	2.6	3.9
K4-20	202101165	3.4	30.106	1.1678	590.8	18.9	1.08	5.49	26.2	1.4	2.1
K5-20	202101166	0.0	30.081	1.1658	1000	30.0	1.08	53.7	30.1	1.6	2.2
K6-20	202101167	10.4	30.170	1.1734	756.8	22.5	1.17	44.2	29.8	1.2	2.1
K7-20	202101168	7.2	30.127	1.1376	861.1	28.6	1.39	5.26	35.5	1.5	2.5
K8-20	202200428	12.8	30.212	1.158	30.212	27.0	1.30	30.4	37.9	1.0	2.2
K9-20	202200429	16.9	30.366	1.157	30.366	18.4	1.57	38.2	40.0	1.1	2.5
K10-20	202200430	0.0	30.187	1.171	30.187	13.3	0.87	16.4	24.9	0.5	1.4
Cottonwood Limestone											
KC1_21	202200433	1.5	30.232	1.135	523.8	8.9	1.03	23.4	25.8	0.6	1.6
KC2_21	202200434	3.7	30.082	1.164	616.3	10.1	1.42	30.1	34.7	0.8	2.3
KC3_21	202200435	4.7	30.880	1.229	535.1	8.8	1.71	47.1	42.7	1.3	3.6
KC4_21	202200436	3.0	30.405	1.127	444.6	7.6	1.38	33.3	32.5	0.9	2.6
KC5_21	202200437	0	30.732	1.166	466.0	9.4	1.31	95.0	28.6	2.3	3.0
KC6_21	202200438	2.3	30.675	1.205	505.4	8.4	1.27	69.2	34.8	2.1	3.1
KC7_21	202200439	1.9	30.294	1.188	425.7	6.9	1.31	26.3	34.8	0.8	2.7
KC8_21	202200440	-0.3	30.296	1.162	523.3	7.8	1.30	44.8	29.8	1.1	2.2
KC9_21	202200441	1.3	30.061	1.251	502.0	7.7	1.11	19.9	27.8	0.5	1.7
KC10_21	202200442	0.2	30.290	1.149	421.6	7.8	1.13	33.6	27.3	0.9	2.0

a – Blank Corrected concentrations

b – Calculated from CRONUS online exposure age calculator (Balco et al., 2008) using LSDn scaling (Lifton et al., 2014).

The surfaces of the large boulders near the edge of the modern Cottonwood bedrock bench range in age from 26 ± 1.6 ka to 42 ± 3.5 ka and increase in age with distance from the modern bench surface (Table 3.1 and Figure 3.3). The linear regression shows that the rate of age increase is 2472 years per meter from the modern bedrock bench ($R^2 = 0.64$). The bare in-situ bedrock of the modern limestone bench is between 27 ± 2.0 ka to 30 ± 2.2 ka. In an analogous manner as above, if we take the reciprocal of the slope of the linear regression, we can estimate the rate of lateral hillslope retreat (Y_{LR}) to be 0.0004 meters per year (0.4 mm/yr). This rate can be interpreted as how quickly the bedrock bench is exposed at the surface as the hillslope above is peeled away via erosion and retreats laterally away from the edge of the limestone bench. At the Cottonwood site (Figure 3.2b) the large cubic boulders are situated near the edge of the modern bedrock bench. Based on field observations these boulders appear to be in locations that correspond closely to where they were when they were once attached to bedrock bench, only changing position mainly in the vertical direction due to detachment and slumping. However, the large boulders have shifted laterally in the downslope direction, leaving space between each boulder and the modern bench edge that is greater than the natural width of the fractures and joints in the in-situ limestone bedrock (Figure 3.2b). I artificially close the gaps to reconstruct the bedrock bench to calculate rates of lateral hillslope retreat (Figure 3.3). I then use these adjusted, gap-closed distances of the boulders to produce “distance corrected” rates of lateral retreat. By accounting for the distances between the large boulders (Figure 3.2b) and the modern bench, the rate of retreat changes to 4500 years per meter ($R^2 = 0.76$), and the rate of lateral uncovering of the bedrock to approximately 0.0002 meters per year (0.2 mm/yr) (Figure 3.3).

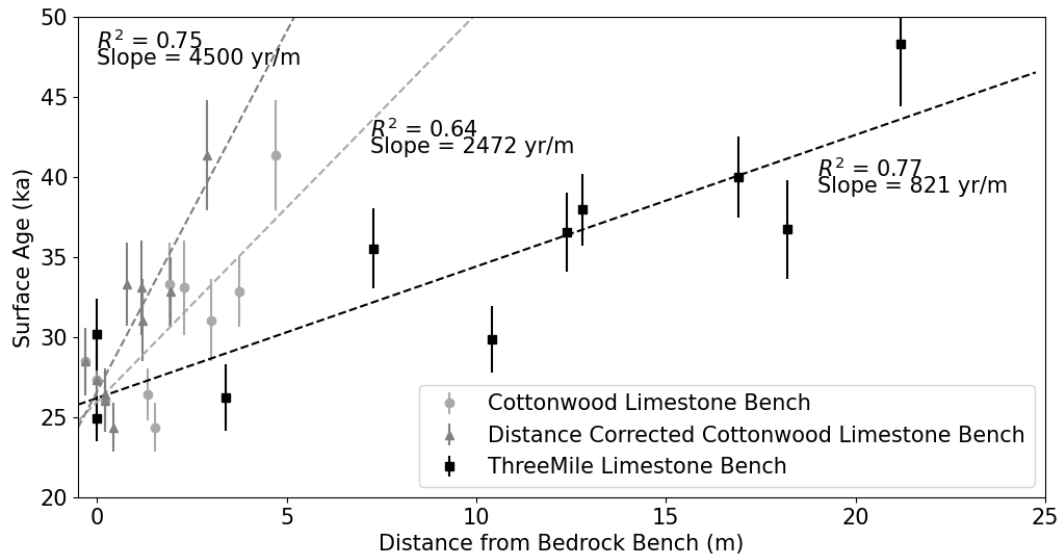


Figure 3. 3 Age-distance regression of boulder and bench surface ages

Uncorrected exposure ages plotted as function of the relative distance of the sample location from the modern bedrock bench edge. Ages are plotted with their external uncertainties. Light grey circles represent the set of samples collected from Cottonwood Limestone surface to understand rates of lateral change. Dark grey triangles represent the set of samples collected from the Cottonwood Limestone surface but the distances from the modern cliff have been corrected to account for lateral shifting of the boulders since being released from the limestone bench. Black squares represent the set of samples collected from the Three-Mile Limestone hillslope boulder armor to understand rates of boulder transport.

3.4.43 Accounting for weathering and inheritance

The exposure ages presented above were calculated with the assumption of negligible surface erosion since deposition. I attempted to establish a reasonable rate of surface erosion, to explore its impact on the ages.

Long-term monitoring of stream chemistry by Macpherson and Sullivan (2019) has shown that the modern landscape denudation rate within my study area is approximately 0.02 mm/yr. However, they suggest that this rate overestimates the actual long-term denudation rate for the bedrock of the landscape, with the temporary decreases due to weathering of calcareous loess deposits. Additionally, limestone weathering is more favorable in the subsurface via karst-related processes and slows down significantly when exposed directly to the atmosphere (Wood

and Macpherson, 2005; Macpherson and Sullivan 2019). Therefore, one can assume that the actual rate of surface weathering over the lifetime of my sampled boulders is substantially less than 0.02 mm/yr.

To understand the potential impact of surface erosion on my chronology, I calculated exposure ages for varying rates of weathering up to 0.02 mm/yr. This analysis revealed that all samples followed a similar pattern, with weathering-corrected ages remaining essentially the same until weathering rates approach 0.02 mm/yr, at which point the ages would be approximately 20% older than those measured at lower erosion rates (Appendix B – Figure B.2). Therefore, I conclude that the effect of erosion on my dataset is negligible when compared to the uncertainty associated with the ^{36}Cl analysis process.

The issue of signal inheritance also needs to be addressed. In many geomorphological settings, sediment grains are the target of dating, however each grain in a deposit has inherited its own geochronological history as it was transported. Fortunately, boulders are much simpler in this regard. Ideally, once the shale and soil covering the limestone is removed and the surface of the limestone is exposed, the accumulation of ^{36}Cl can begin. However, the accumulation of cosmogenic nuclides can also occur in the subsurface before exposure due to the penetration of the cosmic rays into the rock. The production of ^{36}Cl via neutron spallation quickly drops off within the first meter of soil and rock (Balco et al., 2008; Alfimov and Ivy-Ochs, 2009). Additionally, slow muon capture can produce ^{36}Cl at greater depths but at much lower rates (Alfimov and Ivy-Ochs, 2009).

In the Flint Hills landscape, some amount of lateral erosion and hillslope retreat is always occurring, resulting in new portions of the limestone bench coming near the surface, where spallation can cause the accumulation of significant nuclide concentrations (Alfimov and Ivy-

Ochs, 2009). Since inheritance will affect all my samples equally if we assume constant retreat rates, it will not affect my interpretations of rates of lateral retreat and boulder movement. Simulations show that as retreat rates become slower, the relative proportion of inherited ^{36}Cl increases (Figure 3.4). At slower retreat rates, surfaces can look much older than they are, with boulders already having concentrations that are at least 22%-35% made up of subsurface produced nuclide.

I believe using a retreat rate of 0.2 mm/yr to correct these ages for inheritance effects is prudent as it is directly derived from the geochronology of the Cottonwood surfaces (Figure 3.3). Even without correcting for inheritance a rate of lateral bench exhumation is preserved in the geochronology of the modern bench surfaces and nearby boulders (Figure 3.2b) Ideally, the relative change in ages across the bedrock bench and hillslope armor preserves the information relating to retreat and transport independent of the actual absolute age of the surfaces. Because this rate is directly tied to this study location geochronology and it falls between the two end-member rates of Wooster (1903) and Macpherson and Sullivan (2019) I believe that it is the most reasonable lateral retreat rate to use for an inheritance correction. (Table 3.2 and Figure 3.4). Even so there is a level of uncertainty introduced when choosing one rate over another in making a correction. If I use the lateral retreat rates calculated from the denudation rates of Wooster (1903) and Macpherson and Sullivan (2019) (Table 3.2) the inheritance corrected surfaces ages can look between 15% younger (0.4 mm/yr retreat rate of Wooster (1903)) to 20% older (0.1 mm/yr retreat rate of Macpherson and Sullivan (2019)) when compared to the 0.2 mm/yr retreat that I chose to use to correct my ages. In absolute terms surfaces could inherit between 13 to 18 ka worth of signal depending on which lateral retreat rate is used. Nevertheless, most of these ages, even when using inheritance corrections derived from the other rates of lateral retreat

would still be within the last glacial period and so the interpretations presented in the discussion section below would not change significantly.

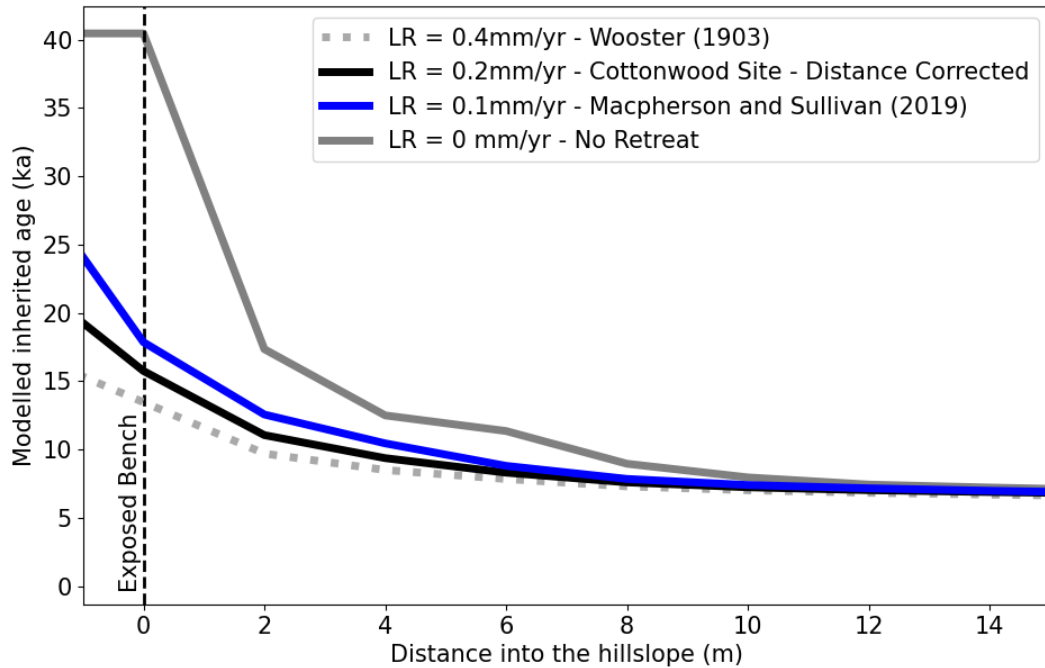


Figure 3. 4 Inheritance modeling curves

Apparent ages of limestone due to subsurface inheritance of ^{36}Cl . The simulation is run for 40,000 years at different rates of lateral hillslope retreat to examine how “old” the limestone bench is when it is first exposed at the surface. There is a general trend of less inherited age as lateral retreat rate increases. Note that the 0.4 mm/yr retreat rate that was estimated for the denudation rate of Wooster (1903) is the same as the rate estimated from the Cottonwood surfaces uncorrected for the boulders moving lateral since they detached from the limestone bench.

When using the chosen 0.2 mm/yr lateral retreat rate results in 15 ka of age is inherited, and the corrected age range for my two sites is $10 \pm 1.4 - 33 \pm 3.5$ ka for the Three Mile Limestone location and $10 \pm 1.6 - 28 \pm 3.5$ ka for the Cottonwood Limestone location. If my estimations of inheritance are correct, then most ages are within the last glacial period but mainly during the height of the LGM (Last Glacial Maximum) and into the period of deglaciation in the Late Pleistocene. A smaller portion of the ages, proximal to the modern cliff face, appear to be just within the Holocene.

Table 3. 2 Boulder and bench surface exposure ages corrected for inheritance based on lateral hillslope retreat

Sample ID	Distance	Geomorphic	Uncorrected	Corrected exposure age (ka)			Shielding
#	from	Surface	exposure	LR* =	LR* = 0.2	LR* = 0.1	Coefficient [%]
	bench (m)		age (ka)	0.4	mm/yr	mm/yr	
				mm/yr	Corrected	Macpherson	
				Wooster	Cottonwood	and Sullivan	
				(1903) [!]	Surfaces -	(2019) ^{&}	
					This study [@]		
Three-Mile Limestone							
K5-20	0	Bench	30.2	17.2	15.2	12.2	0.96
K10-20	0	Bench	24.9	11.9	9.9	6.9	0.96
K4-20	3.4	Boulder	26.2	13.2	11.2	8.2	0.96
K7-20	7.3	Boulder	35.5	22.5	20.5	17.5	0.96
K6-20	10.5	Boulder	29.8	17.0	15.0	12.0	0.96
K1-20	12.4	Boulder	36.5	23.6	21.6	18.6	0.96
K8-20	12.8	Boulder	37.9	24.9	22.9	19.9	0.96
K9-20	16.9	Boulder	40.0	27.0	25.0	22.0	0.96
K2-20	18.2	Boulder	36.7	23.7	21.7	18.7	0.96
K3-20	21.2	Boulder	48.3	35.3	33.3	30.3	0.96
Cottonwood Limestone							
KC8-21	-0.3	Bench	29.8	16.8	14.8	11.8	0.98
KC5-21	0	Bench	28.6	15.6	13.6	10.6	0.97
KC10-21	0.2	Bench	27.3	14.3	12.3	9.3	0.80
KC9-21	1.33	Boulder	27.8	14.8	12.8	9.8	0.87
KC1-21	1.54	Boulder	25.7	12.7	10.7	7.7	1.00
KC7-21	1.9	Boulder	34.8	21.8	19.8	16.8	0.80
KC6-21	2.3	Boulder	34.7	21.7	19.7	16.7	0.75

Sample ID	Distance	Geomorphic	Uncorrected	Corrected exposure age (ka)			Shielding
#	from	Surface	exposure	LR* =	LR* = 0.2	LR* = 0.1	Coefficient%
	bench (m)		age (ka)	0.4	mm/yr	mm/yr	
				mm/yr	Corrected	Macpherson	
				Wooster	Cottonwood	and Sullivan	
				(1903) [!]	Surfaces -	(2019) ^{&}	
					This study [@]		
KC4-21	3	Boulder	32.5	19.5	17.5	14.5	1.00
KC2-21	3.74	Boulder	34.7	21.7	19.7	16.7	0.95
KC3-21	4.7	Boulder	42.6	29.6	27.6	24.6	0.90

- Samples organized by distance from the edge modern bench face.

* - LR = Lateral retreat rate for exhumation of bedrock bench

! - Estimated from geomorphic relationships and volumetric calculations

@ - Corrected distances subtract to account for widening of spaces between cubic boulders that are larger than what the fracture space would be when they slumped from the slope. Uncorrected distances yielded a rate similar to Wooster (1903).

& - Chemical denudation rate calculated from long term monitoring of stream chemistry.

% - Shielding values for Three-Mile Site are topographic shielding only, Cottonwood site shielding values are estimated by Balco (2014) complex geometry shielding MATLAB code.

3.5 Discussion

3.5.44 LGM timing of landscape activity

The chronology of my site indicates that the production and movement of boulder armor, as well as lateral hillslope change, primarily occurred during glacial times. I initially expected that, like in many other landscapes (Gutiérrez et al., 1998; Boroda et al., 2011; Rouqué et al., 2013), boulder ages and the timing of lateral hillslope retreat would typically revolve around times of climate transition, such as the shift from glacial to interglacial, due to the biogeomorphic changes that may lead to increased hillslope activity. However, my chronology, even after accounting for inheritance, shows that geomorphic activity related to the production and transport of boulder armor spans the early Holocene and well into the Late Pleistocene for all inheritance corrected samples. This interpretation suggests that the boulder armor features are mostly related to glacial period landscape activity and that only a few of them are Holocene features. My interpretation below will use the inheritance-adjusted ages ($10 \pm 1.4 - 33 \pm 3.5$ ka).

The inheritance-adjusted ages of this location's hillslope armor are somewhat unexpected when compared to other regional records of hillslope and landscape activity, which shows activity occurring primarily in the Holocene (Lyzell and Mandel, 2020). However, timing of boulder and bench activity present in my chronology may be consistent when compared late Pleistocene and Early Holocene climate records (Figure 3.5). My analysis indicates that a considerable proportion of the ages fall within the range of 15 ka to 35 ka, which corresponds to the Last Glacial Maximum (Marine Isotope Stage "MIS" 2) and the Last Glacial Period (MIS-3). Northern Hemisphere paleoclimate records suggest the region was cooler than present (Figure 3.5A).

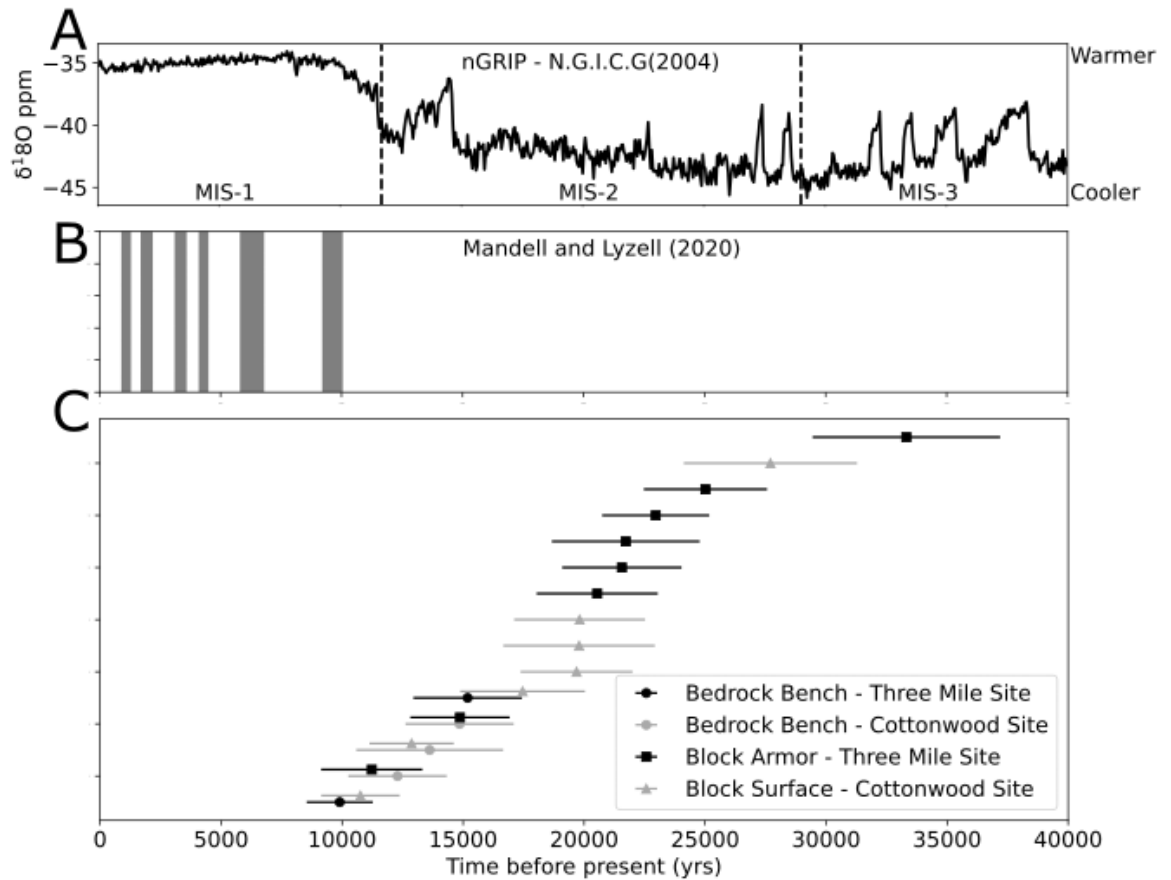


Figure 3. 5 Comparison of paleoclimatic and geomorphic activity to ^{36}Cl chronology

(a) Northern hemisphere ice core temperature proxy data (nGRIP) denoted with Marine Isotope stages (North Greenland Ice Core Group, 2004). (b) Periods of hillslope destabilization described by Mandell and Lyzell (2020) based on soil profiles and stable carbon isotope analysis. (c) My boulder and bench surface ages corrected for inheritance and denoted by sample site and geomorphic surface. Note that bedrock bench exposure ages are clustered around the Pleistocene-Holocene transition, while the majority of boulder armor surfaces cluster with MIS-2.

Regional temperatures at the time have been modeled to be $\sim 10^{\circ}C$ cooler (Shafer et al., 2021). Although this location is not commonly considered “periglacial” during these times, it likely experienced an increased number of temperature oscillations between freezing and thawing conditions. This increase in temperature fluctuations, both annual and diurnal, can enhance various processes like freeze-thaw heave, frost wedging, and soil creep (Hales and Roering, 2007; Remple et al., 2016; Marshall et al., 2017; Schachtman et al., 2019; Marshall et

al., 2021). Paleontological and pollen records suggest that the region and the Great Plains were at least as wet as they are currently during the Pleistocene, when lower temperatures would have increased the effective amount of precipitation due to reduced evapotranspiration (Schultz, 1969; Woodburn et al., 2017). The Pleistocene climate was cool and moderately moist, transitioning to a warmer, drier climate during the Holocene (Woodburn et al., 2017). Therefore, we may expect that there was enough water available during the LGM to enable these processes to occur at a higher rate than they do currently. Interestingly, recent modeling work of Marshall et al., (2021) strongly suggests periglacial processes were pervasive for broad swaths of mid-latitude North America that were not glaciated during the LGM. They suggest that for much of North America paleoclimatic conditions for both temperature and moisture were favorable to the formation of permafrost and the activation of periglacial processes such as frost heave and solifluction. If true, then these more effective processes would be much more successful in moving large boulders as shown in modern alpine settings (Grab et al., 2008). Predicted swell depths of frost heave may have been able to reach up to 2m in depth in the region and would provide force to move boulders (Grab et al., 2008; Marshall et., 2021). Future geomorphic investigations concerning the region need to consider that the Flint Hills and Kansas were indeed periglacial landscapes during the Pleistocene.

The limestones in this region are pre-fractured with joints that have been widened in the subsurface via dissolution (Frye, 1995; Townsend and Macfarlane, 2012). The wedges between these pre-fractured units of limestone are the starting point for increased frost-wedging, causing accelerated cliff retreat and armor production. Once the limestone reaches the near surface and is exposed, freeze-thaw wedging could detach individual boulders of limestone and tilt them onto the slope as new boulders. Initially, water freezes and expands fractures, but once the fracture is

wide enough, soil may collect in it. The swelling and shrinking of the clay in that soil will also act to widen the fracture. Field observations suggest that these fractures eventually fill completely with soil and may even act as preferential pathways for soil transport (i.e., Migoñ et al., 2023) through the limestone benches if fractures are perpendicular to the cliff line. These processes repeat until the limestone becomes a hillslope boulder rather than a portion of the bedrock bench. On the hillslope, glacial-period conditions may have increased rates of freeze-thaw related creep, leading to higher hillslope diffusion, increased removal of material from below the cliff face, and eventually faster slumping and detachment of boulders from the bench. Increases in creep processes also lead to faster transport of boulders and hillslope armor downslope. During this time the more frequent formation and melting of frost in the near surface may be able to repeatedly lift and lower boulders and rock fragments, resulting in movement in the downslope direction in a similar manner as creep (Grab et al., 2008; Chapter 2).

MIS-3 and to a lesser extent MIS-2 are characterized by several high-amplitude Dansgaard-Oeschger (DO) fluctuations, which are abrupt perturbations in climate that last for about a millennium (Kissel et al., 1999; Overpeck and Cole, 2006). These fluctuations would perturb the landscape out of equilibrium and lead to increased hillslope disturbance and fluxes of regolith off the hillslope through a combination of vegetation, hydrologic, and geomorphic drivers. Unstable climate periods or major climatic transitions have been suggested as a mechanism to drive geomorphic change in a variety of landscape ranging from soil mantled and loess covered landscapes like those in the Upper Midwest region of the United State (Knox, 1972) and the Flint Hills in Kansas (Lyzell and Mandel, 2020), to bedrock landscapes like the Valley and Ridge province of Pennsylvania (Del Vecchio, 2018), and on the Colorado Plateau, (McCarroll et al., 2021) as well as in other arid and semi-arid locations around the world (e.g.,

Gutiérrez et al., 1998; Gutiérrez et al., 2010; Boroda et al., 2011; Enzel et al., 2012; Rouqué et al., 2013). These perturbations would contribute to or exaggerate the increases in lateral hillslope retreat, boulder production, and transport downslope.

According to the modeling by Marshall et al. (2021), this location may have experienced periglacial conditions during the Late Pleistocene. If true, then the paleo-climatic conditions may have driven substantial amounts of geomorphic activity on hillslopes. We could expect these conditions to have mimicked activity observed in modern periglacial conditions, which are capable of moving clasts as large as boulders down hillslopes (Grab et al., 2008). If these periglacial conditions modeled by Marshall et al., (2021) did not occur, we still may expect that the paleoclimatic conditions may have at the very least allowed for enhanced creep, frost wedging, and freeze-thaw heave resulting in some amount of boulder transport during the Pleistocene (Deshpande et al., 2021). Nevertheless, these processes rely on specific temperature and moisture conditions that were only achievable in the region during the Pleistocene, as discussed previously. Subsequent climate changes following the Holocene-Pleistocene transition rendered the temperature and moisture conditions unsuitable for the processes to occur or be effective in boulder transportation. After the glacial period ended approximately 12,000 years ago, the production of new boulder armor appears to have ceased, most likely due to unfavorable climatic-geomorphic feedbacks. Consequently, in my two transects at least, no new boulder armor has been deposited on the hillslope, and the efficiency of hillslope processes responsible for downslope movement of these boulders may have significantly declined. Therefore, these boulders should primarily be regarded as relict Pleistocene features. Interestingly, Fame et al. (2023) found that boulder production in the structurally more complex, yet similar latitude, layered landscape of the Blue Ridge Mountains of Virginia overlap with the ages presented here.

Fame et al., (2023) found that exposure ages of boulder surfaces correspond to glacial times (MIS 2 & 3) with boulder production essentially shutting off during the Holocene, mirroring my findings here in the Flint Hills. These two locations with their similar boulder production histories may suggest that production of boulder armor is a consistent feature of layered landscapes while under glacial conditions. Indeed, for hillslopes formed in such layered landscapes, the effects of glacial climates may persist well into the following interglacial periods.

Presently, in Chapter 2 I observe that in the current landscape individual boulders can act as sediment traps that store sediment on their upslope side. This sediment trapping, like the process described by Glade et al. (2017), occurs primarily behind cube-shaped boulders, but also some of the tile-shaped boulders as well (Chapter 2). While there is no direct evidence, there is also anecdotal evidence that these blocks shield the shale hillslopes from weathering and produce steeper hillslopes. Many of the steeper hillslopes in my study area occur in locations of high boulder armor concentration. However, further work will need to be conducted to tease out how boulder armor controls different aspects of hillslope morphology in soil mantled staircase landscapes like the Flint Hills.

3.5.45 Relation to holocene activity

Although most of my inheritance-corrected ages fall within the Last Glacial Period, I also have a small subset of inheritance-corrected ages that range from 10 to 15 ka, spanning the transition from the LGM to the Holocene (Figure 3.5C). Ages closer to 15 ka may be related to landscape perturbations resulting from the transition out of glacial conditions, which is known to drive geomorphic activity and change (Bull 1991; Harvey et al., 1999; Pelletier, 2014). As I discussed earlier, we see a shift from cooler and wetter to warmer and drier climate in the region during this transition (Schultz, 1969; Woodburn et al., 2017). These changes in temperature and

hydrology would drive biogeomorphic changes such as shifts in plant assemblages, particularly grasses, which would result in periods of decreased stabilizing vegetation on the hillslope. The transition between grass assemblages and establishment of new ones during these transitional climates would leave portions of the hillslope vulnerable to the erosive effects of processes like sheet wash and rain splash due to less efficient coverage. The increased efficiency of these processes could then result in fluxes of soil and regolith off the hillslope and reveal and undermine new bench surfaces. For surface ages closer to 10 ka, hillslope destabilization may be related to shifts in the relative proportions of C3/C4 grasses (Lyzell and Mandell, 2020) (Figure 3.5C and D). Although boulder armor has been relatively stable in the Holocene, climate fluctuations appear to have driven the removal of fine materials from the surrounding hillslopes while not affecting the movement of boulder armor. During this time, any soil and regolith would be stripped away from the bedrock bench, exposing it as the bare rock surface we see today.

3.5.46 Boulder transport and lateral retreat of benches

The movement of boulder-sized particles is an area where our process-understanding remains surprisingly incomplete for soil-mantled landscapes. In landscape evolution model experiments it is generally assumed that undermining and tumbling a short distance is the primary way boulder armor moves downslope. However, for landscapes like ours, tumbling seems to be the exception and not the rule. The investigation presented in Chapter 2 concerning boulder armor concluded that the primary mechanism of transport downslope is movement along with the creeping regolith, or creep over the regolith. For the boulder armor below the Three-Mile limestone, the chronology of this site preserves information concerning boulder transport downslope. On the other hand, the boulder surface ages for the large boulders in proximal

positions to the edge of the modern bedrock bench of the Cottonwood Limestone preserve information concerning the rates of lateral change in the landscape. Together, these two sites allow me to make estimates of both lateral landscape change and boulder transport downslope.

When assessing the boulder transport rate below the Three-Mile limestone, it is crucial to acknowledge that the limestone bench is also retreating over time. As I measured the position of these large cubic boulders relative to the current edge of the moving limestone bench, the rate of lateral retreat must be considered when calculating the movement rate derived from the geochronology of these boulders. Therefore, I employ Equation 3.7 to determine the actual rate of downslope boulder movement (X_{BM}). Based on the geochronology data for the boulder armor below the Three-Mile limestone, the apparent rate of boulder movement (X_{ABM}) is 1.2 mm/yr. By examining the geochronology of the boulder and bench surfaces of the Cottonwood Limestone, I estimate the lateral retreat rate of the bedrock bench (Y_{LR}) at 0.2 mm/yr. It is important to note that the rate of lateral hillslope retreat may vary depending on specific location characteristics, such as hillslope aspect or position relative to a stream. It is possible that the Cottonwood Limestone bench retreats slower than the Three-Mile Limestone bench due to the flatter slope of the former. Nonetheless, assuming that hillslopes and limestone benches in the region are all retreating laterally at the same rate and considering the mean hillslope steepness of the sample location ($\sim 12^\circ$) to account for the boulder moving down an inclined surface, I estimate the boulder downslope movement rate (X_{BM}) is 1.0 mm/yr. This corrected rate is approximately 17% slower than the apparent downslope boulder movement rate directly derived from my geochronology. When comparing these rates to known rates of modern average surface creep across the northern hemisphere (1 – 30 mm/yr), the rate here may be considered relatively slow in comparison to soil creep (Oehm and Hallet, 2005). While this rate may be considered

slow by modern standards, it likely reflects a history of transport that encompasses periods of increased activity and relative dormancy, resulting in a long-term averaged rate slower than ongoing modern soil creep.

Interestingly, my estimate of the lateral retreat rate from the cliff and boulder chronology falls between the lateral retreat rates (Table 3.2 and Figure 3.4) based on denudation rates by Wooster (1903) and Macpherson and Sullivan (2019). This geochronology shows a rate twice as fast as the estimated 0.1 mm/yr retreat from Macpherson and Sullivan's denudation rates, and half as much as the 0.4 mm/yr estimation from Wooster's (1903) denudation estimation. As previously discussed, the more favorable climatic conditions in the past may have been the driving force of lateral retreat and boulder production. Therefore, these rates, both boulder transport and lateral retreat, may be relic rates from when the landscape was more active. If that is true, present rates should be much less, indicating a largely dormant landscape from the perspective of cliffs and boulders. However, over geologic timescales, oscillating climates may cause conditions that speed up or slow down landscape activity, and the long-term rates of lateral retreat may be accurately estimated with 0.1 mm/yr for this location. Future research in the area should examine if each limestone bench in the region retreats at the same rate through time or if each bench has its own retreat rate. This can be done by obtaining additional cosmogenic exposure ages from samples taken where the benches are still overlain by regolith.

3.6 Conclusions

Geochronology conducted on hillslope boulder armor in Konza Prairie revealed that these limestone boulders were formed during the Pleistocene period, specifically during the last glacial period. I present observations that show significant increases in the ages of hillslope armor with increasing distance from the source of the boulders, i.e., the limestone bench. Using the

geomorphic relationships between the large boulders that simply slumped when detached from the limestone bench in the past, I estimated the rate of lateral change, i.e., of cliff retreat in this landscape to be 0.02 mm/yr. This rate falls between the geometrically estimated retreat rates based on denudation rates of the Flint Hills region. It is faster than the retreat rate estimated (0.01 mm/yr) from the calculated denudation rate of Macpherson and Sullivan that does not account the slowing down effects of dust and climate variation, but slower than the rough estimations of Wooster (1903). However, I interpret these rates as relict, preserving process information from when this part of the landscape was most active during glacial periods.

I propose that boulder armor ages reflect conditions during the glacial periods, when freeze-thaw processes must have driven boulder production and transport. During the Pleistocene, cooler temperatures must have resulted in more frequent and more effective ice wedging due to the higher effective amount of moisture and more frequent frost-thaw events. This led to more boulders being wedged free from the limestone benches in the landscape. Additionally, transport processes, primarily creep due to expansion and contraction of the soil, were more effective at this time, allowing boulders to be carried away from the bench, providing space for further boulder production from benches. The warmer and drier conditions that followed mostly shut down the production and transport of new boulder armor. However, the modern bench surfaces were exposed during the Holocene, likely due to the stripping of finer hillslope material caused by bio-geomorphic fluctuations such as those reported by Lyzell and Mandel (2020). Today, the boulders we see on this soil-mantled hillslopes are relics from a much earlier time.

Chapter 4 - Fossil hillslopes and the stratigraphic control on rates of adjustment in multi-layered landscapes.

4.1 Abstract

I investigate the intricate relationship between stratigraphic architecture and hillslope dynamics in heterolithic landscapes, shedding light on how the presence of boulder armor influences erosion and diffusion. Using numerical simulations, I examine the effects of the Hardness Ratio (HR) and hillslope armor on hillslope evolution and response to changes in uplift rates. Modeling reveals that heterolithic hillslopes exhibit dynamic steady states, with crest elevations fluctuating as topmost layers are gradually eroded through block-by-block cliff retreat processes. The introduction of boulder armor adds complexity, leading to non-periodic elevation fluctuations and periods of accentuated growth and denudation, depending on hillslope-boulder interactions. Moreover, my simulations show that the response of virtual hillslopes to step changes in uplift rates varies with HR. Higher HR hillslopes exhibit shorter adjustment times following uplift increases, while around an HR of 0.4, optimal boulder armoring and hard layer spacing contribute to distinct adjustment patterns following uplift decreases. These findings suggest that such heterolithic hillslopes may serve as relict features on the landscape, taking significantly longer to adjust than single lithology hillslopes due to the dynamic interplay between boulder armor and stratigraphy.

4.2 Introduction

4.2.47 Plain language summary

Many landscapes across the globe are carved and sculpted out of rock that has layers that alternate between hard and soft. Recent computer modeling work and geologic investigations

have created new understanding of how rivers and streams in such landscapes behave and shape these type of landscape. However, the geomorphic community has not focused as much their efforts on the parts of the landscape that are not streams or rivers, the hillslopes. The work that has been done points to the fact that hard rock units produce boulders and rock fragments that protect and shield softer parts of the hillslope from weathering and erosion. However, we do not have a well-defined model of how the underlying organization of rock as well as boulder on such hillslopes influence the development of the hillslopes in these layered landscapes. Our investigation builds upon previous computer modeling investigations that focused on landforms formed out of one hard and soft layer in tilted rock, here we expand the model to handle multiple layers. We find that the height of a hill in an uplifting landscape varies over time due to the erosion and removal of the topmost level. When boulders are introduced the behavior of the hill through time gets more complicated with the fluctuations becoming harder to predict. We also find that hills in layered landscape with boulder present take longer than expected to erode away due to a complicated interplay between boulder armor, layer spacing, and erosion.

4.2.48 Introduction and conceptual framework

The competition between erosion and the resistance offered by surface rocks represents a fundamental concept in the evolution of landscapes (Lane and Richards, 1997; Gilbert, 1909; Gilbert, 1877). In sedimentary basins worldwide, diverse lithologic layers are cyclically deposited, resulting in stratigraphies that exhibit substantial variations in erodibility (Figure 4.1B). These variations in erodibility, occurring at multiple scales, significantly impact landscape weathering and give rise to distinctive features such as cliffs and hogbacks. The regional-scale organization of stratigraphy plays a pivotal role in shaping landscapes (Ward, 2019; Glade et al., 2019; Yanites et al., 2017; Forte et al., 2016). Previous studies have demonstrated the influence

of lithologic relationships on the propagation of erosion waves within fluvial systems (Forte et al., 2016; Yanites et al., 2017). In heterolithic landscapes, escarpments and hillslopes act as transitional features that preserve valuable information about regional tectonic changes, distinct from those typically observed in fluvial networks (Ward, 2019). However, the majority of investigations into layered landscape evolution have predominantly focused on the fluvial aspects of the terrain.

At the hillslope scale, recent modeling efforts have delved into the impact of lithologic variations on hillslope evolution, with particular attention to the role of boulders in influencing changes (Glade et al., 2019; Glade et al., 2017; Johnstone and Hilley, 2015; Ward et al., 2011). Disparities in erodibility between lithologic units contribute to the formation of cliffs, while boulders play a pivotal role in trapping regolith, thereby reducing erosion and creating steeper slopes (Granger et al., 2001; Glade et al., 2017). Nevertheless, our comprehension of hillslopes within layered landscapes remains incomplete, leaving unanswered questions regarding the timing of equilibrium, landscape responses, and the dynamics of uplift and denudation.

In this study, I adapt Glade et al.'s (2017) model to investigate the controls governing the development of heterolithic hillslopes (Figure 3.1). Employing numerical simulations, I explore the impacts of stratigraphic architecture on hillslope evolution. My objectives encompass the analysis of the influence of resistant layer thickness and spacing on landscape changes under varying uplift rates. Additionally, I aim to examine the rate at which landscapes attain a new steady state and scrutinize the role of substantial boulder armor in shaping hillslope behavior.

4.3 The model

My starting point is the model created by Glade et al. (2017) that examines the impact of large boulders (blocks) on hogback evolution. This model simulated a landscape consisting of a

single tilted hard (resistant) bedrock layer surrounded by softer (erodible) rock. In this study, I have extended this model to incorporate multiple resistant layers. The key parameters I manipulate in these model iterations are the thickness (L_{th}) and separation (L_s) of these hard layers - dictating the stratigraphic architecture of the virtual landscape. The stratigraphy comprises a regularly repeating sequence of harder and softer layers, with nearly horizontal dips. As the virtual landscape undergoes uplift, new hard layers become exposed at the surface and old hard layers. The softer rock undergoes direct conversion into regolith, with the rate of conversion decreasing exponentially with soil depth (Johnstone and Hilley, 2014; Ahnert, 1977). On the other hand, no weathering occurs on the hard layer until a portion of it is undermined and released as a boulder, triggering weathering of the boulder.

I use the linear transport law where soil flux is controlled both by local slope and soil depth (Johnstone and Hilley; 2014).

$$q = -kSh_t(1 - e^{-H/h_t}) \quad \text{Equation 4.1}$$

where q is volumetric soil discharge (L^3/LT), k is the hillslope diffusivity (L/T), S is the local slope gradient, H is the thickness of soil, and h_t is a characteristic soil thickness representing the depth scale of soil transport. This updated model incorporates both boulder armor production and downslope movement of individual boulders on the hillslope. Boulders are deposited immediately downslope when the hard layer undergoes a certain amount of undercutting through diffusion. Individual boulders move down the slope when a specified elevation difference is created between neighboring cells. Boulder armor is converted to regolith when boulders reach a set minimum size. Additionally, once the edge of the topmost hard layer reaches the position of the hillslope ridge crest, that hard layer is removed to simulate the complete erosion and removal of a caprock layer from the hillslope.

In all these experiments, I initiate with an inclined planar hillslope of 15° to ensure the presence of multiple hard layers. The dip angle of these hard layers into the slope is nearly horizontal, approximately 0.1° . To investigate the impact of stratigraphic architecture, I vary the size and spacing of these hard layers, which allows me to define the hardness ratio (HR). HR is determined by the ratio of the average thickness of the hard layers (L_{th}) to the distance separating them (L_s). I explore a range of hardness ratios from 0.1 to 0.6 in increments of 0.1, with L_{th} values ranging from 1.0 to 4.0 meters in 1-meter increments. I limit this investigation to HR values up to 0.6 because values beyond this range would characterize landscapes dominated by catastrophic mass movements like rock falls, a phenomenon my model is not equipped to simulate. To further explore different stratigraphic scenarios, I also consider combinations of L_{th} values ranging from 1.0 to 4.0 meters in 0.5-meter increments and L_s values of 1.5, 3 meters, and up to 15 meters in 3-meter increments. These variations enable me to simulate various stratigraphic configurations while acknowledging the simplification of regularly spaced layers.

The criterion for undermining a hard layer, thus triggering boulder production, is set at 1.5 times the thickness of the hard layer ($1.5 \times L_{th}$). This criterion ensures that thicker layers require more undercutting before they fail and produce a boulder, a concept adapted from Wu and Pollard (1995). In cases where HR is smaller than the amount of undercutting, layer failure is dependent of the next lowest layer to collapse to create the vertical drop needed to induce failure. In each set of experiments, I conducted two subsets of models (Fig 4.1A). One subset involved the release of large boulders from the hard layers, thereby influencing the transport of regolith downslope. The other subset represented a landscape end member in which hillslope armor was instantly converted into regolith, eliminating the influence of large boulders but retaining the

presence of multiple hard layers. This configuration reflects scenarios where the liberated lithology is inherently brittle or poorly cemented.

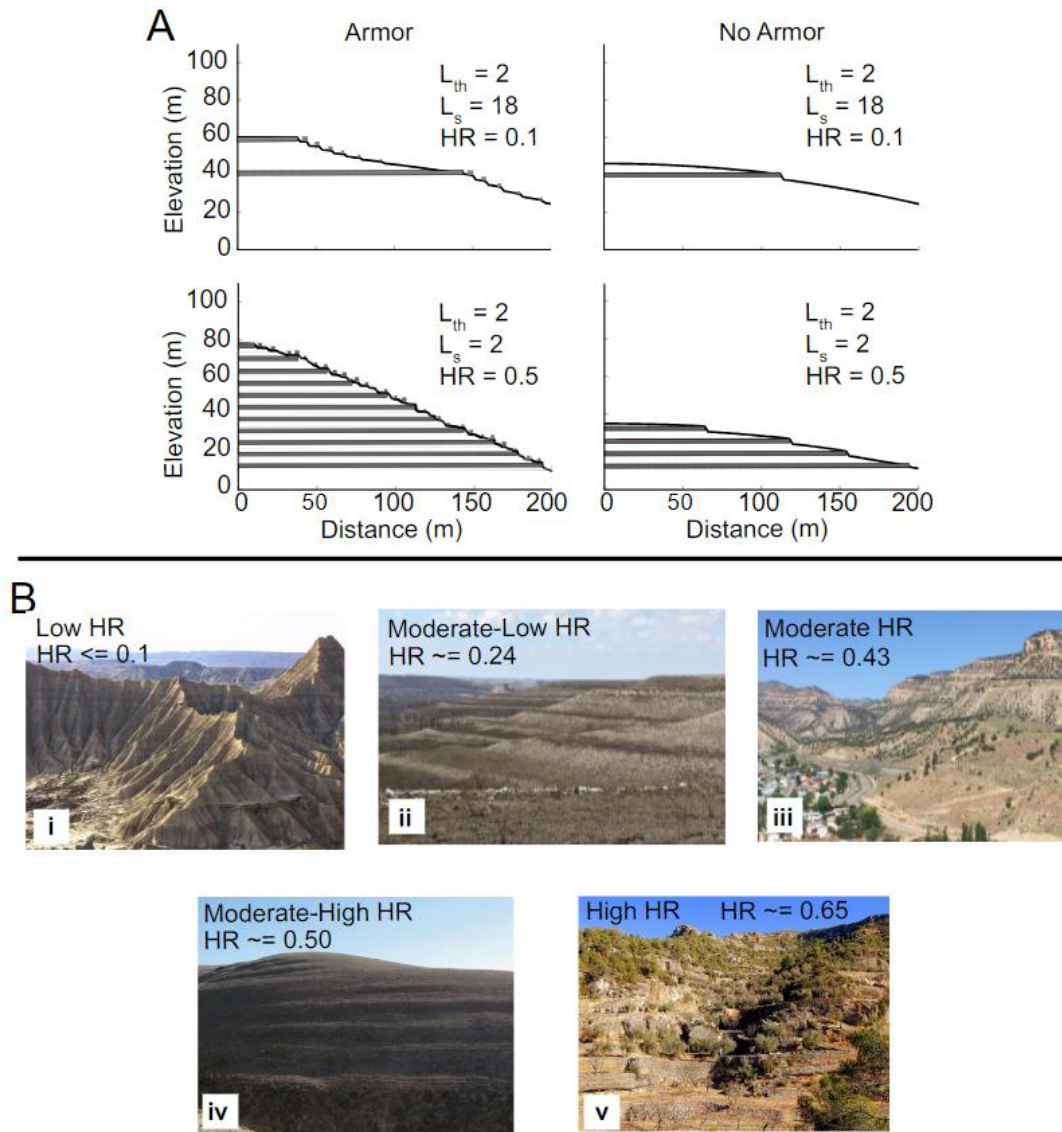


Figure 4. 1 Examples of simulated landscapes and examples of real layered landscapes

Examples of a subset of simulated heterolithic landscapes in dynamic steady state for hillslopes with and without armor. A) Landscapes with and without large rock armor present four combinations of Layer Thickness (L_{th}) and Layer Separation (L_s). The cross section shows hard rock units as grey lines whereas the softer rock unit is white. B) Examples of heterolithic landscapes and hillslopes across the globe and their approximate Hardness Ratios (HR) based on available stratigraphic information of those areas. i) Ebro Basin, Spain ii) Flint Hills, KS, USA iii) Book Cliffs, UT, USA iv) Gabilan Mesa, CA, USA v) Margalef, Spain

I conducted two sets of modeling experiments to investigate the role of HR in hillslope development and its influence on landscape changes. In the first set of experiments, I focused on examining the steady-state characteristics of heterolithic hillslopes developed under various rates of uplift. The uplift rates were varied in the range of 1×10^{-6} to 5×10^{-4} m/yr. I purposely avoided modeling hillslopes at uplift rates exceeding 10^{-4} m/yr since these high-uplift environments typically involve different hillslope processes like landslides and catastrophic failures, which are beyond the scope of this model. In this set of experiments, simulated hillslopes were allowed to reach a steady state during a run time of 5 million years. My objective was to quantitatively assess how both boulder armor and stratigraphy interact and influence hillslope development under differing uplift conditions.

For the second set of models, I initiated the process by allowing the initial landscape to achieve equilibrium through various processes such as diffusion, undercutting, cliff failure, boulder weathering, and boulder movement over a period of 3.5 million years at an uplift rate of 1×10^{-4} m/yr (Fig 1A). Subsequently, I introduced a step change in the uplift rate, with one set of models experiencing a fourfold increase (4×10^{-4} m/yr) and another set with a fourfold decrease in uplift rate (2.5×10^{-5} m/yr). The models ran for an additional 3.5 million years after the uplift change. My goal was to quantify the time required for a hillslope to reach a new steady state following a perturbation in uplift.

Initially, I defined this new steady state as a period during which the rate of change in elevation over time (dz/dt) reached zero. However, due to the complex processes inherent in my simulations, the dz/dt signal exhibited dynamic and oscillatory behavior across various timescales (Fig 4.2). Nevertheless, as the landscape gradually returned to equilibrium, the mean elevation, and consequently the dz/dt signal, exhibited a shape resembling an exponential decay

curve. To determine when a new mean equilibrium elevation was achieved, I employed a Python curve-fitting algorithm, specifically `polyfit`, to fit an exponential decay curve to the mean hillslope elevation time series. This allowed me to precisely quantify the timing of the attainment of a new mean equilibrium elevation. I use the following equation:

$$x = z_{end} - (z_{end} - z_{sc}) * e^{(-t/t_s)} \quad \text{Equation 4.2}$$

Where z_{end} is the final elevation in the elevation time series, z_{sc} is the elevation at the time step right after the uplift change, t is the time step, and t_s is a scaling parameter with units of frequency ($1/t$). However, where the fit of the curve is poor, I visually inspect and manually determine when equilibrium is achieved, if at all. In cases where equilibrium is determined that the hillslope has not achieved steady state, I record the time to steady state as the length of time from the imposed step change to the end of the model run.

4.4 Results

4.4.49 Basic processes of layered landscapes

In each combination of L_s and L_{th} , distinct events unfold across various timescales (Fig 4.2). Over extended periods, the removal or exhumation of hard layers exerts an influence on changes in the landscape surface (Fig 4.2A). On briefer timescales, the movement and extraction of individual boulders play a pivotal role in shaping the landscape surface (Fig 4.2Aii and 4.2Aiii). Furthermore, as L_s (the spacing between hard layers) decreases, a greater number of hard layers populate the hillslope. These higher HR landscape result in more non-periodic swings in landscape change due (Fig 4.1A and 4.2Biii). The periodic oscillations observed in the elevation of the hillslope surface, and consequently in the dz/dt signal, are indicative of hillslopes attaining a dynamic steady state. These oscillations signify the recurring removal of one set of hard and soft units from the landscape. The duration of this process is determined by the

combined value of L_s and L_{th} , divided by the current rate of uplift. Moreover, the amplitude and wavelength of these oscillations are intricately linked to HR, and the presence or absence of boulder armor (Figure 4.2B).

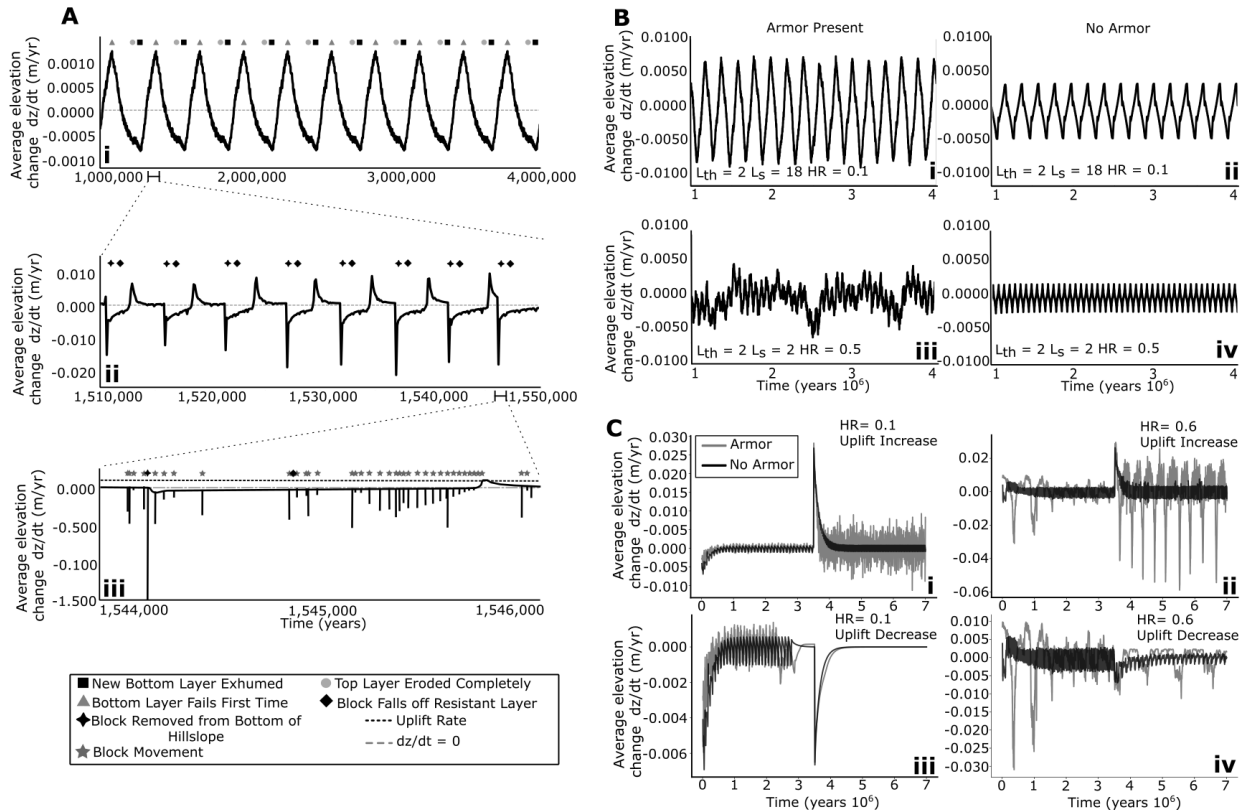


Figure 4. 2 Simulated layered landscape dynamics examples

Changes in landscape elevation for a model run of 1 million years with $L_{th} = 2$ m and $L_s = 15$ m. Geometric symbols plotted above the bold black dz/dt curve represent specific landscape events. i) Averaging changes in dz/dt over 10^4 years reveals that landscape change is primarily influenced by the appearance, disappearance, and activity of the hard layers between 10^4 and 10^5 years. ii) Averaging changes in dz/dt over 10^2 years shows that landscape events occurring over this timescale include the removal and production of large boulders (blocks) from the model domain, specifically at the edge of the domain. iii) Not averaging the dz/dt record shows that the movement of individual boulders downslope is the dominant activity shaping the landscape over hundred-year timescales. Negative spikes are discrete boulder movement event, positive spike soil accumulation behind boulders. B) Subset of model runs showing changes in landscape surface elevation change averaging over 10^4 years. C) Subset of model runs showing dz/dt through time for models where a step change increase or decrease in uplift are imposed at 3.5×10^6 years into the model run.

Layer thickness (L_{th}) and layer separation (L_s) wield significant influence over hillslope development. When L_{th} increases and L_s decreases, the crest elevation of the hillslope rises, and the hillslope takes on a steeper profile (Fig 4.1A). Holding other variables constant, an escalation

in L_{th} yields taller, steeper, and more linear hillslopes. Conversely, an increase in L_s results in shorter, flatter, and more convex hillslopes. Moreover, as HR (hardness ratio) increases, the spacing between the hard layers exerts a more pronounced control over the overall steepness of the landscape when uplift rate is held constant (Fig 4.3B and 4.4Ai).

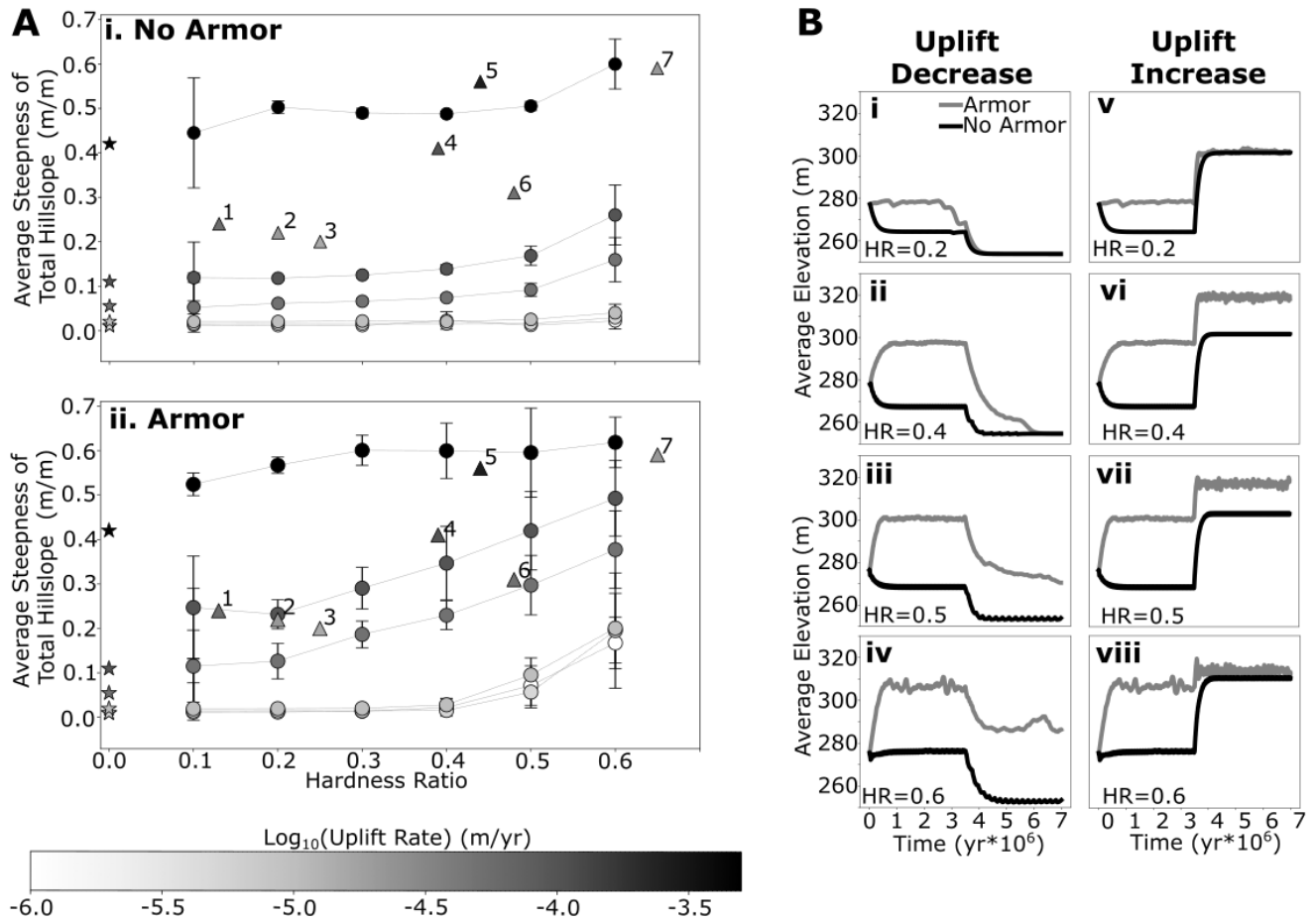


Figure 4. 3 Effect of the presence or absence of armor and response to uplift change

A) Mean landscape steepness for different Hardness Ratios (L_{th}/L_s) under varying uplift rates (1×10^{-6} to 5×10^{-4} m/yr). Circular points represent averages of four model runs with L_{th} values of 1, 2, 3, and 4 m. Stars represent model iterations where no layers are present. Numbered triangular points correspond to real "heterolithic" layered landscapes. The Hardness Ratio and landscape steepness of the real landscapes were determined through landscape analysis, examination of well logs, and published stratigraphic information. Uplift rates were based on previously published values that were geographically closest to the respective landscapes. The numbered landscapes are as follows: 1) Salem Plateau, MS (Rovey et al., 2010; Rovey et al., 2021), 2) State Game Lands 57, PA (DiBiase et al., 2018; McElroy, 2001; Geyer and Wilshusen, 1982), 3) Flint Hills, KS (Macpherson and Sullivan, 2019; Goldberg and Miller, 2019), 4) Monument Valley, UT (Condon, 1997; Cook et al., 2008), 5) Book Cliffs, UT (Seymour and Fielding, 2013; Pederson et al., 2013b), 6) Gabilan Mesa, CA (Roering et al., 2007; Johnstone and Hilley, 2015), 7) Margalef, Spain (Sanjuan et al., 2014; Benito-Calvo et al., 2022). Panel i corresponds to simulations without boulder armor, while Panel ii represents simulations with armor. B) Subset of models runs showing the mean elevation through time for armored and unarmored hillslopes for various HRs and increase or decrease in uplift.

4.4.50 Stratigraphy, armoring, and uplift rates

In the context of landscape uplift rates, the absence of boulder armor appears to lead to minimal variation in landscape steepness until higher uplift rates are reached or when HR (hardness ratio) is greater than or equal to 0.5 (Fig 4.3A). However, with the presence of boulder armor, the relationship between uplift rates, HR, and landscape steepness becomes more evident (Fig 4.3B). At lower uplift rates ($5 \times 10^{-6} - 1 \times 10^{-5}$ m/yr), the trends are similar, whether armor is present or not, with noticeable increases in steepness at higher HR values. Conversely, at higher uplift rates ($5 \times 10^{-5} - 1 \times 10^{-4}$ m/yr), there is a linear increase in steepness with HR. These findings align with real landscapes, as some real-world examples closely resemble my model simulations when boulder armor is considered, based on measured uplift rates, HR values, and hillslope steepness (Fig 4.3B).

4.4.51 Landscape response, adjustment times, and behavior

Much like the findings of Glade et al. (2017), boulder armor exerts a significant influence on hillslope development and its behavior over time. This influence stems from reductions in weathering and mass export across the hillslope (Fig 4.1A and 4.3A). Boulder armor enables hillslopes to attain greater height and develop either concave or linear morphologies (Fig 4.1 and 4.3B). Additionally, the presence of armor leads to steeper hillslope gradients (Fig 4.3B and 4.4Ai). Overall, boulder armor strongly impacts landscape dynamics, affecting the overall dynamic steady state behavior of hillslopes and their response to variations in uplift rates (Fig 4.2B, 4.2C, 4.3B, and Fig 4.4). When armor is present, it introduces a non-periodic signal (Fig 4.2Biii and 4.3B) that overlays atop the periodic signal associated with the exhumation and removal of resistant layers (Fig 4.2Bii). This results in what appears to be a comparatively more irregular dynamic steady state.

Heterolith hillslopes appear to attain steady state conditions differently depending on whether the rate of uplift increases or decreases, as well as the hardness ratio (HR) of the stratigraphy. In cases where uplift decreases, these hillslopes commence denuding and flattening (Fig 4.4B). Therefore, they reduce their steepness and become flatter, a trend observed for all HR values below 0.5, both with and without armor (Fig 4.4Bii). Hillslopes with armor take longer to adjust than those without boulder armor when facing denudation (Fig 4.3B and 4.4Bv). This aligns with the findings of Glade et al. (2017) concerning boulder armor's role in preserving the form of hogback hillslopes over geomorphic timescales. In both cases, with and without armor, the adjustment time remains relatively stable for HRs below 0.3. However, beyond this threshold value (0.4), the adjustment time increases. For unarmored hillslopes, this increase appears to be exponential. The greatest amount of landscape change for these denudating hillslopes occurs when armor is present, and HRs are around 0.4. In cases where uplift is increased, heterolithic hillslopes grow taller and steeper, both with and without armor, as expected (Fig 4.4A). There seems to be a maximum attainable steepness for these heterolithic hillslopes at higher HR values (Fig 4.3Bviii, 4.4Ai, and ii). The time required to reach a new steady state decreases linearly with HR when uplift is increased, with hillslopes featuring armor appearing to require less time to achieve this new steady state steepness. This is unexpected and appears to contradict Glade et al.'s (2017) findings. Furthermore, the degree of steepening that occurs after the step change in uplift decreases for HRs higher than 0.30.

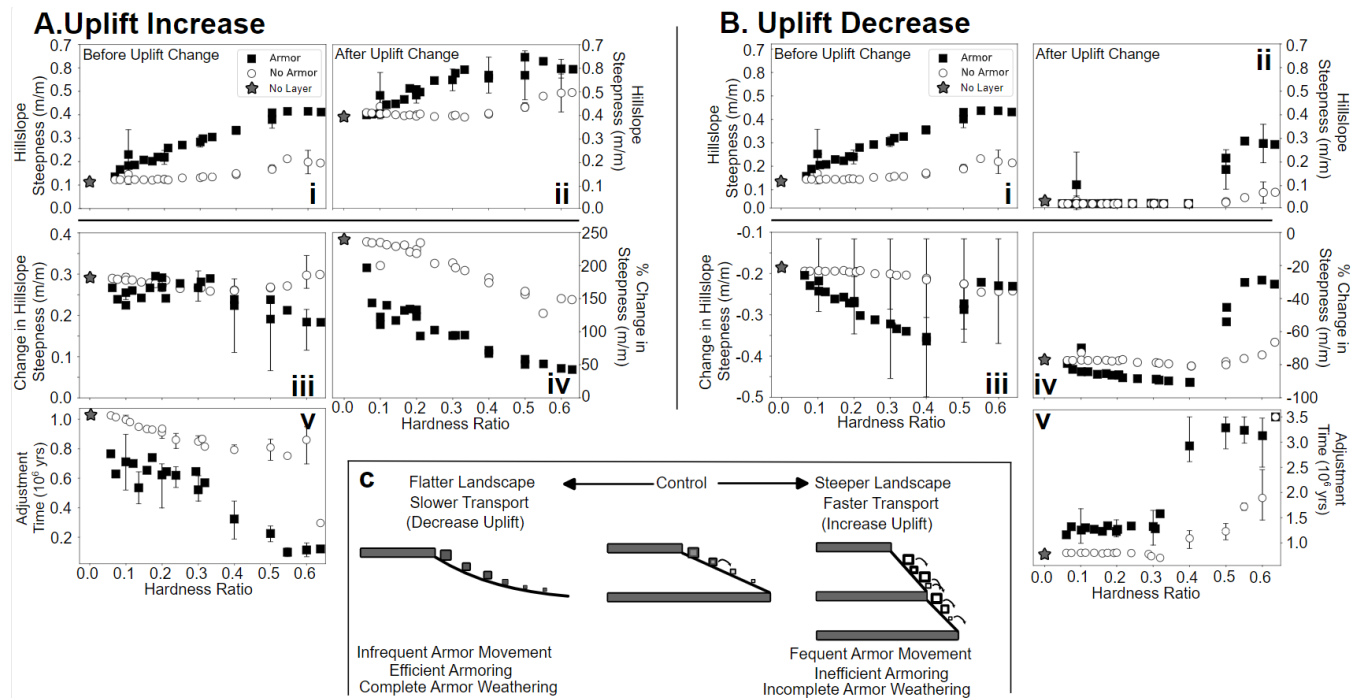


Figure 4. 4 Relationship between hardness ratio landscape properties

The mean landscape steepness is analyzed to examine the effects of hardness ratio (H_R) and the presence of boulder armor on changes in steepness following a step change in uplift rate. The results are presented for landscapes with and without boulder armor, allowing for a comparison of their respective influences on mean landscape steepness. B) The length of time required for a landscape to reach a new steady state after a step change in uplift rate is investigated as a function of hardness ratio. The analysis includes model runs where the hardness ratio is prescribed based on specific values of layer separation (L_s) and layer thickness (L_{th}), as well as model runs where the hardness ratio is determined from unique combinations of L_s and L_{th} . The grey points represent model runs with prescribed HR values, while the white points indicate the mean values for each HR. The black points correspond to model runs with unique H_R combinations, providing additional insights into the relationship between H_R and the time to reach steady state. C) Model of boulder armoring efficiency based on frequency of boulder movement as a function of slope steepness. For uplifting hillslope steepness will increase, but overall armoring effectiveness decrease due to increased movement. For denudating hillslopes steepness will decrease, decreasing frequency of boulder movement, and increase the efficiency of boulder armoring.

4.5 Discussion

4.5.52 Modeled outcomes and real hillslopes

The relationship between stratigraphy and steepness in my simulated landscapes indeed appear to resemble that observed in real landscapes (Fig 4.1B), even when accounting for variations in uplift rates (Fig 4.3A). However, unmodeled factors, such as vegetation, climatic conditions, rock properties, or more complex stratigraphies, may introduce deviations from these simulated landscapes. This divergence may relate to the difference between the single diffusivity

I employ in the modeling versus the distinct diffusivity inherent in each real landscape, influenced by various factors affecting the weathering, erosion of rock, and transport of armor. Nonetheless, we can observe that in nature, as the hardness ratio (HR) increases, landscapes tend to exhibit steeper slopes (Fig 4.2). The rate of uplift remains the primary driver of landscape steepness, as indicated by the increasing steepness for the same HR. However, the organization of stratigraphy exerts a secondary yet profound influence on the steepness that a landscape can achieve. It's noteworthy that as the hardness ratio increases, the spacing between resistant layers becomes smaller, causing the stratigraphy itself to exert more control over hillslope steepness directly (Fig 4.1Bv). This phenomenon is partly due to how the model's resistant layers must be undercut to a certain extent to fail and produce a boulder. As layers come closer together, undermining becomes more challenging, leading to less frequent failures and the growth of higher and steeper landscapes. In real landscape we might expect these higher HR hillslopes to be something closer to an escarpment. While I did not model HRs much beyond 0.6, it's conceivable that in such landscapes, very steep slopes would develop (i.e, Neely et al., 2019). These slopes might not rely on block-by-block failure but instead depend on slow in-situ weathering and disintegration of hard layers. Alternatively, we might expect rapid removal of thin layers of soft rock, creating small voids that cannot support the weight of the overlying hard layer, potentially resulting in limited slumping and block creation. However, it's most likely that HRs above 0.6 would lead to the formation of complex cliffs with more dynamic and catastrophic processes, which are beyond the scope of my current model. The influence of slope armor further complicates the system (Fig 4.3A and 4.3B).

4.5.53 Stratigraphic controls and dynamic steady state

My modeling experiments reveal that heterolithic hillslopes, when reaching “equilibrium”, exhibit continuous growth and denudation over time, characterized by oscillations without settling on a single elevation (Fig 4.2B and 4.3B). As such it may be more appropriate to say that these landscapes reach a dynamic steady state. In uplifting landscapes, the removal of a hard layer serving as the caprock for the hillslope triggers a sudden increase in landscape erosion until the soft rock is entirely weathered and eroded, culminating in the exposure of the next hard unit. This interruption halts the period of heightened hilltop erosion. The exposure of a new hard caprock allows the hillslope to grow in elevation once again. Similar patterns can be observed in landscapes actively denuding due to a decrease in uplift rate, involving periods of intensified weathering and rock removal once the caprock at the top of the landscape is entirely removed. Followed by periods of slow denudation once the next hard layer is reached. The spacing between these hard layers dictates the timing of these fluctuations. However, spacing and thickness are not perfectly regular vertically within real stratigraphic sections or laterally, where layers can pinch out or be disrupted by tectonic features like faults. In real landscapes, we can expect that hillslopes, especially at their summits, may experience varying degrees of weathering and denudation laterally, depending on local lithologic properties. Nevertheless, the long-term average of hillslope elevation change (dz/dt) tends to converge towards zero.

The introduction of boulder armor introduces a level of non-periodicity to these otherwise predictable oscillations of heterolithic hillslopes in a dynamic equilibrium with uplift and weathering. Boulder armor serves as protection against weathering and acts as a repository for mobile regolith buildup. When these boulders move downslope, the stored material is released, resulting in localized increases in regolith movement. Depending on the rate of armor

production, storage on the hillslope, and the pace of downslope movement, we can observe periods of heightened landscape growth when more armor is present and times of increased denudation when less armor is produced (Fig 4.3B). This is evident in the non-periodic fluctuations of the mean elevation over time for slopes with armor (Fig 4.3B). The degree of non-periodic fluctuations in mean elevation increases with HR, as higher HR values correspond to a greater number of hard layers within the hillslope. Consequently, more locations are available for boulder production, resulting in a higher number of blocks that can modify the hillslope's surface and trap mobile regolith, yet there are less locations for boulders to actually armor. Furthermore, these high HR landscapes are steeper and thus block movement is more frequent and results in lower effective armor (Fig 4.4C). I discuss this more in the sections below.

4.5.54 Time to steady state

The modeling of step changes in uplift has revealed intriguing behaviors in both uplifting and denudating hillslopes. For uplifting hillslopes, we observe a relatively linear decrease in the time needed to reach a steady state as the HR (hardness ratio) of the hillslope increases. It's important to note that this trend does not signify that high HR landscapes are more efficient at achieving steady state, but rather that these high HR landscapes are very nearly at their maximum potential steepness prior to the step change. Examining the percent change in steepness (Fig 4.4Aiv), we find that the relative increase from before the step change to after the step change diminishes, indicating that the actual degree of steepening is not substantial relative to the original slope steepness. Due to the modest amount of steepness increase in high HR hillslopes, the time required to reach a new steady state remains relatively brief. In some instances, it appears as though the hillslope is minimally affected by the step change in uplift

(Fig 4.2Biv). This is especially noticeable when blocks are present, as their mere presence already contributes to the steepening of the landscape. Furthermore, the presence of blocks seems to expedite the rate at which a hillslope can attain steady state. Some amount of mass is exported from the hillslope in the form of entire blocks (Fig 4.2A), rather than solely as mobile regolith. This is particularly evident when the resistant layers are situated close to the edge of the simulation domain. In real landscapes, this can be likened to armor entering the fluvial system and being transported relatively swiftly compared to the rate of hillslope processes (see Glade et al., 2019; Shobe et al., 2021).

Conversely, my simulations of denudating landscapes exhibit a markedly different trend. We can observe that for low HR values in both armored and unarmored cases, the time required to reach a new steady state after a decrease in uplift rate is relatively consistent (Fig 4.4Biv). In this set of models, blocks decelerate the rate of landscape change, akin to what is observed in Glade et al.'s (2017) modeling of hogbacks. We can also observe that as the hillslopes denudate, armoring prevents the hillslope from rapidly collapsing to the new steady state mean elevation (Fig 4.3Bi -4.3Biv). Instead, we witness a slower decline of the landscape, with intervals of a "false" new steady state elevation persisting for several hundred thousand years before transitioning to another phase of collapse and reaching the actual new steady state. This phenomenon arises from armor being generated and persisting on hillslopes without being transported for extended periods (Fig 4.4C). Nevertheless, the time required to reach the new steady state for HRs ranging from 0.1 to 0.3 remains relatively consistent, until HR reaches 0.4, at which point the times to steady state increase. For armored landscapes, this change is abrupt, reflecting the intricate interplay between the stratigraphy and the armor on the hillslopes. These

simulated hillslopes suggest that for real layered landscape, denudation may be extended temporally due to the need to remove caprock as well as armor from the slopes.

4.5.55 Optimum armoring and fossil hillslopes

The coupling between armor and hillslope stratigraphy is a phenomenon that becomes apparent in my simulations when hillslopes are no longer actively exhumed at their previous rates, leading to weathering and topographic collapse. Interestingly, hillslopes with an HR of 0.4 exhibit the most pronounced flattening (Fig 4.3Biii). It can also be observed that at this HR, hillslopes take significantly more time to reach a new dynamic steady state (Fig 4.3Bv). I propose that this phenomenon is a result of the interaction between boulder armor and stratigraphy. When the HR is low, resistant layers are spaced farther apart, and the armor generated by weathering cannot effectively shield all parts of the slope. When the HR is high, resistant layers are closer together, slopes are steeper, and blocks do not remain in one position for a sufficient duration (see Fig 4.4C). However, for HRs around 0.4, the hard layers are spaced just right to ensure that boulder armor can cover positions across the hillslope down to the next resistant layer, representing a stratigraphic optimum. In this scenario, armor must span the entire length of the softer sections of the hillslope, while the blocks themselves must remain in place long enough to shield parts of the hillslope from weathering and capture and retain regolith. The presence of armor on a hillslope does not automatically guarantee its maximum effect on the hillslope's evolution; rather, it's about how effectively the armor covers the hillslope and the duration for which it remains in place before being transported downslope to some extent.

In the context of real landscapes, these results suggest that for layered landscapes and hillslopes in denudating environments, may represent "fossilized" features in a geomorphic sense. This is especially true if the hillslopes have reached a false steady state (Fig 4.3Bii and

4.3Biii) and have not yet attained their final long-term equilibrium elevation. The rate of removal of resistant layers and efficiency of block transport appear to be critical factors in the longevity of these hillslopes after a reduction in uplift rate. If caprock remains in place, it will support the landscape, and the rate at which it is removed becomes a controlling factor. Removal is influenced by the rate at which armor in the form of boulders is liberated from the resistant layers through undermining via diffusion processes. However, once a boulder is deposited downslope, it can shield that location from weathering and transport. In scenarios where the landscape is actively flattening, the transport rate slows down, requiring more time for blocks to decrease in size through in-situ weathering. This slowdown in the rate of resistant layer removal contributes to the preservation of the hillslope as it was for a more extended period. Ward (2019) suggests that hillslope features such as cliffs, hogbacks, and cuerdas take significantly longer to adjust than the baselevel fluctuations that would drive their evolution from a bottom-up perspective. My findings here align with Ward's perspective, showing that the adjustment of hillslopes in virtual space can take between 10^5 to 10^6 years, as predicted by Ward (2019). However, the adjustment times for a denudating heterolithic hillslope are notably longer than for an uplifting one, suggesting that if information is preserved in such features, it would be better retained in denudating landscapes where the uplift rate has slowed.

4.6 Conclusion

This study highlights the significance of stratigraphic architecture, particularly the Hardness Ratio (HR), as well as the presence of hillslope armor in controlling hillslope evolution and dynamics. I have demonstrated that for heterolithic hillslopes, achieving a steady state is a dynamic process, with the crest of the hillslope continuously rising and falling as the topmost layer is gradually removed through block-by-block cliff retreat processes. The introduction of

boulder armor into the system further complicates this dynamic, leading to non-periodic fluctuations in elevation and resulting in periods of heightened growth and denudation, contingent on interactions between the hillslope and boulders. Additionally, these simulations shed light on how virtual hillslopes respond differently when subjected to step changes in uplift rates, either increases or decreases. I show that the adjustment times for step increases in uplift decrease with increasing HR, as higher HR hillslopes are already closer to the new steady state steepness, resulting in shorter adjustment times. Conversely, step decreases in uplift rates reveal a shift in adjustment times around an HR of 0.4. This is attributed to the optimal interplay between boulder armoring and hard layer spacing. These findings suggest that such hillslopes may represent relict features on the landscape, taking much longer to adjust than single lithology hillslopes due to the intricate dynamics of boulder armor in these environments. Overall, this study contributes to a deeper understanding of the complex interplay between stratigraphy and hillslope evolution, with potential implications for the interpretation of real landscapes.

Chapter 5 - Layered landscapes future laboratories of hillslope dynamics

5.1 Abstract

This dissertation examined the layered landscape of Flint Hills, situated in northeast Kansas. The geology of this region results in a stair-step hillslope profile that is covered in large fragments of rock that armor the hillslopes. The dissertation research performed here explores the dynamic interplay of geological factors, climatic forces, and boulder armor using a combination of field investigations, geochronology, and landscape evolution modeling. This research focuses on the interaction dynamics of hillslope armor and the interaction with the stratigraphy. Composed of rock fragments and weathered material, boulder armor serves as a geological record of the region's history. My dissertation across three research chapters attempts to begin to unravel the complexities of boulder armor production, its influence on landscape evolution, and its connection with climatic variations. In this final chapter, I will synthesize and contextualize the findings of these research chapters and propose new conceptual models of layered landscape evolution and hillslope armor dynamics. These new insights will expand our understanding of not only layered landscape but also hillslope dynamics in general.

5.2 Introduction

The Flint Hills, a physiographic region in northeast Kansas, is characterized by its rolling terrain, bedrock benches, and extensive outcroppings of limestone. The Flint Hills have presented an opportunity for expanding our understanding of hillslope dynamics in layered landscapes. This chapter delves into the interactions of geology, climatic forces, and boulder

armor described in the previous three research chapters. Here I will synthesize and present a more wholistic understanding of the findings presented in the three previous chapters.

The Flint Hills' stratigraphy and geomorphology provides an ideal natural laboratory for studying landscape evolution in layered landscapes of alternating rock hardness. The resistant limestone layers cause flat benches to form that periodically punctuate the hillslope as well as produce boulder armor. The central theme of this research revolves around boulder armor – a feature intimately tied to the Flint Hills' geological and climatic history. Boulder armor, comprised of rock fragments and weathered material, not only influences the region's topography but also reflects climatic variations that have occurred over geological timescales.

One of the key contributions of this dissertation is the proposal of a new conceptual model for Flint Hills hillslopes, driven by climatic variations across Pleistocene glacial and interglacial periods as they denudate through hard and soft lithologies over geologic time. I also propose that boulder armor is an intrinsic part of many layered landscape systems. In this chapter I also raise important questions about the potential influence of stratigraphic architecture on long term behavior on denudating landscapes like the Flint Hills.

5.2.56 The Flint Hills

Landscapes formed in heterolithic settings, where rocks are oriented nearly horizontally or show minimal deformation, like the Flint Hills, are widespread across the globe (Migoń and Duszyński, 2022). Many interior regions of continents consist of sedimentary basins with rocks that have experienced little structural alteration (Migoń and Duszyński, 2022; Migoń, 2023). Consequently, these landscapes are often referred to as tablelands, characterized by features such as escarpments, mesas, buttes, or stairsteps. All these features share the common characteristic that differences in lithology lead to their development.

The Flint Hills exhibit a unique hillslope profile, resembling stair steps, which are shaped by alternating layers of nearly horizontal shale and limestone (Frye, 1955). This distinctive physiographic province covers approximately 26,000 km² and results from the erosion of Permian-age limestones and shales (Dort, 1987; Aber, 1991; Oviatt, 1999). The soft shale layers comprise the soil-covered sections of the hillslopes, while the limestone layers give rise to small bedrock cliffs and ledges that gracefully curve along the landscape. These limestone layers are well-fractured into regular units at intervals of about one meter, resulting in the deposition of boulders (blocks) on the shale slopes beneath the cliffs (Frye, 1955). These blocks, with various shapes ranging from cubic to tile-shaped, are believed to move through processes such as tumbling and soil rafting, as previously hypothesized. Consequently, the Flint Hills provide an ideal laboratory landscape for studying heterolithic landscape development, the influences of boulder armor, and the history of Pleistocene landscapes. The geology and geomorphology of the Flint Hills offer valuable insights into the processes that shape and evolve landscapes. As such they were natural laboratory and inspiration for the research of my dissertation.

5.3 Results of the previous three research chapters

In this dissertation, I have identified three crucial areas demanding further investigation within the realm of heterolithic landscapes, and the Flint Hills Region has been a promising prospect for exploration for my dissertation. The preceding chapters concentrated on addressing three fundamental research questions, with the Konza Prairie portion of the Flint Hills serving as both my natural laboratory and primary source of inspiration. In the subsequent sections, I will present succinct summaries of the findings from each of the three research chapters, contextualizing the significance of this research within the existing body of knowledge.

5.3.57 Chapter 2 – Limestone boulders (blocks) and hillslope transport

Features within heterolithic landscapes, such as cliffs, benches, hogbacks, and cuestas, actively contribute to landscape development (Glade et al., 2017; Duszyński et al., 2019; Glade et al., 2019). For example, cliffs and valley walls can deposit substantial rock boulders onto hillslopes, influencing the timing and rate of erosional signals across the landscape. This process results in the formation of hillslope armor, further complicating and modulating ongoing landscape changes in the areas below where cliffs, benches, and hogbacks (Glade et al., 2017; Glade et al., 2019; Shobe et al., 2021). The significance of boulders and coarse materials in safeguarding slopes from erosion has long been recognized as a fundamental concept in the study of hillslope geomorphology (Bryan, 1940; Mills, 1984). As outlined by Bryan (1940) and Mills (1984), depressions in hillslopes, such as gullies or stream heads, accumulate coarse colluvial material from a more resistant rock unit located above, resulting in armor at that specific location. This armor shields the hillslope from future erosion caused by runoff and redirects the erosive focus elsewhere. Over time, the armored portion of the hillslope evolves into a prominent high point or hilltop (Bryan, 1940; Mills, 1984; Chilton and Spotila, 2020).

In steep landscapes, boulders form depressions and pockets that capture smaller grains, restraining dry ravel and enhancing surface roughness, thus diminishing the efficiency of erosion caused by overland flow (DiBiase et al., 2017; Bunte and Poesen, 1993). It is widely acknowledged in steep landscapes that boulder armor primarily undergoes movement through mass wasting processes (DiBiase et al., 2017; Caviezel et al., 2021). However, in less steep, soil-mantled landscapes, the transport and removal mechanisms of such boulders are not as well understood. Previous studies have explored the removal pathway of boulders on hillslopes, undergoing breakdown through chemical weathering (Darmody et al., 2005) or physical

processes (Epps et al., 2010; McGrath et al., 2013; Epps et al., 2020), eventually integrating into the mobile regolith. Yet, the physical transportation of boulders off the hillslope has not been thoroughly investigated and has been largely assumed (Glade et al., 2017 and 2019). In Chapter 2, my investigation aims to provide a better understanding of the transport of boulders, specifically large clasts, on soil-mantled hillslopes.

In Chapter 2, the geometric and spatial properties of hillslope boulder armor were utilized to test hypotheses pertaining to boulder armor transport. This research objective was addressed in Chapter 2, revealing that boulders (also referred to as blocks), irrespective of their shape, exhibit a uniform mode of transportation predominantly through creep-related processes. The tumbling of cubic-shaped boulders, in contrast to tile-shaped ones, was found to be infrequent, with freeze-thaw and shrink-swell creep-related processes identified as the primary drivers of boulder movement downslope. Chapter 2 demonstrated a trend of decreasing boulder size with increasing distance from the modern limestone bench edge, the point where new boulders detach. This observation aligns with findings from other landscapes concerning boulder armor below hogbacks. I proposed a novel hypothesis suggesting that large boulders break down into smaller fragments, thereby facilitating their transport through creep processes.

5.3.58 Chapter 3 – Timing and rate of boulder movement and production

In Chapter 3, I addressed the dearth of chronology regarding the production and transport of coarse hillslope boulder armor, both generally and specifically for the Flint Hills. While Chapter 2 provided new insights into the processes governing boulder transport, Chapter 3 seeks to comprehend the rate and timing of those processes. Despite the availability of chronology for the fine portion of hillslope material, uncertainty remains regarding whether coarse hillslope armor is actively undergoing transport. Furthermore, within the geomorphic community, there is

recognition that coarse hillslope armor moves downslope over time; however, there is a lack of spatial data on the rates of movement in temperate, low-relief, soil-mantled settings. This knowledge gap is evident in current models of hillslope armor, where simulated blocks are assumed to "tumble" to the next location in the model when slope steepening or undermining occurs. Nevertheless, based on observations in the Flint Hills (Chapter 2), this assumption appears inappropriate. The evidence suggests that boulders on soil-mantled hillslopes creep downslope while still retaining fine hillslope sediment behind their upslope faces, aligning with the findings of Glade et al. (2017).

In Chapter 3, I addressed this knowledge gap using a combination of cosmogenic chronology, geometric analysis, and simple mathematical modeling to account for inheritance. In Chapter 3, the data shows that landscape activity related to the production and transport of boulders is linked to conditions during the Last Glacial Maximum (LGM). The boulders currently present on the hillslope are relict features from a much colder climate when periglacial conditions prevailed. Furthermore, the lateral retreat rate of the hillslopes and limestone bench in the study location of the Konza Prairie, is approximately 0.02 mm/yr. These rates offer significant insights into geomorphic processes and rates of landscape change, which future modeling work can utilize to constrain rates of boulder movement in soil-mantled settings.

5.3.59 Chapter 4 – Modeling of heterolithic hillslopes

The lithology of underlying rocks constitutes a foundational boundary condition influencing landscape development via geomorphic processes. Nevertheless, when these strata undergo deformation, complexity is added to the control exerted by lithology on landscape evolution, yielding distinct and intricate landscapes (Gilbert, 1877; Gilbert, 1909; Lane and Richards, 1997). The concept of lithology-driven landscape evolution hinges on the interplay

between forces such as tectonics and climate, which induce erosion, and the resistance of surface rocks to this erosion (Gilbert, 1877; Gilbert, 1909; Lane and Richards, 1997). This interplay unfolds across various scales, encompassing weathering and erosion of individual rock outcrops to entire regions. The non-uniform weathering and erosion of rock layers engender diverse topography, where differences in erodibility at the hillslope scale give rise to features like hogbacks and cliffs (Glade et al., 2019; Glade et al., 2017; Ward et al., 2011).

The evolution of hillslope in layered landscapes are intrinsically tied to the underlying stratigraphy and structural properties. Ward (2019) examined the relationship between incision rates and rock dip in the development of heterolithic landscapes. The adjustment time of a landscape with heterogeneous stratigraphy depends on the dip angle of the rock and the coupling between the cliff retreat rate and the escarpment's height. Ward (2019) posits that escarpments and hillslopes function as transitional features that retain information about regional tectonic changes, providing insights on scales distinct from those commonly found in fluvial networks. Nevertheless, the attention paid to hillslopes in these investigations of layered landscapes has been relatively limited, with a predominant focus on their connection to the fluvial components of landscapes. Furthermore, little is known about how the arrangement of these layers influences the broader landscape. As such in my third research chapter (Chapter 4) I use mathematical landscape evolution modeling to produce new insights into how the arrangement of the stratigraphy influences hillslope evolution.

In Chapter 4, I expanded upon Glade et al.'s (2017) 1D hogback model to create a more comprehensive model that simulates hillslope evolution with multiple resistant layers producing blocks as the layers are undermined. Through various simulations of different stratigraphic arrangements, I investigated the effects of changing the spacing between resistant layers and the

thickness of these layers. I found that the interplay between stratigraphy and hillslope armor results in a complex response to ongoing uplift as well as changes in the rate of uplift. In heterolithic landscapes without boulder armor, fluctuations in hillslope characteristics allow the landscape surface elevation to oscillate within a range once it reaches steady state. The wavelength and magnitude of these oscillations are determined by the thickness and spacing between the hard layers of rock. With the introduction of boulder armor, the periodic fluctuations become more non-periodic as blocks move across the hillslope, modulating erosion and regolith transport. Layered landscapes exhibit complex pathways to reach a steady state following a step change. When subjected to increases in uplift, landscapes with higher hillslope retreat rates (HRs) respond more swiftly due to their proximity to maximum steepness, as dictated by stratigraphy. Conversely, when uplift decreases, landscapes with higher HRs take longer to reach a steady state. This is because regolith weathering and diffusion require more time to undermine multiple hard layers, starting from the top of the landscape. The optimal interaction between boulder armor, stratigraphy, and HRs is at approximately ~ 0.4 HR, where the presence of armor significantly prolongs the time required to reach a steady state. These findings shed light on the dynamic interactions between stratigraphy, landscape evolution, and the response to changes in uplift conditions.

5.4 Chapter 5 – Synthesis

5.4.60 Boulder armor and glacial climates

It is evident that in landscapes featuring relatively harder rock units, the production of hillslope armor through weathering is a common occurrence (Chapter 2; Denn et al., 2017; Del Vecchio, 2019; McCarroll and Pederson, 2021; Fame et al., 2023). This phenomenon is observed across various environments, from arid regions to temperate ones, and the presence of

boulder or rock fragment armor plays a significant role in landscape evolution. The Flint Hills, for instance, provide excellent examples of boulder armor protecting hillslopes and trapping material that would otherwise move downslope. However, it is important to note that the production of boulder armor is not constant over time and appears to be influenced by climatic drivers. Furthermore, there appears to be differences in what type of climatic forcing is responsible for production of boulder armor and colluvial material. For more temperate landscapes it appears the significantly cooler temperatures during glacial periods leads to increased amounts of frost shattering of resistant lithologies due to periglacial temperatures (Denn et al, 2017; Del Vecchio, 2019; Fame et al., 2023). For example, Del Vecchio (2019) connected the production of boulder armor on hillslopes to frost shattering under periglacial conditions, particularly in relatively hard-to-weather quartz sandstones of the ridge caprock. In more arid landscapes it appears that climatic disturbances in the form of periodic climatic fluctuations induce periods of toe slope weathering, caprock collapse, and colluvial armor transport and redistribution. McCarroll et al. (2021) showed that the depositional age of colluvial features along the Book Cliffs in semiarid Utah are associated with known periods of climatic instability during the Pleistocene.

In the case of the Flint Hills (Chapter 2), it appears that the climate during the Last Glacial Maximum (LGM) played a crucial role in the delivery of hillslope armor to the region in Kansas. Of the two types of climatic response, my geochronology suggests that the Flint Hills falls under the more temperate, “periglacial,” mode of climatic response to glacial climates (Figure 1). However, there is no evidence in the Flint Hills region of frost shattering being the primary mechanism of armor production. Instead, as discussed in Chapter 2, increases in creep related hillslope process like freeze-thaw, shrink-swell, and frost-heave are the primary drivers of

boulder production and transport (Chapter 2) in the study region. Modeling work of Marshall et al., (2021) strongly suggests periglacial processes were pervasive for broad swaths of mid-latitude North America that were not glaciated during the LGM. The case for periglacial type conditions in the Flint Hills Region are bolstered by Fame et al., (2023) seeing evidence of frost shattering at a similar latitude. Fame et al., (2023) found that exposure ages of boulder surfaces correspond to glacial times (MIS 2 & 3) with boulder production essentially shutting off during the Holocene, mirroring my findings here in the Flint Hills. These two locations with their similar boulder production histories may suggest that production of boulder armor is a consistent feature of layered landscapes while under glacial conditions.

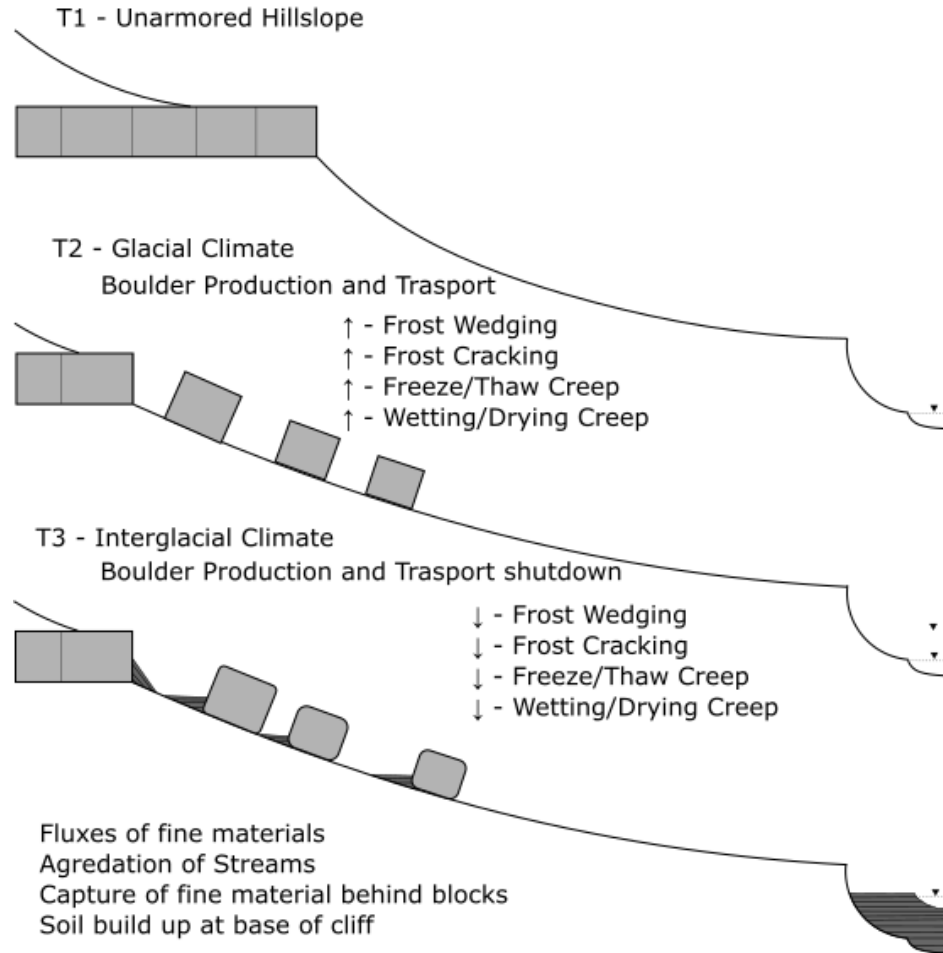


Figure 5. 1 Conceptual model of climate driven boulder armor production and transport

Conceptual hillslope weathering of both softer and harder lithologies, drawing upon field observations, background literature, and findings from Chapters 2 and 3. This model delineates distinct sections of the hillslope that undergo weathering, showcasing heightened activity under specific climatic conditions. Although specifically developed for the Flint Hills, its relevance extends to comparable latitudes or climates in other locations. During glacial climates, there is an intensification of weathering, leading to the fragmentation of resistant rock units. These fragments transform into sizable boulders, actively transported by increased efficiency attributed to elevated levels of freeze/thaw creep processes or periglacial heave. As the climate transitions to interglacial conditions, the removal of material from the resistant lithology ceases. Owing to climatic fluctuations and shifts in stabilizing vegetation, periodic fluxes of fine material from the hillslopes into the stream channels occur (Layzell and Mandell, 2020). The hillslope armor sediment, characterized by its relatively immobile nature, accumulates behind the boulder.

I propose that, for temperate-layered landscapes, boulder armor produced during glacial conditions may persist throughout the following interglacial times. This is especially true in

cases where the layered landscape undergoes glacial conditions, as modeled by Marshall et al. (2021). In Chapter 2, I initially categorized boulder armor as a landscape property with a substantial influence on hillslope evolution. However, if boulder armor is intrinsically tied to layered landscapes, as observed in locations like the Flint Hills, it might be more appropriate to categorize it as a dynamic boundary condition or simply a boundary condition of landscapes, given its production and persistence over geomorphic and geologic time.

If boulder armor stands as a fundamental element within layered landscapes, particularly those subjected to temperate conditions with periglacial influences, the findings from Chapter 3 suggest that we can anticipate the persistence of boulder armor well into the interglacial period (**5.4.59 Boulder weathering in the flint hills**), thereby continuing to exert an impact on landscape evolution and characteristics. This persistence, however, is likely directly influenced by the efficiency of boulder armor weathering, transport, and removal. Studies by Denn et al. (2017), Del Vecchio et al. (2018), and Fame et al. (2023) provide evidence that boulder armor along the Appalachian Mountains, characterized by a temperate climate, has remained relatively unchanged since glacial times. These studies potentially offer insights into how the production and characteristics of boulder armor change with increasing distance from the glacier terminus. It is essential to note that the lithologies in these locations are composed of resistant quartz-rich sandstones. Along the Appalachian Mountains, the terminus of the ice sheet during the Last Glacial Maximum (LGM) reached into northeastern Pennsylvania (Braun, 2004).

Both Denn et al. (2017) and Del Vecchio et al. (2018) conducted their studies within Pennsylvania, with Denn et al.'s study area situated merely 2 km from the terminus of the ice sheet, while Del Vecchio et al.'s study area is further south in central Pennsylvania. In both locales, boulder armor manifests as a boulder field, forming a blanket over the underlying

regolith. The genesis of these boulders is attributed to glacial temperatures sufficiently cold to facilitate frost shattering of bedrock. From the shattered bedrock, resistant units dislodged, tumbling down the valley flanks. Both studies highlight that the boulder armor in Pennsylvania is a multigenerational feature, persisting across several Pleistocene cycles, indicating high endurance over geomorphic timescales. These locations experienced conditions cold enough for frost shattering at multiple points during the Pleistocene. However, it is anticipated that closer to the glacial terminus, frost shattering would be more intense, resulting in higher boulder production, reflected in the thickness of the boulder armor ranging from 3 to 10 meters in both locations. Nevertheless, in these areas, transport processes seem relatively weak outside of the initial tumble when boulders are liberated from the resistant rock unit. This may suggest that in locations closer to the ice sheet, the constant cold may lead to the shutdown of boulder transport via creep processes due to the absence of freeze-thaw cycles. Consequently, boulders accumulate, forming extensive and thick boulder fields in both locations. Once conditions warm up, the boulder field becomes so extensive and thick that creep processes struggle to transport boulders downslope. The system essentially becomes clogged by boulders and may only resume transport when the boulders themselves chemically or physically weather away to a smaller size. Moreover, the boulder armor serves as protection for the underlying regolith, preventing its conversion into soil. This is evident in Del Vecchio et al.'s (2018) field site, where certain portions of the boulder field have weathered down, allowing regolith to separate the boulders and facilitating solifluction that transports boulders with the moving regolith. However, as one moves southward away from the ice sheet, trends in boulder production and transport appear to change.

Fame et al. (2023) directed their research efforts to the Appalachians of central Virginia, a location significantly farther away from the terminus of the Last Glacial Maximum (LGM) ice

sheet. In this area, while boulder fields indicate initial shattering occurred, there is also evidence of discrete boulder armor similar to that observed in the Flint Hills. Although boulders in these locations were formed during glacial periods, the distribution of the boulder armor suggests that conditions were periodically warm enough to enable freeze-thaw creep-related processes to transport and disperse boulders across the hillslopes. While Fame et al. (2023) does not explicitly delve into the drivers of boulder production, it is inferred that, being at a similar latitude as the Flint Hills (Chapter 2 and 3), boulder production in central Virginia may have been either a slower or more discreet process compared to the Pennsylvania locations.

Drawing insights from various studies, including my findings in the Flint Hills, we can formulate hypotheses about changes in boulder production and transport when transitioning from colder-drier climates near the ice sheet to warmer-wetter climates further away. In the coldest locations near the ice sheet margins, high boulder production may result from frost shattering of rock, while transport is limited due to consistently cold and dry conditions, inhibiting creep-related processes. Moving southward away from the ice sheet, boulder production slows, but increasing moisture levels and temperature fluctuations enable creep processes to transport boulders downslope (Chapter 2 and 3). On the landscape, this might be reflected in the prevalence of more boulder fields or talus cones in cooler-drier climates, whereas in moister temperate climates, discrete boulder armor is scattered across hillslopes, separated by areas of soil or weathered regolith. The soil can then transport and move around the boulder via creep related processes like freeze-thaw heave or shrinking and swelling of soils. This trend from colder climates may also be mirrored in the transition from more temperate to warmer-drier climates.

In various semi-arid locations, such as those studied by Schumm (1967), Guitérrez et al. (2010), Boroda et al. (2011), Sheehan and Ward (2018), and McCarroll et al. (2021), boulder armor is a common occurrence. Similar to other landscapes, the production of boulder armor in these semi-arid environments is intricately linked to climatic variables. In an arid landscape, McCarroll et al. (2021) propose that extensive colluvial armor aprons formed below the Book Cliffs, UT during different periods of the Pleistocene and persist as talus flatirons today. The layered landscape of the Colorado Plateau serves as an excellent example of how arid landscapes preserve boulders and colluvial armor. This preservation is more related to the lack of a transport mechanism rather than a lack of boulder weathering. Both McCarroll et al. (2021) and Sheehan and Ward (2018) report that the sandstones in the region are poorly cemented and weather away relatively quickly. The only processes capable of removing these boulders are ongoing gullying on the weak underlying shale causing boulders to tumble into the fluvial system (Sheehan and Ward, 2018; McCarroll et al., 2021) or sheet wash lubrication and expansion/contraction of weathered shales (Schumm, 1967). In either case, in arid locations, boulder transport seems to be limited to the ability of diffusive hillslope properties to remove them, which, again, appears to be ultimately a function of moisture. Therefore, temperate climates with sufficient moisture may be locations where discrete boulder armor, resulting from hillslope processes, can effectively move and spread-out boulders deposited on hillslopes, whereas drier locations, while capable of boulder production, may be more likely to experience boulder accumulation due to poor transport efficiency.

5.4.61 Boulder weathering in the Flint Hills

In cases where boulders are too large to be transported, or conditions are unsuitable for transport, in-situ weathering becomes the sole pathway for the removal of boulder armor from

the hillslope. For instance, the quartzite boulders armoring hilltops in northeastern Kansas (Aber, 1991) are relict features from the Pre-Illinoian glaciation, persisting for at least half a million years, underscoring the potential for boulders to be extremely long-lived features. Studies such as Fame et al. (2023) and Dunn et al. (2017) corroborate this possibility.

Examining the limestone blocks in the Flint Hills, utilizing data and observations from Chapters 2 and 3, we can estimate the lifespan of a boulder on the Flint Hills slopes. In Chapter 2, boulder armor on the hillslope beneath the Cottonwood limestone generally disappears at approximately 30 meters downslope from the cliff. As such we can assume that this is the average distance a boulder can be transported while it is undergoing weathering in this landscape. Beyond this distance most of the boulder have weathered down to a size that can be considered to be part of the underlying regolith. In Chapter 2, I establish that boulders on the hillslope below the Threemile limestone age at approximately 821 years per meter downslope. If we assume constant weathering, we expect, based on this age trend, that a 1m^3 boulder would weather away to nothing in approximately 24.6 thousand years. However, weathering is not constant, and it may take longer for them to completely weather away. Boulders older than 25 thousand years would be expected, if not rarer, especially considering the occurrence of blocks larger than 1m^3 at a relatively frequent rate (Chapter 2 and Chapter 3).

Nevertheless, this time frame allows for a certain number of limestone boulders to persist through interglacial periods, which generally last between 10-15 thousand years (Winograd et al., 2006). This leads to another intriguing question: "How old is the Flint in the Flint Hills?" Now, it becomes apparent that the flint, being more resistant to weathering than the limestone, may be considerably older. If the flint fragments and nodules exhibit weathering resistance comparable to the quartzite boulders related to the Pre-Illonian glaciations, then there is reason to

suspect that the ubiquitous flint in the landscape might be significantly older, encompassing several glacial periods worth of time, compared to the limestone armor. The veneer of flint across the landscape could indeed be the most relict features of this landscape. Further research could attempt to constrain the weathering rate of the flint to verify this hypothesis, or future advances in geochronology may provide insights into the age of the flint in the Flint Hills.

5.4.62 Stratigraphic architecture, geometry, and boulder armor interactions

Chapter 4 of this dissertation revealed a fascinating feedback relationship between boulder armor and stratigraphy in layered landscapes. The optimal spacing of resistant layers relative to the thickness of the erodible package separating them, referred to as the Hardness Ratio (HR), played a crucial role in influencing hillslope adjustment. This optimal spacing seemed to be governed by the geometric relationship between the spacing of resistant layers, the length of the hillslope formed between them, and the amount of boulder armor on the hillslope. When resistant layers were too close together, the resulting erodible hillslope was short and steep, causing boulders to quickly move down the hillslope without effectively shielding the lower portion. On the other hand, when the resistant layers were too far apart, the hillslope became too long, and boulders would weather away before reaching the bottom, leading to faster weathering and material transport in those areas compared to the portions with boulder armor. The optimal range, where hillslopes between hard layers were completely armored, provided the most efficient protection against hillslope weathering and transport. The optimum spacing and thus optimum armoring results in a slowdown effect that preserves the hillslope longer than if it was not armored at all or armored inefficiently. Beyond the armor over time the resistant layers themselves are removed periodically leading to cyclic changes to rates of erosion. The removal of the topmost layer of armor resulted in periods of increased hillslope activity, as the softer

portion of the hillslope below it was rapidly removed. This "landscape heartbeat" or dynamic equilibrium is further complicated by the noise introduced to the movement of blocks on the hillslope.

In the model, block movement was simulated as blocks "falling" or "tumbling" down the hillslope to the next position, a simplification inherited from the original version created by Glade et al. (2017). However, in the presence of blocks, the "heartbeat" signal in the model exhibits more noise, as discussed in Chapter 4. This "heartbeat" serves as a primary observable signal even amid the noise associated with the activity of the boulder armor. Nevertheless, for soil-mantled landscapes where creep-driven movement of blocks is the primary mode of transport (Chapter 2), our models should accurately reflect this reality. A creeping block, hypothetically, would introduce a more subdued effect and contribute less noise to the "heartbeat". While a tumbling block enables the sudden downslope movement of all the regolith it trapped behind it, causing an abrupt increase in sediment fluxes, a slowly creeping block might function more like a very slowly moving dam. The creeping nature would impede the sudden release of trapped sediment, mitigating sudden landscape changes and dampening the overall effect on that "heartbeat". Considering the climate dependence of armor production, the "landscape heartbeat" may be further complicated by the overlaying of climatic forcing. If periods of armor production are relatively spaced apart, there could be times of relatively high landscape change, as the protective armor erodes away, allowing uninterrupted regolith movement. The beat of this cyclic process may be a function of climatic variables changing over geologic time, resulting in a longer-term pattern of speeding up and slowing down.

In actual landscapes characterized by varying thicknesses and spacing of resistant layers, certain sections of the heterolithic hillslope efficiently acquire armor. However, the intricate

processes by which resistant layers shed materials can add complexity to this relationship. In some landscapes, resistant layers may shed boulders through block-by-block failure, with discrete cubic boulders slumping off limestone benches and settling on the hillslope below. In other instances, material shed from resistant layers may manifest as rock falls or collapses, depositing multiple boulders as a jumble of colluvium that is not easily transported by creep-related processes. Therefore, it proves useful to conceptualize boulder armor on a sliding scale (see Figure 5.2), where colluvial blankets with a dense boulder cover represent one end and discrete boulders scattered across the hillslope fall somewhere in the middle. In either end-member case, the armor effectively protects sections of the hillslope. However, a colluvial blanket may induce the most extreme form of slope protection, leading to topographic inversion (e.g., Mills 1981, McCarroll et al., 2021). On the other hand, scattered boulder armor, as observed in the Flint Hills, may result in less visually drastic landscape outcomes but can subtly modulate erosion and hillslope evolution (e.g., Glade et al., 2019, Chapter 4).

of the boulder armor could ultimately be removed, resulting in accelerated landscape change due to the lack of protection. In the case of the Flint Hills, I propose that interglacial periods are a time of inefficient transport with little new boulder production due to inefficient climatic-geomorphic feedbacks.

To test this hypothesis, I can utilize the geochronology data and estimate rates of block transport obtained from Chapter 2 in the context of the geologic setting of the Flint Hills to estimate residence times. The rate of boulder transport via creep on a hillslope with a limestone bench at the top and approximately 30 meters of soil-mantled hillslope below before intersecting another limestone bench is considered. Assuming an apparent transport rate of 1.0 mm/yr, it would take a boulder approximately 30,000 years to travel from the top to the bottom of the hillslope section, provided transport remains constant and the boulder does not decrease in size. Extending our consideration to transport down the entire hillslope to the stream channel, approximately 100 meters downslope of the limestone bench, the transport duration would be 100,000 years. Both timeframes fall within the duration of a glacial period. However, as discussed in the previous section (**5.4.59 Boulder weathering in the Flint Hills**), we might expect that many of the limestone boulders will have weathered down to a size that would be considered part of the regolith much before they reach the age of 100,000 years.

Boulder weathering is not perfectly efficient, so it may be the case that some older boulders are represented somewhere on the entire hillslope. To find these older boulders, we may need to focus our attention on a different portion of the landscape. Steeper, long continuous multi-layered hillslopes not interrupted by a stream channel might be one such location. Older boulders may accumulate near the bottom but be smaller than the boulder-sized fragments sampled in Chapter 3. Determining which boulder or fragment came from which limestone layer

might be challenging, requiring some form of geochemistry or specialized sampling methodology. Another location worth investigating for older boulders is below the Cottonwood Limestone. This approximately 2-meter thick limestone, which was the focus of study in Chapter 2 and Chapter 3, produces large boulders that may persist on the landscape for much longer periods compared to the approximately 1m³ boulders produced from the Threemile limestone. Furthermore, it is relatively isolated from the layers above and below it, and any boulder sampled on these hillslopes would exist solely on that hillslope for its lifetime. This analysis underscores the potential for boulders to preserve a much longer history of activity. Boulder armor can also weather while emplaced on the hillslope, as shown in Chapter 2, and must be considered as a pathway for removing armor.

Expanding beyond the Flint Hills, in regions featuring glacial climate-related boulder armor, a similar pattern of production may reasonably be assumed. Cool glacial periods significantly surpass interglacial periods in duration. Additionally, given a boulder's lithology (limestone versus quartz-rich sandstone), it can easily persist in the landscape through an interglacial period. This suggests that some boulder armor in certain landscapes could be produced and transported cyclically over extended timeframes, spanning multiple glacial and interglacial periods, influencing landscape evolution across geomorphic time under different climatic conditions.

During cooler glacial periods, an increased removal of resistant cap rock might be anticipated. This observation aligns with findings discussed in Chapter 3 and in other temperate regions (Del Vecchio et al., 2022; Fame et al., 2023), where caprock removal appears to be more prominent during glacial times and less active during non-glacial periods. Then, during the interglacial periods, creep-related processes move the blocks around on the hillslopes. The

efficiency of transport is directly connected to underlying lithologic and climatic variables, which are discussed in detail in Chapter 2. Hypothetically, boulder armor is a long-lived geomorphic variable that should be considered for hillslope evolution on at least Holocene and Pleistocene timescales. The cyclic nature of its production and transport, influenced by climatic variations, plays a vital role in shaping landscapes over extended geological timeframes.

5.5 Synthesis – New Flint Hills insights

The research in this dissertation draws its inspiration from the stairstep landscape of the Flint Hills and its distinctive stairstep hillslope morphology. While it's easy to overlook such landscapes, given their central location within North America far from centers of recent uplift, they have been overlooked as a focus of geomorphic investigation. The apparent dynamic nature of the Flint Hills and similar layered landscape (i.e. Denn et al., 2017; Del Vecchio et al., 2022; Fame et al., 2023) provides opportunities to advance our understanding of geomorphology and uncover new insights concerning hillslope processes in relation to boulder armor.

5.5.64 Long timescale behavior of the Flint Hills

A question that arises from this region, as noted by Macpherson and Sullivan (2019), pertains to the apparent slower rate of erosion in the Flint Hills compared to erosion rates calculated using geochemistry-based methods. Considering the age of the exposed Permian rocks, the known thickness of rock layers, and an assumed denudation rate of 0.02 mm/year, it's puzzling that the Permian rock hasn't eroded completely. Macpherson and Sullivan suggest that the presence of calcite-rich dust could explain the too-high denudation rate. They propose that chemical weathering at the surface may preferentially target the dust, slowing the overall weathering process. However, this hypothesis remains untested in the field or in model space.

The simulations of layered landscapes conducted in Chapter 4 can help unravel the mismatch between expected landscape relief and what remains in the landscape. The data presented in Chapter 4 suggest that landscapes like the Flint Hills can achieve higher-than-expected relief due to a combination of resistant layers and boulder armor. In particular, the presence of boulder armor, a signature characteristic of the Flint Hills, has a significant effect on the relief of a landscape, especially at lower uplift rates. When boulders are present, the virtual landscapes can be 10-15% taller than when boulders are not present. The influence of the presence of layers is slightly more complicated. When resistant layers are spread far apart, the landscape behaves more similarly to one without any resistant layers at all. However, when there are more layers closer together, with a higher Hardness Ratio (HR, Chapter 4), the topography can be between 5-7% taller. Therefore, assuming that over long geologic times, boulder armor is present, its effect on modulating erosion could be one factor in slowing down the rate of landscape erosion. In these models, we observe that a denudating hillslope takes considerably longer to adjust and reach equilibrium compared to hillslopes experiencing a rise in the rate of uplift or incision. These adjustment times span million-year timescales when all factors remain stable after the uplift change. However, climate fluctuations over this time scale could theoretically slow down activity at certain periods like in the Flint Hills (Chapter 3).

This echoes the findings of Ward (2019) in his modeling experiments with tilted layered landscapes. Ward (2019) suggests that hillslopes and cliffs within layered landscapes can hold valuable information about past conditions due to their relatively slow rate of change, especially when compared to the rapid shifts in boundary conditions like uplift, river incision, or climate. The extent of information preserved in the form and geomorphic properties of a cliff or hillslope may be debatable. For a landscape like the Flint Hills, where the underlying rocks are flat lying,

they may be more informative in preserving uplift and river incision compared to features preserved in tilted rocks. Chapter 4 suggests that given enough time and in steady state, a layered landscape hillslope will attempt to become an overall convex shape punctuated by convexities related to where the resistant layer outcrops. When an increase in uplift was introduced, a “knickpoint” could sometimes be observed propagating up the hillslope as the heterolithic hillslope adjusts. This observation may suggest that relatively flat-lying rock may be better at preserving uplift and incision rate changes compared to tilted rock.

The exposure ages of hillslope boulder armor (Chapter 3) reveal that armor transport, boulder generation, and bench retreat primarily occur during glacial periods when climatic variables are favorable. Layzell and Mandel (2020) show that the mobile regolith and fine-grained portions of the hillslopes are actively transported due to vegetation changes controlled by climatic variation over the Holocene. In the context of MacPherson and Sullivan's (2019) findings, the mismatch between streamflow-based denudation calculations and the presumed excessive relief of the landscape could result from the partitioning of hillslope activity. Different portions of the hillslope may become active in weathering and transport under specific conditions. Glacial conditions are essential for removing resistant portions of the hillslopes, while climate fluctuations are needed to mobilize finer-grained soil and regolith for transport. Inactive benches and caprock hold up the landscape, even if weathering and transport of the softer lithology are actively ongoing. The presence of boulder armor, while protecting the softer lithology from weathering, may also trap otherwise mobile regolith.

The observed stop-and-go denudation pattern and the prolonged adjustment times in the models (Chapter 4) may perhaps be applicable to the geological reality of the Flint Hills over geologic time. However, it's important to emphasize that these changes should be viewed as

temporary perturbations within the broader trajectory toward equilibrium, aligning with the rate of uplift or river incision. Modeled hillslopes (Hardness Ratio = 0.4 with boulder armor present) that showed this behavior took an extra 1 to 2 million years longer to adjust which is 2 to 4 times as long compared to when boulders are absent. At higher Hardness Ratios it could be argued that the landscapes never truly reached equilibrium before the end of the model run. Once again, the presence of both boulder armor and heterolithic stratigraphy on the hillslope scale is the source of this protracted path to equilibrium. Without boulder armor heterolithic hillslopes act closer to the as if they had no resistant layers at all (i.e. Johnstone and Hilley, 2014), simple soil mantled hillslope. According to the modeling results, the protracted adjustment of this landscape can be attributed to its nature as a denudating layered landscape. Lowering the landscape effectively involves the removal of the uppermost caprock supporting it. This process becomes particularly challenging when the caprock is undermined through diffusion, providing additional protection to the hillslopes beneath it and thereby slowing down the overall landscape adjustment process. Only upon the removal of this uppermost layer can the landscape initiate more rapid denudation, as illustrated in the simulated models (Chapter 4).

Nevertheless, over geological timescales, these factors could contribute to the variation in material removal from the landscape and result in a slower-than-expected rate of denudation, as highlighted by MacPherson and Sullivan (2019). When these factors interact, the landscape denudates at a slower rate over extended periods than expected when calculating the denudation rate based on the current landscape. The interplay of climate, armor, and stratigraphy requires a nuanced understanding of the varied conditions, and their temporal dynamics are crucial for accurately interpreting the geological history of the Flint Hills and other similar layered landscapes. However, as demonstrated in this dissertation, their interactions can be complex, and

thus further attention will be needed to understand and quantify how they affect the evolution of layered landscapes. Modeling exploring the effects of climate, most easily varying diffusivity over time, will need to be explored within the model space developed in Chapter 4. In my modeling, climate was explicitly ignored due to its complicated factor in landscape activity but may be useful to explore in a model set up where the uplift of the hillslope is kept constant through time. Boulder movement rules would also need to be updated to more accurately reflect how boulders move in soil-mantled hillslopes via creep. To fully reflect the reality of boulder movement, diffusion would have to be connected to the rate of movement. In the context of the Flint Hills, exploring the interaction between climate, boulder armor, and stratigraphy would provide greater insights into how climate can quicken or slow down landscape denudation.

5.5.65 Boulder and armor dynamics

In the Flint Hills, the presence of hillslope armor, primarily sourced from limestone layers, is a ubiquitous and prominent feature. This armor has a significant impact on landscape evolution, as discussed in Chapter 3 and in previous studies by Glade et al. (2017) and Glade et al. (2019). However, in the Flint Hills, there has been a lack of a clear hypothesis regarding when and by what mechanisms this armor is formed. While it may be a common assumption that boulder armor production is a relatively continuous and uniform process (Yeend, 1973; Koons, 1981), this notion is challenged by previous research conducted in other regions that links armor production to specific climatic conditions (Denn et al., 2017; McCarroll et al., 2021; Fame et al., 2023; Chapter 3). Boulder armor production in the Flint Hills is tied to cooler climatic conditions, particularly during the Pleistocene that can drive increase creep efficiency (Chapter 2 and Chapter 3). The production and placement of armor on hillslopes predominantly occurred during Ice Age conditions (Chapter 3). These boulders and rock fragments are primarily

transported through creep, as the relatively low gradient of these hillslopes makes tumbling an uncommon form of downhill transport. Even in the present-day, with changing climate conditions that have apparently led to a cessation of boulder production, some degree of creep transport likely continues, albeit at a reduced rate compared to the peak glacial periods.

Different portions of the hillslopes in the Flint Hills exhibit activity at distinct times, and the composition of materials transported across the hillslope varies with the prevailing climatic conditions (Layzell and Mandell, 2020; Chapter 3). This leads to the proposal of a new conceptual model for Flint Hills hillslopes, primarily driven by variations in the efficiency of creep and physical weathering during glacial and interglacial periods. During glacial periods, resistant limestone layers actively generate new boulders, and these boulders are effectively transported downslope. However, during interglacial periods, boulder production decreases, and the rate of boulder transport slows down. Any hillslope activity during interglacial periods is primarily associated with the movement of fine hillslope materials downslope (Mandell and Lyzell in 2020).

Interestingly, there is anecdotal evidence of ongoing boulder movement via creep or sliding, and this movement results in the armor shifting slightly downslope. This activity creates a small gap on the upslope side between the boulder or rock fragment and the soil that has accumulated on the upslope side of the boulder. Furthermore, some of these boulders look like they have overridden grasses that now appear to grow out and around the overriding boulder or fragment. These grasses may also act to reduce friction and cause downslope movement. The coefficient of friction between the limestone boulder and the grass may be lower compared to the boulder and the underlying soil. Alternatively, wetted grass may be a relatively low friction surface and thus allow movement during intense rain events or high snow melt events. An

investigation of this process is outlined in the following section below (**5.7.69 Creeping boulders and grass sliding**). This process could be an interesting part of the overall dynamics of Flint Hills hillslopes.

5.5.66 Hillslope erosional signals

The geochronology data from Chapter 3, focusing on two spatially and stratigraphically separate sets of bedrock benches and boulder armor, indicates a synchrony in the timing of activity between these sets. This observation leads to the conclusion that the activity of limestone benches is synchronous across the entire hillslope. I have therefore proposed that in the Flint Hills, geomorphic activity over the Holocene and Pleistocene has been primarily driven by climatic factors.

However, the presence of resistant layers, interrupting the mostly diffusive softer units, leads to the propagation of "knickpoints" up the hillslope (Chapter 4). In the model, these knickpoints can be attributed to various factors, such as interactions between boulders, diffusion, uplifting landscapes, or changes in uplift rates. The model demonstrates a wave of activity moving up the hillslope, with accentuated changes occurring as we move upward through the landscape. This implies that in a bottom-up driven landscape, the lowermost layers are the first to feel the full effect of changes. The question arises as to whether actual layered landscapes exhibit a similar trend of the lower most bench being active before the uppermost benches on a hillslope. A new chronology of boulders or bench surfaces in this location would show decreasing age of surfaces with increasing elevation of bedrock bench and associated boulders on the hillslope. In the case of the Flint Hills, without significant uplift or incision, there is a conceptual landscape in which signals propagating from the bottom-up may fail to reach the top due to the overriding influence of climatic forcing, resulting in synchronized changes across the hillslopes. This

concept is worthy of further exploration, as it implies that different portions of the landscape may essentially be unaware of the conditions in areas below them, only being affected by the sediment transported from higher elevations. However, further research and geochronological studies across the various limestone benches of the region are needed to validate this hypothesis. I discuss such investigation in the following section (**5.7.70. Expanded cliff retreat chronology**).

One notable result from my modeling in Chapter 4 is the finding that denudating hillslopes take longer to adjust compared to hillslopes with a constant uplift rate (HR hillslopes). The Flint Hills, and the Great Plains in general, can be considered landscapes that have been undergoing denudation for a significant duration. While quantifying this timescale is challenging without comprehensive geochronological data, we can infer, based on my modeling results, that this magnitude of time aligns with the landscape's history. Drawing from the research by Ward et al. (2021), which indicates that the adjustment of strike valleys with tilted rock takes significantly longer compared to fluvial portions of the landscape, it is suggested that hillslopes, hogbacks, cuerdas, and cliffs have likely experienced multiple pulses of erosional signals that have yet to fundamentally alter their forms. As per Ward et al. (2021), these hillslopes are preserving information about past landscape conditions within their morphology. While fully deciphering the signature of these past conditions is beyond the scope of this work, it provides a useful perspective when considering the hillslopes and the overall landscape of the Flint Hills within the context of the modeling of complex hillslopes of layered landscape (Chapter 4). For the portion of the modeling where I simulated denudating landscapes after a significant decrease in the rate of landscape, I believe that it may provide some valuable insights to the dynamics of the Flint Hills.

Denudating heterolithic hillslopes, especially when the spacing between hard layers allows for efficient armoring of the hillslopes, can persist on the landscape for a significant period even after the initial reduction in uplift. Although a specific diffusivity was selected for modeling in the study, it's essential to recognize that diffusivity can significantly vary across landscapes, influenced by factors like climate, vegetation, and underlying rock properties. In the case of the Flint Hills, we have evidence (as discussed in Chapter 2 and 3) that hillslope activity and diffusivity vary with climatic changes. If the region has not experienced recent and significant base-level fall, then the hillslopes in the Flint Hills have been primarily denudating through diffusion-based processes. Given that heterolithic hillslopes are expected to have longer adjustment times, we may anticipate that fluctuations in hillslope transport efficiency, spanning much of the Pleistocene to the present and future, contribute to slowing down the overall landscape adjustment. Periodic slowdowns during interglacial periods may further extend the lifespan of these hillslopes and maintain the relief of the terrain in the Flint Hills. As discussed earlier, researchers have noted that the denudation of the landscape appears to be occurring more slowly than expected. While this phenomenon may not have a single, straightforward explanation, it can be attributed, at least in part, to the intrinsic nature of a denudating heterolithic landscape. This nature results in an overall slower topographic decline, as the process of lowering the landscape is periodically challenged by the removal of resistant lithologies across all hillslopes within the region (**5.5.62 Long timescale behavior of the Flint Hills**).

5.6 The future of layered landscape research

5.6.67 Signal shredding in heterolithic hillslope

In locations where hillslopes are primarily composed of a single lithology, we typically consider these features to undergo diffusive processes. The growth and denudation of such hillslopes progress relatively smoothly, with erosional signals propagating from the fluvial system upward without significant interruption. However, in the case of heterolithic landscapes, a complication arises in the form of a resistant layer that does not erode or change at a rate comparable to the surrounding, more erodible rock. Essentially, this introduces a lithologic knickpoint in the hillslope, akin to what is found in fluvial systems. In my modeling, it becomes evident that any baselevel signal must cause the failure of this hard layer before it can propagate over and beyond the resistant layer. This implies that, depending on the criteria required for a resistant layer to fail, base level signals may become trapped below this resistant layer. While the process by which a resistant layer fails and triggers a step back may vary, the presence of a barrier to erosional signals is still apparent.

The scenarios involving multiple sets of hard layers, we might encounter a significant obstruction to baselevel signals propagating from the fluvial system. Research by Jerolmack and Paola (2010) illustrates that external signals applied to a system can be obliterated depending on the frequency and magnitude of the signal. The signal effectively becomes “smeared” across a range of scales due to the various processes operating within the system at different timescales. In my simulated heterolithic hillslopes, we observe that different processes exert influence at different timescales. These processes introduce “noise” into the system. In the modeling performed in Chapter 3, the shorter time scale processes of boulder movement and resistant layer failure obscure or alter the more periodic long term signals of resistant layer removal. Visual

inspection of the change in elevation through time or mean elevation suggests that there may be autogenic feedbacks between boulders and the landscape that result in non-periodic increases or decreases in the simulated hillslope surface. The method of spectral analysis presented by Jerolmack and Paola (2010)

Future modeling experiments should investigate the fluctuations in the hillslope surface using power spectral analysis to dissect the different cyclic processes that may result in modifying and fragmenting uplift signals. One such cyclic signal that would be of interest is the duration it takes for a resistant layer to be eroded away and the underlying softer lithology to be reduced to the next resistant layer, as demonstrated in Chapter 3. This process exhibits a highly periodic nature and can be detected through power spectral analysis. Much like the work of Jerolmack and Paola (2010), any modeling experiment will need to vary and modulate the uplift to assess how a periodic uplift signal can propagate up a hillslope. An examination of the relationship between HR (hillslope relief) and boulder armor, along with the magnitude of signal fragmentation, may provide valuable insights into whether layered landscapes even register the influence of baselevel signals, even within a simulated context.

5.6.68 Cliff preservation and fracture soil routing

A common feature in the Flint Hills landscape and other layered terrains is the presence of resistant layers that give rise to cliffs or benches with regular fractures and joints. In the context of boulder armor production and the lateral erosion of these resistant rock formations, these fractures facilitate block-by-block retreat. The resistant lithology is already divided into discrete units that, through various processes, can lead to the detachment of individual boulders onto the hillslope below. However, these fractures themselves may play a fascinating role in landscape evolution.

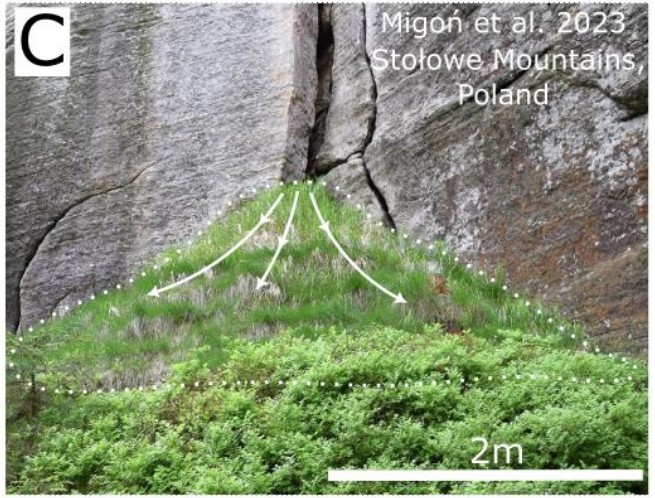
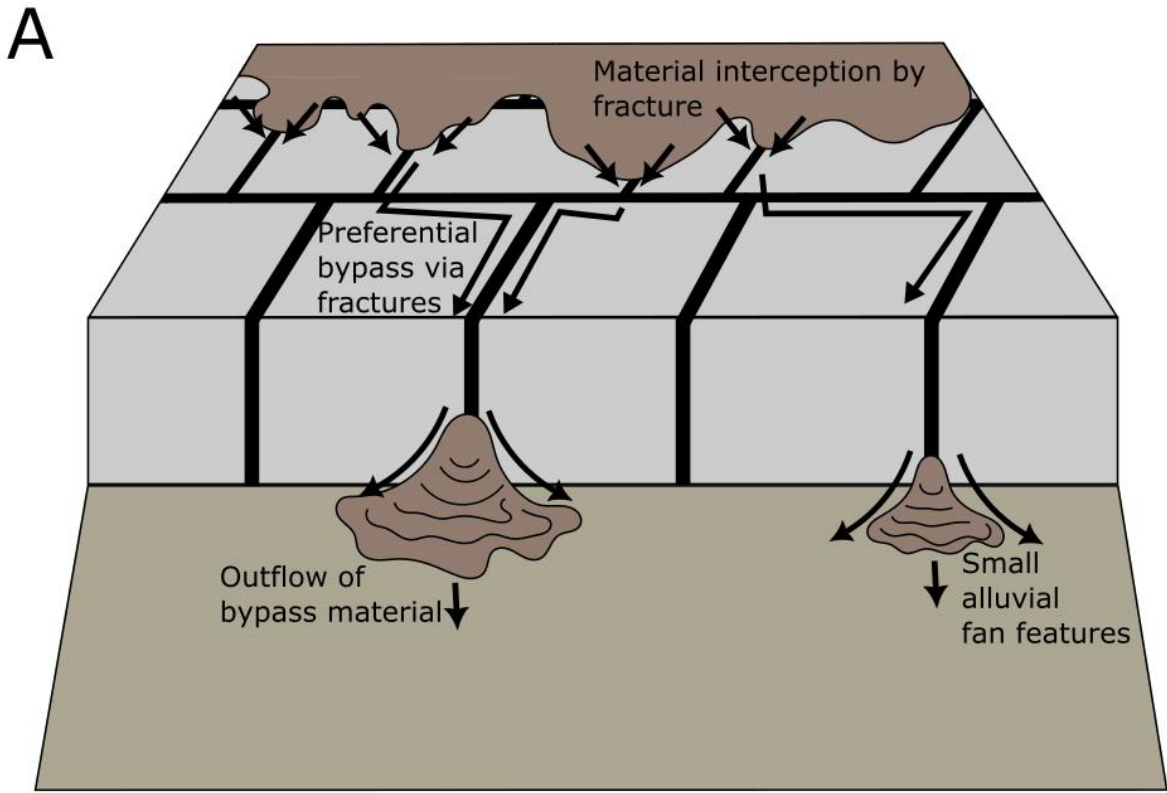


Figure 5. 3 Conceptual model of fracture piping and field examples

a) Model illustrates how fractured and resistant rock, functioning as a caprock or bench former, can channel finer hillslope material through fractures to the hillslope below, ultimately resulting in a bare rock surface. The rerouted soil accumulates below the bench, forming small alluvial fan-like features as it follows the path of fractures. The bypass of soil through fractures serves as one mechanism that generates a bare-rock bench, distinct from surfaces covered or draped under a layer of mobile regolith. b) Example of fracture piping of sediments through fractures of the Cottonwood Limestone in the Konza Prairie portion of the Flint Hills. Arrows have been added to indicate

direction of fracture piping. Dashed lines are used to outline alluvial fan-like features. c) Example of fracture piping of sediments documented by Migon et al. (2023) in Poland. Arrows have been added to indicate direction of fracture piping. Dashed lines are used to outline alluvial fan-like features.

In the Flint Hills, it appears that the regular fractures and joints in the limestone are widened through subsurface dissolution processes associated with karst phenomena. Observations by Migon et al. (2017) and (2023) in a sandstone tabletop landscape in Germany and Poland along with my own observations in the Flint Hills suggest that bedrock fractures may play a crucial role in soil transport around a resistant bedrock unit. As soil moves downslope and encounters the resistant unit, it can be captured in the large cracks and fractures in the rock. These fractures may act as channels, facilitating the preferential movement of sediment past the cliff face (see Figure 5.3) In European tablelands, the scale of these fractures is on the order of meters. Migon et al. (2023) demonstrate that fractures in sandstones can have connectivity resembling those developed in karst systems found in carbonate rocks. These sandstone fracture conduits can transport significant volumes of water, along with weathered and loosened sand grains, through and out of the sandstone caprocks. Migon et al., (2023) report small scale alluvial fans that build up from vertical fractures in the cliff face (Figure 5.3c). In the field area of the Flint Hills, the limestones that are the bench forming rock units are also regular fractured (Frye, 1955). In contrast to the European table lands, the fractures in the Flint Hills limestones are typically much smaller, measuring tens of centimeters in width and around a meter in height at most.

Nevertheless, in both locations, there is evidence (Figure 3A and B) that small fans of material, resembling landscape features like alluvial fans, extend out from the openings of these fractures. The presence of similar features at different fracture scales suggests the movement of weathered material through the rock via the fractures. The process could be termed “fracture piping” as it may share similarities to piping processes that can occur on soil mantled hillslopes

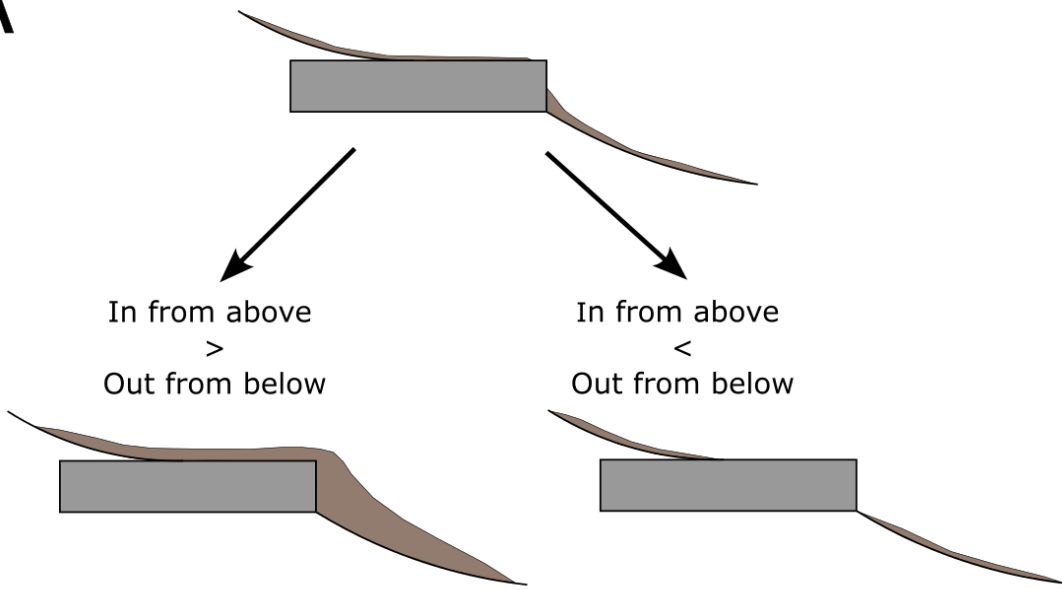
in other settings (Jones, 1994; Jones, 2010). Fracture piping is the preferential transport of weathered regolith or soil through a resistant rock unit via cracks, joints, or fractures rather than over the top and across the resistant rock unit. That fracture piping of regolith through caprock may be a process that can occur across different scales. Integrating fracture piping phenomenon into the model developed in Chapter 3 may also pave the way for future modeling work to establish the influence of fractures before field investigations are conducted. Further discussion of this potential research is provided in the “Future Work” section below. More importantly, the presence of these features in the Flint Hills indicates that material is being transported through these fractures. The role of these fractures may be essential in preserving the exposed rock surfaces of benches and small to moderately sized cliffs in the landscape that are not draped and covered in soil.

In the Flint Hills, the soil mantle covering the hillslopes often stops a few meters before reaching the actual edge of the bedrock bench. If soil transport were continuous, one might expect the soil cover to extend all the way to the edge of the bedrock bench or even drape over it, entirely concealing it. However, what is frequently observed is that the soil is preferentially routed downward into the fractures, where it then gets transported "through" the resistant rock unit. This process preserves a bare bedrock surface. The Flint Hills offer an excellent opportunity to investigate whether fractures indeed play a role in preserving the morphology of bedrock features in a layered landscape, particularly at the sub-hillslope scale. Here, I propose a basic conceptual model of bench morphology that can be expanded to heterolithic hillslopes. This model draws insights from the findings of Chapters 2, 3, and 4, Ward et al.'s (2011) model of cliff evolution, and field observations. Bench morphology, in this model, refers to both the exposure of the bedrock bench and its vertical extent. At its core, bench morphology is a function

of the mass balance between material input from above and material removal from below the resistant layer (see Figure 5.4A).

If more material is removed than is transported in from above, the bench becomes exposed and grows in relief. Conversely, if the material coming in from above exceeds what is being removed, the bench becomes buried and draped in a blanket of regolith. In extreme settings, the resistant bedrock layer is not expressed as a convexity but instead samples a continuous hillslope (see Figure 5.4B). Observations suggest that the presence of fractures allows soil to "bypass" the cliff face, resulting in a bench being exposed when, without fractures, it would be covered in soil. This process is evidenced by small-scale alluvial fan-like features composed of soils extending from fractures within the bench face (see Figure 3). Regardless of the scenario, the balance between accumulation and removal is the primary control on how a bench is expressed in the landscape. This balance may be influenced by factors such as the distance from a drainage or vegetation cover, directly affecting the equilibrium. Ultimately, if true, bench morphology can give a quick glance at the mass balance history of material moving down the hillslope. Zooming out, if this simple model is applied across an entire hillslope it may reveal places of increased sediment fluxes and recent transport conditions. Further investigations are required to rigorously test this model of bench morphology.

A



B

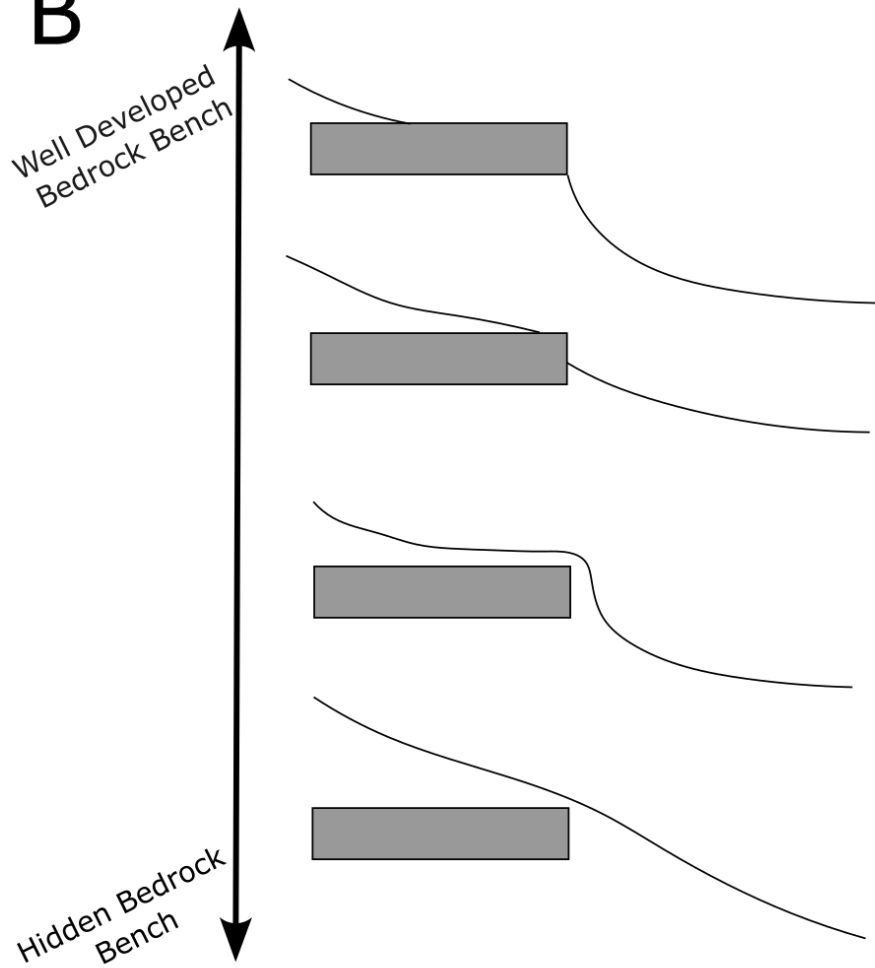


Figure 5. 4 Mass balance model of bench morphology

a) The simplified mass balance model of bench morphology is dependent on the downslope transport of fine hillslope material. In scenarios where more material is traveling over the resistant bench-forming layer than is being removed, the soil cover extends over, drapes, and conceals the layer from view. Conversely, in cases where more material is being removed below the bench than is being transported in from above, a pronounced bench with a vertical drop develops. b) The sliding scale of bench morphologies that may arise from the mass balance model is based on field observations. This scale reflects the continuum of possible bench expressions, ranging from fully covered by soil to exposed with a distinct vertical relief. The observed variations align with the dynamic equilibrium between material input and removal, illustrating the range of bench morphologies that can be encountered in the landscape along a single cliff.

5.6.69 Improved modeling of hillslope armor

In Chapter 4, my modeling approach for hillslope boulder armor was based on the rules formulated by Glade et al. (2017). These rules essentially state that when sufficient relief is created below a boulder, it will “fall” down to the next cell. While this modeling approach replicates one of the processes responsible for material transport down hillslopes, it doesn't capture the actual physical processes that govern armor transport downslope. The transport of boulders is influenced by a complex interplay of forces. For instance, when dealing with a large single boulder located on a hillslope undergoing active erosion, one would need to consider several forces acting on the boulder. These forces include the gravitational pull, the resistance to movement caused by friction, and the force exerted by the regolith trapped behind the boulder, pushing it downslope. Accurate modeling would require determining the boulder's center of gravity to calculate when movement initiates and to predict whether and how far it will tumble downslope. On the other hand, when modeling the movement of smaller rock fragment armor, as observed in Chapter 2, the approach should account for more continuous, slower processes resembling creep. This could involve linking the rate of movement to the rate of soil creep occurring at the surface of the hillslope. Additionally, it might be necessary to simulate the

periodic raising and lowering of armor, a phenomenon driven by processes such as frost wedging and clay expansion.

These proposed improvements would make the modeling of boulder armor more realistic, as there are multiple mechanisms involved in driving boulder transport. However, for a comprehensive understanding, these mechanistic improvements should be coupled with an enhanced understanding of how to model hillslope armor at scales smaller than the resolution of the model. In landscapes like the Flint Hills and other similar regions, hillslope armor varies in size, generally decreasing as you move downslope. Frequently, individual armor units are much smaller than the meter-scale resolution of the model, and there are numerous individual armor units of various sizes within a single model cell.

5.7 Future research in the Flint Hills

The Flint Hillslope still provides opportunities to answer fundamental questions concerning layered landscapes, hillslope boulder armor, landscape dynamics. There are also further opportunities to explore the geomorphology and landscape history of the region.

5.7.70 Understanding bedrock bench and cliff morphology

The primary and commonly cited control on cliff, escarpment, and cuesta morphology is the relative difference in rock properties between the overriding cap rock and the underlying slope or plinth rock, specifically rock strength and resistance to weathering. Essentially, the presence of a significant difference in the rate of the conversion of rock into regolith between two rock units once exposed at the surface is enough to allow the development of cliff-like features. Various factors such as cliff face aspect, vegetation, climate, fracture density, and heterogeneity within the rock itself can lead to differences in morphology across a landscape. However, for cliffs and bedrock benches there is not well-defined understanding as to what

directly controls the expression of a resistant layer as vertical cliff or bare bedrock benches. For example, the limestone bedrock benches here in the Flint Hills, can range in morphology and expression. Moving along a bedrock bench in the study area various expressions of cliff morphology can be observed (Figure 5.4b). In some places there is a well-developed bench with a vertical face and top where the soil has been stripped away in other the cliff is hidden below a cover of regolith a continue surface connecting the hillslope above and below the resistant layers. These observations prompt the question of what controls how a lithological difference is expressed in a hillslope setting. The Flint Hills present an excellent opportunity to investigate the processes and factors that control bench morphology. Field observations suggest that the primary control on bench morphology in the Flint Hills is the balance between the regolith provided from the hillslope above the edge of the bedrock bench and the rate at which the regolith is removed from below the bottom of the bedrock bench (Figure 5.4a). Ward et al. (2011) proposed a similar concept for large arid escarpments in the American Southwest. In this case, if debris production from the caprock is higher than the rate of debris weathering and removal, the cliff can bury itself. In the Flint Hills, the bedrock bench does not appear to produce enough sediment to bury itself; instead, sediment from the higher portions of the hillslope above a given bench is what can bury the bench.

The balance between the input of regolith that may blanket the bench and processes removing that regolith is influenced by several factors. The presence or absence of extensive fractures or joints is one such factor, as these features can affect the lateral transport of regolith past the edge of the bench-forming unit (Migon et al., 2023). The width and density of fractures may vary laterally across the landscape, partially controlled by ongoing karst activity in the subsurface. If fractures are absent or not wide enough, regolith must travel across the bench

surface, potentially covering it. Another factor that may control bench expression in the Flint Hills is the bench's relative position on the hillslope, including its aspect, distance from a drainage, and position on a convex or concave portion of the hillslope (Temme et al., 2022). Anecdotal observations suggest that well-expressed benches are often found on convex portions of the hillslope, pointing outward, while less developed benches are in concave areas. Differences in exposure to the elements and vegetation density may play a role in these variations.

Understanding the factors and processes that control the morphologic expression of resistant layers as bench or cliff features may enable the decoding of information preserved in the larger hillslope or cliff system morphology. According to Ward (2019), cliffs, hogbacks, cuestas, and similar features may preserve information in their morphology about long-term changes in landscape boundary conditions, such as river incision or climate fluctuations. Cliffs and similar features may adjust on timescales that are comparatively slower than the drivers of landscape evolution like river incision, preserving important landscape history information if decoded. The first step in decoding the morphology of cliff and, by extension, hillslope systems developed in layered landscapes would be to target and understand the morphology of individual small benches and cliffs. Future investigations should focus on different aspects of the bench system in the Flint Hills.

5.7.71 Creeping boulders and grass sliding

In the current conceptual model of rock fragment and boulder movement in the Flint Hills, as based on the findings of Chapter 2, the dominant mechanism is creep-driven transport. However, there have been anecdotal field observations suggesting that boulder movement, in some instances, has occurred more recently. This movement is evidenced by “imprints” on the

upslope side of rock fragments, formed into the soil that has collected on the upslope side of the rock. These imprints indicate that the rock fragment has moved several centimeters in the downslope direction. Additionally, observations include grasses that appear to have been partially overridden by a creeping boulder, with the grass having to grow around the now-overriding boulder or rock fragment.

The frequency of these features across the hillslopes of the Konza Prairie area in the Flint Hills appears to be relatively rare. Nevertheless, these observations suggest that some movement events are small-scale, sudden in timing, and have occurred relatively close to the present, within the lifetime of a grass that has established itself in a location and is now growing out from under the rock fragment or boulder that has moved over them. The mechanisms allowing for such short-distance, rapid movement could be related to sheet wash during high-intensity storms. Schmidt (1967) reported on the movement of rock fragments on bare shale slopes due to friction reductions resulting from sheet wash lubrication. Future research in grassland hillslopes should investigate the processes behind relatively sudden, short-distance movements. While sheet wash lubrication may be a plausible driver of downslope movement of boulders, there could be an alternative mechanism for friction reduction on these hillslopes.

One possibility is that when a boulder creeps over a clump of grass, the grass beneath the boulder may act as a source of surface friction reduction. There is also anecdotal evidence of recent movement due to grass stems growing out and around the downslope side of the boulder that has shifted over the plant at some time in the recent past. This grass may facilitate faster creep compared to the forested portions of the Flint Hills landscape. Grass stems, especially when wet, may act as a smooth, slippery surface, like a slide, that allows blocks to glide more easily than over bare soil. This reduction in friction may be particularly significant when the

grass is wetted during rainy periods. This process of “grass sliding” could occur during storm events when sheet wash is at its highest, and the movement of water may get underneath the boulder or rock fragment, fully lubricating it and allowing it to move under its own weight. Once a block gets moving and overrides more wet grass, it can slide even further due to the grass acting as a slippery surface.

To explore this further, a series of physical experiments could be conducted to test the likelihood of rock fragments sliding on hillslopes that resemble those of a grassland hillslope and replicate the hillslope gradient where these rock fragments and boulders are found. This would help clarify the role of grasses in friction reduction and movement events on these hillslopes. Conceptually, this “grass sliding” would allow faster or further movement on grassland hillslopes compared to those in forest settings where there is no grass on the forest floor. However, the frequency or likelihood of this process would have to be explored by future research. One possible observation that can be used to test if this process may be occurring is seeing the maximum distance that boulders or large rock fragments occur downslope relative to the cliff in both grassland and forest settings. Hypothetically, blocks and fragments in the grassland settings should reach further down the hillslope compared to those in a forested setting due to this proposed “grass-sliding” process.

Directly measuring the rate of boulder creep may be quantified using geochronology, in this case optically stimulate luminescence. The soils in the study location are in part composed of loess that can be measured using luminescence techniques because they are composed of quartz. As the boulder slowly creeps over the soil the quartz grains are “buried”, where the boulder prevents light from beaching the grains in the near surface. As the boulder moves in the downslope direction new portions of the hillslope will be protected. The OSL signal

would accumulate while the soil surface is covered, and going from the upslope to downslope side of the boulder the OSL signal would decrease (Figure 5.5). The rate of this decrease would reflect the rate of boulder movement. A sequence of samples would need to be taken from underneath a large enough boulder to be sure that bioturbation is left to a minimum.

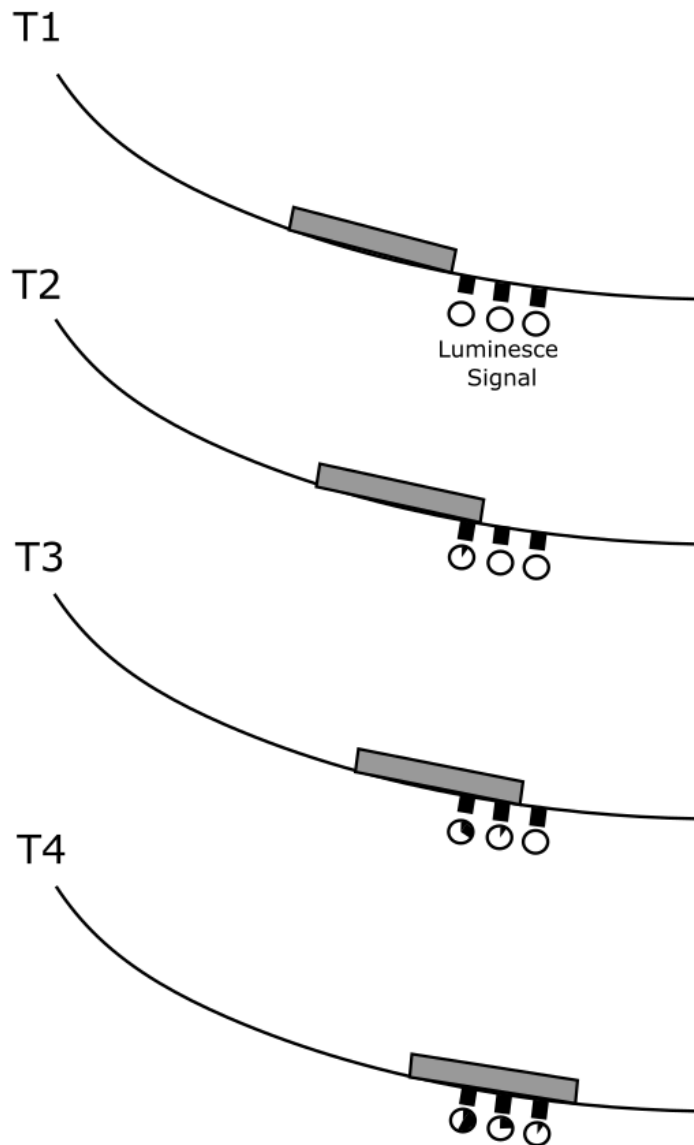


Figure 5. 5 Optically stimulated luminescence record of block movement

A conceptual model illustrating how the movement of a boulder over a hillslope could influence the luminescence signal of surficial material through time. This impact on the luminescence signal may be measured through sample collection from beneath the boulder.

5.7.72 Expanded cliff retreat chronology

The evidence presented in Chapter 2 suggests that limestone bench retreat and armor transport occur contemporaneously across the two sample locations, which are separated vertically in the stratigraphy. The proposed explanation in Chapter 3 is that climatic forcing

primarily drove Pleistocene cliff evolution, a relatively uncontroversial conclusion supported by various investigations into hillslope activity, cliff retreat, and lateral erosion in different locations and climate types (Denn et al., 2017; McCarroll et al., 2021; Layzell and Mandel, 2020; Fame et al., 2023; Chapter 3). However, it remains unclear whether the ultimate driver of landscape evolution, the lowering of baselevel, exerts a strong influence on the higher portions of the hillslope due to signal shredding (e.g. Jerolmack and Paola, 2010). This can be challenging to assess, especially considering that erosional signals within the landscape may become fragmented as they propagate up the hillslope, interacting with mobile hillslope armor and multiple resistant limestone layers.

The behavior of the hillslopes in the Flint Hills can be conceptually distilled into two end-member models (Figure 5.6). The top-down, climate-driven model posits that all portions of the hillslope exhibit similar timings of bench activity (e.g., bench retreat and armor production) due to climatic forcing. The Holocene record demonstrates that climatic fluctuations cause pulses of fine material to move from the hillslopes into the stream valleys. Chapter 2 suggests that more optimal climatic conditions during the Last Glacial Maximum increased the rate of block-by-block failure of the limestone layer and enhanced transport. In this model, because climatic variables affect the entire hillslope, the resulting geochronology across all portions of the hillslope would be contemporaneous, with all benches shedding material and retreating laterally.

In contrast, the bottom-up baselevel incision-driven model proposes that a propagating incision signal moving up the hillslope would cause periods of activity at each limestone bench, with geochronological ages becoming older as you move toward the top of the hillslope. In this scenario, rather than distinct periods of boulder ages or surfaces, a systematic change might be observed as you move up the stratigraphy toward the top of the landscape. The expected pattern

of retreat rates may involve a slowing of retreat as you move away from the ultimate driver of activity, the fluvial system. However, if this pattern exists, substantial future geochronological work will be required across multiple limestone benches in vertical succession to test the proposed ideas.

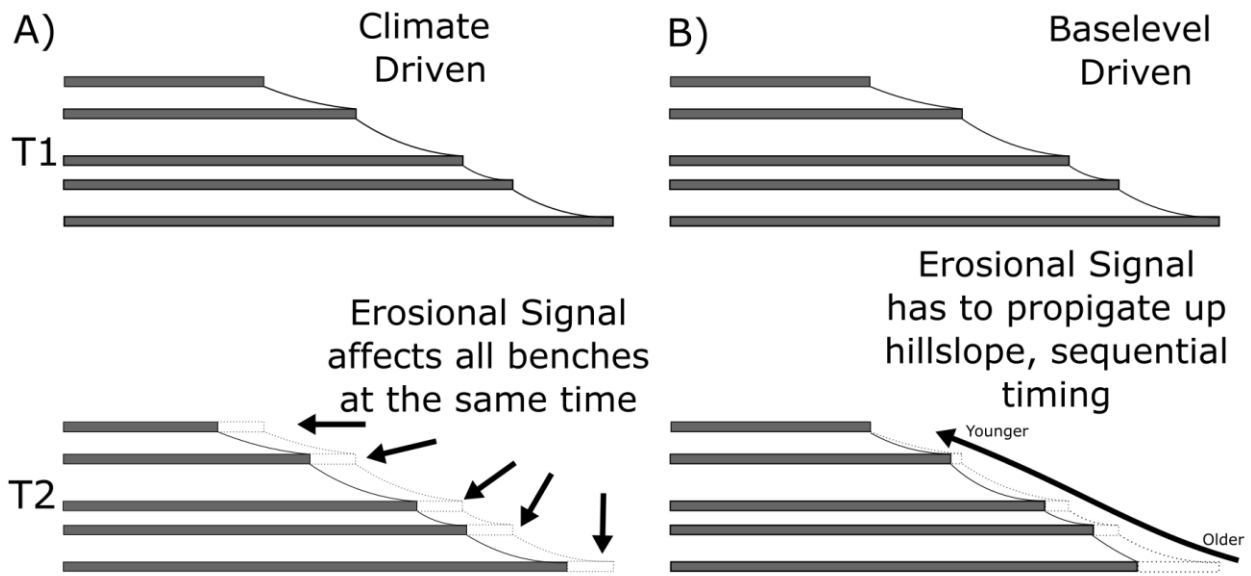


Figure 5. 6 Models of erosional signal propagation in layered landscape

a) Climate-driven hillslope change and bench retreat across the entire hillslope. All benches will retreat simultaneously due to the climate signal affecting the cliff at the same time. The form of the hillslope stays relatively the same. b) Base-level-driven hillslope change and bench retreat. Results in decreasing amounts of retreat and activity moving up the hillslope. The overall hillslope becomes steeper and more convex.

5.7.73 Hilltop gravels and dating the age of the current landscape

It's clear that there is an important gap in our understanding of the geomorphic history of northeast Kansas, particularly concerning the Pre-Illinoian hilltop gravels (i.e. Aber, 1991; Aber 2018; Aber 2019; Aber, 2022) described by Aber (2018 & 2019). These gravels represent a previous drainage system that existed before the ~700ka glaciation in northeast Kansas. This period, associated with the hilltop chert gravels, likely predates the formation of the modern Flint Hills as we recognize them today. While it's estimated that the current landscape configuration is

at least 3 million years old, without geochronological work, this estimation remains unverified. The hilltop chert gravels are thought to be contemporaneous with, or at least related to, the deposition of the Ogallala Formation, which spans a broad depositional surface across Kansas. Conducting a chronological investigation into these hilltop chert gravels would be groundbreaking in enhancing our understanding of the region's development and geomorphic history. Specifically, it could provide insights into the rate at which this landscape evolved over the Pleistocene. Techniques like cosmogenic burial isochron dating would be crucial in constraining the age of these features. Future research in this area would be a valuable contribution to advancing our knowledge of the Flint Hills and the broader Great Plains landscape. This aspect of the landscape development was outside the bounds of my dissertation, however the development and evolution of the regional drainages has significant influences over the development of hillslopes. Exploring this poorly explored aspect of the Flint Hills landscape may further reveal the dynamic nature of this type of landscape over geomorphic and geologic timescales.

5.8 Conclusions

The Flint Hills, characterized by its distinctive limestone layers and stair-step terrain, exemplifies the dynamic interplay of geological processes and climatic influences. This dissertation has delved into various facets of Flint Hills geomorphology, shedding light not only on the landscape evolution of this region but also providing useful insights into the dynamics of layered landscapes in general. One prominent feature of the Flint Hills landscape is the ubiquitous presence of hillslope armor, sourced from limestone layers. This armor, comprising boulders and rock fragments, plays a pivotal role in landscape evolution. Through meticulous fieldwork, geochronology, and modeling efforts, the research presented in the previous three

chapters of the dissertation has expanded our knowledge of heterolithic landscapes and boulder armor.

In this chapter, I examined the findings of the three research chapters in the context of each other to create new understanding. Boulder armor production and transport appear to be in part a function of climatic variables such as temperature and moisture availability. I examined previous work along the Appalachian Mountains in conjunction with the findings of Chapters 2 and 3 and propose that moisture is a key climate variable for the transport of boulders by creep processes. When moisture is not available, boulder armor may pile up and form talus cones or boulder fields, and when it is, the boulders are spread out into discrete boulder armor as in the Flint Hills. This trend also seems to be the case for arid locations like the Colorado Plateau. This research and previous work may suggest that temperate landscapes may be the best at spreading boulder armor across the hillslope as discrete clasts. The boulder, depending on lithology and weathering rate, can persist across interglacial periods. For the Flint Hills, data from Chapters 2 and 3 suggest that limestone boulders may exist on the hillslope as "armor" for an estimated 25-30 thousand years.

I also attempted to apply the insights gained from the modeling in Chapter 4 to current questions concerning mismatches between the current relief of the landscape and what may be expected concerning the erosion rates calculated for the region. Modeling suggests that a heterolithic landscape could be 10-15% taller than those without boulder armor and resistant layers. The presence of both in the Flint Hills may be one of the possible contributing factors to the Flint Hills being taller than otherwise expected.

Future research can build upon the work presented here, and I present some possible avenues that can be pursued. Optically stimulated luminescence could be utilized to determine

the block creep rate directly rather than estimated from the distribution of dated boulders on the hillslope, providing current, Holocene rates of boulder movement. The concept of "fracture piping" may be an interesting avenue of future research allowing for better understanding of bedrock bench morphology as well as establishing a new type of geomorphic process. Future research can also explore the timing of bench and boulder production across all the bedrock bench on the hillslope to test if boulder production is a bottom-up base-level process or a top-down climate-driven process. The Flint Hills, as well as layered landscapes in general, can be excellent laboratories for future advances in geomorphology.

References

- Aber, J. S. (1991). The glaciation of northeastern Kansas. *Boreas*, 20(4), 297–314.
<https://doi.org/10.1111/j.1502-3885.1991.tb00282.x>
- Aber, J. S. (1997). Chert Gravel and Neogene Drainage in East-Central Kansas. *Current Research in Earth Sciences*, 29–41. <https://doi.org/10.17161/cres.v0i240.11776>
- Aber, J. S. (2018). Upland Chert Gravel in the Emporia, Kansas Vicinity: New Exposures, Observations, and Stratigraphic review. *Transactions of the Kansas Academy of Science*, 121(1–2), 103–110. <https://doi.org/10.1660/062.121.0211>
- Aber, J. S. (2019). High-Terrace Chert-Gravel Deposits in the Toledo Vicinity, Chase County, Kansas. *Transactions of the Kansas Academy of Science*, 122(3–4), 251–256.
<https://doi.org/10.1660/062.122.0308>
- Aber, J. S. (2022). Reappraisal of the Glaciation of Northeastern Kansas. *Transactions of the Kansas Academy of Science*, 125(1–2), 41–51. <https://doi.org/10.1660/062.125.0104>
- Aber, S. W., & Grisafe, D. A. (1982). Petrographic Characteristics of Kansas Building Limestones (Bulletin No. 224). Kansas Geological Survey. Retrieved from <https://www.kgs.ku.edu/Publications/Bulletins/224/>
- Abrahams, A. D., Parsons, A. J., Cooke, R. U., & Reeves, R. W. (1984). Stone movement on hillslopes in the Mojave Desert, California: A 16-year record. *Earth Surface Processes and Landforms*, 9(4), 365–370. <https://doi.org/10.1002/esp.3290090409>
- Ahnert, F. (1960). The Influence OF Pleistocene Climates Upon the Morphology of Cuesta Scarps on the Colorado Plateau. *Annals of the Association of American Geographers*, 50(2), 139–156. <https://doi.org/10.1111/j.1467-8306.1960.tb00341.x>
- Ahnert, F. (1977). Some comments on the quantitative formulation of geomorphological

- processes in a theoretical model. *Earth Surface Processes*, 2(2–3), 191–201.
<https://doi.org/10.1002/esp.3290020211>
- Aitken, M. J. (1985). Thermoluminescence dating: Past progress and future trends. *Nuclear Tracks and Radiation Measurements* (1982), 10(1), 3–6. [https://doi.org/10.1016/0735-245X\(85\)90003-1](https://doi.org/10.1016/0735-245X(85)90003-1)
- Alfimov, V., & Ivy-Ochs, S. (2009). How well do we understand production of ^{36}Cl in limestone and dolomite? *Quaternary Geochronology*, 4(6), 462–474.
<https://doi.org/10.1016/j.quageo.2009.08.005>
- Atkinson, R. J. C. (1975). British prehistory and the radiocarbon revolution. *Antiquity*, 49(195), 173–177. <https://doi.org/10.1017/S0003598X00070034>
- Axelrod, D. I. (1985). Rise of the grassland biome, central North America. *The Botanical Review*, 51(2), 163–201. <https://doi.org/10.1007/BF02861083>
- Balco, G. (2014). Simple computer code for estimating cosmic-ray shielding by oddly shaped objects. *Quaternary Geochronology*, 22, 175–182.
- Balco, G., Stone, J. O., Lifton, N. A., & Dunai, T. J. (2008). A complete and easily accessible means of calculating surface exposure ages or erosion rates from ^{10}Be and ^{26}Al measurements. *Quaternary Geochronology*, 3(3), 174–195.
<https://doi.org/10.1016/j.quageo.2007.12.001>
- Balco, G., Briner, J., Finkel, R. C., Rayburn, J. A., Ridge, J. C., & Schaefer, J. M. (2009). Regional beryllium-10 production rate calibration for late-glacial northeastern North America. *Quaternary Geochronology*, 4(2), 93–107.
<https://doi.org/10.1016/j.quageo.2008.09.001>

- Banerjee, D., Hildebrand, A. N., Murray-Wallace, C. V., Bourman, R. P., Brooke, B. P., & Blair, M. (2003). New quartz SAR-OSL ages from the stranded beach dune sequence in south-east South Australia. *Quaternary Science Reviews*, 22(10), 1019–1025.
[https://doi.org/10.1016/S0277-3791\(03\)00013-1](https://doi.org/10.1016/S0277-3791(03)00013-1)
- Baykasoğlu, A., Güllü, H., Çanakçı, H., & Özbakır, L. (2008). Prediction of compressive and tensile strength of limestone via genetic programming. *Expert Systems with Applications*, 35(1), 111–123. <https://doi.org/10.1016/j.eswa.2007.06.006>
- Beeton, J. M., & Mandel, R. D. (2011). Soils and late-Quaternary landscape evolution in the Cottonwood River basin, east-central Kansas: Implications for archaeological research. *Geoarchaeology*, 26(5), 693–723. <https://doi.org/10.1002/gea.20367>
- Benito-Calvo, A., Moreno, D., Fujioka, T., López, G. I., Martín-González, F., Martínez-Fernández, A., et al. (2022). Towards the steady state? A long-term river incision deceleration pattern during Pleistocene entrenchment (Upper Ebro River, Northern Spain). *Global and Planetary Change*, 213, 103813.
<https://doi.org/10.1016/j.gloplacha.2022.103813>
- Bernard, T., Sinclair, H. D., Gailleton, B., Mudd, S. M., & Ford, M. (2019). Lithological control on the post-orogenic topography and erosion history of the Pyrenees. *Earth and Planetary Science Letters*, 518, 53–66. <https://doi.org/10.1016/j.epsl.2019.04.034>
- Bhanwariwal, K., & Ravi, K. (2021). Laboratory Swell Pressure Determination of Expansive Clays. In T. G. Sitharam, C. R. Parthasarathy, & S. Kolathayar (Eds.), *Ground Improvement Techniques* (pp. 309–315). Singapore: Springer.
https://doi.org/10.1007/978-981-15-9988-0_28
- Bierman, P. R., Marsella, K. A., Patterson, C., Davis, P. T., & Caffee, M. (1999). Mid-

- Pleistocene cosmogenic minimum-age limits for pre-Wisconsinan glacial surfaces in southwestern Minnesota and southern Baffin Island: a multiple nuclide approach. *Geomorphology*, 27(1), 25–39. [https://doi.org/10.1016/S0169-555X\(98\)00088-9](https://doi.org/10.1016/S0169-555X(98)00088-9)
- Black, T. A., & Montgomery, D. R. (1991). Sediment transport by burrowing mammals, Marin County, California. *Earth Surface Processes and Landforms*, 16(2), 163–172. <https://doi.org/10.1002/esp.3290160207>
- Blackmore, P. (2019). GIS20 GIS coverages defining Konza elevations. Environmental Data Initiative.
- Boroda, R., Amit, R., Matmon, A., ASTER Team, Finkel, R., Porat, N., et al. (2011). Quaternary-scale evolution of sequences of talus flatirons in the hyperarid Negev. *Geomorphology*, 127(1), 41–52. <https://doi.org/10.1016/j.geomorph.2010.12.003>
- Braucher, R., Bourlès, D., Merchel, S., Vidal Romani, J., Fernandez-Mosquera, D., Marti, K., et al. (2013). Determination of muon attenuation lengths in depth profiles from in situ produced cosmogenic nuclides. *Nuclear Instruments and Methods in Physics Research Section B: Beam Interactions with Materials and Atoms*, 294, 484–490. <https://doi.org/10.1016/j.nimb.2012.05.023>
- Braun, J., Heimsath, A. M., & Chappell, J. (2001). Sediment transport mechanisms on soil-mantled hillslopes. *Geology*, 29(8), 683–686. [https://doi.org/10.1130/0091-7613\(2001\)029<0683:STMOSM>2.0.CO;2](https://doi.org/10.1130/0091-7613(2001)029<0683:STMOSM>2.0.CO;2)
- Briggs, J. M., Knapp, A. K., & Brock, B. L. (2002). Expansion of Woody Plants in Tallgrass Prairie: A Fifteen-year Study of Fire and Fire-grazing Interactions. *The American Midland Naturalist*, 147(2), 287–294. [https://doi.org/10.1674/0003-0031\(2002\)147\[0287:EOWPIT\]2.0.CO;2](https://doi.org/10.1674/0003-0031(2002)147[0287:EOWPIT]2.0.CO;2)

- Ramsey, C. (2008). Radiocarbon Dating: Revolutions in Understanding*. *Archaeometry*, 50(2), 249–275. <https://doi.org/10.1111/j.1475-4754.2008.00394.x>
- Brooks, S. M., Crozier, M. J., Preston, N. J., & Anderson, M. G. (2002). Regolith stripping and the control of shallow translational hillslope failure: application of a two-dimensional coupled soil hydrology-slope stability model, Hawke's Bay, New Zealand. *Geomorphology*, 45(3), 165–179. [https://doi.org/10.1016/S0169-555X\(01\)00153-2](https://doi.org/10.1016/S0169-555X(01)00153-2)
- Bryan, K. (1940). Gully gravure—a method of slope retreat. *Journal of Geomorphology*, 3, 89–107.
- Bull, W. B. (1991). Geomorphic responses to climatic change. Retrieved from <https://www.osti.gov/biblio/5603696>
- Bunte, K., & Poesen, J. (1993). Effects of rock fragment covers on erosion and transport of noncohesive sediment by shallow overland flow. *Water Resources Research*, 29(5), 1415–1424. <https://doi.org/10.1029/92WR02706>
- Carriere, A., Le Bouteiller, C., Tucker, G. E., Klotz, S., & Naaim, M. (2020). Impact of vegetation on erosion: Insights from the calibration and test of a landscape evolution model in alpine badland catchments. *Earth Surface Processes and Landforms*, 45(5), 1085–1099. <https://doi.org/10.1002/esp.4741>
- Carson, M. A., & Kirkby, M. J. (1972). Hillslope form and process. (No Title). Retrieved from <https://cir.nii.ac.jp/crid/1130000798298766848>
- Caviezel, A., Ringenbach, A., Demmel, S. E., Dinneen, C. E., Krebs, N., Bühler, Y., et al. (2021). The relevance of rock shape over mass—implications for rockfall hazard assessments. *Nature Communications*, 12(1), 5546. <https://doi.org/10.1038/s41467-021-25794-y>

- Cecil, C. B. (1990). Paleoclimate controls on stratigraphic repetition of chemical and siliciclastic rocks.
- Cecil, C. B., & Edgar, N. T. (2003). Climate Controls on Stratigraphy. SEPM Society for \ Sedimentary Geology. <https://doi.org/10.2110/pec.03.77>
- Chapot, M. S., Roberts, H. M., Duller, G. A. T., & Lai, Z. P. (2016). Natural and laboratory TT-OSL dose response curves: testing the lifetime of the TT-OSL signal in nature. *Radiation Measurements*, 85, 41–50.
- Chilton, K. D., & Spotila, J. A. (2020). Preservation of Valley and Ridge topography via delivery of resistant, ridge-sourced boulders to hillslopes and channels, Southern Appalachian Mountains, U.S.A. *Geomorphology*, 365, 107263. <https://doi.org/10.1016/j.geomorph.2020.107263>
- Condon, S. M. (1997). Geology of the Pennsylvanian and Permian cutler group and Permian Kaibab limestone in the Paradox Basin, southeastern Utah and southwestern Colorado. US Government Printing Office.
- Cook, K. L., Whipple, K. X., Heimsath, A. M., & Hanks, T. C. (2009). Rapid incision of the Colorado River in Glen Canyon – insights from channel profiles, local incision rates, and modeling of lithologic controls. *Earth Surface Processes and Landforms*, 34(7), 994–1010. <https://doi.org/10.1002/esp.1790>
- Culling, W. E. H. (1960). Analytical Theory of Erosion. *The Journal of Geology*, 68(3), 336–344. <https://doi.org/10.1086/626663>
- Cunningham, A. C., Wallinga, J., Hobo, N., Versendaal, A. J., Makaske, B., & Middelkoop, H. (2014). Does deposition depth control the OSL bleaching of fluvial sediment? *Earth Surface Dynamics Discussions*, 2(2), 575–603.

- Darmody, R. G., Thorn, C. E., & Allen, C. E. (2005). Chemical weathering and boulder mantles, Kärkevage, Swedish Lapland. *Geomorphology*, 67(1), 159–170.
<https://doi.org/10.1016/j.geomorph.2004.07.011>
- Davis, W. M. (1892). The Convex Profile of Bad-Land Divides. *Science*, ns-20(508), 245–245.
<https://doi.org/10.1126/science.ns-20.508.245.a>
- Del Vecchio, J., DiBiase, R. A., Denn, A. R., Bierman, P. R., Caffee, M. W., & Zimmerman, S. R. (2018). Record of coupled hillslope and channel response to Pleistocene erosion and deposition in a sandstone headwater valley, central Pennsylvania. *GSA Bulletin*, 130(11–12), 1903–1917. <https://doi.org/10.1130/B31912.1>
- Denn, A. R., Bierman, P. R., Zimmerman, S. R. H., Caffee, M. W., Corbett, L. B., & Kirby, E. (2018). Cosmogenic nuclides indicate that boulder fields are dynamic, ancient, multigenerational features. *GSA Today*, 4–10. <https://doi.org/10.1130/GSATG340A.1>
- Deshpande, N. S., Furbish, D. J., Arratia, P. E., & Jerolmack, D. J. (2021). The perpetual fragility of creeping hillslopes. *Nature Communications*, 12(1), 3909.
<https://doi.org/10.1038/s41467-021-23979-z>
- DiBiase, R. A., Lamb, M. P., Ganti, V., & Booth, A. M. (2017). Slope, grain size, and roughness controls on dry sediment transport and storage on steep hillslopes. *Journal of Geophysical Research: Earth Surface*, 122(4), 941–960. <https://doi.org/10.1002/2016JF003970>
- DiBiase, R. A., Denn, A. R., Bierman, P. R., Kirby, E., West, N., & Hidy, A. J. (2018). Stratigraphic control of landscape response to base-level fall, Young Womans Creek, Pennsylvania, USA. *Earth and Planetary Science Letters*, 504, 163–173.
<https://doi.org/10.1016/j.epsl.2018.10.005>
- Dietrich, W. E. (1987). Overview: "Zero-order basins" and problems of drainage density,

- sediment transport and hillslope morphology. International Association of Hydrological Sciences Publication, 165, 27–37.
- Dietrich, William E., Bellugi, D. G., Sklar, L. S., Stock, J. D., Heimsath, A. M., & Roering, J. J. (2003). Geomorphic Transport Laws for Predicting Landscape form and Dynamics. In Prediction in Geomorphology (pp. 103–132). American Geophysical Union (AGU). <https://doi.org/10.1029/135GM09>
- Dorn, R. I. (2003). Boulder weathering and erosion associated with a wildfire, Sierra Ancha Mountains, Arizona. *Geomorphology*, 55(1), 155–171. [https://doi.org/10.1016/S0169-555X\(03\)00138-7](https://doi.org/10.1016/S0169-555X(03)00138-7)
- Dort Jr, W. (1987). Type descriptions for Kansas River terrace. *Quaternary Environments of \ Kansas*, 5, 103–107.
- Dredge, L. A. (1992). Breakup of Limestone Bedrock by Frost Shattering and Chemical Weathering, Eastern Canadian Arctic. *Arctic and Alpine Research*, 24(4), 314–323. <https://doi.org/10.2307/1551286>
- Drever, J. I. (1988). *The geochemistry of natural waters (Vol. 437)*. Prentice hall Englewood Cliffs
- Dunne, J., Elmore, D., & Muzikar, P. (1999). Scaling factors for the rates of production of cosmogenic nuclides for geometric shielding and attenuation at depth on sloped surfaces. *Geomorphology*, 27(1), 3–11. [https://doi.org/10.1016/S0169-555X\(98\)00086-5](https://doi.org/10.1016/S0169-555X(98)00086-5)
- Duszyński, F., & Migoń, P. (2015). Boulder aprons indicate long-term gradual and non-catastrophic evolution of cliffed escarpments, Stołowe Mts, Poland. *Geomorphology*, 250, 63–77. <https://doi.org/10.1016/j.geomorph.2015.08.007>
- Duszyński, F., Jancewicz, K., Kasprzak, M., & Migoń, P. (2017). The role of landslides in

- downslope transport of caprock-derived boulders in sedimentary tablelands, Stołowe Mts, SW Poland. *Geomorphology*, 295, 84–101.
<https://doi.org/10.1016/j.geomorph.2017.06.016>
- Duszyński, F., Migoń, P., & Strzelecki, M. C. (2019). Escarpment retreat in sedimentary tablelands and cuesta landscapes – Landforms, mechanisms and patterns. *Earth-Science Reviews*, 196, 102890. <https://doi.org/10.1016/j.earscirev.2019.102890>
- Duveiller, G., Hooker, J., & Cescatti, A. (2018). The mark of vegetation change on Earth's surface energy balance. *Nature Communications*, 9(1), 679.
<https://doi.org/10.1038/s41467-017-02810-8>
- Enzel, Y., Amit, R., Grodek, T., Ayalon, A., Lekach, J., Porat, N., et al. (2012). Late Quaternary weathering, erosion, and deposition in Nahal Yael, Israel: An “impact of climatic change on an arid watershed”? *Geological Society of America Bulletin*, 124(5–6), 705–722.
<https://doi.org/10.1130/B30538.1>
- Eppes, M. C., Magi, B., Scheff, J., Warren, K., Ching, S., & Feng, T. (2020). Warmer, Wetter Climates Accelerate Mechanical Weathering in Field Data, Independent of Stress-Loading. *Geophysical Research Letters*, 47(24), 2020GL089062.
<https://doi.org/10.1029/2020GL089062>
- Eppes, Martha Cary, McFadden, L. D., Wegmann, K. W., & Scuderi, L. A. (2010). Cracks in desert pavement rocks: Further insights into mechanical weathering by directional insolation. *Geomorphology*, 123(1), 97–108.
<https://doi.org/10.1016/j.geomorph.2010.07.003>
- Eppes, M.-C., & Keanini, R. (2017). Mechanical weathering and rock erosion by climate-

- dependent subcritical cracking. *Reviews of Geophysics*, 55(2), 470–508.
<https://doi.org/10.1002/2017RG000557>
- Fame, M. L., Chilton, K. D., Spotila, J. A., Kelly, M. A., & Caton, S. A. (n.d.). Periglacial resurfacing of hillslopes and channels with large boulders in the Virginia Appalachians. *Earth Surface Processes and Landforms*, n/a(n/a). <https://doi.org/10.1002/esp.5713>
- Forte, A. M., Yanites, B. J., & Whipple, K. X. (2016). Complexities of landscape evolution during incision through layered stratigraphy with contrasts in rock strength. *Earth Surface Processes and Landforms*, 41(12), 1736–1757. <https://doi.org/10.1002/esp.3947>
- Frye, J. C. (1955). The Erosional History of the Flint Hills. *Transactions of the Kansas Academy of Science (1903-)*, 58(1), 79–86. <https://doi.org/10.2307/3625588>
- Gilbert, G. K. (1877). *The Geology of the Henry Mountains*. Washington, D.C., United States: Geographical and Geological Survey.
- Gilbert, G. K. (1909). The Convexity of Hilltops. *The Journal of Geology*, 17(4), 344–350.
<https://doi.org/10.1086/621620>
- Gilbert, Grove Karl, & Murphy, E. C. (1914). *The transportation of debris by running water*. US Government Printing Office.
- Glade, R. C., & Anderson, R. S. (2018). Quasi-Steady Evolution of Hillslopes in Layered Landscapes: An Analytic Approach. *Journal of Geophysical Research: Earth Surface*, 123(1), 26–45. <https://doi.org/10.1002/2017JF004466>
- Glade, Rachel C., Anderson, R. S., & Tucker, G. E. (2017). Block-controlled hillslope form and persistence of topography in rocky landscapes. *Geology*, 45(4), 311–314.
<https://doi.org/10.1130/G38665.1>
- Glade, Rachel C., Shobe, C. M., Anderson, R. S., & Tucker, G. E. (2019). Canyon shape and

- erosion dynamics governed by channel-hillslope feedbacks. *Geology*, 47(7), 650–654.
<https://doi.org/10.1130/G46219.1>
- Gomes, L., Miranda, H. S., Silvério, D. V., & Bustamante, M. M. C. (2020). Effects and behaviour of experimental fires in grasslands, savannas, and forests of the Brazilian Cerrado. *Forest Ecology and Management*, 458, 117804.
<https://doi.org/10.1016/j.foreco.2019.117804>
- Gorynski, K. E., & Mandel, R. D. (2009). Bioclimatic Change; Late-Quaternary Alluvial Fan in Western Kansas (Open-file Report No. 21). Kansas Geological Survey. Retrieved from https://www.kgs.ku.edu/Publications/OFR/2009/OFR09_21/index.html
- Gosse, J. C., & Phillips, F. M. (2001). Terrestrial in situ cosmogenic nuclides: theory and application. *Quaternary Science Reviews*, 20(14), 1475–1560.
[https://doi.org/10.1016/S0277-3791\(00\)00171-2](https://doi.org/10.1016/S0277-3791(00)00171-2)
- Goudie, A. S., Allison, R. J., & McLaren, S. J. (1992). The relations between modulus of elasticity and temperature in the context of the experimental simulation of rock weathering by fire. *Earth Surface Processes and Landforms*, 17(6), 605–615.
<https://doi.org/10.1002/esp.3290170606>
- Govers, G., & Poesen, J. (1998). Field experiments on the transport of rock fragments by animal trampling on scree slopes. *Geomorphology*, 23(2), 193–203.
[https://doi.org/10.1016/S0169-555X\(98\)00003-8](https://doi.org/10.1016/S0169-555X(98)00003-8)
- Grab, S. W., Dickinson, K. J. M., Mark, A. F., & Maegli, T. (2008). Ploughing boulders on the Rock and Pillar Range, south-central New Zealand: Their geomorphology and alpine plant associations. *Journal of the Royal Society of New Zealand*, 38(1), 51–70.
<https://doi.org/10.1080/03014220809510546>

- Gran, K. B., Finnegan, N., Johnson, A. L., Belmont, P., Wittkop, C., & Rittenour, T. (2013). Landscape evolution, valley excavation, and terrace development following abrupt postglacial base-level fall. *Geological Society of America Bulletin*, 125(11–12), 1851–1864. <https://doi.org/10.1130/B30772.1>
- Granger, D. E., & Muzikar, P. F. (2001). Dating sediment burial with in situ-produced cosmogenic nuclides: theory, techniques, and limitations. *Earth and Planetary Science Letters*, 188(1), 269–281. [https://doi.org/10.1016/S0012-821X\(01\)00309-0](https://doi.org/10.1016/S0012-821X(01)00309-0)
- Granger, D. E., Riebe, C. S., Kirchner, J. W., & Finkel, R. C. (2001). Modulation of erosion on steep granitic slopes by boulder armoring, as revealed by cosmogenic ^{26}Al and ^{10}Be . *Earth and Planetary Science Letters*, 186(2), 269–281. [https://doi.org/10.1016/S0012-821X\(01\)00236-9](https://doi.org/10.1016/S0012-821X(01)00236-9)
- Granger, D. E., Fabel, D., & Palmer, A. N. (2001). Pliocene–Pleistocene incision of the Green River, Kentucky, determined from radioactive decay of cosmogenic ^{26}Al and ^{10}Be in Mammoth Cave sediments. *GSA Bulletin*, 113(7), 825–836. [https://doi.org/10.1130/0016-7606\(2001\)113<0825:PPIOTG>2.0.CO;2](https://doi.org/10.1130/0016-7606(2001)113<0825:PPIOTG>2.0.CO;2)
- Grieve, S. W. D., Mudd, S. M., & Hurst, M. D. (2016). How long is a hillslope? *Earth Surface Processes and Landforms*, 41(8), 1039–1054. <https://doi.org/10.1002/esp.3884>
- Gutiérrez Elorza, M., & Sesé Martínez, V. H. (2001). Multiple talus flatirons, variations of scarp retreat rates and the evolution of slopes in Almazán Basin (semi-arid central Spain). *Geomorphology*, 38(1), 19–29. [https://doi.org/10.1016/S0169-555X\(00\)00051-9](https://doi.org/10.1016/S0169-555X(00)00051-9)
- Gutiérrez, M., Sancho, C., & Arauzo, T. (1998). Scarp retreat rates in semiarid environments from talus flatirons (Ebro Basin, NE Spain). *Geomorphology*, 25(1), 111–121. [https://doi.org/10.1016/S0169-555X\(98\)00034-8](https://doi.org/10.1016/S0169-555X(98)00034-8)

- Gutiérrez, M., Lucha, P., Moreno, A., Guerrero, J., Martín-Serrano, A., Nozal, F., et al. (2010). Are talus flatiron sequences in Spain climate-controlled landforms? *Zeitschrift Fur Geomorphologie - Z GEOMORPHOLOGIE*, 54, 243–252. <https://doi.org/10.1127/0372-8854/2010/0054-0013>
- Hales, T. C., & Roering, J. J. (2007). Climatic controls on frost cracking and implications for the evolution of bedrock landscapes. *Journal of Geophysical Research: Earth Surface*, 112(F2). <https://doi.org/10.1029/2006JF000616>
- Harvey, A. M. (2002). Effective timescales of coupling within fluvial systems. *Geomorphology*, 44(3), 175–201. [https://doi.org/10.1016/S0169-555X\(01\)00174-X](https://doi.org/10.1016/S0169-555X(01)00174-X)
- Harvey, A. M., Wigand, P. E., & Wells, S. G. (1999). Response of alluvial fan systems to the late Pleistocene to Holocene climatic transition: contrasts between the margins of pluvial Lakes Lahontan and Mojave, Nevada and California, USA. *CATENA*, 36(4), 255–281. [https://doi.org/10.1016/S0341-8162\(99\)00049-1](https://doi.org/10.1016/S0341-8162(99)00049-1)
- Hayden, B. P. (1998). Regional climate and the distribution of tallgrass prairie. *Grassland Dynamics: Long-Term Ecological Research in Tallgrass Prairie*. Oxford University Press, New York, 19–34.
- Heimsath, A. M., Dietrich, W. E., Nishiizumi, K., & Finkel, R. C. (1997). The soil production function and landscape equilibrium. *Nature*, 388(6640), 358–361. <https://doi.org/10.1038/41056>
- Heimsath, A. M., Chappell, J., Spooner, N. A., & Questiaux, D. G. (2002). Creeping soil. *Geology*, 30(2), 111–114.
- Heimsath, A. M., Furbish, D. J., & Dietrich, W. E. (2005). The illusion of diffusion: Field

- evidence for depth-dependent sediment transport. *Geology*, 33(12), 949.
<https://doi.org/10.1130/G21868.1>
- Heisinger, B., Lal, D., Jull, A. J. T., Kubik, P., Ivy-Ochs, S., Neumaier, S., et al. (2002).
Production of selected cosmogenic radionuclides by muons: 1. Fast muons. *Earth and Planetary Science Letters*, 200(3), 345–355. [https://doi.org/10.1016/S0012-821X\(02\)00640-4](https://doi.org/10.1016/S0012-821X(02)00640-4)
- Heisinger, B., Lal, D., Jull, A. J. T., Kubik, P., Ivy-Ochs, S., Knie, K., & Nolte, E. (2002).
Production of selected cosmogenic radionuclides by muons: 2. Capture of negative muons. *Earth and Planetary Science Letters*, 200(3), 357–369.
[https://doi.org/10.1016/S0012-821X\(02\)00641-6](https://doi.org/10.1016/S0012-821X(02)00641-6)
- Hirano, M. (1968). A Mathematical Model of Slope Development: An approach to the. *Journal of Geosciences Osaka City University*, 11, 13–52.
- Horton, R. E. (1945). Erosional development of streams and their drainage basins; hydrophysical approach to quantitative morphology. *Geological Society of America Bulletin*, 56(3), 275–370.
- Imbrie, J., Laporte, L. F., & Merriam, D. F. (1964). Beattie Limestone facies (Lower Permian) of the northern midcontinent. *Kansas Geological Survey Bulletin*, 169(1), 219–238.
- Jerolmack, D. J., & Paola, C. (2010). Shredding of environmental signals by sediment transport. *Geophysical Research Letters*, 37(19). <https://doi.org/10.1029/2010GL044638>
- Johnson, W. C., Willey, K. L., & Macpherson, G. L. (2007). Carbon isotope variation in modern soils of the tallgrass prairie: Analogues for the interpretation of isotopic records derived from paleosols. *Quaternary International*, 162–163, 3–20.
<https://doi.org/10.1016/j.quaint.2006.10.036>

- Johnstone, S. A., & Hilley, G. E. (2015). Lithologic control on the form of soil-mantled hillslopes. *Geology*, 43(1), 83–86. <https://doi.org/10.1130/G36052.1>
- Kalantari, B. (2012). Foundations on expansive soils: a review. *Research Journal of Applied Sciences, Engineering and Technology*, 4(18), 3231–3237.
- Kirkby, M. (1988). Hillslope runoff processes and models. *Journal of Hydrology*, 100(1–3), 315–339.
- Kissel, C., Laj, C., Labeyrie, L., Dokken, T., Voelker, A., & Blamart, D. (1999). Rapid climatic variations during marine isotopic stage 3: magnetic analysis of sediments from Nordic Seas and North Atlantic. *Earth and Planetary Science Letters*, 171(3), 489–502. [https://doi.org/10.1016/S0012-821X\(99\)00162-4](https://doi.org/10.1016/S0012-821X(99)00162-4)
- Knight, C. L., Briggs, J. M., & Nellis, M. D. (1994). Expansion of gallery forest on Konza Prairie Research Natural Area, Kansas, USA. *Landscape Ecology*, 9(2), 117–125. <https://doi.org/10.1007/BF00124378>
- Knox, J. C. (1972). Valley alluviation in southwestern Wisconsin. *Annals of the Association of American Geographers*, 62(3), 401–410. <https://doi.org/10.1111/j.1467-8306.1972.tb00872.x>
- Kohn, M. J. (2010). Carbon isotope compositions of terrestrial C₃ plants as indicators of (paleo)ecology and (paleo)climate. *Proceedings of the National Academy of Sciences*, 107(46), 19691–19695. <https://doi.org/10.1073/pnas.1004933107>
- Koons, E. D. (1955). Cliff retreat in the southwestern United States. *American Journal of Science*, 253(1), 44–52. <https://doi.org/10.2475/ajs.253.1.44>
- Lal, D. (1991). Cosmic ray labeling of erosion surfaces: in situ nuclide production rates and

- erosion models. *Earth and Planetary Science Letters*, 104(2), 424–439.
[https://doi.org/10.1016/0012-821X\(91\)90220-C](https://doi.org/10.1016/0012-821X(91)90220-C)
- Lane, S. N., & Richards, K. S. (1997). Linking River Channel Form and Process: Time, Space and Causality Revisited. *Earth Surface Processes and Landforms*, 22(3), 249–260.
[https://doi.org/10.1002/\(SICI\)1096-9837\(199703\)22:3<249::AID-ESP752>3.0.CO;2-7](https://doi.org/10.1002/(SICI)1096-9837(199703)22:3<249::AID-ESP752>3.0.CO;2-7)
- Langston, A. L., Tucker, G. E., Anderson, R. S., & Anderson, S. P. (2015). Evidence for climatic and hillslope-aspect controls on vadose zone hydrology and implications for saprolite weathering. *Earth Surface Processes and Landforms*, 40(9), 1254–1269.
<https://doi.org/10.1002/esp.3718>
- Layzell, A. L., & Mandel, R. D. (2020). Late Quaternary landscape evolution and bioclimatic change in the central Great Plains, USA. *GSA Bulletin*, 132(11–12), 2553–2571.
<https://doi.org/10.1130/B35462.1>
- Lee, M. K., Lee, Y. I., Lim, H. S., Lee, J. I., Choi, J. H., & Yoon, H. I. (2011). Comparison of radiocarbon and OSL dating methods for a Late Quaternary sediment core from Lake Ulaan, Mongolia. *Journal of Paleolimnology*, 45(2), 127–135.
<https://doi.org/10.1007/s10933-010-9484-7>
- Lee, X., Goulden, M. L., Hollinger, D. Y., Barr, A., Black, T. A., Bohrer, G., et al. (2011). Observed increase in local cooling effect of deforestation at higher latitudes. *Nature*, 479(7373), 384–387. <https://doi.org/10.1038/nature10588>
- Leopold, L. B., Wolman, M. G., Miller, J. P., & Wohl, E. E. (2020). *Fluvial processes in geomorphology*. Courier Dover Publications.
- Libby, W. F., Anderson, E. C., & Arnold, J. R. (1949). *Age Determination by Radiocarbon*

- Content: World-Wide Assay of Natural Radiocarbon. *Science*, 109(2827), 227–228.
<https://doi.org/10.1126/science.109.2827.227>
- Lifton, N., Sato, T., & Dunai, T. J. (2014). Scaling in situ cosmogenic nuclide production rates using analytical approximations to atmospheric cosmic-ray fluxes. *Earth and Planetary Science Letters*, 386, 149–160. <https://doi.org/10.1016/j.epsl.2013.10.052>
- Macpherson, G. L., & Sullivan, P. L. (2019). Watershed-scale chemical weathering in a merokarst terrain, northeastern Kansas, USA. *Chemical Geology*, 527, 118988.
<https://doi.org/10.1016/j.chemgeo.2018.12.001>
- Madsen, A. T., & Murray, A. S. (2009). Optically stimulated luminescence dating of young : A review. *Geomorphology*, 109(1), 3–16.
<https://doi.org/10.1016/j.geomorph.2008.08.020>
- Marrero, S. M., Phillips, F. M., Borchers, B., Lifton, N., Aumer, R., & Balco, G. (2016). Cosmogenic nuclide systematics and the CRONUScale program. *Quaternary Geochronology*, 31, 160–187. <https://doi.org/10.1016/j.quageo.2015.09.005>
- Marshall, J. A., Roering, J. J., Rempel, A. W., Shafer, S. L., & Bartlein, P. J. (2021). Extensive Frost Weathering Across Unglaciaded North America During the Last Glacial Maximum. *Geophysical Research Letters*, 48(5), e2020GL090305.
<https://doi.org/10.1029/2020GL090305>
- Marshall, Jill A., Roering, J. J., Gavin, D. G., & Granger, D. E. (2017). Late Quaternary climatic controls on erosion rates and geomorphic processes in western Oregon, USA. *GSA Bulletin*, 129(5–6), 715–731. <https://doi.org/10.1130/B31509.1>
- Marston, R. A. (2010). Geomorphology and vegetation on hillslopes: Interactions, dependencies,

- and feedback loops. *Geomorphology*, 116(3), 206–217.
<https://doi.org/10.1016/j.geomorph.2009.09.028>
- Martin, Y. (2000). Modelling hillslope evolution: linear and nonlinear transport relations. *Geomorphology*, 34(1), 1–21. [https://doi.org/10.1016/S0169-555X\(99\)00127-0](https://doi.org/10.1016/S0169-555X(99)00127-0)
- McCarroll, N., & Temme, A. (2022). RFP01 Properties of large hillslope blocks and cliff faces along the cottonwood limestone near the konza prairie nature trail [Data set]. Environmental Data Initiative.
<https://doi.org/10.6073/PASTA/65F917EDEA2318F7F7D63AE4239091C3>
- McCarroll, Nicholas R. (2019). Evolution of the Book Cliffs Dryland Escarpment in Central Utah – Establishing Rates and Testing Models of Escarpment Retreat (M.S.). Utah State University, United States -- Utah.
- McCarroll, Nicholas R., & Temme, A. J. A. M. (2022). Transport and Weathering of Large Limestone Blocks on Hillslopes in Heterolithic Sedimentary Landscapes. *Journal of Geophysical Research: Earth Surface*, 127(9), e2022JF006609.
<https://doi.org/10.1029/2022JF006609>
- McCarroll, Nicholas R., Pederson, J. L., Hidy, A. J., & Rittenour, T. M. (2021). Chronostratigraphy of talus flatirons and piedmont alluvium along the Book Cliffs, Utah – Testing models of dryland escarpment evolution. *Quaternary Science Reviews*, 274, 107286. <https://doi.org/10.1016/j.quascirev.2021.107286>
- McCarroll, Nicholas Reilly, & Temme, A. (2024). The lasting legacy of glacial landscape dynamics: Capturing the transport of boulder armor and hillslope retreat with geochronology in the Flint Hills of Kansas. *Geomorphology*, 445, 108980.
<https://doi.org/10.1016/j.geomorph.2023.108980>

- McFadden, L. D., Eppes, M. C., Gillespie, A. R., & Hallet, B. (2005). Physical weathering in arid landscapes due to diurnal variation in the direction of solar heating. *GSA Bulletin*, 117(1–2), 161–173. <https://doi.org/10.1130/B25508.1>
- McGrath, G. S., Nie, Z., Dyskin, A., Byrd, T., Jenner, R., Holbeche, G., & Hinz, C. (2013). In situ fragmentation and rock particle sorting on arid hills. *Journal of Geophysical Research: Earth Surface*, 118(1), 17–28. <https://doi.org/10.1029/2012JF002402>
- McLauchlan, K. K., Commerford, J. L., & Morris, C. J. (2013). Tallgrass prairie pollen assemblages in mid-continental North America. *Vegetation History and Archaeobotany*, 22(3), 171–183. <https://doi.org/10.1007/s00334-012-0369-8>
- Menting, F., Langston, A. L., & Temme, A. J. A. M. (2015). Downstream fining, selective transport, and hillslope influence on channel bed sediment in mountain streams, Colorado Front Range, USA. *Geomorphology*, 239, 91–105. <https://doi.org/10.1016/j.geomorph.2015.03.018>
- Migoń, P., & Duszyński, F. (2022). Landscapes and landforms in coarse clastic sedimentary tablelands – Is there a unifying theme? *CATENA*, 218, 106545. <https://doi.org/10.1016/j.catena.2022.106545>
- Migoń, P., Duszyński, F., Jancewicz, K., Kotowska, M., & Poręba, W. (2023). Surface-subsurface connectivity in the morphological evolution of sandstone-capped tabular hills – How much analogy to karst? *Geomorphology*, 440, 108884. <https://doi.org/10.1016/j.geomorph.2023.108884>
- Mills, H. H. (1981). Boulder Deposits and the Retreat of Mountain Slopes, or, “Gully Gravure” Revisited. *The Journal of Geology*, 89(5), 649–660. <https://doi.org/10.1086/628628>
- Monson, R. K., Edwards, G. E., & Ku, M. S. B. (1984). C3-C4 Intermediate Photosynthesis in

- Plants. *BioScience*, 34(9), 563–574. <https://doi.org/10.2307/1309599>
- Montgomery, D. R. (2001). Slope distributions, threshold hillslopes, and steady-state topography. *American Journal of Science*, 301(4–5), 432–454.
- Mudd, S. M., & Furbish, D. J. (2004a). Influence of chemical denudation on hillslope morphology. *Journal of Geophysical Research: Earth Surface*, 109(F2).
<https://doi.org/10.1029/2003JF000087>
- Mudd, S. M., & Furbish, D. J. (2004b). Influence of chemical denudation on hillslope morphology. *Journal of Geophysical Research: Earth Surface*, 109(F2).
<https://doi.org/10.1029/2003JF000087>
- Murray, A. S., & Olley, J. M. (2002). Precision and accuracy in the optically stimulated luminescence dating of sedimentary quartz: a status review. *Geochronometria: Journal on Methods & Applications of Absolute Chronology*, 21. Retrieved from
http://www.geochronometria.pl/pdf/geo_21/Geo21_01.pdf
- Neely, A. B., DiBiase, R. A., Corbett, L. B., Bierman, P. R., & Caffee, M. W. (2019). Bedrock fracture density controls on hillslope erodibility in steep, rocky landscapes with patchy soil cover, southern California, USA. *Earth and Planetary Science Letters*, 522, 186–197.
<https://doi.org/10.1016/j.epsl.2019.06.011>
- Nelson, M. S., Gray, H. J., Johnson, J. A., Rittenour, T. M., Feathers, J. K., & Mahan, S. A. (2015). User Guide for Luminescence Sampling in Archaeological and Geological Contexts. *Advances in Archaeological Practice*, 3(2), 166–177.
<https://doi.org/10.7183/2326-3768.3.2.166>
- Nishiizumi, K., Winterer, E. L., Kohl, C. P., Klein, J., Middleton, R., Lal, D., & Arnold, J. R.

- (1989). Cosmic ray production rates of ^{10}Be and ^{26}Al in quartz from glacially polished rocks. *Journal of Geophysical Research: Solid Earth*, 94(B12), 17907–17915.
<https://doi.org/10.1029/JB094iB12p17907>
- Nishiizumi, Kunihiro, Imamura, M., Caffee, M. W., Southon, J. R., Finkel, R. C., & McAninch, J. (2007). Absolute calibration of ^{10}Be AMS standards. *Nuclear Instruments and Methods in Physics Research Section B: Beam Interactions with Materials and Atoms*, 258(2), 403–413. <https://doi.org/10.1016/j.nimb.2007.01.297>
- North Greenland Ice Core Project members, Andersen, K. K., Azuma, N., Barnola, J.-M., Bigler, M., Biscaye, P., et al. (2004). High-resolution record of Northern Hemisphere climate extending into the last interglacial period. *Nature*, 431(7005), 147–151.
<https://doi.org/10.1038/nature02805>
- Oh, J.-S., Seong, Y. B., Larson, P. H., Hong, S.-C., & Yu, B. Y. (2020). Asymmetric Hillslope Retreat Revealed from Talus Flatirons on Rock Peak, San Tan Mountains, Arizona, United States: Assessing Caprock Lithology Control on Landscape Evolution. *Annals of the American Association of Geographers*, 110(1), 98–119.
<https://doi.org/10.1080/24694452.2019.1624421>
- Ouimet, W. B., Whipple, K. X., Royden, L. H., Sun, Z., & Chen, Z. (2007). The influence of large landslides on river incision in a transient landscape: Eastern margin of the Tibetan Plateau (Sichuan, China). *GSA Bulletin*, 119(11–12), 1462–1476.
<https://doi.org/10.1130/B26136.1>
- Overpeck, J. T., & Cole, J. E. (2006). Abrupt Change in Earth's Climate System. *Annual Review of Environment and Resources*, 31(1), 1–31.
<https://doi.org/10.1146/annurev.energy.30.050504.144308>

- Oviatt, C. G. (1998). *Geomorphology of Konza prairie*. *Grassland Dynamics: Long-Term Ecological Research in Tallgrass Prairie*. Oxford University Press, New York, 35–47.
- Paronuzzi, P., & Serafini, W. (2009). Stress state analysis of a collapsed overhanging rock slab: A case study. *Engineering Geology*, 108(1), 65–75.
<https://doi.org/10.1016/j.enggeo.2009.06.019>
- Pazzaglia, F. J. (2003). Landscape evolution models. In *Developments in Quaternary Sciences* (Vol. 1, pp. 247–274). Elsevier. [https://doi.org/10.1016/S1571-0866\(03\)01012-1](https://doi.org/10.1016/S1571-0866(03)01012-1)
- Pederson, J., Burnside, N., Shipton, Z., & Rittenour, T. (2013). Rapid river incision across an inactive fault—Implications for patterns of erosion and deformation in the central Colorado Plateau. *Lithosphere*, 5(5), 513–520.
- Pelletier, J. D. (2014). The linkages among hillslope-vegetation changes, elevation, and the timing of late-Quaternary fluvial-system aggradation in the Mojave Desert revisited. *Earth Surface Dynamics*, 2(2), 455–468. <https://doi.org/10.5194/esurf-2-455-2014>
- Pelletier, Jon D., & Rasmussen, C. (2009). Quantifying the climatic and tectonic controls on hillslope steepness and erosion rate. *Lithosphere*, 1(2), 73–80.
<https://doi.org/10.1130/L3.1>
- Pérez, F. L. (1985). Surficial Talus Movement in an Andean Paramo of Venezuela. *Geografiska Annaler: Series A, Physical Geography*, 67(3–4), 221–237.
<https://doi.org/10.1080/04353676.1985.11880148>
- Perron, J. T. (2011). Numerical methods for nonlinear hillslope transport laws. *Journal of Geophysical Research: Earth Surface*, 116(F2). <https://doi.org/10.1029/2010JF001801>
- Rempel, A. W., Marshall, J. A., & Roering, J. J. (2016). Modeling relative frost weathering rates

- at geomorphic scales. *Earth and Planetary Science Letters*, 453, 87–95.
<https://doi.org/10.1016/j.epsl.2016.08.019>
- Rhoads, B. L. (2006). The Dynamic Basis of Geomorphology Reenvisioned. *Annals of the Association of American Geographers*, 96(1), 14–30. <https://doi.org/10.1111/j.1467-8306.2006.00496.x>
- Richardson, P. W., Perron, J. T., & Schurr, N. D. (2019). Influences of climate and life on hillslope sediment transport. *Geology*, 47(5), 423–426. <https://doi.org/10.1130/G45305.1>
- Roering, J. J. (2008). How well can hillslope evolution models “explain” topography? Simulating soil transport and production with high-resolution topographic data. *Geological Society of America Bulletin*, 120(9–10), 1248–1262.
<https://doi.org/10.1130/B26283.1>
- Roering, Joshua J. (2004). Soil creep and convex-upward velocity profiles: theoretical and experimental investigation of disturbance-driven sediment transport on hillslopes. *Earth Surface Processes and Landforms*, 29(13), 1597–1612. <https://doi.org/10.1002/esp.1112>
- Roering, Joshua J., Kirchner, J. W., & Dietrich, W. E. (1999). Evidence for nonlinear, diffusive sediment transport on hillslopes and implications for landscape morphology. *Water Resources Research*, 35(3), 853–870. <https://doi.org/10.1029/1998WR900090>
- Roering, Joshua J., Kirchner, J. W., & Dietrich, W. E. (2001a). Correction to “Hillslope evolution by nonlinear, slope-dependent transport: Steady state morphology and equilibrium adjustment timescales” *Journal of Geophysical Research: Solid Earth*, 106(B11), 26787–26787. <https://doi.org/10.1029/2001JB900018>
- Roering, Joshua J., Kirchner, J. W., Sklar, L. S., & Dietrich, W. E. (2001). Hillslope evolution by

- nonlinear creep and landsliding: An experimental study. *Geology*, 29(2), 143–146.
[https://doi.org/10.1130/0091-7613\(2001\)029<0143:HEBNCA>2.0.CO;2](https://doi.org/10.1130/0091-7613(2001)029<0143:HEBNCA>2.0.CO;2)
- Roering, Joshua J., Kirchner, J. W., & Dietrich, W. E. (2001b). Hillslope evolution by nonlinear, slope-dependent transport: Steady state morphology and equilibrium adjustment timescales. *Journal of Geophysical Research: Solid Earth*, 106(B8), 16499–16513.
<https://doi.org/10.1029/2001JB000323>
- Roering, Joshua J., Perron, J. T., & Kirchner, J. W. (2007). Functional relationships between denudation and hillslope form and relief. *Earth and Planetary Science Letters*, 264(1–2), 245–258.
- Román-Sánchez, A., Willgoose, G., Giráldez, J. V., Peña, A., & Vanwalleghem, T. (2019). The effect of fragmentation on the distribution of hillslope rock size and abundance: Insights from contrasting field and model data. *Geoderma*, 352, 228–240.
<https://doi.org/10.1016/j.geoderma.2019.06.014>
- Roqué, C., Linares, R., Zarroca, M., Rosell, J., Pellicer, X. M., & Gutiérrez, F. (2013). Chronology and paleoenvironmental interpretation of talus flatiron sequences in a sub-humid mountainous area: Tresp Depression, Spanish Pyrenees. *Earth Surface Processes and Landforms*, 38(13), 1513–1522. <https://doi.org/10.1002/esp.3391>
- Roth, D. L., Doane, T. H., Roering, J. J., Furbish, D. J., & Zettler-Mann, A. (2020). Particle motion on burned and vegetated hillslopes. *Proceedings of the National Academy of Sciences*, 117(41), 25335–25343. <https://doi.org/10.1073/pnas.1922495117>
- Rovey, C. W., Forir, M., Balco, G., & Gaunt, D. (2010). Geomorphology and paleontology of Riverbluff Cave, Springfield, Missouri
- Rovey, C. W., Bassett, D. J., & McKay, M. P. (2021). Ordovician and Mississippian stratigraphy

in southwestern Missouri, USA.

- Ruedrich, J., Bartelsen, T., Dohrmann, R., & Siegesmund, S. (2011). Moisture expansion as a deterioration factor for sandstone used in buildings. *Environmental Earth Sciences*, 63(7), 1545–1564. <https://doi.org/10.1007/s12665-010-0767-0>
- Sanjuan Girbau, J., Martín-Closas, C., Costa, E., Barberà, X., & Garces, M. (2014). Calibration of Eocene-Oligocene charophyte biozones in the Eastern Ebro Basin (Catalonia, Spain). *Stratigraphy*, 11, 61–81. <https://doi.org/10.29041/strat.11.1.03>
- Schachtman, N. S., Roering, J. J., Marshall, J. A., Gavin, D. G., & Granger, D. E. (2019). The interplay between physical and chemical erosion over glacial-interglacial cycles. *Geology*, 47(7), 613–616. <https://doi.org/10.1130/G45940.1>
- Schaller, M., Blanckenburg, F. von, Hovius, N., Veldkamp, A., van den Berg, M. W., & Kubik, P. W. (2004). Paleoerosion Rates from Cosmogenic ¹⁰Be in a 1.3 Ma Terrace Sequence: Response of the River Meuse to Changes in Climate and Rock Uplift. *The Journal of Geology*, 112(2), 127–144. <https://doi.org/10.1086/381654>
- Schanz, S. A., & Montgomery, D. R. (2016). Lithologic controls on valley width and strath terrace formation. *Geomorphology*, 258, 58–68. <https://doi.org/10.1016/j.geomorph.2016.01.015>
- Schlager, W. (1993). Accommodation and supply—a dual control on stratigraphic sequences. *Sedimentary Geology*, 86(1), 111–136. [https://doi.org/10.1016/0037-0738\(93\)90136-S](https://doi.org/10.1016/0037-0738(93)90136-S)
- Schmidt, K. M., & Montgomery, D. R. (1995). Limits to Relief. *Science*, 270(5236), 617–620. <https://doi.org/10.1126/science.270.5236.617>
- Schmidt, K.-H. (1996). Talus and pediment flatirons, indicators of climatic change on scarp

- slopes on the Colorado Plateau, USA. *Zeitschrift Für Geomorphologie. Supplementband*, (103), 135–158.
- Schultz, G. E. (1969). Geology and Paleontology of a Late Pleistocene Basin in Southwest Kansas. In G. E. Schultz (Ed.), *Geology and Paleontology of a Late Pleistocene Basin in Southwest Kansas* (Vol. 105, p. 0). Geological Society of America.
<https://doi.org/10.1130/SPE105-p1>
- Schumm, S. A. (1967). Rates of Surficial Rock Creep on Hillslopes in Western Colorado. *Science*, 155(3762), 560–562. <https://doi.org/10.1126/science.155.3762.560>
- Schumm, S. A. (1985). Patterns of Alluvial Rivers. *Annual Review of Earth and Planetary Sciences*, 13(1), 5–27. <https://doi.org/10.1146/annurev.ea.13.050185.000253>
- Schumm, Stanley Alfred, & Chorley, R. J. (1966). Talus weathering and scarp recession in the Colorado Plateaus. US Geological Survey.
- Seymour, D. L., & Fielding, C. R. (2013). High resolution correlation of the Upper Cretaceous stratigraphy between the Book Cliffs and the western Henry Mountains Syncline, Utah, USA. *Journal of Sedimentary Research*, 83(6), 475–494.
- Shafer, S. L., Bartlein, P. J., & Izumi, K. (2021). PMIP3/CMIP5 lgm simulated temperature data for North America downscaled to a 10-km grid: US Geological Survey data release.
- Shobe, C. M., Bennett, G. L., Tucker, G. E., Roback, K., Miller, S. R., & Roering, J. J. (2020). Boulders as a lithologic control on river and landscape response to tectonic forcing at the Mendocino triple junction. *GSA Bulletin*, 133(3–4), 647–662.
<https://doi.org/10.1130/B35385.1>
- Shobe, C. M., Turowski, J. M., Nativ, R., Glade, R. C., Bennett, G. L., & Dini, B. (2021). The

- role of infrequently mobile boulders in modulating landscape evolution and geomorphic hazards. *Earth-Science Reviews*, 220, 103717.
<https://doi.org/10.1016/j.earscirev.2021.103717>
- Shtober-Zisu, N., & Wittenberg, L. (2021). Long-term effects of wildfire on rock weathering and soil stoniness in the Mediterranean landscapes. *Science of The Total Environment*, 762, 143125. <https://doi.org/10.1016/j.scitotenv.2020.143125>
- Sklar, L. S., & Dietrich, W. E. (2001). Sediment and rock strength controls on river incision into bedrock. *Geology*, 29(12), 1087. [https://doi.org/10.1130/0091-7613\(2001\)029<1087:SARSCO>2.0.CO;2](https://doi.org/10.1130/0091-7613(2001)029<1087:SARSCO>2.0.CO;2)
- Smith, G. N. (1991). *Geomorphology and geomorphic history of the Konza prairie research natural area, Riley and Geary Counties, Kansas* (PhD Thesis). Kansas State University.
- Stock, J. D., & Montgomery, D. R. (1999). Geologic constraints on bedrock river incision using the stream power law. *Journal of Geophysical Research: Solid Earth*, 104(B3), 4983–4993. <https://doi.org/10.1029/98JB02139>
- Stone, J. O., Allan, G. L., Fifield, L. K., & Cresswell, R. G. (1996). Cosmogenic chlorine-36 from calcium spallation. *Geochimica et Cosmochimica Acta*, 60(4), 679–692.
[https://doi.org/10.1016/0016-7037\(95\)00429-7](https://doi.org/10.1016/0016-7037(95)00429-7)
- Stone, John O. (2000). Air pressure and cosmogenic isotope production. *Journal of Geophysical Research: Solid Earth*, 105(B10), 23753–23759. <https://doi.org/10.1029/2000JB900181>
- Strudley, M. W., Murray, A. B., & Haff, P. K. (2006). Emergence of pediments, tors, and piedmont junctions from a bedrock weathering–regolith thickness feedback. *Geology*, 34(10), 805–808. <https://doi.org/10.1130/G22482.1>
- Stumpff, M. L. (2021). Characterizing the evolution of detached limestone blocks on hillslopes:

Konza Prairie, Kansas, United States of America.

- Sweeney, K. E., Roering, J. J., & Ellis, C. (2015). Experimental evidence for hillslope control of landscape scale. *Science*, 349(6243), 51–53. <https://doi.org/10.1126/science.aab0017>
- Szramek, K., Walter, L. M., Kanduč, T., & Ogrinc, N. (2011). Dolomite Versus Calcite Weathering in Hydrogeochemically Diverse Watersheds Established on Bedded Carbonates (Sava and Soča Rivers, Slovenia). *Aquatic Geochemistry*, 17(4), 357–396. <https://doi.org/10.1007/s10498-011-9125-4>
- Taylor Perron, J., & Fagherazzi, S. (2012). The legacy of initial conditions in landscape evolution. *Earth Surface Processes and Landforms*, 37(1), 52–63. <https://doi.org/10.1002/esp.2205>
- Temme, A. J., Schoorl, J. M., Claessens, L., & Veldkamp, A. (2013). Quantitative modeling of landscape evolution. Retrieved from <http://oar.icrisat.org/id/eprint/7445>
- Temme, A. j. a. m., Armitage, J., Attal, M., van Gorp, W., Coulthard, T. j., & Schoorl, J. m. (2017). Developing, choosing and using landscape evolution models to inform field-based landscape reconstruction studies. *Earth Surface Processes and Landforms*, 42(13), 2167–2183. <https://doi.org/10.1002/esp.4162>
- Thaler, E. A., & Covington, M. D. (2016). The influence of sandstone caprock material on bedrock channel steepness within a tectonically passive setting: Buffalo National River Basin, Arkansas, USA. *Journal of Geophysical Research: Earth Surface*, 121(9), 1635–1650. <https://doi.org/10.1002/2015JF003771>
- Tieszen, L. L., Reed, B. C., Bliss, N. B., Wylie, B. K., & DeJong, D. D. (1997). Ndvi, C3 and C4

- Production, and Distributions in Great Plains Grassland Land Cover Classes. *Ecological Applications*, 7(1), 59–78. [https://doi.org/10.1890/1051-0761\(1997\)007\[0059:NCACPA\]2.0.CO;2](https://doi.org/10.1890/1051-0761(1997)007[0059:NCACPA]2.0.CO;2)
- Todd, J. E. (1916). History of Kaw Lake. *Transactions of the Kansas Academy of Science* (1903-), 28, 187–199. <https://doi.org/10.2307/3624356>
- Townsend, M. A., & Macfarlane, P. A. (2012). Seasonality Effects on Karst Aquifers, Flint Hills Region, Central Kansas, 277–286. [https://doi.org/10.1061/40698\(2003\)25](https://doi.org/10.1061/40698(2003)25)
- Tucker, G. E., & Hancock, G. R. (2010). Modelling landscape evolution. *Earth Surface Processes and Landforms*, 35(1), 28–50. <https://doi.org/10.1002/esp.1952>
- Vero, S. e., Macpherson, G. l., Sullivan, P. l., Brookfield, A. e., Nippert, J. b., Kirk, M. f., et al. (2018). Developing a Conceptual Framework of Landscape and Hydrology on Tallgrass Prairie:A Critical Zone Approach. *Vadose Zone Journal*, 17(1), 170069. <https://doi.org/10.2136/vzj2017.03.0069>
- Wahrhaftig, C. (1965). Stepped Topography of the Southern Sierra Nevada, California. *Geological Society of America Bulletin*, 76(10), 1165. [https://doi.org/10.1130/0016-7606\(1965\)76\[1165:STOTSS\]2.0.CO;2](https://doi.org/10.1130/0016-7606(1965)76[1165:STOTSS]2.0.CO;2)
- Ward, D. J., Berlin, M. M., & Anderson, R. S. (2011). Sediment dynamics below retreating cliffs. *Earth Surface Processes and Landforms*, 36(8), 1023–1043. <https://doi.org/10.1002/esp.2129>
- Ward, Dylan J. (2019). Dip, layer spacing, and incision rate controls on the formation of strike valleys, cuernas, and cliffbands in heterogeneous stratigraphy. *Lithosphere*, 11(5), 697–707. <https://doi.org/10.1130/L1056.1>
- Wells, T., Willgoose, G. R., & Hancock, G. R. (2008). Modeling weathering pathways and

- processes of the fragmentation of salt weathered quartz-chlorite schist. *Journal of Geophysical Research: Earth Surface*, 113(F1). <https://doi.org/10.1029/2006JF000714>
- Wentworth, C. K. (1922). A Scale of Grade and Class Terms for Clastic Sediments. *The Journal of Geology*, 30(5), 377–392. <https://doi.org/10.1086/622910>
- Whittaker, A. C. (2012). How do landscapes record tectonics and climate? *Lithosphere*, 4(2), 160–164. <https://doi.org/10.1130/RF.L003.1>
- Wood, H. K., & Macpherson, G. L. (2005). Sources of Sr and implications for weathering of limestone under tallgrass prairie, northeastern Kansas. *Applied Geochemistry*, 20(12), 2325–2342. <https://doi.org/10.1016/j.apgeochem.2005.08.002>
- Woodburn, T. L., Johnson, W. C., Mason, J. A., Bozarth, S. R., & Halfen, A. F. (2017). Vegetation dynamics during the Pleistocene–Holocene transition in the central Great Plains, USA. *The Holocene*, 27(1), 155–163. <https://doi.org/10.1177/0959683616652710>
- Wooster, L. C. (1903). Some Notes on Kansas Geology. *Transactions of the Kansas Academy of Science (1903-)*, 19, 118–121. <https://doi.org/10.2307/3624188>
- Yanites, B. J., Becker, J. K., Madritsch, H., Schnellmann, M., & Ehlers, T. A. (2017). Lithologic Effects on Landscape Response to Base Level Changes: A Modeling Study in the Context of the Eastern Jura Mountains, Switzerland. *Journal of Geophysical Research: Earth Surface*, 122(11), 2196–2222. <https://doi.org/10.1002/2016JF004101>
- Yeend, W. E. (1973). Slow-Sliding Slumps, Grand Mesa, Colorado. *The Mountain Geologist*. Retrieved from <https://archives.datapages.com/data/rmag/mg/1973/yeend.htm>
- Zondervan, J. R., Whittaker, A. C., Bell, R. E., Watkins, S. E., Brooke, S. A. S., & Hann, M. G. (2020). New constraints on bedrock erodibility and landscape response times upstream of an active fault. *Geomorphology*, 351, 106937. <https://doi.org/10.1016/j.geomorph.2019.106937>

Appendix A Chapter 2

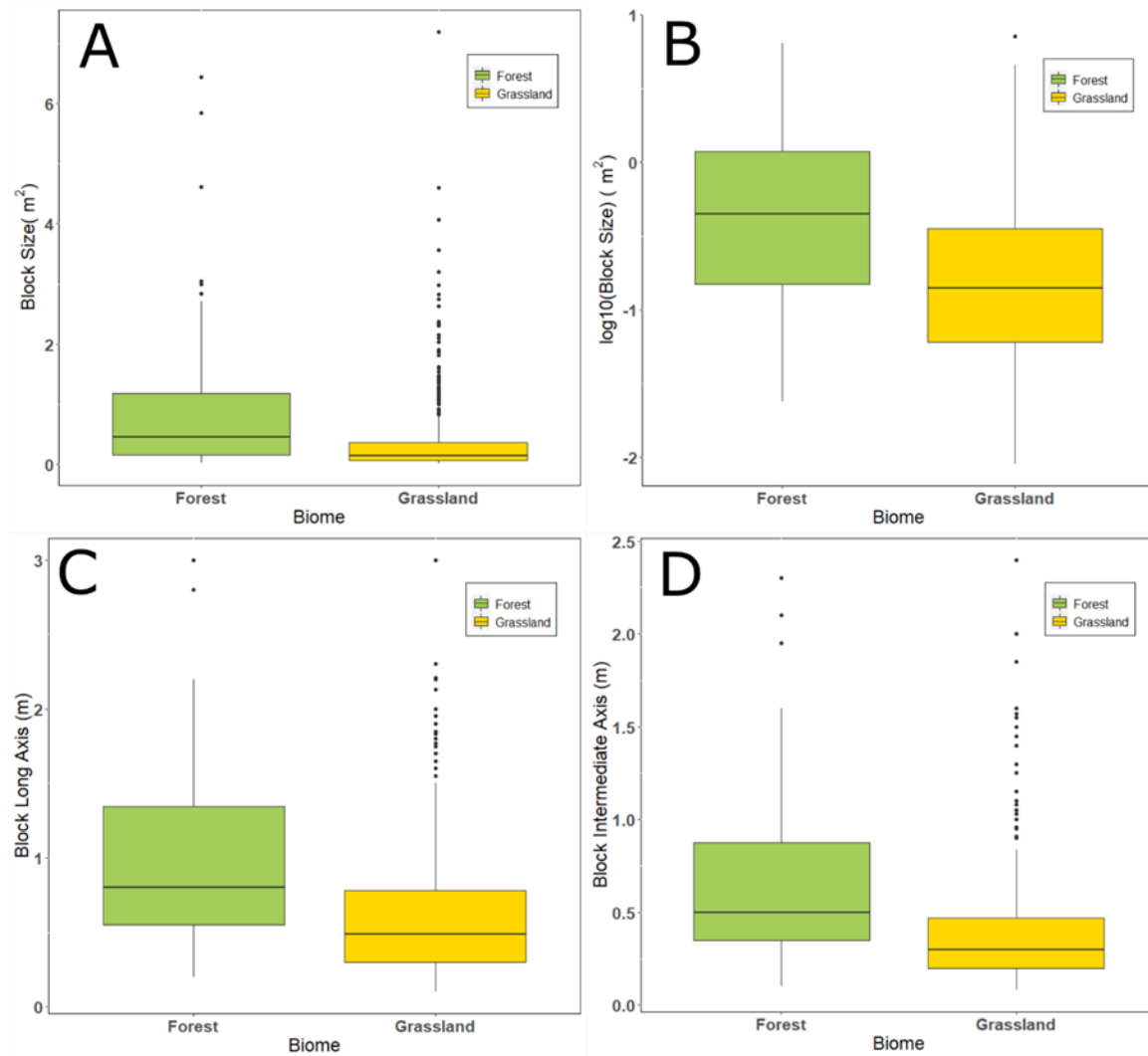


Figure A.1 Block size data presented for land cover types of forest and grassland

A) Block size separated by land cover type. B) Log₁₀ of block size separated by landcover type. C) Block long axis length separated by landcover type. D) Block Intermediate axis length separated by land cover type.

Appendix A Table A.1 Regression results comparison for largest grain size fractions on hillslopes

Grain Size of Rock Block	Linear Regression			Logarithmic Regression		
	b*	p-value	Adjusted R ²	b ^{\$}	p-value	Adjusted R ²
Largest Block	-0.160	0.02	0.407	-1.63	0.02	0.436
5 th Largest Block	-0.071	<0.001	0.776	-0.742	<0.001	0.874
10 th Largest Block	-0.047	<0.001	0.884	-0.458	<0.001	0.865
15 th Largest Block	-0.037	< 0.001	0.842	-0.354	<0.001	0.770

Table presents regression results for data presented in Figure 4C.

*Slope of linear regression with units of m²/m.

\$ Is for regression of [b*log(x)] where units of b are in m².

To get this to work, you may have to highlight the numbering of the sections in the Appendix...Set Numbering Value as follows, and ensure that the first of the sequence is correct, whether the value is 6 or 7 or 8 or whatever (based on the number of chapters you have prior with the Heading 1 label).

Appendix B Chapter 3

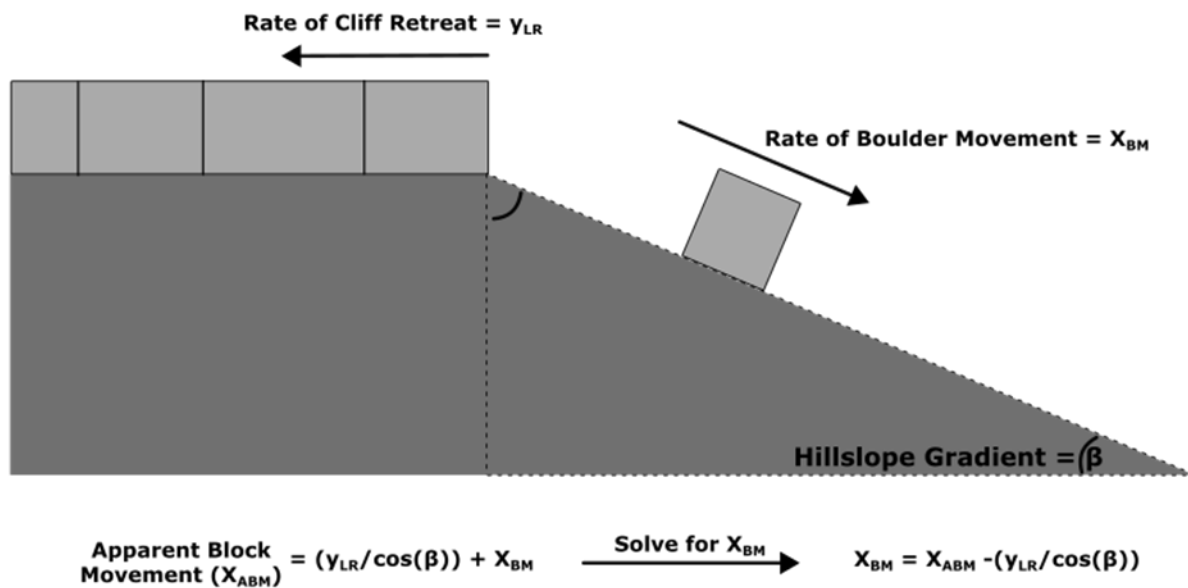


Figure B.1 Schematic of the geometric relationships on hillslope.

Schematic of the geometric relationships between the rate of lateral bench retreat and the rate of boulder transport downslope. Below shows how an apparent measured rate of block movement from geochronology may be the sum of both the rate of lateral bench retreat as well as the rate of boulders downslope. The derivation of the actual block movement rate is show.

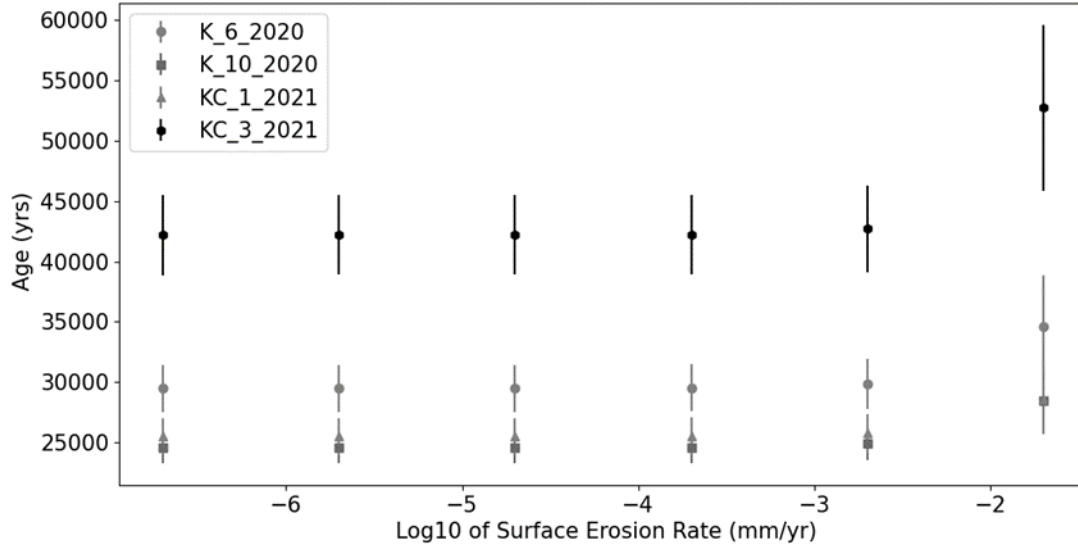


Figure B.2 **Influence of erosion rates on block surface ages**

Subset of ^{36}Cl geochronology to show the effect of increasing erosion rates on the surface exposure rates calculated from CRONUS.

Table B.1. Bulk rock chemistry of limestone boulders in Konza Prairie, KS (1 of 2).

Sample Name	Sample Type	Lithologic Unit	SiO ₂ %	Al ₂ O ₃ %	Fe ₂ O ₃ %	MgO %	CaO %	Na ₂ O %	K ₂ O %	TiO ₂ %	P ₂ O ₅ %
K1-20	Bulk	Three Mile Limestone	4.9	0.38	0.27	0.64	51.71	0.02	0.1	0.02	0.03
K3-20	Bulk	Three Mile Limestone	5.17	0.45	0.29	0.65	51.42	0.06	0.12	0.02	0.03
K5-20	Bulk	Three Mile Limestone	3.51	0.29	0.28	0.48	52.67	0.04	0.09	0.02	0.01
KC1-21	Bulk	Cottonwood	6.17	0.66	0.33	0.63	50.27	0.03	0.17	0.03	0.03
KC2-21	Bulk	Cottonwood	4.97	0.65	0.27	0.64	51	0.04	0.16	0.03	0.03

Geochemical Analysis performed by Bureau Veritas, Vancouver, Canada. Bulk samples were analysis using lithium borate fusion, dissolution, and analyzed with ICP-ES/MS.

Table B.2. Bulk rock chemistry of limestone boulders in Konza Prairie, KS (2 of 2).

Sample Name	Sample Type	Lithologic Unit	MnO %	Cr ₂ O ₃ %	Ba %	Ni %	Sr %	Zr %	Y %	Nb %	Sc %	LOI %
K1-20	Bulk	Three Mile Limestone	0.04	<0.02	14	<20	197	<5	<3	<5	<1	41.8
K3-20	Bulk	Three Mile Limestone	0.04	<0.02	14	<20	214	<5	3	<5	<1	41.7
K5-20	Bulk	Three Mile Limestone	0.04	<0.02	10	<20	221	<5	3	<5	<1	42.5
KC1-21	Bulk	Cottonwood	0.03	<0.02	301	<20	191	8	3	3.3	<1	41.6
KC2-21	Bulk	Cottonwood	0.03	<0.02	28	<20	203.9	6.5	2.9	3.7	<1	42.1

Geochemical Analysis performed by Bureau Veritas, Vancouver, Canada. Bulk samples were analysis using lithium borate fusion, dissolution, and analyzed with ICP-ES/MS.

Table B.3. Target rock chemistry of limestone boulders in Konza Prairie, KS (1 of 5).

Sample Name	Sample Type	Lithologic Unit	SiO ₂ %	Al ₂ O ₃ %	Fe ₂ O ₃ %	MgO %	CaO %	Na ₂ O %	K ₂ O %	TiO ₂ %	P ₂ O ₅ %
				3	3						
K1-20	Target	Three Mile Limestone	4.9	0.45	0.28	0.64	52.01	0.05	0.11	0.02	0.02
K3-20	Target	Three Mile Limestone	4.62	0.41	0.23	0.62	51.99	0.04	0.1	0.02	0.05
K5-20	Target	Three Mile Limestone	3.39	0.31	0.31	0.48	52.67	0.04	0.08	0.02	0.01
KC1-21	Target	Cottonwood	6.06	0.64	0.33	0.64	50.39	0.04	0.15	0.03	0.03
KC2-21	Target	Cottonwood	5.02	0.61	0.26	0.64	51.06	0.05	0.16	0.03	0.03

Geochemical Analysis performed by Bureau Veritas, Vancouver, Canada. Bulk samples were analysis using lithium borate fusion, dissolution, and analyzed with ICP-ES/MS.

Table B.4. Target rock chemistry of limestone boulders in Konza Prairie, KS (2 of 5).

Sample Name	Sample Type	Lithologic Unit	MnO %	Cr ₂ O ₃ %	Ba PPM	Ni PPM	Sc PPM	LOI %	Sum %	Be PPM	Co PPM	Cs PPM
K1-20	Target	Three Mile Limestone	0.04	<0.02	21	<20	<1	41.4	99.95	<1	0.7	0.2
K3-20	Target	Three Mile Limestone	0.04	<0.02	20	<20	<1	41.8	99.93	<1	0.8	0.1
K5-20	Target	Three Mile Limestone	0.04	<0.02	14	<20	<1	42.6	99.95	<1	0.4	<0.1
KC1-21	Target	Cottonwood	0.03	0.003	360	<20	<1	41.6	99.97	<1	1.3	0.3
KC2-21	Target	Cottonwood	0.03	0.003	32	<20	<1	42	99.96	<1	0.3	0.2

Geochemical Analysis performed by Bureau Veritas, Vancouver, Canada. Bulk samples were analysis using lithium borate fusion, dissolution, and analyzed with ICP-ES/MS.

Table B.5. Target rock chemistry of limestone boulders in Konza Prairie, KS (3 of 5).

Sample Name	Sample Type	Lithologic Unit	Ga PPM	Hf PPM	Nb PPM	Rb PPM	Sn PPM	Sr PPM	Ta PPM	Th PPM	U PPM
K1-20	Target	Three Mile Limestone	<0.5	0.1	0.5	3.7	<1	216.1	<0.1	0.4	1.9
K3-20	Target	Three Mile Limestone	<0.5	0.2	0.4	3.3	<1	233.8	<0.1	0.5	1.7
K5-20	Target	Three Mile Limestone	<0.5	0.2	0.3	2.6	<1	249.7	<0.1	0.3	1.7
KC1-21	Target	Cottonwood	<0.5	0.2	1	5.5	4	191	<0.1	0.4	2.3
KC2-21	Target	Cottonwood	<0.5	0.2	0.5	4.7	<1	203.9	<0.1	0.4	2.2

Geochemical Analysis performed by Bureau Veritas, Vancouver, Canada. Bulk samples were analysis using lithium borate fusion, dissolution, and analyzed with ICP-ES/MS.

Table B.6. Target rock chemistry of limestone boulders in Konza Prairie, KS 4 of 5).

Sample Name	Sample Type	Lithologic Unit	V PPM	W PPM	Zr PPM	Y PPM	La PPM	Ce PPM	Pr PPM	Nd PPM	Sm PPM	Eu PPM
K1-20	Target	Three Mile Limestone	<8	<0.5	5.1	4.1	7.7	13.3	1.51	5.5	0.89	0.22
K3-20	Target	Three Mile Limestone	<8	<0.5	7.7	4.4	8.1	16.1	1.78	7.1	1.25	0.25
K5-20	Target	Three Mile Limestone	<8	<0.5	5.8	3.4	6.2	11.7	1.26	4.7	0.78	0.2
KC1-21	Target	Cottonwood	<8	<0.5	8	3	5	8.3	1	3.3	0.6	0.13
KC2-21	Target	Cottonwood	<8	<0.5	6.5	2.9	4.5	8.6	0.96	3.7	0.67	0.15

Geochemical Analysis performed by Bureau Veritas, Vancouver, Canada. Bulk samples were analysis using lithium borate fusion, dissolution, and analyzed with ICP-ES/MS.

Table B.7. Target rock chemistry of limestone boulders in Konza Prairie, KS (5 of 5).

Sample Name	Sample Type	Lithologic Unit	Gd	Tb	Dy	Ho	Er	Tm	Yb	Lu
K1-20	Target	Three Mile Limestone	PPM							
K3-20	Target	Three Mile Limestone	1.01	0.14	0.69	0.11	0.32	0.05	0.21	0.04
K5-20	Target	Three Mile Limestone	1.21	0.16	0.81	0.14	0.28	0.05	0.23	0.04
KC1-21	Target	Cottonwood	0.9	0.12	0.6	0.11	0.25	0.03	0.19	0.02
KC2-21	Target	Cottonwood	0.69	0.1	0.53	0.09	0.2	0.04	0.19	0.03

Geochemical Analysis performed by Bureau Veritas, Vancouver, Canada. Bulk samples were analysis using lithium borate fusion, dissolution, and analyzed with ICP-ES/MS.
